2022

Water Quality in the Yangtze River at Shanghai and the Role of Coastal Reservoirs in Shanghai's Water Supply

Samuel Finnian Kelly

UNIVERSITY OF WOLLONGONG AUSTRALIA

Water Quality in the Yangtze River at Shanghai and the Role of Coastal Reservoirs in Shanghai's Water Supply

Samuel Finnian Kelly

Supervisors:
A/Prof. Shu-qing Yang
A/Prof. Muttucumaru Sivakumar
Prof. Jerry Ongerth

This thesis is presented as part of the requirement for the conferral of the degree:
Master of Philosophy in Environmental Engineering

This research has been conducted with the support of the Australian Government Research Training Program Scholarship

The University of Wollongong
School of Civil, Mining and Environmental Engineering

July 2022

Abstract

Shanghai is the largest city in China and third largest in the world. It is home to more than 24 million people and is the largest commercial and industrial centre in China. Challenges to water supply in coastal mega cities are becoming apparent worldwide, and Shanghai was predicted to be among one of the most likely to suffer severe water crisis. To meet its rapidly growing demand for municipal water supply, Shanghai has turned to the enormous fresh water resource provided by the Yangtze River at its estuary. Coastal reservoirs have been constructed to capture, store and protect water supplies in the estuary; these reservoirs now provide around 70% of Shanghai's water supply.

This thesis is designed to examine the implications of using coastal reservoirs in Shanghai's municipal water supply system by describing relevant water quality characteristics of the Yangtze River at points of diversion to Shanghai's coastal reservoirs and evaluating the effect of water quality processes in these reservoirs on downstream water treatment operations. A critical literature review covering Shanghai's municipal water supply and the water quality at the Yangtze River Estuary was undertaken. From literature sources, data on key water quality parameters at the estuary and the Qingcaosha Reservoir, Shanghai's largest coastal reservoir, has been collected. The data has been assembled and compared with relevant standards, and Mann-Kendall analysis applied to trends in key nutrients and total suspended solids concentrations. The settling characteristics of the Qingcaosha Reservoir have been assessed by treating the reservoir as an ideal settling basin and potential algal growth behaviour analysed using the lake ecology model PCLake+. Potential management options for algal blooming in the Qingcaosha Reservoir are explored.

This study concludes that additional storage in Shanghai's coastal reservoirs, potentially in the form of an additional coastal reservoir, as well as expanded pumping and treatment capacity is required to secure Shanghai's water supply to 2050. Additionally, nutrient levels in the Yangtze Estuary have resulted in algal blooms in the Qingcaosha Reservoir and will continue to cause problematic algal blooming in Shanghai's coastal reservoirs unless appropriate management strategies are applied. It is recommended that more extensive and intensive sampling be undertaken in the estuary and Shanghai's coastal reservoirs to accurately describe water quality in these locations and so that more advanced modelling and statistical techniques can be applied. Alternative reservoir management strategies should also be explored to determine if the cost of providing treated water to Shanghai can be reduced.

Acknowledgments

During the preparation of this thesis, I have received significant support and assistance from those around me.

Firstly, I would like to thank my supervisors, A/Prof. Shu-qing Yang, A/Prof. Muttucumaru Sivakumar and Prof Jerry Ongerth for sharing their experience and insight, and whose advice I relied upon to complete this body of work. I would also like to thank Dr Mehdi Robati, for his willingness to talk through ideas in the early days of my thesis and for his staunch support as my student representative, as well as Joshua Atkinson, who generously donated his time as a sounding board and gave helpful advice on environmental modelling. My thanks also go to the university support staff, especially Rhondalee Cambareri who helped me keep everything on track during the latest stages of my study.

I am extremely grateful to my family and friends for their love and encouragement, especially my wife Moonue who graciously sacrificed her time to keep things going and supported me while I pursued my studies. I also appreciate the patience and flexibility of my colleagues at Cardno, especially Craig Hood and Adam Clarke, who helped me to balance my work and study successfully.

Without all the people mentioned above, I would have not completed this thesis and I am fortunate indeed that they were there to support me in this endeavour.

Certification

I, Samuel Finnian Kelly, declare that this thesis submitted in fulfilment of the requirements for the conferral of the degree Master of Philosophy in Environmental Engineering, from the University of Wollongong, is wholly my own work unless otherwise referenced or acknowledged. This document has not been submitted for qualifications at any other institution.

_____

Samuel Finnian Kelly

19th July 2022

List of Names or Abbreviations

a =	year (annum)
d =	days
^{o}C =	degrees Celsius
DIP =	dissolved inorganic phosphorous
g =	grams
h =	hours
ha =	hectares
HRT =	Hydraulic Retention Time
kg =	kilograms
km =	kilometres
km^2 =	square kilometres
km^3 =	cubic kilometres
L =	litres
m =	metres
m^2 =	square metres
m^3 =	cubic metres
mg =	milligrams
mm =	millimetres
NO_3-N =	nitrate measured by nitrogen content
NH_4-N =	ammonium measured by nitrogen content
Pa =	Pascals
s =	seconds
s^2 =	square seconds
t =	tonnes
TDS =	total dissolved solids
TGD =	three Gorges Dam
TN =	total Nitrogen
TP =	total Phosphorous
TSS =	total suspended solids

Table of Contents

1. Introduction 8
   1.1 Background 8
   1.2 Problem Statement 9
   1.3 Specific Objectives 10
   1.4 Scope 10
   1.5 Structure of this Thesis 11
2. Shanghai and the Yangtze River 12
   2.1 Local Geography and Raw Water Sources 12
   2.2 The Yangtze River and its Estuary 19
      2.2.1 Climate and Streamflow 23
      2.2.2 People and Land Use in the Yangtze River Basin 32
   2.3 Shanghai's Municipality Water Supply 43
      2.3.1 Water Quantity and Quality 43
      2.3.2 Configuration of Shanghai's Water Supply 49
   2.4 Shanghai's Water Security 56
   2.5 Summary 58
3. Water Quality in the Yangtze River at Shanghai 60
   3.1 Water Quality Summary 60
   3.2 Saline Intrusion 69
   3.3 Nutrients and Sediment Concentrations at the Yangtze Estuary 75
      3.3.1 Characterisation of Nutrient and Sediment Concentrations 75
      3.3.2 Factors Affecting Nutrients and Sediments in the Yangtze Estuary 93
      3.3.3 Eutrophication and Algal Blooms 105
   3.4 Summary 109
4. Water Quality Shanghai's Qingcaosha Reservoir 111
   4.1 Qingcaosha Reservoir and its Water Quality 113
      4.1.1 Physical Characteristics 113
      4.1.2 Nutrients 121
      4.1.3 Algae 126
   4.2 Water Quality Processes Occurring in the Qingcaosha Reservoir 129
      4.2.1 Sedimentation 129
      4.2.2 Biological Processes 134
   4.3 The Effect of Coastal Reservoir and Potential Management Strategies 146
   4.4 Summary 154
5. Conclusions and Recommendations 156
   5.1 Conclusions from this Study 156
   5.2 Recommendations for Further Research 159
6. Bibliography 161
7. Appendices 171
   A1 - Supplementary Data Tables 171
   A2 - Chinese Water Quality Standards 176
   A3 – PCLake+ input data 179

List of Tables and Figures

Figure 1-1: Problem Statement Schematic 9
Figure 2-1: Location of Shanghai in China 12
Figure 2-2: The Yangtze River Delta Region 13
Figure 2-3: Shanghai's Local Water Resources and Major Abstraction Points 15
Figure 2-4: The Yangtze River Basin 20
Figure 2-5: Tributaries of the Yangtze River and Key Hydrometric Stations 21
Figure 2-6: The Yangtze River Estuary 22
Figure 2-7: Average Monthly Rainfall in the Yangtze Basin (1970-2000) 24
Figure 2-8: Average Annual Streamflow at Datong Station (1950 – 2015) 29
Figure 2-9: Average Monthly flow at Datong Station (1950 – 2015) 30
Figure 2-10: Minimum Monthly Streamflow at Datong Station (1950 – 2015) 31
Figure 2-11: Population Density Distribution in the Yangtze River Basin 33
Figure 2-12: Land Use in the Yangtze Basin 34
Figure 2-13: Shanghai 1989-2019 36
Figure 2-14: Location of Key Projects in Shanghai's Nearshore Zone 38
Figure 2-15: Large Dams in the Yangtze River Basin 41
Figure 2-16: Growth in Shanghai's Population and Total GDP (1978-2013) 43
Figure 2-17: Population Growth and Historical Water Supply Consumption in Shanghai 46
Figure 2-18: Historical and Predicted Annual Municipal Water Supply Consumption in Shanghai 47
Figure 2-19: Shanghai's Municipal Water Supply Assets 50
Figure 2-20 Comparison of Historical and Predicted Annual Municipal Water Supply Consumption and Municipal Treatment Capacity in Shanghai 52
Figure 2-21: Typical Types of Water Treatment Processes 54
Figure 3-1: Schematic of Shanghai's Municipal Supply 60
Figure 3-2: The Yangtze Estuary and Distances from Xuliujing 70
Figure 3-3: Comparison between flow at Datong with 7-day lag and TDS at the estuary. 72
Figure 3-4: Annual Average Concentration (1990-2013) of Total Nitrogen, Nitrate and Ammonium at Datong and the Estuary 76
Figure 3-5: Annual Average Concentration (1990-2013) of Total Phosphorous, Dissolved Inorganic Phosphorous and Total Suspended Solids at Datong and the Estuary. 77
Figure 3-6: Nitrate-N concentration at the Yangtze Estuary. 81
Figure 3-7: Nitrate-N concentration at the Datong 82
Figure 3-8: Ammonium-N concentration at the Datong 83
Figure 3-9: DIP Concentration at the Estuary 84
Figure 3-10: DIP Concentration at Datong 85
Figure 3-11: TSS Concentration at Datong 86
Figure 3-12: Particle size distribution of Suspended Sediment (SS) and Bed Material (BM) at Jiangyin and Datong 88
Figure 3-13: Monthly Average Concentration (1990-2013) of Total Nitrogen, Nitrate and Ammonium at Datong and the Estuary 90
Figure 3-14: Monthly Average Concentration (1990-2013) of Total Phosphorous, Dissolved Inorganic Phosphorous and Total Suspended Solids at Datong and the Estuary 91
Figure 3-15: Population in the Yangtze Basin 98
Figure 3-16: Total Fertiliser Application in the Yangtze Basin 99
Figure 3-17: Nitrogenous Fertiliser Application in the Yangtze Basin 100
Figure 3-18: Phosphorous Fertiliser Application in the Yangtze Basin 101
Figure 3-19: Irrigated Area in the Yangtze Basin 102
Figure 3-20: Livestock in the Yangtze River Basin 103
Figure 3-21: Aquaculture area in the Yangtze Basin 104
Figure 4-1: Locations of Shanghai's coastal reservoirs 111
Figure 4-2: Data sources and sample locations in the Qingcaosha Reservoir 112
Figure 4-3: The Qingcaosha Reservoir 113
Figure 4-4: Bathymetry in the Qingcaosha Reservoir 114
Figure 4-5: Average Monthly Water Temperature in the Qingcaosha Reservoir 117
Figure 4-6: Average monthly DO concentration in the Qingcaosha Reservoir 117
Figure 4-7: Average monthly pH in the Qingcaosha Reservoir 118

Figure 4-8: Average Transparency in the Qingcaosha Reservoir Jun 2009 to Oct 2013 119
Figure 4-9: Average Monthly Transparency in the Qingcaosha Reservoir 119
Figure 4-10: Longitudinal Change in Transparency in the Qingcaosha Reservoir. 120
Figure 4-11: Longitudinal Change in Turbidity in the Qingcaosha Reservoir. 120
Figure 4-12: Average TN the Qingcaosha Reservoir 2009-2017 121
Figure 4-13: Average Monthly TN the Qingcaosha Reservoir 2011-207 122
Figure 4-14: Longitudinal Change in TN in the Qingcaosha Reservoir. 122
Figure 4-15: Average TP the Qingcaosha Reservoir 2009-2017 123
Figure 4-16: Average Monthly TP the Qingcaosha Reservoir 2009-2017 124
Figure 4-17: Longitudinal Change in TP in the Qingcaosha Reservoir. 124
Figure 4-18: TN, TP, and estimated TN:TP molar ratio 125
Figure 4-19: Chlorophyll a, Cyanobacteria and Chlorophyta in the Qingcaosha Reservoir 127
Figure 4-20: Monthly Average Chlorophyll-a concentration in the Qingcaosha Reservoir 127
Figure 4-21: Longitudinal Change in TP in the Qingcaosha Reservoir. Chen and Zhu (2018) 128
Figure 4-22: Sediment particle distribution at Jiangyin and estimated minimum settleable particle size at the overflow rates calculated in **Table 4-7** 132
Figure 4-23: Aerial Photo captured in 2016 where Suspended Sediment the Qingcaosha Reservoir can be observed 133
Figure 4-24: Comparison of estimated annual and summer Chlorophyll-a concentrations at varying phosphorous concentrations under typical operating conditions 137
Figure 4-25: Comparison of estimated annual Chlorophyll-a concentrations at varying phosphorous concentrations under different hydraulic loading 138
Figure 4-26: Comparison of estimated summer Chlorophyll-a concentrations at varying phosphorous concentrations under different hydraulic loading 139
Figure 4-27: Comparison of estimated annual Chlorophyll-a concentrations at varying phosphorous concentrations with different marsh coverage fractions 141
Figure 4-28: Comparison of estimated summer Chlorophyll-a concentrations at varying phosphorous concentrations with different marsh coverage fractions 142
Figure 4-29: Chlorophyll a response to clay fraction of suspended sediment 143
Figure 4-30: Annual average and summer average Chlorophyll a response to suspended sediment concentration 144
Figure 4-31: Example of Implementation of Reservoir Management Measures in Qingcaosha Reservoir. 153

Table 2-1: Key information on the Yangtze River's Major Tributaries 19
Table 2-2: Key data on Provinces in the Yangtze Basin. 35
Table 2-3: Total abstraction in Jiangsu present and 2030 planned 42
Table 2-4: Class III Basic Water Quality Parameter Guidelines (SEPA 2002) 48
Table 2-5: Pumping Stations and Treatment Plants in Shanghai 51
Table 2-6: Estimated Removal Rates at Two Water Treatment Plants in Shanghai 54
Table 2-7: Cost Estimates for Future Water Treatment Plants in Shanghai under Various Growth Scenarios. 55
Table 3-1: Water Quality Summary at the Yangtze Estuary 61
Table 3-2: Mann-Kendall Test Summary for Nutrient Data in the Yangtze Estuary 80
Table 3-3: Estimated Annual Loads of TSS, PN and PP from the Yangtze Estuary 88
Table 3-4: Mean Concentration of Nutrients in Rivers and Estuaries 92
Table 3-5: Mann-Kendall Summary for Land Uses in the Yangtze Basin 97
Table 4-1: Shanghai's Coastal Reservoirs Key Data Summary 112
Table 4-2: Estimated Average Depth and Storage under various operating water levels. 115
Table 4-3: Typical Wind Direction (%) at the Qingcaosha Reservoir 115
Table 4-4: Estimated Average Wind Speed (m/s) at the Qingcaosha Reservoir 115
Table 4-5: Estimated Reservoir Fetch. 116
Table 4-6: Estimated Settling Velocities based on Particle Grading Classification (ISO 14688-1:2017) and Classification of Suspended Solids and Bed Material at Jiangyin and Datong 131
Table 4-7: Estimated Horizontal Velocity and Overflow Rate at various Hydraulic Retention Times 131
Table 4-8: Potential Management Measures for Algal Blooms in Drinking Water Reservoirs 148

1. Introduction

1.1 Background

Shanghai is the largest city in China and third largest in the world with a population of more than 24 million people within the municipal boundary and is the largest industrial and commercial centre in China. Megacities (cities with populations over 10 million) such as Shanghai are facing challenges where water demand is unable to be met as a result of natural, socioeconomic, water quality or environmental reasons (Sun, Michelsen et al. 2015). A situation where water demand is unable to be met with available water supply is called a water crisis. In 1996 at the UN Centre for Human Settlements Conference, Habitat II, Shanghai was predicted to be one of the dozen cities most likely to suffer sever water crisis by 2010. A water crisis has the potential to threaten the health of Shanghai's citizens and be a critical factor in limiting further economic growth in the region (Li, Mander et al. 2009, Finlayson, Barnett et al. 2012, Yang and Kelly 2015).

Historically, Shanghai has had problems with sourcing sufficient good quality water for municipal supply and despite significant nearby water resources, Shanghai's drinking water supply is not guaranteed (Ward and Liang 1995, Finlayson, Barnett et al. 2012). As described by Shen Yiyun, the deputy director of Shanghai Municipal Bureau of Water Resources:

"The water quality of the rivers is unacceptable and Shanghai does not have a lot of drinking water even though the city is practically surrounded by water." (Xinhua News Agency 2006)

To source a reliable water supply, Shanghai has turned to the Yangtze River Estuary and its enormous supply of what is perceived to be high quality water. Drawing water from the estuary is complicated however, because the only part of the estuary available to Shanghai for water withdrawals is prone to intense periodic saline intrusions. To solve this problem, coastal reservoirs are used to capture, store, and protect water supply during periods of saline intrusions, with these reservoirs, the largest being the Qingcaosha Reservoir, currently providing around 70% of Shanghai's water supply. Coastal reservoirs are now a critical component of Shanghai's water supply system, storing water until such time it is treated for municipal and industrial use.

Coastal reservoirs are capable of collecting a significant amount of runoff that would normally be lost to the sea, however they also can collect pollutants generated in the catchment. The Yangtze River is 6,300 km long, draining a basin of around 1.8 million m^2, and receives the waste of more than 440 million people, industry and agriculture. As a result, the Yangtze estuary has the potential to be affected by water poor quality originating from anthropogenic activities upstream in the basin. By extension, the Coastal Reservoirs in the Yangtze Estuary are also at risk of being affected. In particular concerns have been raised about the high nutrient loads and subsequent algal blooming in these reservoirs, which has the potential to result in problems with water

treatment operations downstream and could result in complications in downstream treatment operations or increased risk to public health (Webber, Barnett et al. 2018). Shanghai relies on predominantly conventional water treatment processes for its municipal supply. Conventional water treatments have a limited capacity to treat contaminants other than particulates and micro-organisms and water quality in Shanghai's coastal reservoirs could have implications for the efficacy of Shanghai's current water treatment operations.

1.2 Problem Statement

This project is designed to examine the implications of using coastal reservoirs in Shanghai's municipal water supply system by describing relevant water quality characteristics of the Yangtze River at points of diversion to Shanghai's coastal reservoirs and evaluating the effect of water quality processes in these reservoirs on downstream water treatment operations.

Figure 1-1: Problem Statement Schematic. Aerial photo sourced from NASA Earth Observatory (2017)

1.3 Specific Objectives

The specific objectives of this project are to:

1. Critically review Shanghai's available water resources, in particular the Yangtze River, and Shanghai's water supply operations;
2. Characterise the concentrations and behaviours of water quality parameters in the Yangtze Estuary relevant to Shanghai's water supply via the Qingcaosha Reservoir; and
3. Identify relevant water quality processes occurring within the Qingcaosha Reservoir and determine the implications on downstream treatment operations using conventional water treatment processes.

1.4 Scope

In meeting specific objective 1, a critical literature review of published articles is undertaken. Topic covered in this literature review include Shanghai's available raw water sources, the Yangtze River and its estuary and the current configuration of Shanghai's water supply. The literature review is aimed to provide insight into what options Shanghai has for water supply, the quantity of water available from these options, Shanghai's specific requirements for raw water quantity and quality, and the configuration of the current municipal water supply system.

To meet specific objective 2, water quality data from selected articles is assembled and compared with relevant raw water quality standards to determine constituents of concern (i.e. parameters relevant to Shanghai's water supply). No attempt was made to contact authorities or universities in Shanghai to collect additional data for this study. Only data that is available in currently published material will be used and this thesis will involve no collection of new data. Collected data will be from locations and time-periods relevant to Shanghai's Coastal Reservoirs and only parameters that can be reasonably expected to be affected by coastal reservoir design and operation will be considered in detail. Data on constituents of concern will be plotted and a Mann-Kendall trend analysis applied to annual time series data.

Specific objective 3 requires data to be collected representing conditions within the coastal reservoirs. Due to its relative significance and available data, this thesis will focus on Shanghai's largest coastal reservoir, Qingcaosha. Key data is assembled and plotted to characterise the Qingcaosha reservoir and its water quality. Potential sedimentation in the reservoir is analysed by treating the Qingcaosha reservoir as an ideal settling basin and a lake ecology model, PCLake+ is used to assess the potential for algal growth in the reservoir under various nutrient loading conditions and operating scenarios. The implications of observed and modelled water quality behaviour are compared with the capabilities of Shanghai's municipal supply and potential reservoir management strategies are explored.

1.5 Structure of this Thesis

This thesis is structured into 5 chapters, which are organised as follows:

- **Chapter 1: Introduction –** This chapter defines the problem statement, specific objectives and scope for this thesis;
- **Chapter 2: Shanghai and the Yangtze River** – This chapter addresses specific objective 1 and focuses on the context in which Shanghai's coastal reservoirs operate. It features a discussion of Shanghai's local geography and available water resources, a description of the Yangtze River system, quantification of the requirements of Shanghai's municipal supply and an overview of the current configuration of Shanghai's water supply;
- **Chapter 3: Water Quality in the Yangtze River at Shanghai** – This chapter addresses specific objective 2 and includes the collection and analysis of water quality data at locations and time periods relevant to Shanghai's coastal reservoirs. Salinity, nutrients and sediment loading are identified as water quality constituents of concern and covered in further detail;
- **Chapter 4: Shanghai's Coastal Reservoirs** – This chapter addresses specific objective 3 and introduces Shanghai's coastal reservoirs, characterises water quality in the Qingcaosha Reservoir, examines significant processes occurring in the reservoir and discusses implications and potential management strategies;
- **Chapter 5: Conclusions and Recommendations** – This chapter summarises the conclusions of this thesis and makes recommendations for future research.

2. Shanghai and the Yangtze River

2.1 Local Geography and Raw Water Sources

Shanghai is the largest city in China and third largest in the world with a population of more than 24 million people within the municipal boundary and is the largest industrial and commercial centre in China (Shanghai Municipal People's Government 2010, UN DESA 2018, Webber, Barnett et al. 2018). The Shanghai Municipality is located on the eastern extent of the Yangtze River Delta, adjacent to where the Yangtze River (also referred to as the Changjiang) meets the East China Sea (**Figure 2-1**). Shanghai has a total area of 6,340 km^2 and is bordered by Zhejiang Province, Jiangsu Province and Lake Tai to the West, the Yangtze River Estuary to the North and the East China Sea to the South and East. The Yangtze Delta (**Figure 2-2**) is an alluvial plain formed by sediment deposits from the Yangtze River and is one of the world's largest; supporting a population of 74 million people and is one of the most densely populated and economically important regions in China (Yin, Walcott et al. 2005, Zhang, Gemmer et al. 2008, Qiu and Zhu 2013, Webber, Barnett et al. 2018).

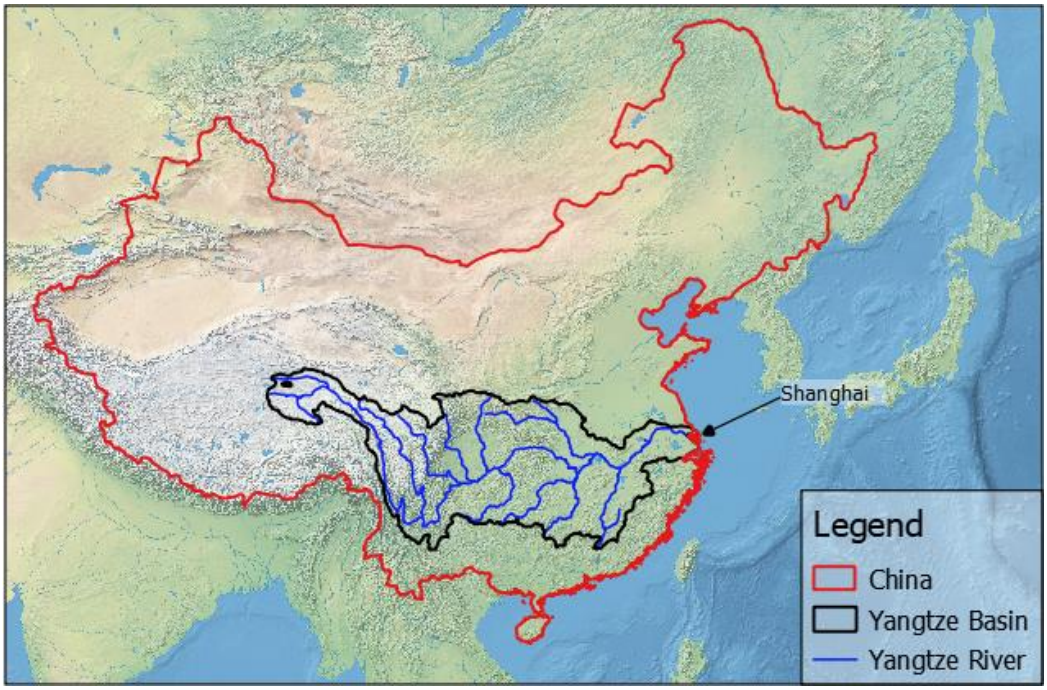

Figure 2-1: Location of Shanghai in China. Boundaries were extracted from the GADM database (www.gadm.org), version 2.8. Yangtze River Data from Crissman and Berman (2012)

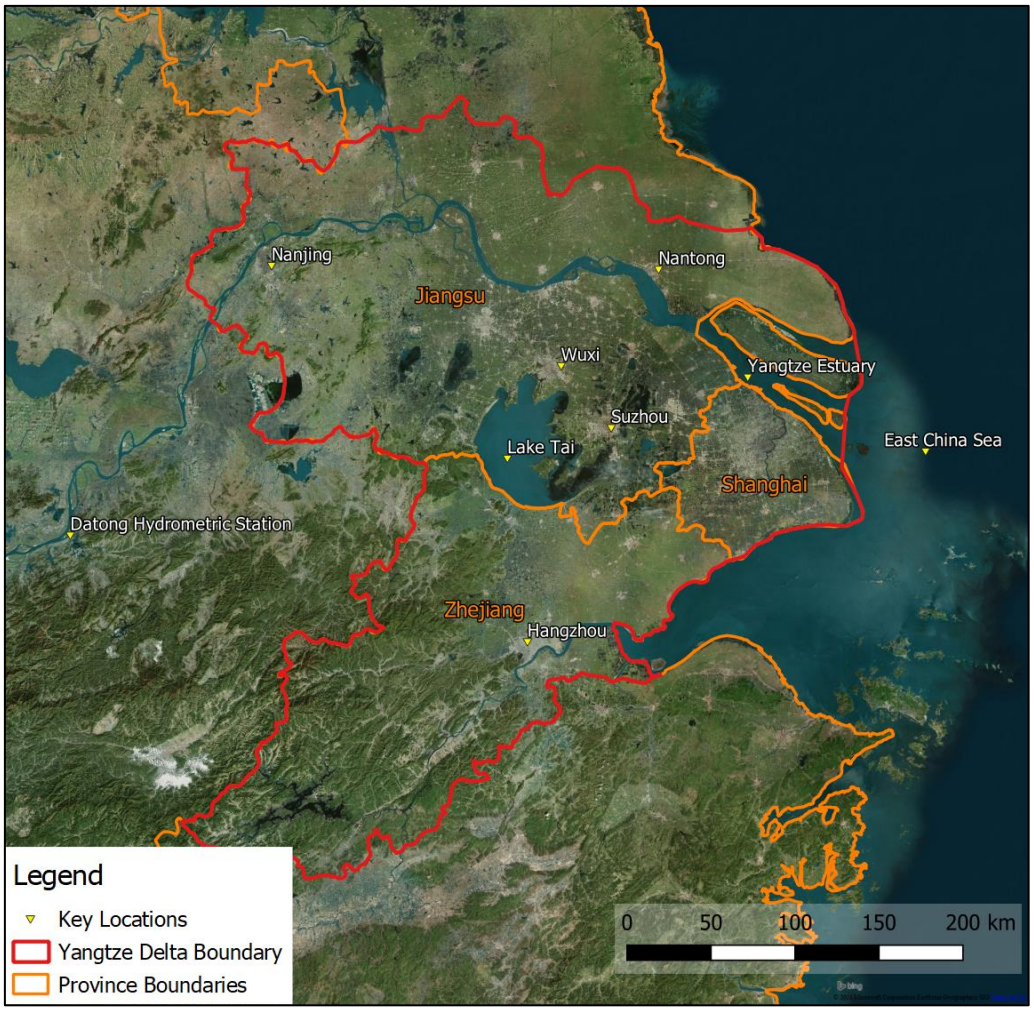

Figure 2-2: The Yangtze River Delta Region. Aerial Photo source from Bing Aerial, Microsoft Corporation Earthstar Geographics SIO (2021). Boundaries were extracted from the GADM database (www.gadm.org), version 2.8.

Most areas of modern day Shanghai have only become dry land as late as the Tang Dynasty (618-907 CE) and the modern coastline of Shanghai to the east of the Huangpu River only formed as late as the Ming Dynasty (1368-1661 CE) (Shanghai Municipal People's Government 2010). As a result, Shanghai Municipality is mostly low and flat, with an average elevation of around 4 m above sea level (Shanghai Municipal Government 2009). Shanghai is intersected by many rivers, creeks, and numerous drainage and transport canals, with the most significant being the Huangpu River and Suzhou Creek.

Shanghai Municipality has three major sources of water; surface water drawn from local rivers and canals, groundwater, and surface water from the Yangtze Estuary. All three of these sources have been used by Shanghai to varying extents in the past and with consumers accessing these sources through both the public and private supply (Webber, Barnett et al. 2018). Other potential supplementary water sources include rainwater harvesting, wastewater recycling. A map showing Shanghai's local water resources and current major abstraction points for water supply is displayed in **Figure 2-3**.

Local surface water from rivers and canals has supplied a significant proportion of Shanghai's drinking water throughout its history. The majority of Shanghai's local rivers and canals originate from the Lake Tai Basin, an interconnected series of lakes, rivers, and smaller waterways. Lake Tai is the third largest lake in China, with a surface area of 2,238 km^2 and containing 4.66 billion m^3 of water (Yang and Kelly 2015). The Lake Tai Catchment comprises portions of Shanghai's neighbouring provinces, Jiangsu and Zhejiang and receives inflows from the Tiaoxi River, the highlands to the west of the Lake, and from precipitation onto the lake surface (Finlayson, Barnett et al. 2012). In addition, since 2002 water has been diverted from the Yangtze River to Lake Tai via the Wangyu River in an attempt to improve water quality in the lake. Additional diversions from the Yangtze to Meiliang Bay in the northwest of Lake Tai have been added or are planned to supplement the initial diversion (Li, Tang et al. 2013).

The Taipu River is the main discharge from Lake Tai, which then flows to the Huangpu River. The Huangpu River is the largest of Shanghai's local rivers and until 2011, it was the primary source of Shanghai's municipal water supply (Ward and Liang 1995, Bai, Zhang et al. 2006, Webber, Barnett et al. 2018). The Huangpu River is 113.4 km long, has a mean annual discharge of 319 m^3/s and an annual runoff volume of approximately 10.06 billion m^3 (Liu 2007, Shanghai Municipal People's Government 2010). The first municipal drinking water treatment plant in Shanghai (and China) was constructed at Yangshupu (in central Shanghai) by foreign concession holders in 1881 and withdrew water from the Huangpu River at its confluence with Suzhou Creek (Ward and Liang 1995, Shanghai Municipal People's Government 2010, Webber, Barnett et al. 2018).

Historically, water quality in Shanghai has been a significant concern for officials and residents (Ward and Liang 1995). Water quality issues in the Huangpu River have resulted from the large quantities of urban, industrial, and agricultural waste it receives. Water in the Huangpu River is characterised by high turbidity and high concentrations of organic matter and ammonia (Bai, Zhang et al. 2006, Song, An et al. 2010). High pollutant concentrations limit the Huangpu River's capacity for natural purification and as much as 70% of pollution is reported to be not effectively removed using conventional water treatment systems consisting of flocculation, sedimentation and sand filtration (Bai, Zhang et al. 2006, Song, An et al. 2010). High turbidity and concentrations of organic matter can also interfere with effective disinfection or cause disinfection by-products to occur (World Health Organization 2017). The Huangpu River is also heavy utilised for purposes other than raw drinking water, and any sudden water pollution accidents can have a severe effect on water supply as well as induce public panic. Examples include more than 52 t of petrochemical oil spilled in the River in January 2012, and 16,000 diseased pig carcasses found in the river in the following March (Yang and Kelly 2015).

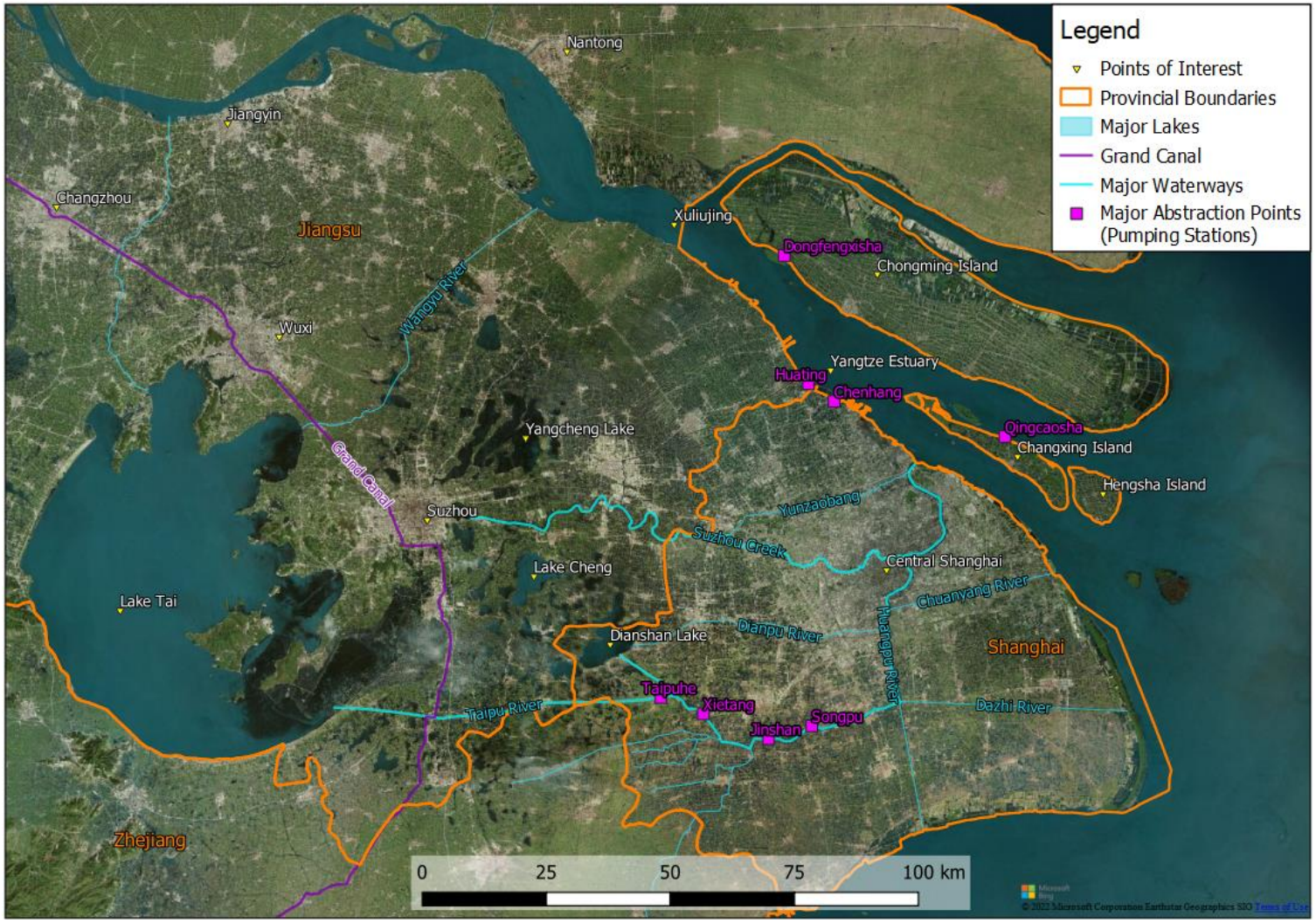

Figure 2-3: Shanghai's Local Water Resources and Major Abstraction Points. Aerial Photo source from Bing Aerial, Microsoft Corporation Earthstar Geographics SIO (2022). Boundaries were extracted from the GADM database (www.gadm.org), version 2.8. Water Resources were mapped from aerial photography.

Efforts to move the locations of water supply intakes along the Huangpu River from areas within central Shanghai upstream towards Dianshan Lake and the Taipu River have been occurring as early as the 1980's in an attempt to improve the quality of Shanghai's water supply by avoiding the most polluted areas closer to the city centre (Ward and Liang 1995, Finlayson, Barnett et al. 2012, Webber, Barnett et al. 2018). The upper extent of the Huangpu River is Dianshan Lake which is the furthest upstream raw water intakes can be moved to capture good quality water due to the municipal/provincial boundaries between Shanghai and Jiangsu. The area between the north of Dianshan Lake and Lake Tai is entirely within Jiangsu Province. Despite these attempts to relocate intakes, as well as other actions to remediate the problem, problems arising from poor water quality in the Huangpu river have not been resolved (Ward and Liang 1995, Webber, Barnett et al. 2018). This is mainly due to increasing pollution in upstream water sources, for example Dianshan Lake is now heavily utilised for tourism, retirement villages, sports facilities and more; the water discharge from nearby developments has resulted in some eutrophication of the lake (Ward and Liang 1995, Wang, Yuan et al. 2014). Similarly, inflow originating from Lake Tai is also of poor quality, with the main sources of pollution being municipal and industrial wastes, fertilisers and pesticides, as well as aquaculture and animal husbandry wastes (Li, Mander et al. 2009, Finlayson, Barnett et al. 2012). In particular, Lake Tai's nutrient loading from urban, agricultural, and industrial runoff can have significant effects on water quality, like in 2007 when a large algal bloom suddenly polluted 70% of local water supplies for Wuxi City, affecting water supply for more than 2 million people (Jiang 2009, Li, Mander et al. 2009).

In addition to pollution induced issues, both Jiangsu and Zhenjiang provinces also draw large quantities of water from Lake Tai, with the result being that the system is already over-committed as a water resource (Finlayson, Barnett et al. 2012). Pollution in Taihu and the extraction of its water are controlled by the Taihu Basin Administration Bureau, directly under the control of the State Council not the Shanghai Municipal Government, and as such Shanghai has little control over available water coming from Lake Tai or its quality (Finlayson, Barnett et al. 2012, Webber, Barnet et al. 2015, Webber, Barnett et al. 2018).

Groundwater was previously used as an alternative water source, supplementing surface water supplies. This practice was discontinued in the 1960's due to the significant subsidence that resulted from over-exploitation of the groundwater resource (Ward and Liang 1995). During the period of extreme groundwater exploitation (between 1920 and the mid-1960's) around 0.2 billion m^3/a was withdrawn from the groundwater resource, resulting in average annual subsidence rates of 40 mm and with total subsidence amounting to several meters; this is a significant issue considering that the majority of Shanghai is an average of around 4 m above sea level (Jiang 2009, Li, Finlayson et al. 2017, Webber, Barnett et al. 2018). The natural recharge rate of groundwater was insufficient to maintain the hydrological balance and artificial recharge using local tap water was required to slow subsidence rates to around 2 mm/a (Ward and Liang 1995, Finlayson, Barnett et al. 2012, Shi, Jiang et al. 2016, Li, Finlayson et al. 2017). The current water supply from

ground water is around 10 million m^3/a, and the recharge rate (including artificial recharge) is between 2-10 million m^3/a (Finlayson, Barnett et al. 2012, Webber, Barnett et al. 2018). Groundwater use is now controlled by strict local legislation to prevent further subsidence in Shanghai, however some households in suburban areas and some farmers still use groundwater wells (Cheng, Chen et al. 2018, Webber, Barnett et al. 2018).

Supplementary sources of water such as harvesting rainwater and water recycling are presently not being considered by the Municipal Government having previously been ignored or not pursued in any serious way (Webber, Barnet et al. 2015, Webber, Barnett et al. 2018). In part, this is due to the politics of water resources management in China, where as a legacy of the planned economy, water resource policies and management are largely supply-driven, engineering-based, single-sector solutions that often only involve a single stakeholder (Cheng and Hu 2011). As a result, in Shanghai, like many other Chinese cities, capital intensive centralised solutions dominate the water management sector at the expense of more local and distributed options (Webber, Barnet et al. 2015, Webber, Barnett et al. 2018). For the application of stormwater harvesting and storage, and wastewater recycling, there are also practical reasons why they have not been implemented in Shanghai.

Urban rainwater harvesting in large cities is thought to be an effective method of resolving water shortages, however despite this, uptake of rainwater harvesting systems in China is still relatively low (Webber, Barnett et al. 2018). In Beijing, which is considered a pioneer of rainwater collection in large cities, despite the relatively high benefit to cost ratio, less than 1% of annual rainfall in the city is captured for use (Webber, Barnett et al. 2018). The primary issues behind this low uptake of stormwater harvesting are firstly the difficulties of implementing storage systems in high density cities where most of the population live in apartment towers (household scale tanks are generally inappropriate and large underground tanks are considered to be expensive) and secondly Chinese water supply bureaucracies are ill-equipped to manage small decentralised systems of water supply (Webber, Barnet et al. 2015). There is approximately 7-8 billion m^3/a of local precipitation in Shanghai that is currently not used to supply residents (Webber, Barnett et al. 2018). A benefit cost analysis conducted by Jing, Zhang et al. (2017) into assessing the economic viability of rainwater harvesting systems in China found that the application of rainwater harvesting systems for the irrigation of public spaces in humid and semi-humid climates such as Shanghai is not economically viable. This study did however find that the use of rainwater harvesting for toilet flushing or toilet flushing combined with lawn irrigation was a promising option for Shanghai especially when small scale systems (5–30 m^3) were used. If Shanghai were to adopt rainwater harvesting, it is likely to be only applied at small scales, and difficulties with overcoming the implementation and management of small, distributed storages would need to be overcome.

Municipal wastewater recycling in China is still in its infancy with further developments limited

by the cost of advanced treatment (Cheng and Hu 2011). While water recycling is an effective means of coping with water shortage, the primary issue for water supply in Shanghai at this stage is not a shortage of water, but a shortage of water with sufficient quality for municipal supply. Considering the relatively good quality of water from the Yangtze River, it is likely that water recycling would require the same or greater investment in water treatment as supply from the Yangtze Estuary (Webber, Barnett et al. 2018).

The Yangtze River is the only other significant freshwater resource near Shanghai. With a mean annual discharge of around 900 billion m^3 of water, the volume of available water is significantly larger than any other alternative available for Shanghai's use; nearly 90 times more than that of the Huangpu River and 4500 times more than peak groundwater extraction (pre-1960s). However, sourcing water from the Yangtze is not without its difficulties. At present there is not integrated water sharing plan for water in the Yangtze River, with all rights to the water in the Yangtze River are held by the Changjiang Water Resources Commission directly under the authority of the Ministry of Water Resources. The Water Resources Commission is planning to distribute those rights to provinces and municipalities along the river but only at points where the river is within the province (Webber, Barnet et al. 2015). As a result, Shanghai only has access to the water from the Yangtze Estuary in locations that fall within its municipal boundary, which roughly corresponds to the last 100 km before it meets the East China Sea. This area is affected by regular salt water intrusions that can affect the entire area where Shanghai has access and is affected by pollution sources both originating locally and in the Yangtze River Basin (Chen, Webber et al. 2013). The Yangtze, its catchment and key water quality parameters are discussed further in **Section 2.2** and **Chapter 3**.

2.2 The Yangtze River and its Estuary

The Yangtze River (**Figure 2-4**) is the third longest river on Earth with a length of 6300 km stretching from the Qinghai-Tibet Plateau to the East China Sea at Shanghai, draining a total catchment area of approximately 1,800,000 km^2 with a mean annual discharge of around 28,500 m^3/s (Zeng, Kundzewicz et al. 2012, Qiu and Zhu 2013, Wang, Xing et al. 2013, Webber, Barnett et al. 2018). The Yangtze River Basin can be divided into three main regions, the Upper Basin with an elevation of over 3000 m, the Middle Basin with an average elevation of 1000 m and the Lower Basin with an average elevation of 100 m (Wang, Xing et al. 2013). The Yangtze River main stem passes through seven provinces and municipalities. Its tributaries collect water from an additional twelve provinces. The Yangtze River Basin has nine major tributaries as shown in **Figure 2-5**; key data about these tributaries is presented in **Table 2-1**. The Jinsha River, the Tongtian River and the Dam Chu are considered to be a part of the Yangtze River's main stem.

Table 2-1: Key information on the Yangtze River's Major Tributaries. Adapted from Liu, Zhang et al. (2003) and Shen and Liu (2009).

Tributary	Length (km)	Catchment Area (1000 km^2)	Annual Average Discharge (m^3/s)	Sediment Load (million t/a)
Yalong Jiang	1,810	128.4	1,810	27.5
Min Jiang (incl. Dadu He)	735	133.0	2,840	50.2
Tuo Jiang	702	27.9	402.7	12.4
Jialing Jiang	1,120	160.0	2,120	145.0
Wu Jiang	1,037	87.9	1,650	32.4
Han Jiang (incl. Dan Jiang)	1,557	159.0	1,710	124
Yuan Jiang	1033	89.2	2,115	15.2
Xiang Jiang	856	94.7	2,406	11.6
Gan Jiang (incl. Mei Jiang)	744	80.9	2,105.5	11.2

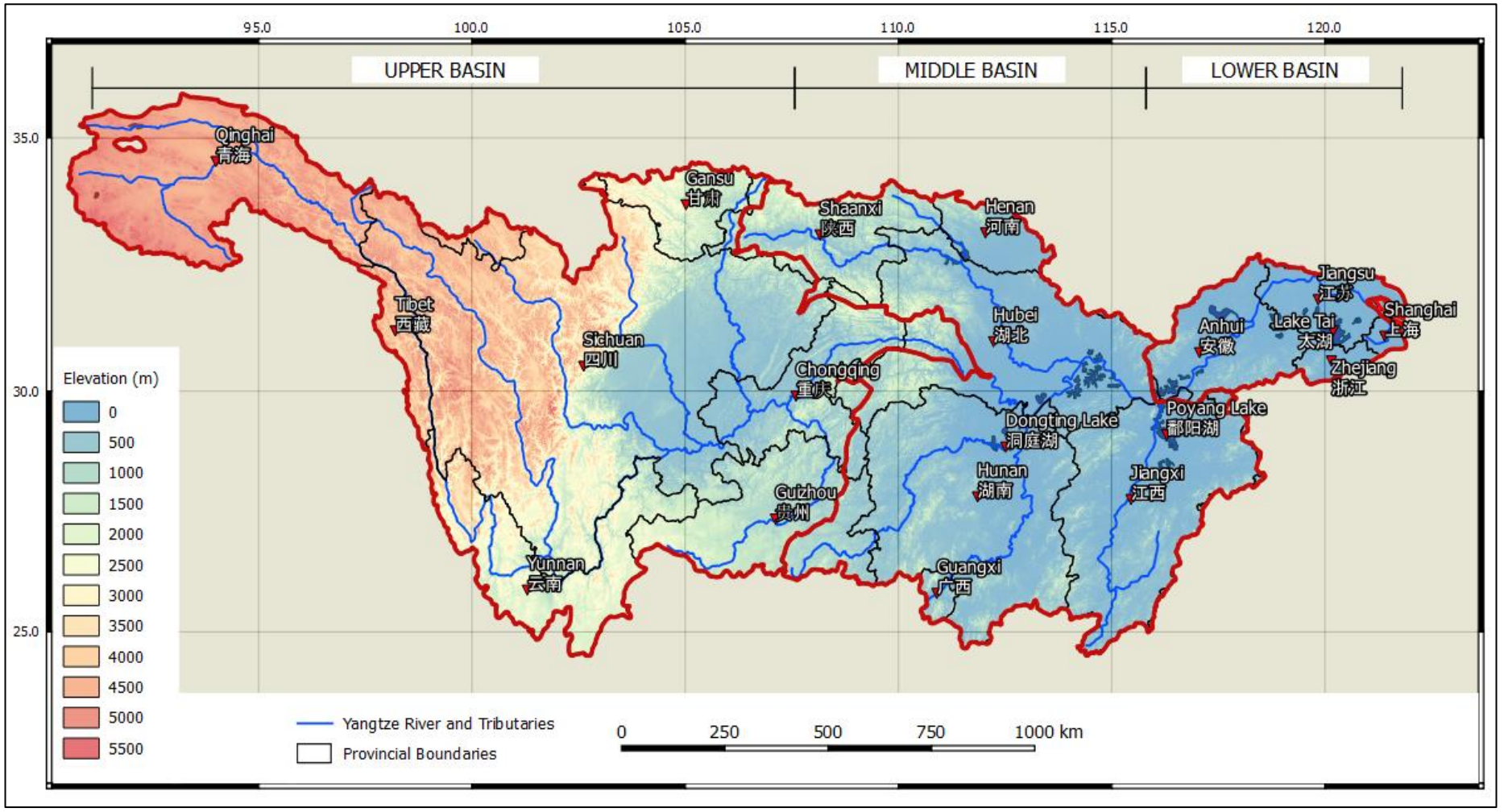

Figure 2-4: The Yangtze River Basin. Digital elevation data sourced from Robinson, Regetz et al. (2014). Boundaries were extracted from the GADM database (www.gadm.org), version 2.8. Yangtze River Data from Crissman and Berman (2012)

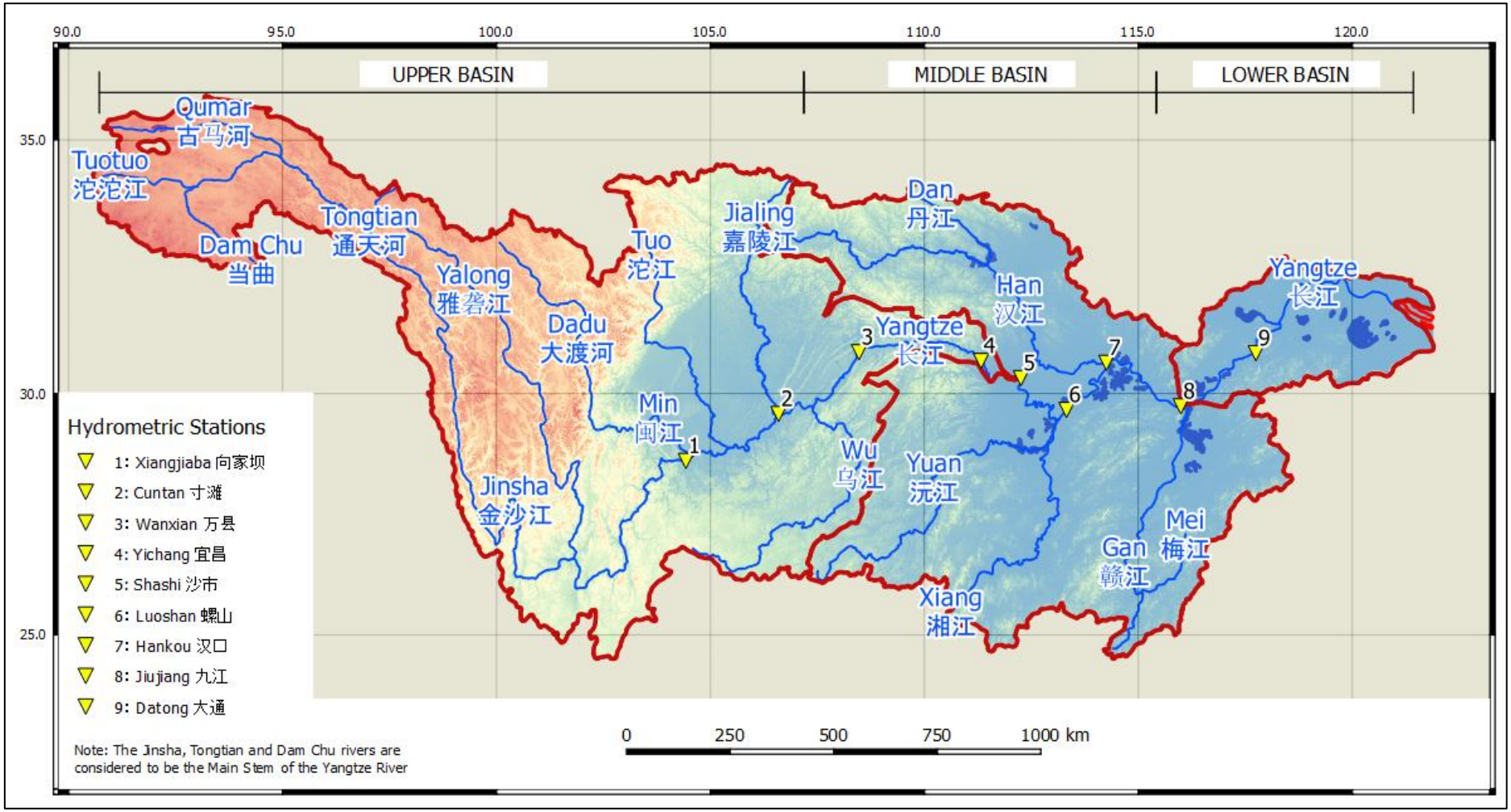

Figure 2-5: Tributaries of the Yangtze River and Key Hydrometric Stations. Digital elevation data sourced from Robinson, Regetz et al. (2014). Boundaries were extracted from the GADM database (www.gadm.org), version 2.8. Yangtze River Data from Crissman and Berman (2012)

The Lower Yangtze River is the reach of the river that passes through the Yangtze River Delta Region and is subject to tidal effects (**Figure 2-2**). This reach of the river is approximately 600 km long, beginning roughly between Datong Town in Anhui Province, before passing through Jiangsu Province and finally discharging to the East China Sea though the Yangtze Estuary, adjacent to Shanghai Municipality.

The Yangtze Estuary (**Figure 2-6**) is 90 km at its widest point where it meets the ocean (Zhang, Savenije et al. 2011). It is a third order bifurcation estuary with the first bifurcation located at the tip of Chongming Island where it divides into the North and South Branches. The second bifurcation occurs at Changxing Island where the south branch divides into the south and north channels and the final bifurcation is located at Jiuduansha island which separates the North and South Passages (Zhang, Savenije et al. 2011, Qiu and Zhu 2013, Wan, Gu et al. 2014, Yang, Deng et al. 2015). The Yangtze Estuary experiences a mean and maximum tidal range of 2.67 m and 4.62 m respectively, and an irregular semi-diurnal character with an average flood and ebb duration of 5 h and 7.4 h respectively (Zhang, Savenije et al. 2011, Qiu and Zhu 2013).

Figure 2-6: The Yangtze River Estuary. Satellite photo sourced from Google Satellite Imagery - Google Terrametrics (2017)

2.2.1 Climate and Streamflow

Sources of streamflow in the Yangtze River include both precipitation and glacial melting in the upper basin. There are 1,332 glaciers in the upper basin of the Yangtze with a total area of 1,894.98 km^2 and total ice volume of 147.52 km^3. While these glaciers are melting (which is expected to accelerate due to climate change), the total volume of meltwater is less than 1% of the annual flow of the Yangtze River and as such, glacial melting is not a significant contributor to annual runoff in the Yangtze River (Finlayson, Barnett et al. 2012, Chen, Webber et al. 2013).

The Yangtze River Basin is subject to an annual monsoon season where warm moist air from the south meets cold dry air from the north, causing heavy rainfall over the entire basin. Most of the basin is subject to this monsoon climate, with both the southwest monsoon and southeast monsoon having an effect on climate, however precipitation is mainly influenced by the southeast monsoon (Zeng, Kundzewicz et al. 2012, Wang, Xing et al. 2013). Mean annual rainfall ranges between 270 and 500 mm in the western regions, and 1600 and 1900 mm in the east, with 70-80% of this precipitation falling between the wet season between May and October (Wang, Xing et al. 2013). Mean monthly rainfall for 1970-2000 is presented in **Figure 2-7**. The majority of rain falls within the middle basin above the southern tributaries between March and June, with a rainfall peak occurring in the upper basin between July and September. October to February is typically dry across the entire basin.

Differences in precipitation from year to year in the Yangtze catchment are small. The coefficient of variation of annual precipitation for the basin as a whole was 0.066 for the period of 1955-2011 (Webber, Barnett et al. 2018). The high precipitation across the whole Yangtze catchment combined with relatively low average annual temperatures produces a high runoff ratio (close to 50%) with very low inter-annual variability. In this regard, the Yangtze behaves more like the rivers in the equatorial tropics (e.g. the Amazon, Parana, Congo Rivers) that other sub-tropical rivers (Webber, Barnett et al. 2018). Over the long term, the climate in the Yangtze Basin follows a 25-28 year cycle between hotter and colder periods, which is potentially driven by changes in solar radiation, resulting in a 22.2 year cycle between flood and dry periods that follows this change temperature change; catastrophic floods and droughts are usually the result of abrupt temperature change (Zhang, Gemmer et al. 2008, Zhang, Savenije et al. 2012).

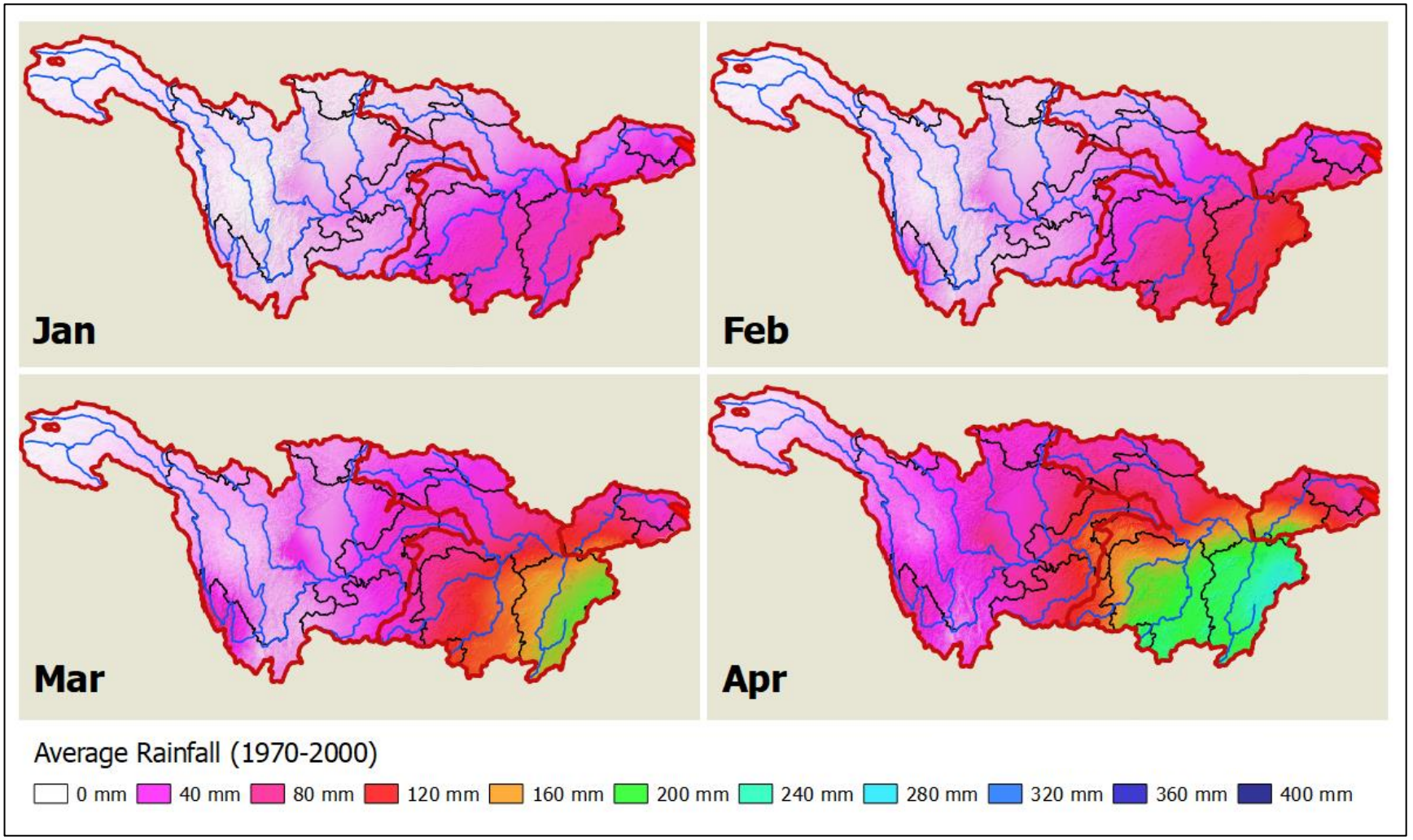

Figure 2-7: Average Monthly Rainfall in the Yangtze Basin (1970-2000). Rainfall data sourced from Fick and Hijmans (2017) accessible from http://worldclim.org. Boundaries were extracted from the GADM database (www.gadm.org), version 2.8. Yangtze River Data from Crissman and Berman (2012).

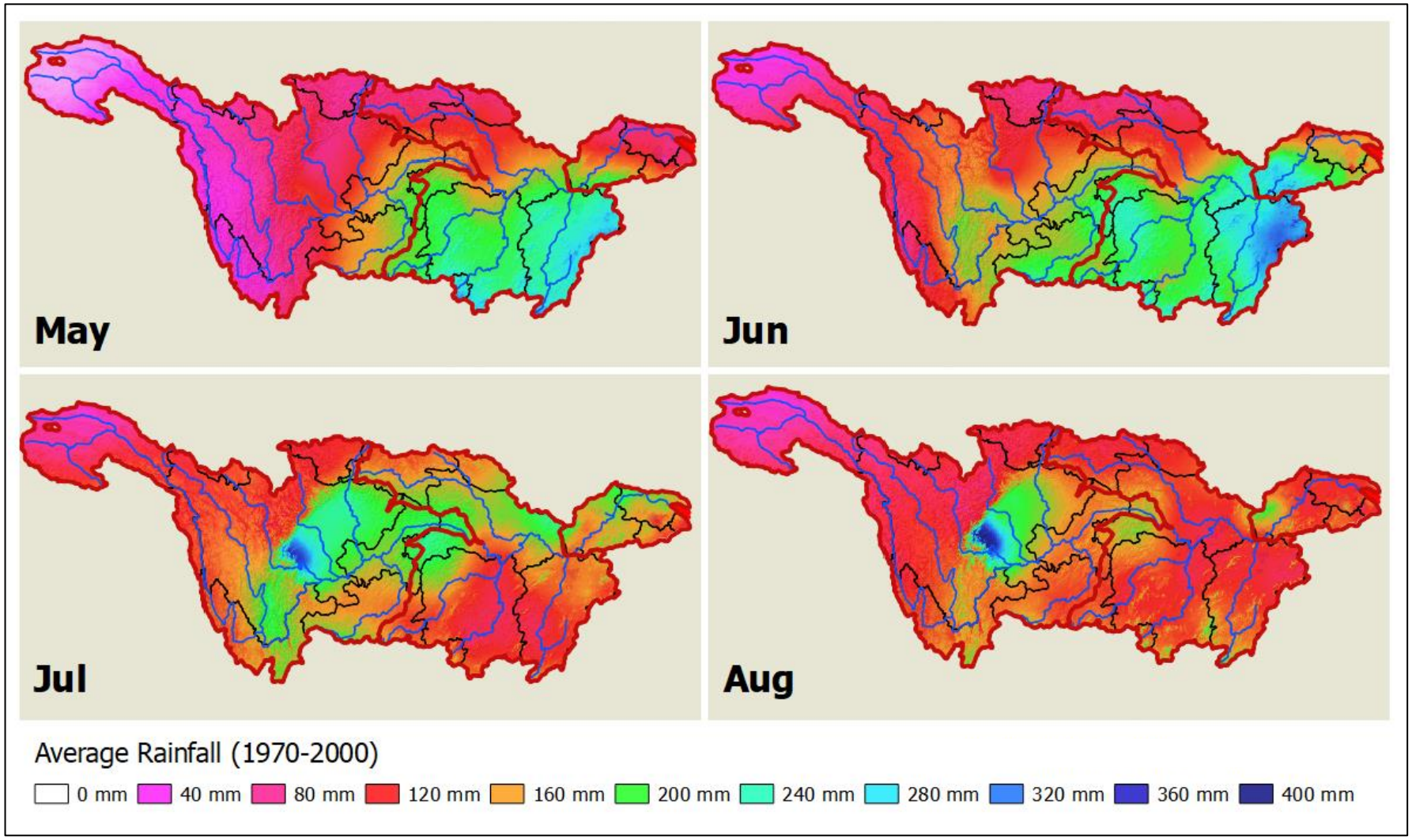

Figure 2-7 (continued): Average Monthly Rainfall in the Yangtze Basin (1970-2000). Rainfall data sourced from Fick and Hijmans (2017) accessible from http://worldclim.org. Boundaries were extracted from the GADM database (www.gadm.org), version 2.8. Yangtze River Data from Crissman and Berman (2012).

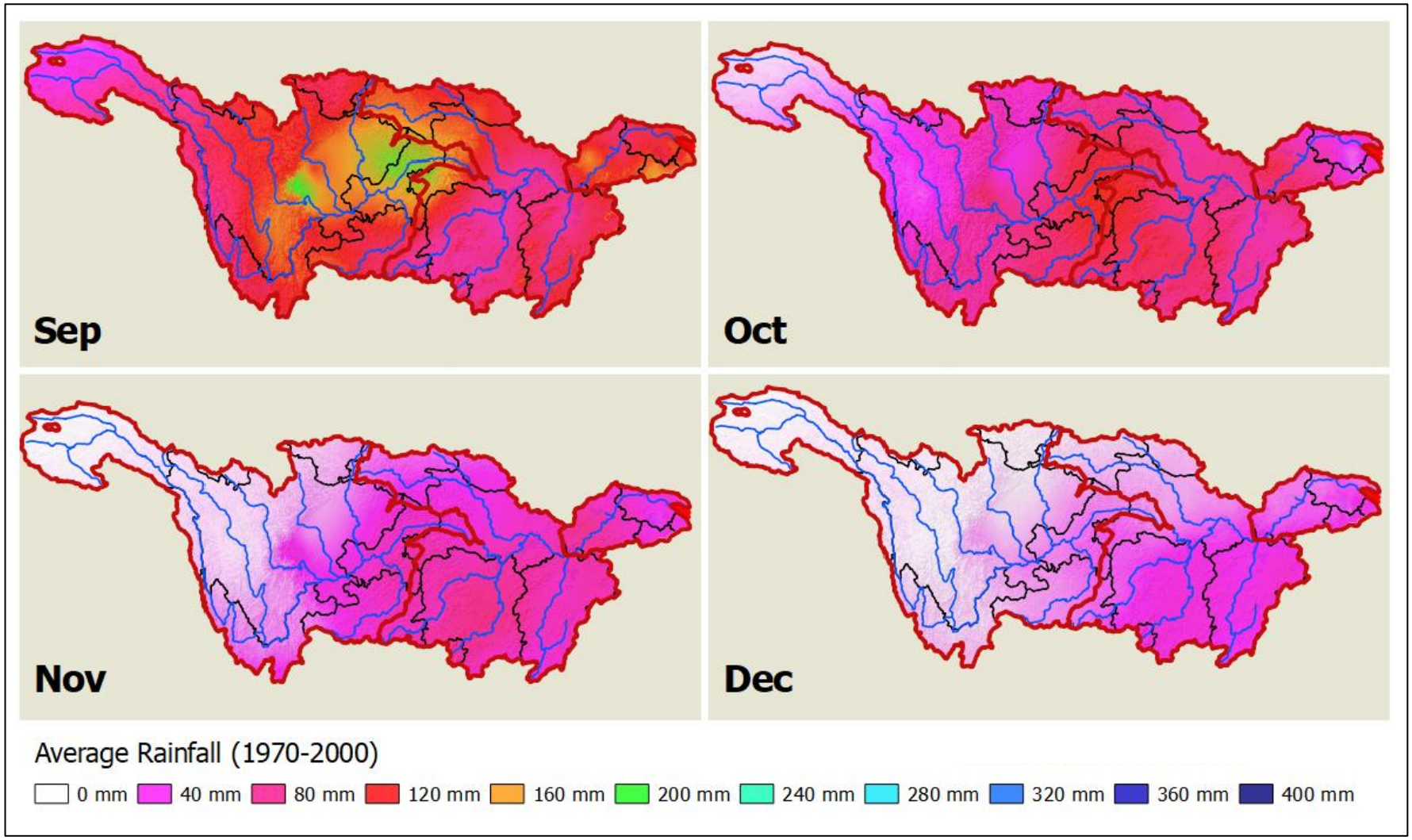

Figure 2-7 (continued): Average Monthly Rainfall in the Yangtze Basin (1970-2000). Rainfall data sourced from Fick and Hijmans (2017) accessible from http://worldclim.org. Boundaries were extracted from the GADM database (www.gadm.org), version 2.8. Yangtze River Data from Crissman and Berman (2012).

From 1960, annual temperatures have been increasing in the Yangtze Basin, however annual runoff over this time period has shown no significant change; this has been accompanied by an increasing population and level of economic development (Finlayson, Barnett et al. 2012). There has however been a significant change in the distribution of precipitation and discharge within annual cycles during the past 50 years. Statistically significant increases have been observed in January, March, June and July, and decreases in April, May, September and December. The increase in summer and winter and decrease in spring and autumn is reflected in runoff. The changes in precipitation have been ascribed to changes in the monsoon pattern, which is driven by temperature change over the East China Sea (Finlayson, Barnett et al. 2012, Zeng, Kundzewicz et al. 2012). Climate Change is expected to cause further uneven distributions of rainfall and based on the predictions of the Intergovernmental Panel on Climate Change (IPCC) for the middle of the 21st century, the Yangtze River discharge is predicted to increase in early and mid-summer due to increased precipitation in the preceding months and decrease in the late summer and autumn due to the early cessation of the monsoon and increased evaporation (Finlayson, Barnett et al. 2012, Wang, Xing et al. 2013, Webber, Barnett et al. 2018).

Streamflow measurements for the Lower Yangtze River and Estuary used in most research relies on data from Datong Hydrometric Station. Datong Hydrometric Station is located in Datong Town, Anhui, at the upper limit of tidal influence in the Yangtze River (Refer **Figure 2-4** and **Figure 2-5**). At just over 600 km from the mouth of the Estuary, it is the farthest downstream permanent hydrometric station with long term records. Due to the tidal nature of the reach of river below this point, discharge is more complicated to observe (Zhang, Savenije et al. 2012). The basin above Datong comprises of approximately 94% of the Yangtze River Basin's total area and is therefore responsible for the vast majority of its rainfall. The Yangtze River Delta accounts for the remaining 6% of land area contributing runoff to the estuary (Dai, Chu et al. 2011, Chen, Webber et al. 2013). The travel time of water in the river from Datong to the Estuary at Xuliujing is approximately 7 days (Zhang, Savenije et al. 2012).

Using the streamflow at Datong as the discharge of the Yangtze River to its mouth, the average discharge of the Yangtze River would be approximately 28,500 m^3/s (Zeng, Kundzewicz et al. 2012, Qiu and Zhu 2013, Wang, Xing et al. 2013). The variation in annual average flows from 1950 to 2010 at Datong Station are summarised in **Figure 2-8** with error bars representing the monthly minimum and maximum streamflow. The minimum monthly discharge at Datong was 6,730 m^3/s and was observed in February 1963 and the daily minimum discharge at the estuary was 4,620 m^3/s observed on the 31st of January in 1979 (Zhang, Savenije et al. 2011). The maximum monthly discharge at the estuary was 84,200 m^3/s observed in August 1954 and the maximum daily discharge at the estuary was 92,600 m^3/s and was observed on the 1st of August 1954 (Zhang, Savenije et al. 2012). Like precipitation in the basin, discharge from the Yangtze River has low inter-annual variability; compared to rivers in similar climate zones, the discharge of the Yangtze River is very stable delivering predictable flows to the estuary (Finlayson, Barnett

et al. 2012, Webber, Barnett et al. 2018). Despite this relative stability, major floods, such as the 1998 flood and major droughts like the ones that occurred in 2006 and 2011 may become more common possibly in relation to global warming (Wang, Xing et al. 2013).

Flow in the Yangtze River displays an annual cycle peaking in summer with flows averaging about five times higher than those in winter which can be observed in **Figure 2-9**. As highlighted in the previous section, streamflow in the river is predominantly driven by surface runoff, without much groundwater or snowmelt contribution, and as a result the monthly distribution of streamflow matches that of precipitation. In general, the streamflow peak is one month behind that of rainfall, which is to be expected, however it is interesting to note that the peak average flow for extreme flood years appears to be one month behind that of the average year occurring in August instead of July. **Figure 2-9** also shows that there is a large amount of variability in monthly flow from year to year, however on average the driest month is January and the wettest is July.

The data in **Figure 2-8** is divided into three time periods representing years prior to the first major dam crossing the mainstem of the Yangtze River, the Gezhou Dam (GZD), the years between the construction of the Gezhou Dam and the second major dam crossing the mainstem of the river, the Three Gorges Dam (TGD), and the period after the Three Gorges Dam. There is a drop in average annual streamflow after the closure of the Three Gorges Dam, however, this has been demonstrated to be the result of a wet rainfall period preceding the damming and a dry period including several very low rainfall years following it (Yang, Xu et al. 2015). Dry season minimum monthly streamflow at Datong between 1950 and 2015 is presented in **Figure 2-10**. Average minimum monthly streamflow has been divided into the same three time periods as **Figure 2-8**. Before the 1980's (pre Gezhou Dam) the average minimum monthly streamflow in the dry season was approximately 9,700 m^3/s while after the closure of the Three Gorges Dam, the average minimum monthly streamflow in the dry season increased to around 11,700 m^3/s, which represents an approximate 20% increase in average minimum flow. This effect indicates that the Three Gorges Dam has resulted in an observable increase in minimum monthly flows during the dry season. The effects of dams and diversions on flow in the Yangtze River is discussed further in **Section 2.2.2**.

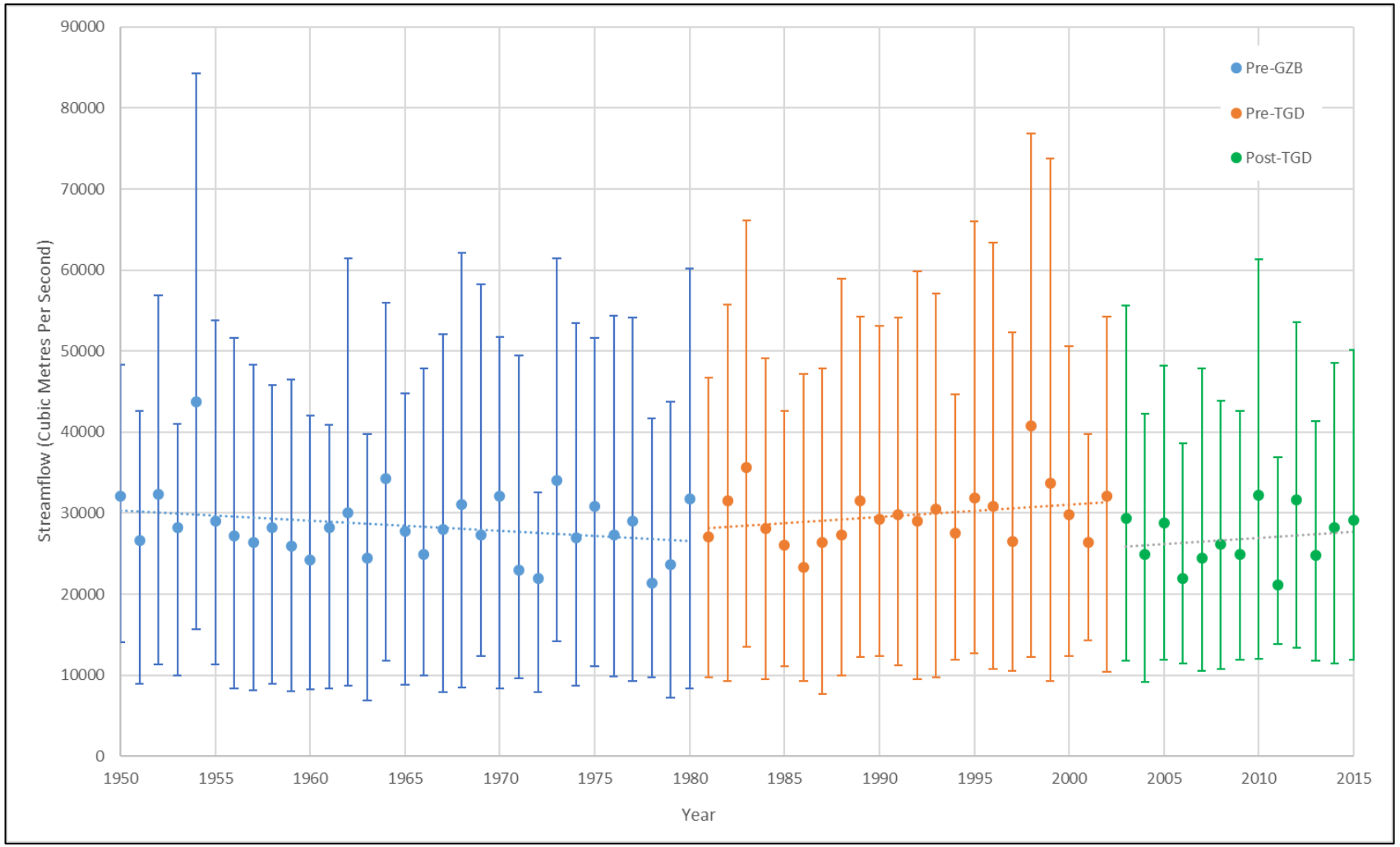

Figure 2-8: Average Annual Streamflow at Datong Station (1950 – 2015). Streamflow data from Changjiang Water Resources Commission, digitised from Gao, Li et al. (2012). Colours represent time periods divided by the commencement of operation of Gezhou Dam (GZB) and the Three Gorges Dam (TGD). Dotted lines represent lines of best fit in each time period.

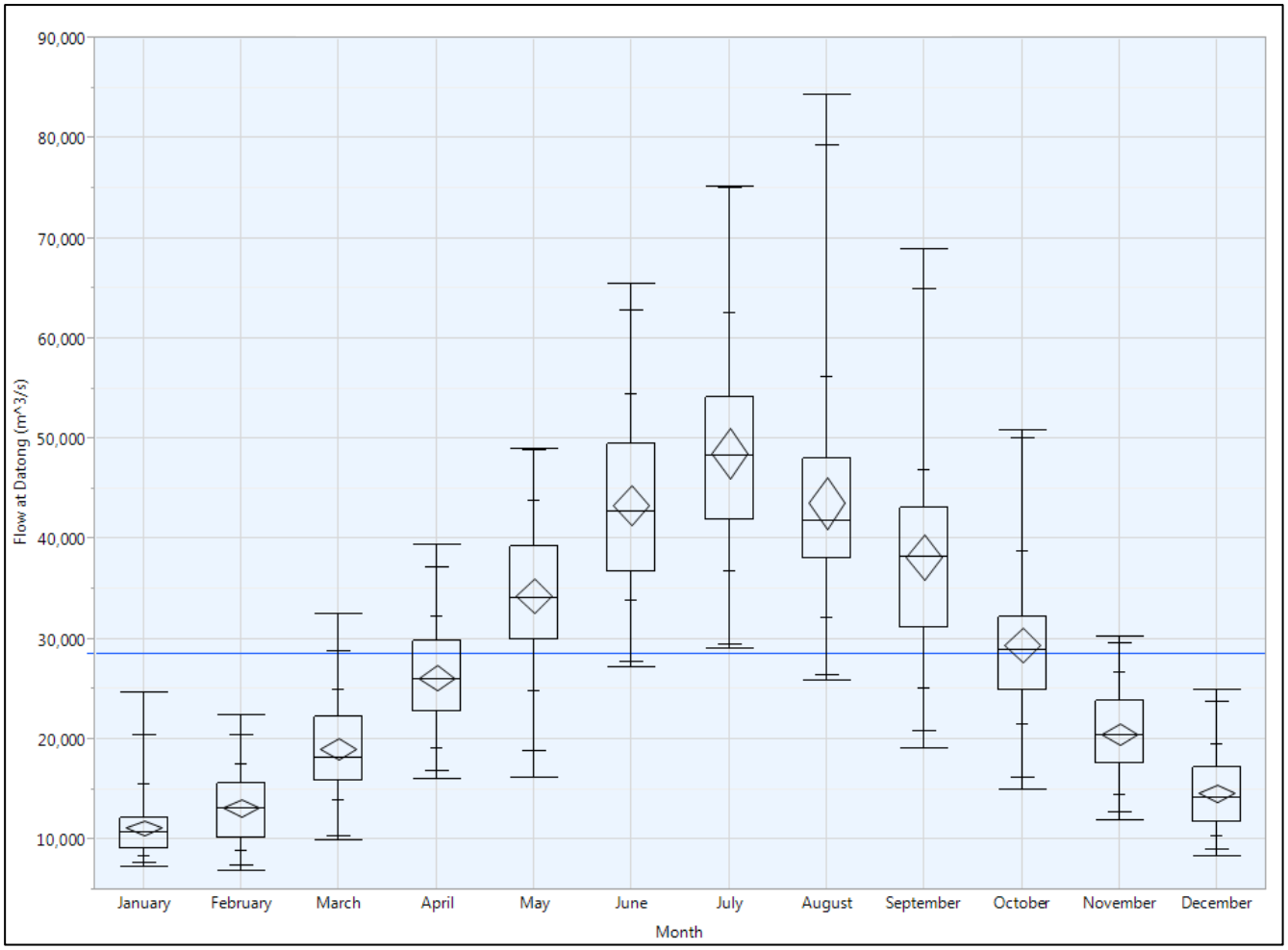

Figure 2-9: Average Monthly flow at Datong Station (1950 – 2015). Streamflow data from Changjiang Water Resources Commission, digitised from Gao, Li et al. (2012). Diamonds represent an estimation of the mean with 95% confidence intervals. The quantiles on the box plots represent the 0th, 5th, 10th, 25th, 50th, 75th, 90th, 95th and 100th quantiles. Blue line represents annual average flow of approximately 28,500 m^3/s.

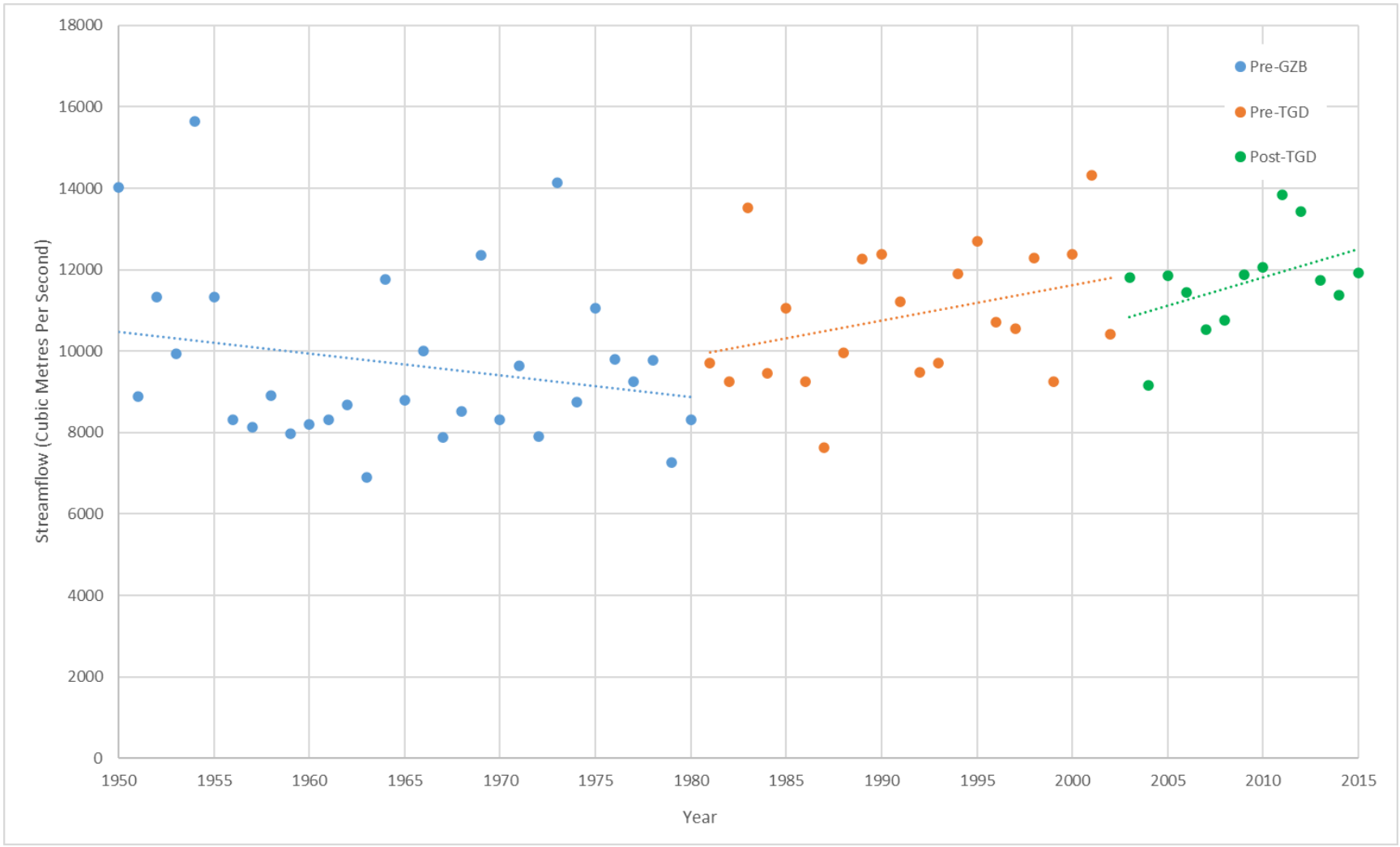

Figure 2-10: Minimum Monthly Streamflow at Datong Station (1950 – 2015). Streamflow data from Changjiang Water Resources Commission, digitised from Gao, Li et al. (2012). Colours represent time periods divided by the commencement of operation of Gezhou Dam (GZB) and the Three Gorges Dam (TGD). Dotted lines represent lines of best fit in each time period

2.2.2 People and Land Use in the Yangtze River Basin

The Yangtze River Basin is of critical importance to the Chinese people being the home of over 440 million people; the region plays a vital role in the economic development and ecological environmental conservation of China (Zhang, Xu et al. 2009, Yang, Milliman et al. 2011). The Yangtze River basin encompasses approximately 24% of China's arable land, provides 32% of the national gross output for agriculture, 34.5% of national gross output for industry and accounts for around 40% of China's freshwater resources, more than 70% of the Country's rice production, 50% of its grain and more than 70% of its fishery production (Wang, Wang et al. 2013) (Wong, Williams et al. 2007). Within the basin there are seventeen provinces and two major municipalities. The population centres of these administrative divisions are concentrated along the main stem of the river, around the lakes and tributaries of the middle basin, and in the Sichuan Basin (in the upper basin). Key data on the administrative divisions is presented in **Table 2-2** and spatial distribution of population can be observed in **Figure 2-11**. A significant proportion of land around these areas has been cultivated, while the dominant land cover in the upper basin is grassland and the mountainous area between the upper and lower basin is mostly forested. Basin land use can be observed in **Figure 2-12**.

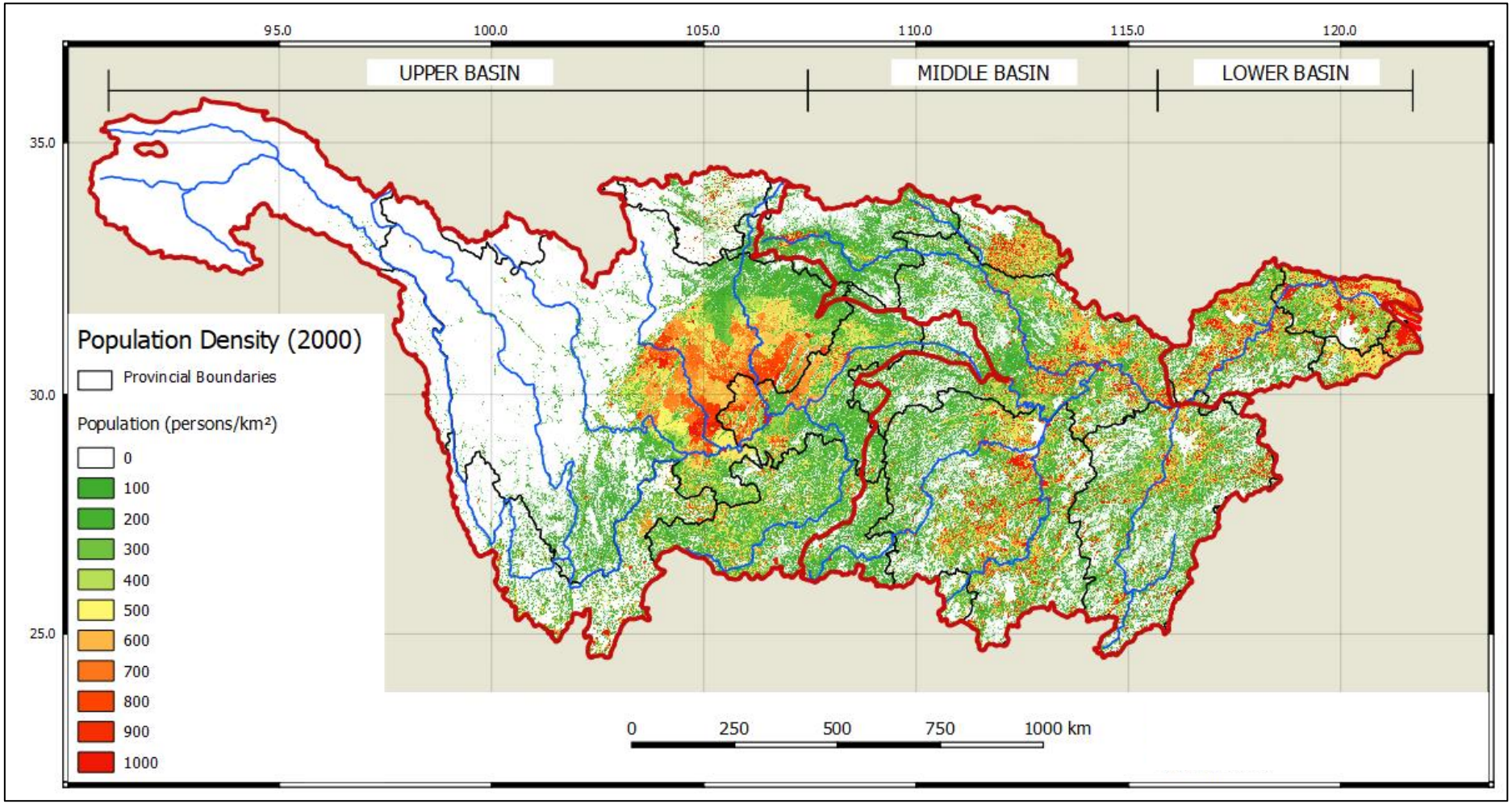

Figure 2-11: Population Density Distribution in the Yangtze River Basin. Population data from Wang, Chen et al. (2015), Boundaries were extracted from the GADM database (www.gadm.org), version 2.8. Yangtze River Data from Crissman and Berman (2012).

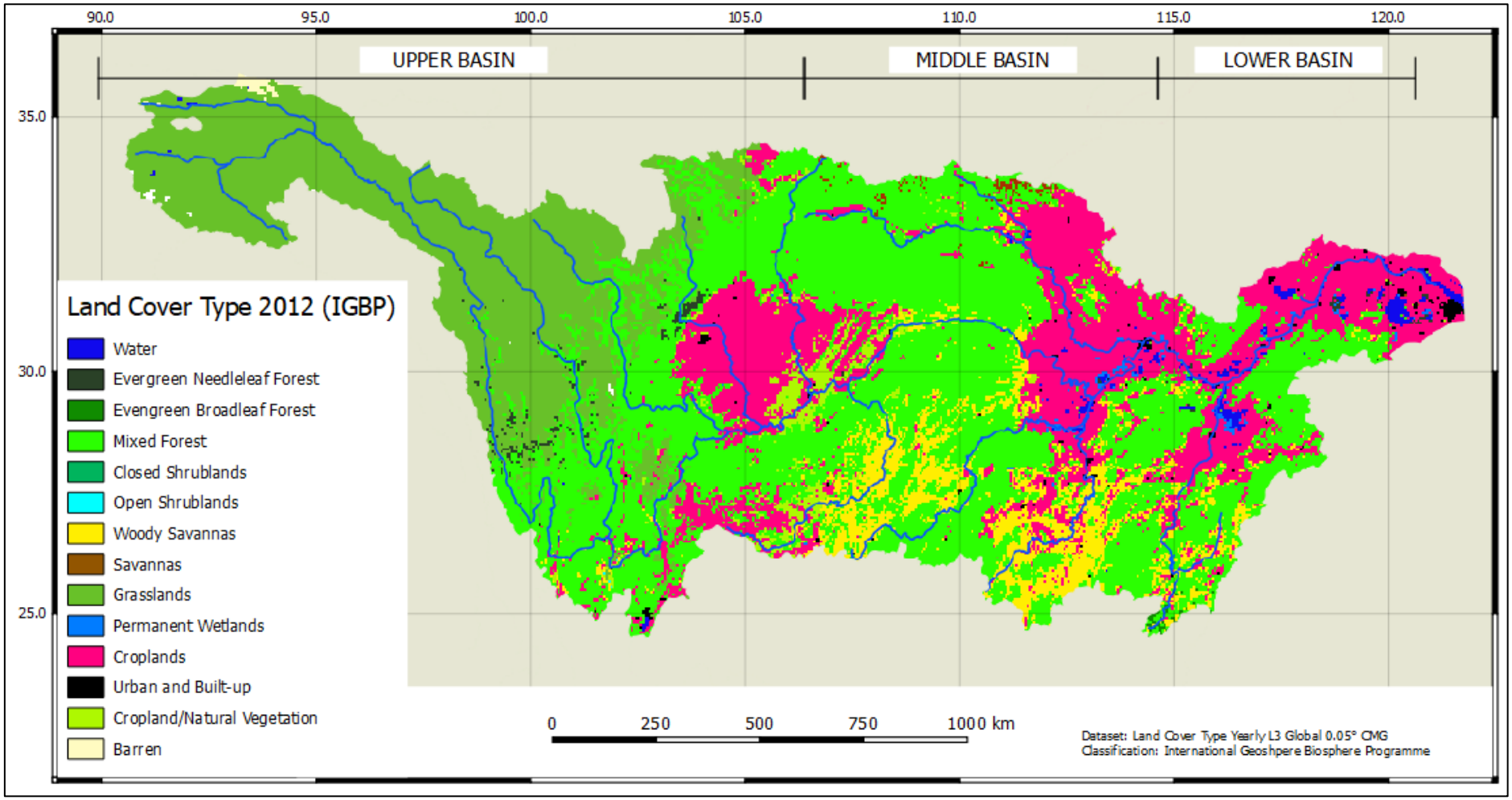

Figure 2-12: Land Use in the Yangtze Basin. Land use data from NASA LP DAAC (2015), Yangtze River Data from Crissman and Berman (2012).

Table 2-2: Key data on Provinces in the Yangtze Basin. Wang, Wang et al. (2007) and the NBS China (National Bureau of Statistics of China 2017); Provinces were ranked with locations along the main stem first (light blue), followed by those surrounding Poyang and Dongting Lakes (green) and finally provinces along tributaries (red).

Province/ Municipality	Province Area (1000 km^2)	Area Within Yangtze Basin (1000 km^2)	Area within the Yangtze Basin (%)	Population (Million People; 2014 census)	Urbanisation Level (%)
Shanghai	6.3	6.3	100.0	24.2	89.6
Jiangsu	102.6	39.9	38.9	79.6	65.2
Anhui	139.4	65.6	47.1	60.8	49.2
Hubei	185.9	185.9	100.0	58.2	55.7
Sichuan (+ Chongqing)	567.4	567.4	100.0	111.3	49.9
Qinghai	721.2	169.3	23.5	5.8	49.7
Jiangxi	163.2	163.2	100.0	45.4	50.2
Hunan	211.8	211.8	100.0	67.4	49.3
Guizhou	176.0	115.7	65.7	35.1	40.0
Henan	167.0	27.4	16.4	94.4	45.2
Yunnan	394.1	109.1	27.7	47.1	41.7
Shanxi	205.6	72.8	35.4	36.5	53.8
Zhejiang	101.8	12.2	12.0	55.1	64.9
Gansu	454.0	38.4	8.5	25.9	41.7
Guangxi	236.7	8.4	3.5	47.5	46.0
Fujian	121.4	1.0	0.8	38.1	61.8
Guangdong	177.9	0.3	0.2	107.2	68.0
Tibet	1200.0	29.2	2.4	3.2	25.8

Like many developing countries, industrialisation and economic growth in the China have been prioritised over environmental protection (Yin, Walcott et al. 2005). Increasing population and rapid economic development have led to the water quality degrading drastically due to the application of fertilisers, pesticides and discharge of industrial wastes (Wang, Webber et al. 2008, Song, Ji et al. 2010). In Shanghai municipality in particular, there has been significant urban development and other human activities over the last few decades to support a rapidly growing population and economic activities including manufacturing and shipping. These activities have significantly altered the local landscape and nearshore geomorphology; the pace and extent of these can be observed in **Figure 2-13**. With increasing urbanisation, the development of factories and harbours and increased shipping and transportation comes the increased potential for both point and non-point sources of water pollution that can find their way into the Yangtze Estuary via Shanghai's large network of streams or through wastewater outlets. Such practices can not only lead to nutrient enrichment, but also the addition of local heavy metals, potentially impacting the aquatic ecosystem and can be problematic for municipal water supply (Song, Ji et al. 2010).

Figure 2-13: Shanghai 1989-2019 (NASA Earth Observatory 2017)

36

Figure 2-13 (Continued): Shanghai 1989-2019 (NASA Earth Observatory 2017)

37

Additionally, there have been many projects in the Yangtze Estuary that have altered Shanghai's nearshore geomorphology including the North Branch Reclamation Project, the Hengsha Reclamation Project, The Pudong International Airport and Nanhui Siltation Reclamation Project and the Deepwater Navigation Channel Project (Refer **Figure 2-14**). These projects have been carried out for a variety of reasons including improving shipping, transportation and environmental protection, however they represent significant interventions in natural processes and have implications for hydrodynamic behaviour in the estuary, saline intrusion and local sea level rise (Wan, Gu et al. 2014, Cheng, Chen et al. 2018, Mei, Dai et al. 2018).

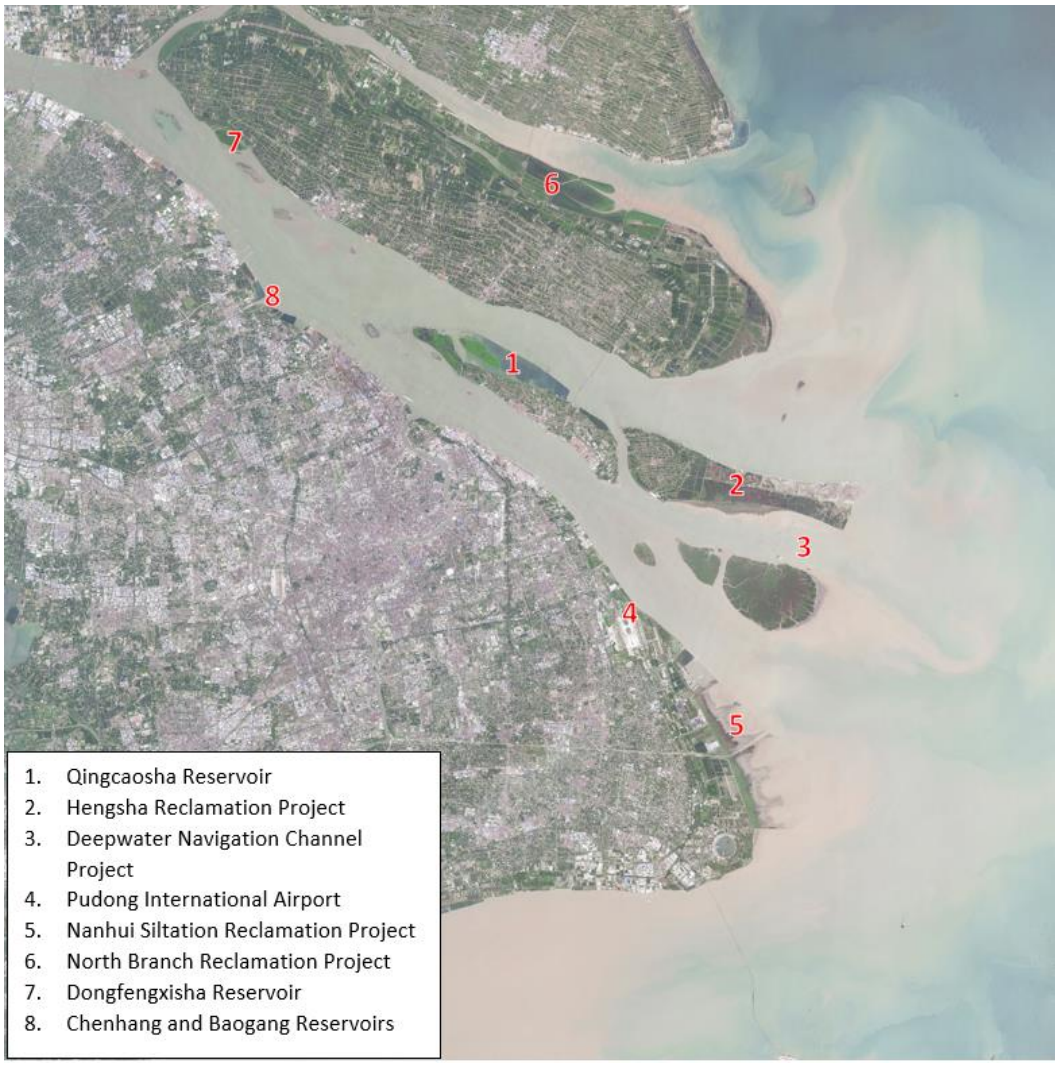

Figure 2-14: Location of Key Projects in Shanghai's Nearshore Zone. Photo was captured in 2019 (NASA Earth Observatory 2017)

Along with the urbanisation and economic development in the Yangtze River Basin, major infrastructure such as dams and diversion schemes have been implemented to provide water for cities, irrigation, and hydropower, or to improve the navigability of the Yangtze River for transportation. It is estimated that around 46,000 dams have been constructed within the Yangtze River Basin and are estimated to have a cumulative storage capacity of 230 billion m^3 (Finlayson, Barnett et al. 2012). Most of these dams were constructed after 1950, with the peak construction period falling between 1970 and 2000. As of 2002, there were 162 dams with a storage capacity of greater than 0.1 km^3; these dams account for nearly 155 km^3 cumulatively (Finlayson, Barnett et al. 2012). The spatial distribution of these dams can be observed in **Figure 2-15**.

The largest and most well-known dams on the Yangtze River are the Three Gorges Dam and the Gezhou Dam which are used for hydropower and to improve the navigability of the Yangtze River so that shipping can reliably reach Chongqing and the Sichuan Basin. The Gezhou Dam commenced operation in 1981 and was the first dam to cross the mainstem of the Yangtze River. The Three Gorges Dam, upstream of the Gezhou Dam was the second on the main stem of the Yangtze River and is now the largest dam in China and amongst the largest in the world. Filling of the Three Gorges Reservoir began in 2003 and full operation began in 2010. More large dams are planned for the Yangtze, with another five reservoirs, each as large as the Three Gorges Reservoir to be constructed in the upper basin along the Jinsha River and Jialing River(Dai and Lu 2014). By 2050, an additional 184 new large dams in the Yangtze catchment are expected to be constructed, with a total volume of 222.83 km^3 (Finlayson, Barnett et al. 2012).

Dams disrupt the continuity of flow and sediment regimes in rivers and the downstream impact of dams can include significant hydrological and geomorphological changes after impoundment (Luo, Yang et al. 2012, Dai, Fagherazzi et al. 2016). Through these disruptions to river regimes, dams can influence water quality in the estuaries of rivers in two main ways:

- The adjustment to the flow regime of the river can influence the pattern and intensity of saline intrusion into the estuary region (Qiu and Zhu 2013);
- The capture of sediment within the reservoir behind the dam can result in a change of deposition/erosion behaviour in the river downstream and the particle grading curves of suspended and deposited sediments (Luo, Yang et al. 2012, Dai, Fagherazzi et al. 2016). The amount, type and size of sediment transported in rivers has implications for the transport of nutrients to the estuary and water treatment operations (Dai and Lu 2014, Mines 2014, Dai, Fagherazzi et al. 2016)

Since 2003, frequent droughts in China, especially the spring drought of 2011, have caused public concern about the role of dams. Of all the dams in the Yangtze River Basin, the Three Gorges Dam has generated more concern and discussion than all the other dams in the catchment

combined, particularly around its effects on the hydrologic regime of the Yangtze River (Finlayson, Barnett et al. 2012). Subsequent analysis has shown that:

- The Three Gorges Dam and other dams in the basin have had no net effect on the total annual flow discharging from the Yangtze River (Finlayson, Barnett et al. 2012);
- The seasonality of the flows discharging from the Yangtze River has changed over time with significant increases in January, February and March (dry season) caused by the release of water for hydroelectricity generation, while significant decrease in the September to October discharge occurs as water is stored for later release (Chen, Webber et al. 2013, Qiu and Zhu 2013). This effect on flows in the dry season is probably responsible for the higher minimum monthly stream flow at Datong post Three Gorges Dam that is observable in **Figure 2-10**; and
- This effect is not necessarily negative; for example, during the 2011 drought, stored water was released from the dam at a higher rate than inflowing water, increasing the available water downstream to a level higher than it would have been without the dam (Chen, Webber et al. 2013, Qiu and Zhu 2013).

While the influence of damming on hydrology in the Yangtze River is predominantly redistributive and potentially beneficial for dry season water supply in the Lower Yangtze River, the implementation of water transfer systems from the Yangtze to other cities and rivers is more concerning for streamflow arriving at the Yangtze Estuary; in some cases, water transferred can be lost from the system entirely. Streamflow data at Datong suggest that these extractions of flow in the upper and middle basin are having little effect so far, there are many more schemes planned for the future, in particular in the lower river downstream of Datong (Finlayson, Barnett et al. 2012).

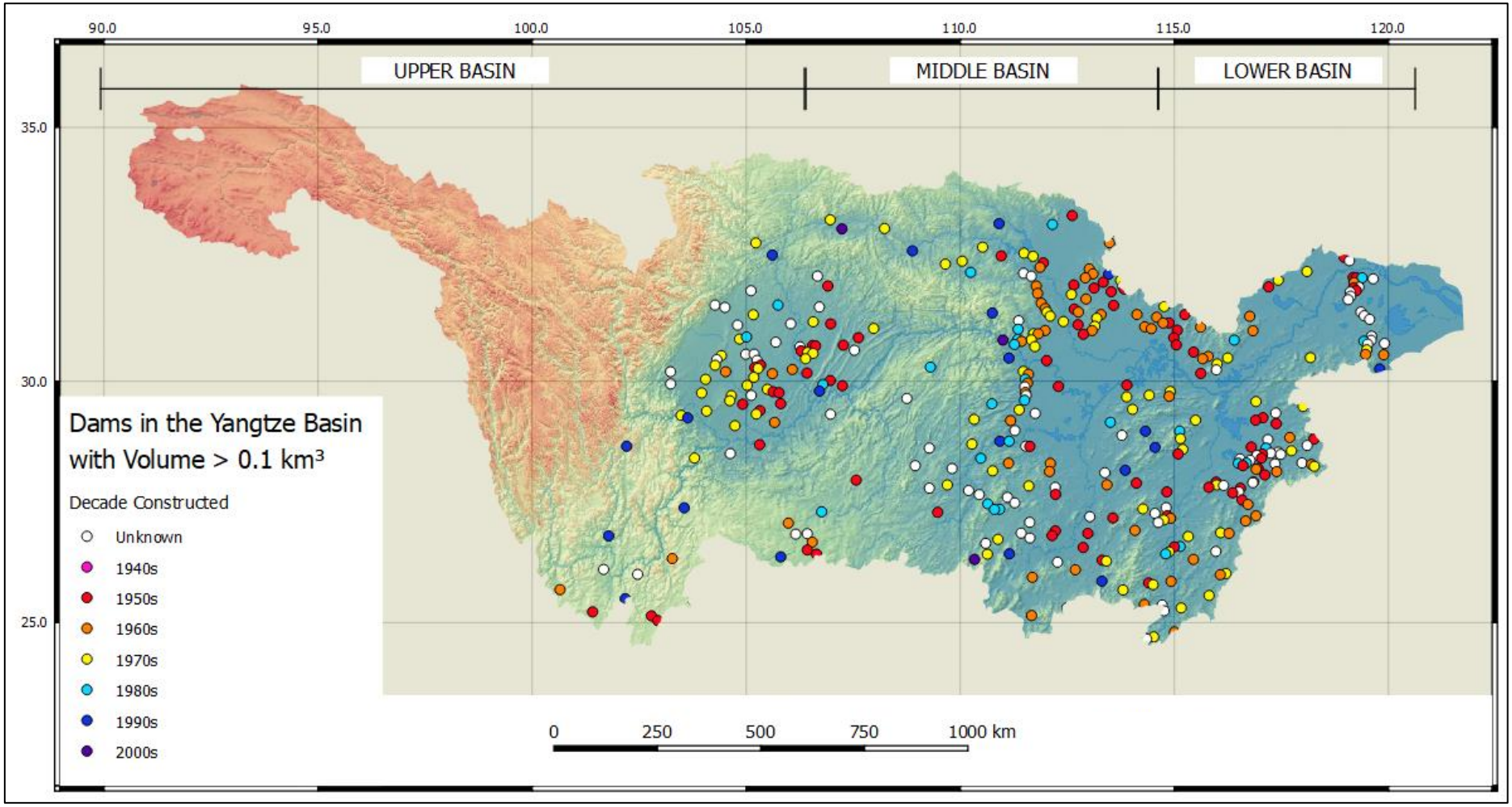

Figure 2-15: Large Dams in the Yangtze River Basin. Digital elevation data sourced from Robinson, Regetz et al. (2014). Dam data sourced from Lehner, Reidy Liermann et al. (2011).

Due to rapid economic development in the Yangtze Delta, demand for water has increased significantly, with many water transfer systems being constructed in the Jiangsu reach of the Yangtze Delta including the eastern route of the South North Water Transfer Project. Water in this region is used for agriculture, industry and urban supply, as well as to improve water quality in local tributaries (Chen, Zong et al. 2001, Zhang, Savenije et al. 2012). The main water transfer facilities for each of the major uses (agricultural, industrial, and municipal) along the Yangtze River downstream of Datong include sluices, pumping stations, culverts, water works and water intakes. (Chen, Webber et al. 2013).

Pre-2000, there were 64 diversion projects downstream of Datong with a combined capacity of 145.8 billion m^3/a, by 2010 this capacity had grown to 649 billion (total annual discharge of the Yangtze River is around 900 billion m^3). In May 2011, the Jiangsu Provincial Government approved increased withdrawals of water; the 2008 and planned 2030 abstraction volumes are shown in **Table 2-3** (Chen, Webber et al. 2013). It can be seen that in Jiangsu province alone extraction capacity is planned to nearly double by 2030 to approximately 9% of the Yangtze's annual flow.

Table 2-3: Total abstraction in Jiangsu present and 2030 planned, adapted from Chen, Webber et al. (2013)

Type of water use	2008	2030 (estimated)
Provincial Use (m^3)	25.35 billion	32.70 billion
Industrial and Power Generation (m^3)	14.20 billion	35.50 billion
South-North Water Transfer Project - Eastern Route (m^3)	8.94 billion (2007 value)	14.82 billion
Total (m^3)	**48.49 billion**	**83.02 billion**

Different facilities operate with different mechanisms diverting water and drainage returns. Sluices can abstract water during periods of high water levels, including high tides; pumping stations intensively abstract water during the dry season and periods of high water demand (Chen, Webber et al. 2013). During periods of high-water demand water abstraction from the Yangtze is increased. This has the potential to severely lower the flow discharged to the estuary during hot and dry years (Zhang, Savenije et al. 2012, Chen, Webber et al. 2013). While extractions during the dry season are limited because the water level drops to below many of the intakes for pumps and sluices, there are dry season pumps and sluices that can access water even during periods of low water level, with a total capacity of around 5,600 m^3/s which is as much as 50% of dry season flow (Chen, Webber et al. 2013). This is a significant risk for availability of freshwater at the estuary during dry months and years and can have implications for saline intrusion at the estuary. This is discussed further in **Section 3-2**.

2.3 Shanghai's Municipality Water Supply

2.3.1 Water Quantity and Quality

To support its significant population and economy, Shanghai requires a reliable supply of good quality water. As such, the two main factors that control water demand in Shanghai are population and growth in GDP (Webber, Barnett et al. 2018). The change in Shanghai's population and GDP are shown in **Figure 2-16**. Shanghai generates a significant portion of China's gross domestic product (GDP) and its economy has grown much faster than the national average. In the period 1994–2000, Shanghai's average annual GDP growth rate was 14.7%, and during 2000–2007, it was 9.8% (Finlayson, Barnett et al. 2012, Chen, Webber et al. 2013). Between 1978 and 2015, Shanghai's population increased from 11 to 24.2 million. Of this, the local population rose slowly from 11 to 14.3 million while the migrant population increased from 50,000 in 1978 to about 10 million in 2015 (Webber, Barnett et al. 2018). To accommodate these changes, Shanghai is increasingly urbanised, with large amounts of fields being converted to make way for roads and buildings. As shown in **Figure 2-13** (**Section 2.2.2**), in 1989 Shanghai Municipality and the area around Lake Tai was predominantly green and has undergone a massive transformation over the following 30 years.

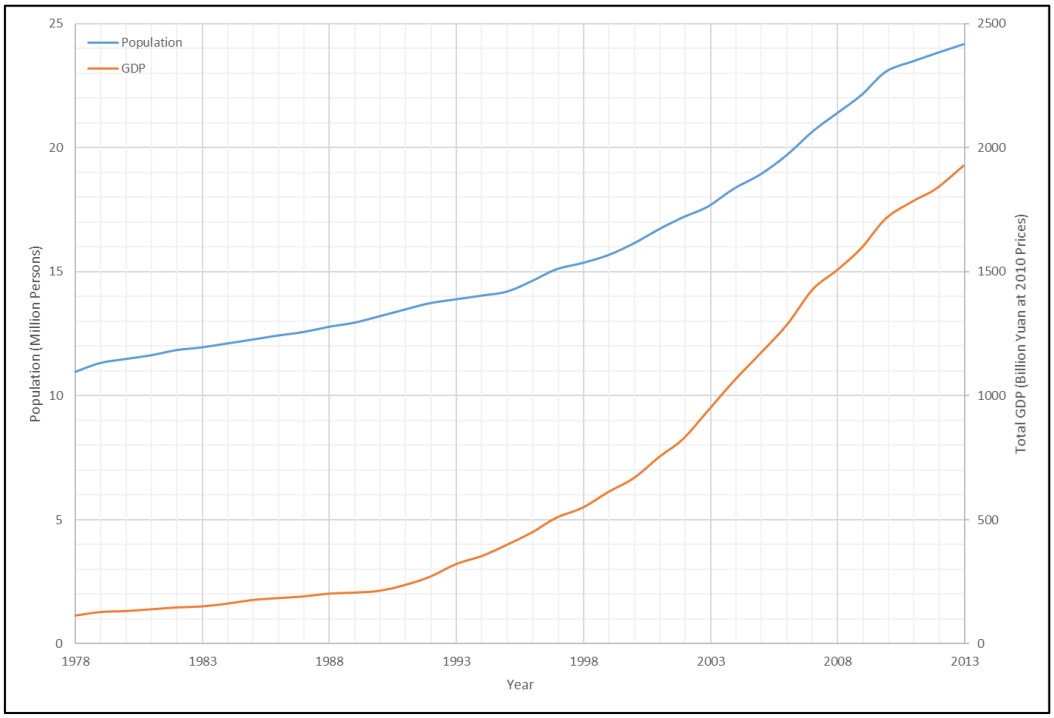

Figure 2-16: Growth in Shanghai's Population and Total GDP (1978-2013). Shanghai Statistical Yearbook (adapted from Li, Finlayson et al. (2017))

The total annual water use (municipal supply and self-supply) in Shanghai is approximately 12.26 billion m^3 and based on average sector water use (2006-2010) Shanghai water users can be broken down generally as follows:

- ~59 % for cooling in power stations;
- ~14 % for agriculture;
- ~10 % for household use;
- ~9 % for use in public spaces; and
- the remaining 8% used by industry other than power stations (Finlayson, Barnett et al. 2012).

Power station water supply, agriculture water supply, around half of the industrial (non-power station) water supply, and a quarter of both household and public space water supply (in total circa 80.4% in 2006-2010) are self-supplied from direct withdrawals from raw sources around Shanghai and as such are not considered in this thesis (Finlayson, Barnett et al. 2012). The remaining water for households, public spaces and the remaining industrial water (circa 19.6% in 2006-2010) is processed in the municipal water supply system before use (Finlayson, Barnett et al. 2012, Webber, Barnett et al. 2018). The current trend in water users is that direct withdrawals for agriculture and industry are decreasing and the use of treated water from the distribution system increasing due to the closure or relocation of industrial plants and the expansion of urban area into farmland; by around 2015, the treated water supply accounted for just over 25% of total water use in Shanghai (Webber, Barnett et al. 2018).

From 1978 to the present there have been changes in consumptive behaviour in Shanghai. Between 1978 and 2000 there was a significant increase in end users in Shanghai connected to the municipal supply, the number of parks and their irrigated area increased and until 1990 there was also continuing growth in Shanghai's industrial sector. As a result, during this period the per capita water use in Shanghai rose from less than 90 m^3/a to almost 150 m^3/a (Webber, Barnett et al. 2018). After 2000, many water intensive industries have shifted out of Shanghai and the per capita demand for non-industrial water has dropped and remained constant at about 100-110 m^3/a which is equivalent to about 300L/day (Webber, Barnett et al. 2018). As a result of increased population and changes in consumptive behaviour, water consumption from the municipal water supply system (i.e. tap water) has increased from about 0.97 billion m^3/a in 1978 to 3.1 billion m^3/a in 2013 (Li, Finlayson et al. 2017). Population growth and historical water supply consumption is presented in **Figure 2-17**.

A study conducted by Li, Finlayson et al. (2017) used a method of extrapolation and principle component analysis to forecast public water demand by projecting the growth in population and GDP, assuming that demand for water per unit of population and GDP will continue to change at their historically observed rates of change (Li, Finlayson et al. 2017). As such, potential effects of changes in source water or water conservation practices are not explicitly considered in these

estimates. Use estimate scenarios were based on a population growth of 200,000 (low), 300,000 (medium) and 400,000 (high) per year and a rate of GDP growth of 3%, 5% and 7% per annum (**Figure 2-18**).

Three future scenarios were considered in Li, Finlayson et al. (2017)'s study:

- **Scenario 1** - Shanghai's population is estimated to grow from 24.2 million in 2014 to 31.5 million in 2050, and its GDP is estimated grow from ¥1931.73 billion to ¥5766.64 billion by this time;
- **Scenario 2** - Shanghai's population is estimated to grow to 35.3 million by 2050, and GDP is estimated grow to ¥11,747.60 billion; and
- **Scenario 3** - Shanghai's population is estimated to grow to 39 million by 2050, and GDP to ¥23,612.66 billion.

Based on the above scenarios, the annual demand for water from the municipal water supply in Shanghai in 2050 is estimated to be between 4.2 billion m^3 (scenario 1) and 5.7 billion m^3 (scenario 3), representing increases of between 35% and 83% relative 2013 levels.

To meet this demand, a sufficient supply must be available for treatment and ultimate use. In addition to the quantity requirements, these raw water sources must meet minimum quality standards that conform to the Environmental Quality Standards for Surface Water, GB3838 – 2002 (SEPA 2002) or require extensive additional treatment. The Environmental Quality Standards for Surface Water is subdivided into 5 categories, representing different grades of water:

- **Class I**: Natural protection areas
- **Class II**: Level one drinking water source
- **Class III**: Level two drinking water source
- **Class IV**: Industrial water source
- **Class V**: Agricultural water source

Water that exceeds the maximum concentration thresholds for **Class V** (often denoted as **Class V+**) is considered by the Chinese government to be unusable for any purpose. For municipal supply, **Class II** is the desirable source quality, however with sufficient treatment, a **Class III** supply is acceptable. Water quality parameters targeted by the standards include dissolved oxygen (DO) levels, pH, chemical and 5-day biochemical oxygen demands (COD and BOD_5), turbidity, nutrient concentrations, oils, phenols, heavy metals, and some key toxic compounds. A summary of key parameters and thresholds for **Class III** water is presented in **Table 2-4**. For a full translated list of standard requirements, please refer to **Appendix 2**.

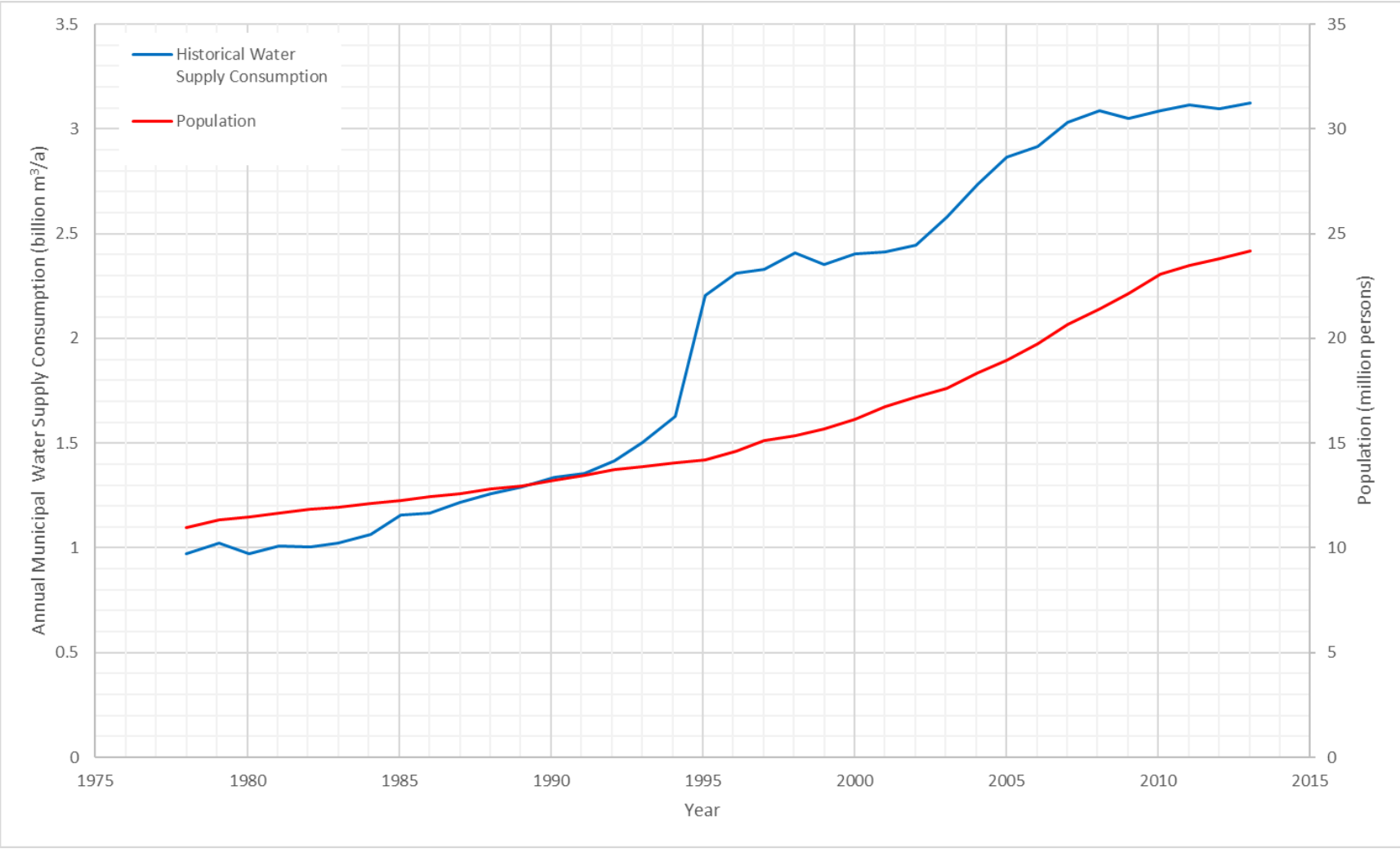

Figure 2-17: Population Growth and Historical Water Supply Consumption in Shanghai. Adapted from Li, Finlayson et al. (2017). Historical data is originally from Shanghai Statistical Yearbook (2014).

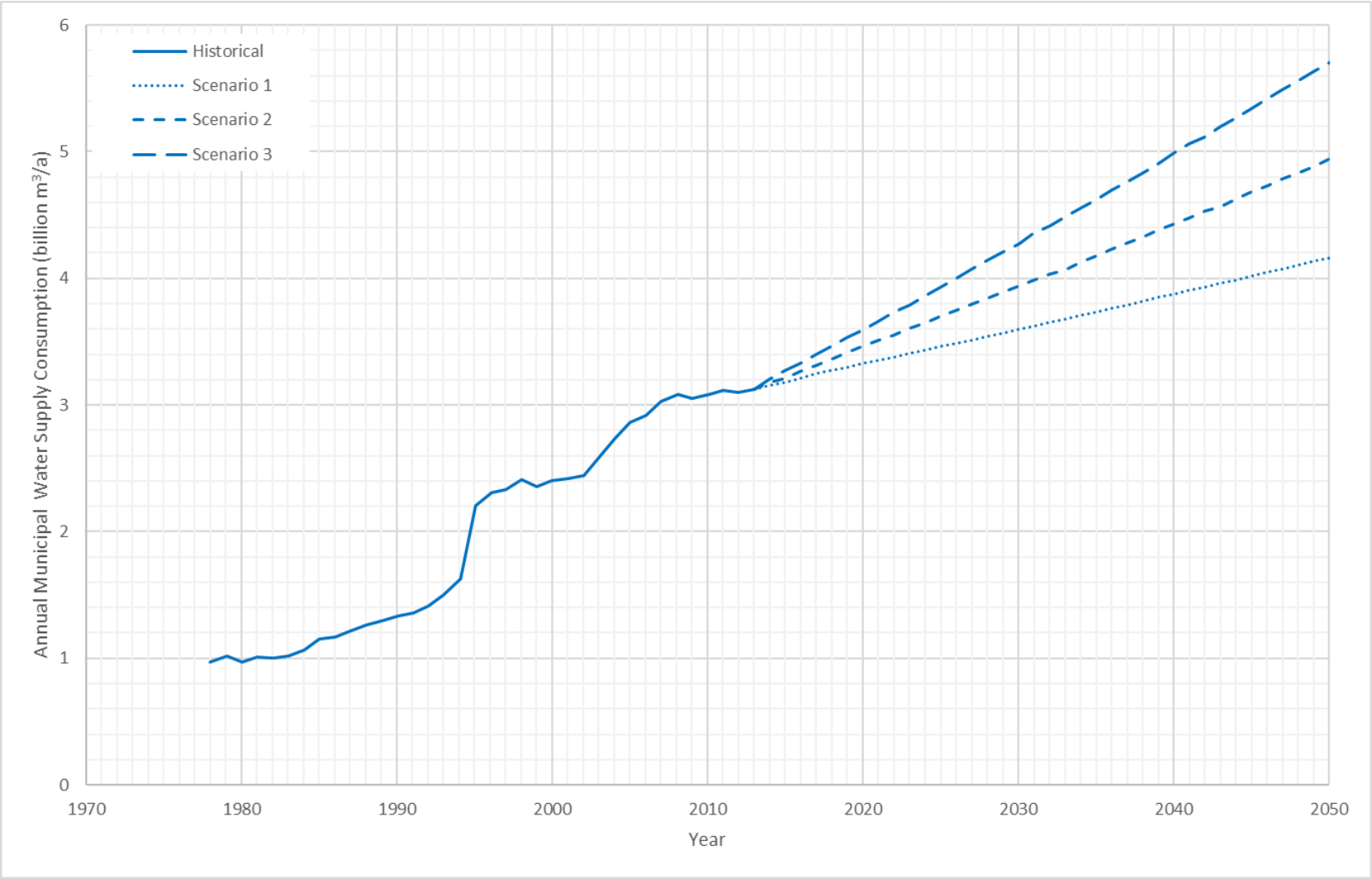

Figure 2-18: Historical and Predicted Annual Municipal (treated) Water Supply Consumption in Shanghai. Adapted from Li, Finlayson et al. (2017). Historical data is originally from Shanghai Statistical Yearbook (2014).

Table 2-4: Class III Basic Water Quality Parameter Guidelines (SEPA 2002)

Parameter	Unit	Threshold
Water temperature	(ºC)	The change in temperature in the man-made environment should be limited to: Rise in weekly average maximum temperature ≤ 1 Drop in weekly average maximum temperature ≤ 2
pH	-	6 to 9
Dissolved Oxygen	(mg/L)	5
Permanganate Index	(mg/L)	6
COD	(mg/L)	20
BOD_5	(mg/L)	4
NH_3-N	(mg/L)	1
TP (rivers)	(mg/L)	0.2
TP (lake/reservoir)	(mg/L)	0.05
TN	(mg/L)	1
Copper (Cu)	(mg/L)	1
Zinc (Zn)	(mg/L)	1
Fluoride (Fl^-)	(mg/L)	1
Selenium (Se)	(mg/L)	0.01
Arsenic (As)	(mg/L)	0.05
Mercury (Hg)	(mg/L)	0.0001
Cadmium (Cd)	(mg/L)	0.005
Hexavalent Chromium (Cr^{6+})	(mg/L)	0.05
Lead (Pb)	(mg/L)	0.05
Cyanide (CN^-)	(mg/L)	0.2
Volatile Phenol	(mg/L)	0.005
Oils	(mg/L)	0.05
Anionic Surfactants	(mg/L)	0.2
Sulphide (S^{2-})	(mg/L)	0.2
Total Coliforms	(count/L)	10000

2.3.2 Configuration of Shanghai's Water Supply

Shanghai's first water treatment plant was constructed at Yangshupu in central Shanghai by foreign concession holders in 1883 to withdraw and treat water from the confluence of the Huangpu River and Suzhou Creek; this plant is still in operation today and is one of the largest in the city (Shanghai Municipal People's Government 2010). By 1987, there were 12 water intake treatment plants that were governed by the Shanghai Water Treatment Company. 11 of these plants processed water from the Huangpu. The other plant at was located at Taopu (inland) and processed water for industrial use only. (Ward and Liang 1995).

Presently there are 36 public water treatment plants in Shanghai, and the majority of the water for residential and public uses is processed through these plants prior to distribution (Finlayson, Barnett et al. 2012, Webber, Barnett et al. 2018). The 36 public water treatment plants (**Figure 2-19**, **Table 2-5**) have a total combined treatment capacity of 4.177 billion m^3/a (in 2013) and are located:

- on Chongming Island (3 plants, Yangtze Water Source);
- near Chenhang and Huating reservoirs (7 plants, Yangtze Water Source);
- near the Qingcaosha reservoir (12 plants, Yangtze Water Source); and
- along the Huangpu River (14 plants) (Webber, Barnett et al. 2018).

Shanghai's two largest water treatment plants are the Yangshupu and Changqiao water treatment plants, which each have the capacity to treat 1.48 and 1.40 million m^3/d (0.54 and 0.511 billion m^3/a) respectively (Li, Finlayson et al. 2017). Approximately 75% of treatment capacity is provided by plants with the Yangtze River as their water source and the remaining 25% from the Huangpu and Taipu Rivers.

The public water treatment plants are supplied from eight raw water pumping stations with a combined capacity of 5.827 billion m^3/a. The eight pumping stations are located in remote and rural areas of the municipality with four located along the upper Huangpu River and Taipu River (accounting for 43% of available pump capacity), and the remaining four draw water from the Yangtze Estuary (accounting for the remaining 57% of available pump capacity). Of the available pump capacity, pumps in the Yangtze estuary are 90% utilised while only 42% of pump capacity from the Huangpu and Taipu rivers is utilised (based on treatment volume from each source compared with pumping capacity at each source in **Table 2-5**).

The municipal distribution system consists of 30,000km of pipeline and 40000 storage tanks (Li, Chen et al. 2019).

As discussed in **Section 2.3.1**, Shanghai has a significant demand for water to meet the needs of its population and economy. Up to 2050, even under the most optimistic scenarios, future growth in population and GDP will lead to further increase in the demand for municipal water supply. **Figure 2-20** reproduces the water consumption trends from **Section 2.3.1** and makes comparison with historical water supply capacity (up to 2013). This figure shows that the 2013 supply is capable of meeting up to around 2025 under the high growth projection (**Scenario 3**; annual population growth of 400,000 and GDP growth of 7%), up to 2030 for the medium growth projection (**Scenario 2**; annual population growth of 300,000 and GDP growth of 5%), and 2040 for the low growth projection (**Scenario 1**; annual population growth of 200,000 and GDP growth of 3%). To meet 2050 demand under all projections, additional water supply intakes capacity and treatment capacity will need to be increased. Assuming the highest projection of 5.7 billion m^3/a with a 20% factor to make provision for losses in the distribution system (as recommended in Li, Finlayson et al. (2017)), municipal supply requirements could reach as high as 6.8 billion m^3/a, with the vast majority of new facilities sourcing their water from the Yangtze River. Under the same projection, by 2050, as many as 5 additional water treatment plants the size of Yangshupu may be required. In addition, pump capacity from the Yangtze will need to be increased as current capacity is already 90% utilised.

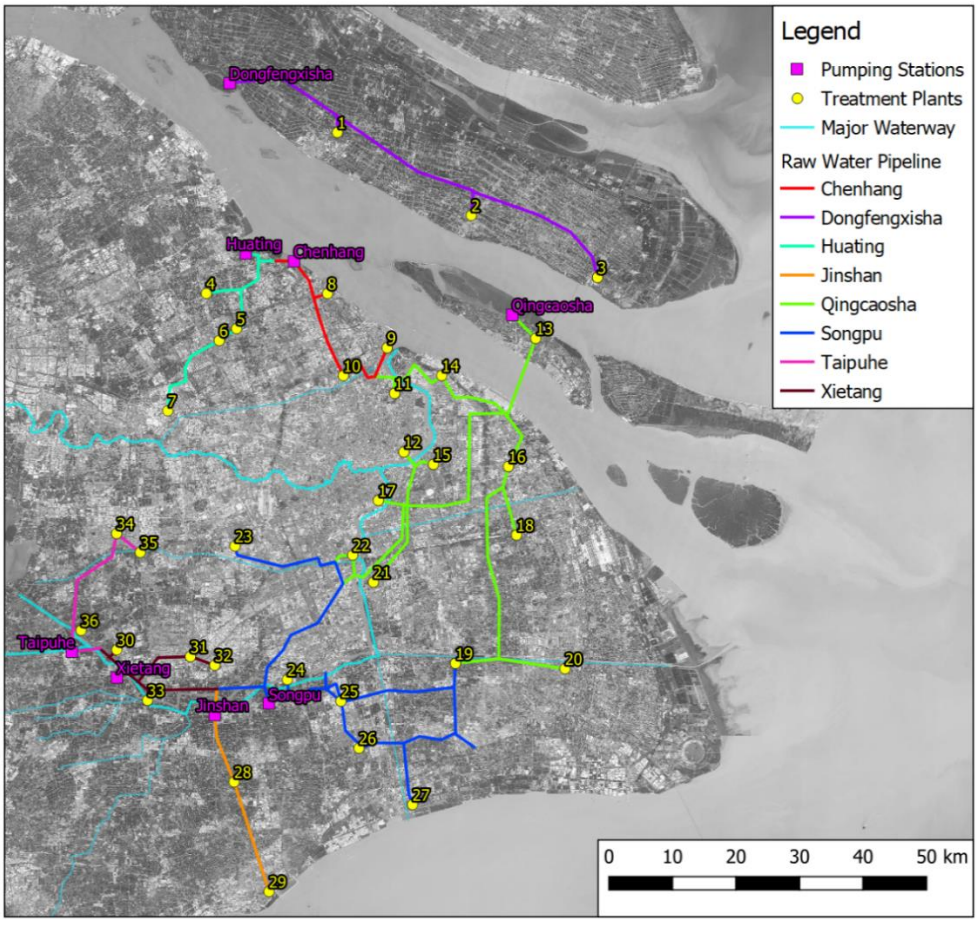

*Figure 2-19: Shanghai's Municipal Water Supply Assets. Numbers correspond to treatment plant in **Table 2-5**. Municipal supply information sourced from Li, Chen et al. (2019). Aerial photo sourced from NASA Earth Observatory (2017)*

Table 2-5: Pumping Stations and Treatment Plants in Shanghai. Adapted from Li, Chen et al. (2019).

Pumping Stations		Treatment Plants		
Name	**Capacity (million m^3/d)**	**Plant Number***	**Name**	**Capacity (million m^3/d)**
Dongfengxisha	0.215	1	Chengqiao	0.075
		2	Baozhen	0.020
		3	Chenjiazhe	0.040
Huating	0.400	4	Bei	0.150
		5	Yongsheng	0.220
		6	Jiading	0.080
		7	Anting	0.120
Chenhang	1.800	8	Yuepu	0.400
		9	Wusong	0.180
		10	Taihe	0.800
Qingcaosha	7.190	11	Zhabei	0.280
		12	Yangshupu	1.480
		13	Changxing	0.100
		14	Lingqiao	0.400
		15	Pudong	0.200
		16	Jinhai	0.800
		17	Linjiang	0.600
		18	Chuansha	0.200
		19	Hangtou	0.200
		20	Huainan	0.240
		21	Nanshi	0.700
		22	Changqiao	1.400
Songpu	5.000	23	Xujing	0.070
		24	Minhang #2	0.900
		25	Fengxian #3	0.350
		26	Fengxian #2	0.100
		27	Xinghuo	0.100
Jinshan	0.400	28	Jinshan #1	0.220
		29	Shihua	0.160
Xietang	0.600	30	Xiaokunshan	0.200
		31	Songjiang #1	0.100
		32	Songjiang #2	0.160
		33	Chedun	0.040
Taipuhe	0.360	34	Qingpu #1	0.060
		35	Qingpu #2	0.200
		36	Qingpu #3	0.100
Total	**15.965 (million m^3/d) 5.827 (billion m^3/a)**			**11.445 (million m^3/d) 4.177 (billion m^3/a)**

Refer to **Figure 2-19 for treatment plant locations*

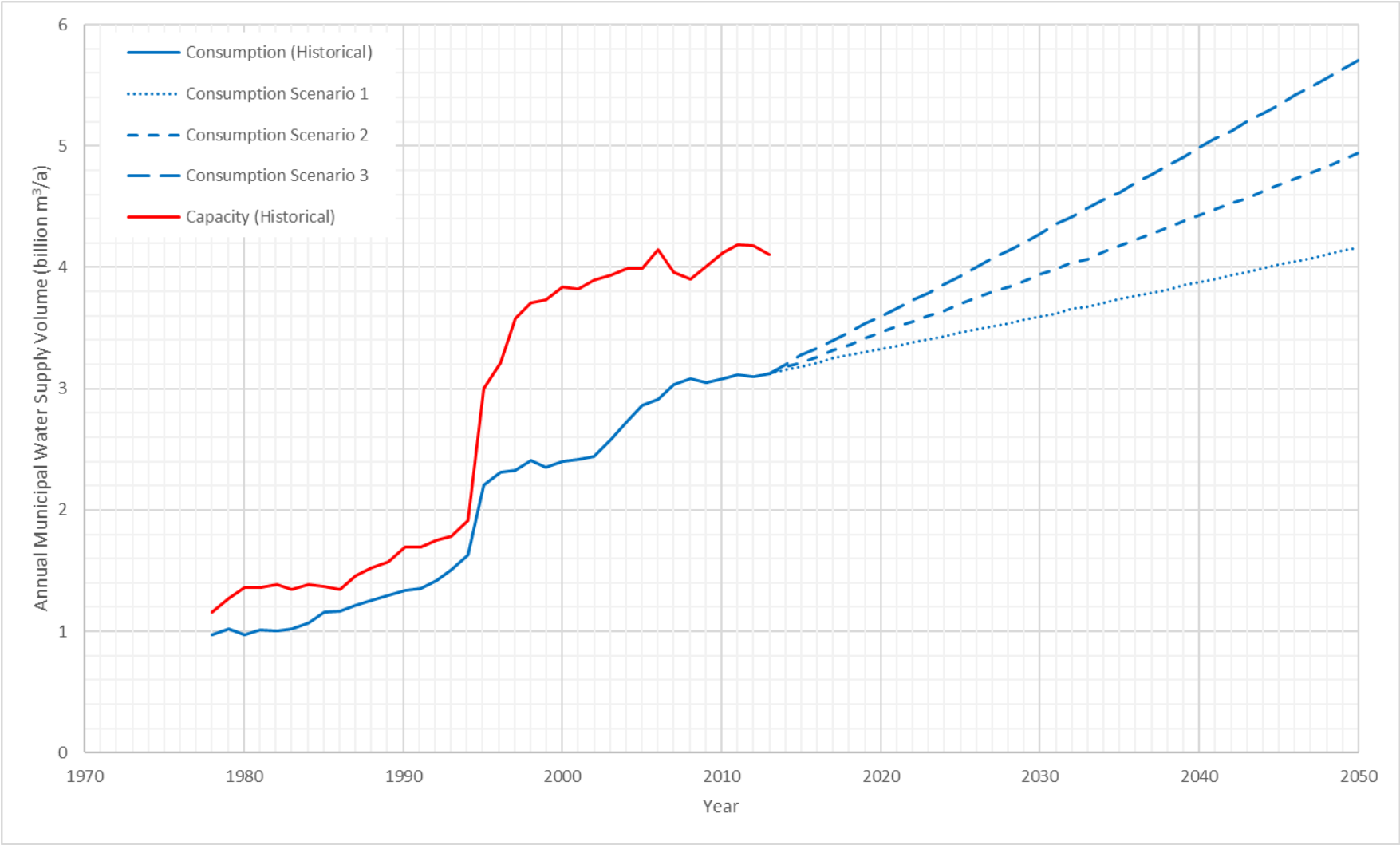

Figure 2-20 Comparison of Historical and Predicted Annual Municipal (treated) Water Supply Consumption and Municipal Treatment Capacity in Shanghai. Adapted from Li, Finlayson et al. (2017). Historical data is originally from Shanghai Statistical Yearbook (2014).

Incoming raw water quality has implications on the overall cost of treatment because it determines the type and intensity of water treatment needed to reach drinking water standards. Better raw water quality reduces the need for sediment removal, makes filtration easier, and reduces the need for additional processes such as pre-oxidation, activated carbon and membrane filtration(McDonald, Weber et al. 2016). In particular, a lower concentration of phosphorus and nitrogen reduces algal growth and the amount of organic matter in the water, which simplifies filtration and reduces the prevalence of disinfection by-products in treated water (McDonald, Weber et al. 2016). Ultimately, water treatment plants using raw water of high quality can be designed using simpler treatment technologies, which lead to a lower capital cost during construction and lower operations and maintenance (O&M) costs (McDonald, Weber et al. 2016).

Presently, water treatment plants in Shanghai predominantly use a conventional filtration process (Refer **Figure 2-21**) consisting of chemical coagulation and flocculation, sedimentation and filtration followed disinfection by chlorination (Webber, Barnett et al. 2018). There are currently only two treatment plants out of 36 that have experimented with applying advanced treatment technologies (Li, Chen et al. 2019). The estimated treatment performance of two of the larger water treatment plants in Shanghai, Minhang #2 which treats water from the Huangpu River and Yuepu, which treats water from the Yangtze via the Chenhang Reservoir, is summarised in **Table 2-6**. Results demonstrate that the treatment technologies applied are effective at removing physical and biological constituents (Turbidity and Total Bacteria Count) but not effective at treating organic compounds (COD, Detergent, Volatile Phenols) as well as TN and ammonium. Analysis by Li, Chen et al. (2019) suggests that the average concentrations of all parameters assessed (Colour, Turbidity, Bacteria Count, Ammonium, Iron, Manganese, COD) in finished water are below the Chinese treated drinking water quality requirements. There are however maximum concentrations of ammonium, iron and COD in treated water originating from both the Huangpu and Yangtze Rivers that exceed drinking water requirements (Li, Chen et al. 2019). High concentrations of COD and ammonium indicate that water supplies are affected by organic and domestic contaminants likely originating from wastewater discharge and may require the upgrade of treatment plants to include advanced treatment technologies to ensure adequate quality treated water (Li, Chen et al. 2019).

Estimates of the annual cost for Shanghai's municipal water treatment have been undertaken and are presented in **Table 2-7**. In the absence of protection of source water from saline intrusion (i.e. no coastal reservoirs), advanced filtration (desalination) would be required for water from the Yangtze. Poor water quality or the occurrence of algal blooming would require Shanghai's municipal supply to increase from using conventional treatment technology to use technologies such as granular activated carbon and oxidation (Filtration Plus). Under all growth scenarios, by 2050, the difference between a conventional and advanced treatment could double the cost of water treatment in Shanghai per year, reaching as high as $USD 1,634 million under the highest

growth projection. The cost of implementing filtration plus treatments is estimated to increase treatment cost by approximately 40%.

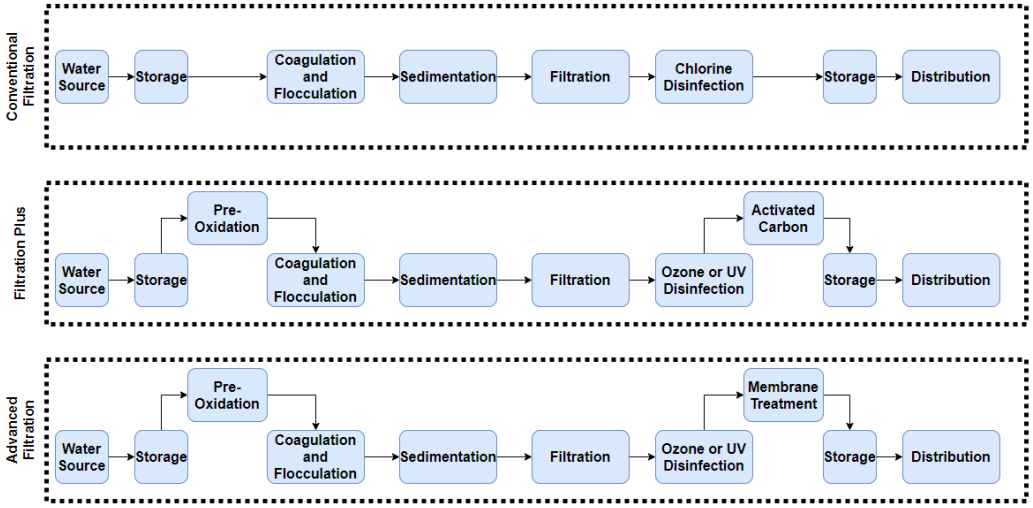

Figure 2-21: Typical Types of Water Treatment Processes. Adapted from Webber, Barnett et al. (2018)

Table 2-6: Estimated Removal Rates at Two Water Treatment Plants in Shanghai. Adapted from Li, Chen et al. (2019).

Parameter	**Estimated Removal Rate at Water Treatment Plants (%)**	
	Minhang #2 (Huangpu River)	**Yuepu (Yangtze via Chenhang Reservoir)**
Colour	56	69
Turbidity	97	99
Total Bacteria Count	99	100
TP	89	55
Iron	97	84
Manganese	67	52
COD	27	34
Detergent	44	24
Volatile Phenols	0	5
TN	-17	47
Ammonium	10	-6

Table 2-7: Cost Estimates for Future Water Treatment Plants in Shanghai under Various Growth Scenarios.

*Estimated Water Supply Consumption from Li, Finlayson et al. (2017), refer Figure **2-20**. Required Water Supply Capacity is assumed as 20% higher than consumption for growth scenarios to make provision for losses in the distribution system (as recommended in Li, Finlayson et al. (2017)), except for where estimated to be below the 2013 supply capacity of 4.2 billion m^3/a. Categories for Treatment Technologies have been adopted from McDonald, Weber et al. (2016). Filtration Plus refers to conventional filtration with a supplementary treatment process such as granular activated carbon, pre-ozonation, etc. Advanced filtration refers to treatment using membrane technology. Cost estimates for different treatment technologies were calculated based on cost estimates from McDonald, Weber et al. (2016) for a 250 ML/d plant. Replacement costs were annualised by McDonald, Weber et al. (2016) assuming a 30y bond at a 5% interest rate and prices are in $USD for 2015.*

Scenario		Estimated Water Supply Consumption (billion m^3/a)	Required Water Supply Capacity (billion m^3/a)	Conventional Filtration			Filtration Plus			Advanced Filtration		
				Annualised Replacement Cost ($Million)	Annual O&M Costs ($Million)	Total Annual Costs ($Million)	Annualised Replacement Cost ($Million)	Annual O&M Costs ($Million)	Total Annual Costs ($Million)	Annualised Replacement Cost ($Million)	Annual O&M Costs ($Million)	Total Annual Costs ($Million)
Historical	2013	3.1	4.2	391	87	479	529	147	677	852	152	1003
Low	2030	3.5	4.2	391	87	479	529	147	677	852	152	1003
	2040	3.9	4.7	436	97	533	590	164	754	949	169	1118
	2050	4.2	5.0	469	105	574	635	177	812	1022	182	1204
Medium	2030	3.9	4.7	436	97	533	590	164	754	949	169	1118
	2040	4.4	5.3	492	110	602	665	185	851	1070	191	1261
	2050	4.9	5.9	548	122	670	741	206	947	1192	213	1405
High	2030	4.3	5.2	481	107	588	650	181	831	1046	187	1233
	2040	5.0	6.0	559	125	684	756	210	967	1216	217	1433
	2050	5.7	6.8	637	142	780	862	240	1102	1387	247	1634

2.4 Shanghai's Water Security

As Shanghai continues to grow and develop, so will its demand for high-quality water supply. The traditional water sources that Shanghai has relied on, the Huangpu River and other local water resources, are no longer suitable for Shanghai's needs both with regards to quantity and quality, and it is necessary to draw on the massive water resource provided by the Yangtze River which delivers on average 900 billion m^3 of water to estuary every year, which is 90 times more than the nearest alternative, the Huangpu River. Because Shanghai has access to the large and reliable annual supply of water from of the Yangtze River, it is the infrastructure necessary to supply potable water to consumers that is considered to be the primary barrier to meeting Shanghai's future public water needs (Li, Finlayson et al. 2017). By 2050, Shanghai could require between 4.2 and 5.7 billion m^3 of raw water for municipal supply per year, which represents a 35% to 83% increase in consumptions (relative to 2013 levels). At present, Shanghai's municipal supply has a raw water pumping capacity of 5.8 billion m^3/a (with most spare capacity associated with pumps in the Huangpu River) and a treatment capacity of 4.2 billion m^3/a.

To meet future demand as many as five new 1.5 million m^3/d treatment plants could be required along with expanded pumping capabilities in the estuary. The cost of expanding Shanghai's treatment capabilities is dependent on raw water quality and which constituents need to be removed prior to end-use. Currently, Shanghai mainly relies of conventional filtration systems to improve water to the required standards. These systems are effective at the removal of physical and microbial constituents, but not effective at removing organic compounds and nitrogen or at treating salinity. Direct withdrawal from the estuary would require the addition desalination so that freshwater could be obtained even during times where saline intrusion into the estuary was occurring. A system such as this would be the most expensive option for upgrading Shanghai's treatment system.

Withdrawing water further upstream is another potential option to minimise the impact of saline intrusions on Shanghai's water supply, however the decision was made not to because firstly of the costs associated constructing the diversion system and secondly because of the administrative issues and potential illegalities of inter-provincial water transfers (Chen, Webber et al. 2013). As noted in **Section 2.1**, at present there is not integrated water sharing plan for water in the Yangtze River and all rights to the water in the Yangtze River are held by the Changjiang Water Resources Commission that is directly under the authority of the Ministry of Water Resources. The Water Resources Commission is planning to distribute those rights to provinces and municipalities along the river but only at points where the river is within the province (Webber, Barnet et al. 2015). To build intakes and pipelines within Jiangsu would need the approval and probable compensation of the Jiangsu provincial government as well as negotiations with the National Ministry of Water Resources' Changjiang (Yangtze River) Water Resources Commission (Webber, Barnet et al. 2015, Webber, Barnett et al. 2018)

Policy options to improve water security in Shanghai such as applying an integrated water resource management approach, improving water use efficiency, clarifying water rights, improved enforcement of water laws and regulations, and catchment scale water pollution control are potential options. These options have been suggested for China more broadly, however due to the political and administrative structure around water resource management in China, the successful application of these options is difficult (Cheng and Hu 2011). There are 8 central government agencies that hold certain responsibilities over aspects of water resource management including the Ministry of Water Resources, Ministry of Environmental Protection, Ministry of Housing and Urban-Rural Development, Ministry of Agriculture, State Forest Administration, National Development and Reform Commission, Ministry of Transport and Ministry of Health. There is an obscure delineation of authority and responsibilities between these agencies at multiple levels of government ranging from the national to local levels that undermines the allocation of water resources, the coordination water resources exploitation, the conservation of water resources and enforcement of water resources planning (Cheng and Hu 2011). This results in inconsistent policies and conflicting interests among the different ministries that weaken overall management of water resources in China (Cheng and Hu 2011). In the case of Shanghai, the primary issues affecting the implementation of water management policies include a lack of legal basis for addressing water use and pollution control at the basin level, a lack of clear policy responsibility in the government, a lack of effective cross-jurisdictional coordination, a focus on largely supply-driven, engineering-based, single-sector solutions, and a low level of stakeholder and public participation (Cheng and Hu 2011, Webber, Barnet et al. 2015). It has been argued that China is not ready to implement integrated water resource management in any successful way unless it can be adapted to China's political landscape or the political landscape changes (Cheng and Hu 2011).

As the only viable alternative to secure water supplies, the Shanghai Government has already decided to implement a long-term strategy to secure water supply from the Yangtze Estuary using Coastal Reservoirs (Finlayson, Barnett et al. 2012). Coastal reservoirs can be filled with water from the river during conditions where incoming water quality is acceptable, and during periods where the water at the intake is too saline or to low quality for drinking water use, the reservoir can be closed, protecting the stored water (Chen, Webber et al. 2013). However, the use of coastal reservoirs does not preclude poor raw water quality outcomes. Chronic occurrence of pollutants in the Yangtze Estuary would prevent the reservoir from being able to selectively avoid these contaminants and result in additional treatment options like activated carbon being required for the treatment process. Similar to other heavily developed catchments, elevated nutrient concentrations resulting from wastewater, food production and industry could also result in the risk of algal blooms occurring in the reservoir, which would also require enhancement to Shanghai's existing water treatment facilities. For this reason, it is important to consider the water quality being diverted to the coastal reservoirs in more detail.

2.5 Summary

- The majority of Shanghai's water supply have historically been drawn from three main sources, local surface water such as the Huangpu River, groundwater and the Yangtze River. Local surface waters are subject to poor water quality and groundwater is no longer used as a major water source to prevent subsidence in Shanghai.
- The Yangtze River is the only available significant freshwater resource near Shanghai. The Yangtze River has a catchment area of approximately 1,800,000 km^2 mean annual discharge of around 900 million m^3 (28,500 m^3/s). Shanghai has access to the Yangtze's water at its estuary in the last 100 km before it reaches the sea.
- Flow in the Yangtze River displays an annual cycle peaking in summer with flows averaging about five times higher than those in winter. Compared with other rivers in similar climate zones, the discharge of the Yangtze is relatively stable and delivers predictable flows to the estuary each year.
- The Yangtze River Basin is home to over 440 million people and is important to China's economic development and environmental conservation. The basin provides a significant proportion of China's arable land, agricultural and industrial production and accounts for around 40% of China's freshwater resources.
- Additionally, a lot of major infrastructure such as dams for irrigation and hydropower, or diversion schemes have been implemented in the basin. This infrastructure is of sufficient scale to alter the hydrology of the Yangtze River. Of particular concern are the diversion schemes planned in the Lower Yangtze River which during the dry season could abstract as much as 5,600 m^3, equivalent to approximately 50% of flow in the driest months.
- Shanghai's current municipal water supply demand is approximately 3.1 billion m^3/a. It is estimated that by 2050, municipal water supply demand could be between 4.2 and 5.7 billion m^3/a.
- For drinking water use, raw water quality must comply with the Class III drinking water standards specified in the Environmental Quality Standards for Surface Water, GB3838 – 2002.
- Shanghai's municipal water supply is currently services by 8 pumping stations with cumulative capacity of 5.827 billion m^3/a and 36 municipal water treatment plants with cumulative capacity of 4.177 billion m^3/a. Of these assets, 57% of the total pumping capacity and 75% of the treatment capacity is associated with the Yangtze Estuary as a water source.
- To meet the estimated 2050 demand (with a +20% factor to make provision for losses in the distribution system), as much as 6.8 billion m^3/a capacity in the municipal supply could be required. An increase of this magnitude would require as many as 5 additional treatment plants the size of Shanghai's largest, the Yangshupu drinking water treatment plant. Additional pumping stations in the estuary will also be required.
- Shanghai presently relies on a conventional filtration process to treat water in its

municipal supply. These systems are effective at the removal of physical and microbial constituents, but not effective at removing organic compounds and nitrogen or at treating salinity. The type of treatment technologies applied depend on the quality of the raw water used. High salinity would require the application of advanced filtration technologies such as membrane treatment, while issues like algal blooms would require additional treatment processes like activated carbon to be incorporated into the treatment process.

- Upgrading Shanghai's treatment plants to incorporate additional treatments is estimated to cost around 40% more than the current system while upgrading to an advanced filtration system could nearly double the overall cost.

3. Water Quality in the Yangtze River at Shanghai

3.1 Water Quality Summary

Understanding the quality of a raw water supply is important because it dictates the treatment requirements to improve the raw water to drinking water standards and also has implications for operation rules for diversion systems and storages. Better raw water quality reduces the need for sediment removal, makes water treatment processes easier, and reduces the need for additional processes required to meet drinking water standards (McDonald, Weber et al. 2016). This chapter aims to characterise the water quality in the Yangtze Estuary with specific interest in composition for public water supply.

To determine which constituents are considered to be of concern for Shanghai's municipal supply, the following must be considered:

- Chinese Government water quality targets for drinking water quality. In this case, the Class III thresholds from **Environmental Quality Standards for Surface Water**, GB3838 – 2002 (SEPA 2002) are relevant (refer **Section 2.3.1**);
- The components of municipal supply system implemented and their capabilities. Any constituent that could be affected by operation of Shanghai's coastal reservoirs or has implications for Shanghai's municipal water treatment should be considered (refer **Figure 3-1**);
- The frequency that elevated concentrations of these constituents occur. Coastal reservoirs can be closed during short periods where elevated concentrations occur and therefore only constituents with consistently high concentrations should be considered; and
- The risk that the constituents pose to public health.

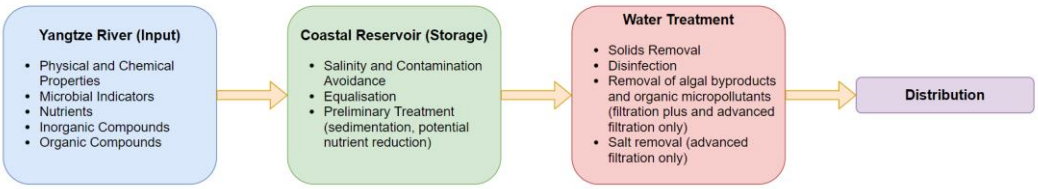

Figure 3-1: Schematic of Shanghai's Municipal Supply

Data on a range of potential water quality constituents was collected from literature. As Shanghai is only able to withdraw water from areas of the Yangtze Estuary that falls within its municipal boundary, only measurements representative of the estuary between Xuliujing and the mouth of the Yangtze River were selected. Data reduction techniques were applied so that only one estimate of average concentration is made for each month. The median, maximum and minimum monthly estimates of mean concentration for each constituent are reported in **Table 3-1** and where available, comparison is made to Chinese raw water standard Class III.

Table 3-1: Water Quality Summary at the Yangtze Estuary. Note: Green text denotes compliance with Chinese Raw Water Standard Class III, red denotes failure and blue denotes no applicable criteria. N.D. = below limits of detection

Constituent	Units	Concentration			Guidelines (SEPA 2002)	Data Sources
		Min	Median	Max		
Temperature	Celsius	8.04	22.3	30.7	N/A	Chetelat, Liu et al. (2008), Liu, Yu et al. (2009), Pan and You (2010)
pH	-	7.76	7.95	8.47	6-9	Chetelat, Liu et al. (2008), Pan and You (2010), Pan, Ying et al. (2014), Liu, Zhao et al. (2015)
DO	mg/L	5.68	6.89	9.53	> 6 mg/L (CIII)	Liu, Yu et al. (2009), Liu, Zhao et al. (2015)
Conductivity	µs/cm	289	333	1295	N/A	Pan, Ying et al. (2014), Liu, Zhao et al. (2015)
Total Suspended Solids	mg/L	37.6	122.9	406.5	N/A	Yang, Shen et al. (2007), Muller, Berg et al. (2008), Chai, Yu et al. (2009), Liu, Yu et al. (2009), Guo and He (2011), Gao, Li et al. (2012), Zhang, Dong et al. (2012), Ding, Gao et al. (2014), Meng, Yu et al. (2015)
COD	mg/L	1.8	8.88	38.1	20 mg/L (CIII)	Meng, Qin et al. (2004), Wu (2005), Lu, Zhang et al. (2010), Pan, Ying et al. (2014), Liu, Zhao et al. (2015)
BOD_5	mg/L	0.79	3.19	4.05	4 mg/L (CIII)	Liu, Zhao et al. (2015)
Chlorophyll a	mg/L	0.56	1.4	1.57	N/A	Liu, Yu et al. (2009), Lu, Zhang et al. (2010)
Bicarbonate (HCO_3)	mg/L	96.2	120	143	N/A	Ding, Gao et al. (2014)
Dissolved Organic Carbon (DOC)	mg/L	1.623	5.84	11.22	N/A	Muller, Berg et al. (2008), Wu, Huang et al. (2014), Nie, Yan et al. (2015)
Total Nitrogen (TN)	mg/L	0.62	1.81	2.85	1 mg/L (CIII)	Meng, Qin et al. (2004), Yang, Shen et al. (2007), Muller, Berg et al. (2008), Chai, Yu et al. (2009), Shen and Liu (2009), Lu, Zhang et al. (2010), Chen, Liu et al. (2012), Huang, Xie et al. (2014), Wu, Huang et al. (2014), Liu, Zhao et al. (2015)
Nitrate-N (NO_3-N)	mg/L	0.06	1.61	2.23	10 mg/L (note: NO_3-N concentrations of > 1 mg/L will result in failing the TN target)	Fu and Shen (2002), Meng, Qin et al. (2004), Zhou, Liu et al. (2006), Yang, Shen et al. (2007), Chetelat, Liu et al. (2008), Muller, Berg et al. (2008), Liu, Yu et al. (2009), Shen and Liu (2009), Gao, Li et al. (2012), Jiang, Liu et al. (2014), Wu, Huang et al. (2014), Gao, Li et al. (2015)

Constituent	Units	Concentration			Guidelines (SEPA 2002)	Data Sources
		Min	Median	Max		
Ammonium-N (NH_4-N)	mg/L	0.003	0.051	0.43	1 mg/L (CIII)	Fu and Shen (2002), Meng, Qin et al. (2004), Zhou, Liu et al. (2006), Yang, Shen et al. (2007), Muller, Berg et al. (2008), Liu, Yu et al. (2009), Gao, Li et al. (2012), Yan, Chen et al. (2013), Wu, Huang et al. (2014), Gao, Li et al. (2015), Liu, Zhao et al. (2015)
Total Phosphorous (TP)	mg/L	0.03	0.20	0.84	0.05 mg/L (CIII Lakes/Reservoirs)	Duan, Zhang et al. (2000), Yan and Shen (2003), Muller, Berg et al. (2008), Shen and Liu (2009), Yao, Yu et al. (2009), Yan, Chen et al. (2013), Liu, Zhao et al. (2015)
Dissolved Inorganic Phosphorous (DIP)	mg/L	0.005	0.040	0.19	N/A	Duan, Shen et al. (2000), Fu and Shen (2002), Meng, Qin et al. (2004), Zhou, Liu et al. (2006), Muller, Berg et al. (2008), Chai, Yu et al. (2009), Shen and Liu (2009), Gao, Li et al. (2012), Jiang, Liu et al. (2014), Gao, Li et al. (2015) , Meng, Yu et al. (2015)
Potassium	mg/L	2.24	4.19	17.2	N/A	Chetelat, Liu et al. (2008), Muller, Berg et al. (2008), Ding, Gao et al. (2014)
Boron	µg/L	14.1	31.3	383	500	Muller, Berg et al. (2008), Ding, Gao et al. (2014)
Bromine	µg/L	35.0	76.0	109	N/A	Ding, Gao et al. (2014)
Chloride	mg/L	9.87	15.7	777	250	Chetelat, Liu et al. (2008), Muller, Berg et al. (2008), Ding, Gao et al. (2014)
Fluoride	mg/L	0.13	0.27	0.38	1.0 (CIII)	Chetelat, Liu et al. (2008), Ding, Gao et al. (2014)
Iodine	µg/L	0.65	1.00	1.00	N/A	Muller, Berg et al. (2008), Ding, Gao et al. (2014)
Sulphate-S	mg/L	6.68	12.6	39.7	250	Chetelat, Liu et al. (2008), Muller, Berg et al. (2008), Ding, Gao et al. (2014)
Aluminium	mg/L	-	16.4	-	N/A	Muller, Berg et al. (2008)
Barium	µg/L	2.00	58.0	60.0	N/A	Muller, Berg et al. (2008), Ding, Gao et al. (2014)
Iron	µg/L	-	9.2	-	300	Muller, Berg et al. (2008)
Manganese	µg/L	0.059	0.17	18	100	Muller, Berg et al. (2008), Ding, Gao et al. (2014)

Constituent	Units	Concentration			Guidelines (SEPA 2002)	Data Sources
		Min	Median	Max		
Calcium	mg/L	22.9	41.3	60.4	N/A	Chetelat, Liu et al. (2008), Muller, Berg et al. (2008), Ding, Gao et al. (2014)
Magnesium	mg/L	5.28	8.1	61.4	N/A	Chetelat, Liu et al. (2008), Muller, Berg et al. (2008), Ding, Gao et al. (2014)
Sodium	mg/L	6.3	11.9	418	200	Chetelat, Liu et al. (2008), Muller, Berg et al. (2008), Ding, Gao et al. (2014)
Antimony	μg/L	0.88	0.965	1.05	5	Muller, Berg et al. (2008)
Arsenic	μg/L	1.45	2	4.08	50 C(III)	Wu (2005), Muller, Berg et al. (2008), Ding, Gao et al. (2014)
Cadmium	μg/L	0.016	0.039	0.082	5 C(III)	Wu (2005), Muller, Berg et al. (2008), Ding, Gao et al. (2014)
Chromium	μg/L	0.57	0.61	0.65	50 C(III)	Muller, Berg et al. (2008)
Cobalt	μg/L	0.21	0.24	0.27	1000	Muller, Berg et al. (2008)
Copper	μg/L	0.69	2.51	5	1000 C(III)	Wu (2005), Muller, Berg et al. (2008), Ding, Gao et al. (2014)
Lead	μg/L	0.07	0.455	1.4	50 C(III)	Wu (2005), Muller, Berg et al. (2008)
Mercury	μg/L	0.005	0.021	0.024	0.1 C(III)	Wu (2005), Muller, Berg et al. (2008)
Nickel	μg/L	2.42	3	5	20	Muller, Berg et al. (2008), Ding, Gao et al. (2014)
Selenium	μg/L	-	2.41	-	10 C(III)	Muller, Berg et al. (2008)
Thallium	μg/L	-	0.009	-	0.1	Muller, Berg et al. (2008)
Atrazine	ng/L	N.D.		140	3000	Han, Chen et al. (2009), Han, Chen et al. (2013)
Carbendazim	ng/L	0.43	52.8	104	N/A	Liu, Zhao et al. (2015)
DDT	ng/L	N.D.	0.32	78.0	1000	Hu, Sun et al. (2009), Liu, Yuan et al. (2010), Shi, Wang et al. (2011), Han, Chen et al. (2013), Tang, Huang et al. (2013)
Dimethoate	μg/L	N.D.	1.16	1.67	80	Muller, Berg et al. (2008), Han, Chen et al. (2009), Han, Chen et al. (2013)

Constituent	Units	Concentration			Guidelines (SEPA 2002)	Data Sources
		Min	Median	Max		
HCH	ng/L	0.06	2.03	84.5	5000	Hu, Sun et al. (2009), Liu, Yuan et al. (2010), Shi, Wang et al. (2011), Tang, Huang et al. (2013)
4-tert-OP	ng/L	0.127	1.66	4.85	N/A	Nie, Yan et al. (2015)
BPA	ng/L	N.D.	5.32	160	N/A	Shi, Wang et al. (2011), Shi, Hu et al. (2013), Shi, Liu et al. (2014), Nie, Yan et al. (2015)
DEHP	ng/L	N.D.	479	13095	8000	Muller, Berg et al. (2008), Shi, Wang et al. (2011), Zhang, Dong et al. (2012), Shi, Wei et al. (2013)
ΣPAEs	ng/L	250	420	1255	N/A	Zhang, Dong et al. (2012), Han, Chen et al. (2013)
PFOA	ng/L	7.38	9.19	119	N/A	Lu, Yang et al. (2013), Pan, Ying et al. (2014)
PFOS	ng/L	0.682	1.07	13.5	N/A	Lu, Yang et al. (2013), Pan, Ying et al. (2014)
Anthracene	ng/L	N.D.	2.65	7.20	N/A	Muller, Berg et al. (2008), He, Hu et al. (2011), Zhang, Dong et al. (2012), Shi, Hu et al. (2013)
Benzo(a)anthracene	ng/L	N.D.	1.40	94.9	N/A	Muller, Berg et al. (2008), He, Hu et al. (2011), Zhang, Dong et al. (2012), Shi, Hu et al. (2013)
Benzo(a)pyrene	ng/L	N.D.	0.60	11.9	2.8	Muller, Berg et al. (2008), He, Hu et al. (2011), Zhang, Dong et al. (2012), Han, Chen et al. (2013), Shi, Hu et al. (2013)
Benzo(b)fluoranthene	ng/L	N.D.	5.0	18.6	N/A	Muller, Berg et al. (2008), Ou, Liu et al. (2009), He, Hu et al. (2011), Zhang, Dong et al. (2012), Shi, Hu et al. (2013)
Benzo(k)fluoranthene	ng/L	N.D.	1.60	14.8	N/A	Muller, Berg et al. (2008), Ou, Liu et al. (2009), He, Hu et al. (2011), Zhang, Dong et al. (2012), Shi, Hu et al. (2013)
Fluorene	ng/L	N.D.	93.8	225	N/A	Muller, Berg et al. (2008), Ou, Liu et al. (2009), He, Hu et al. (2011), Zhang, Dong et al. (2012), Shi, Hu et al. (2013)
Indeno[1,2,3-cd]pyrene	ng/L	N.D.	1.70	88.9	N/A	Muller, Berg et al. (2008), Ou, Liu et al. (2009), He, Hu et al. (2011), Zhang, Dong et al. (2012), Shi, Hu et al. (2013)
Phenanthrene	ng/L	N.D.	5.45	702	N/A	Muller, Berg et al. (2008), Ou, Liu et al. (2009), He, Hu et al. (2011), Zhang, Dong et al. (2012), Shi, Hu et al. (2013)

Constituent	Units	Concentration			Guidelines (SEPA 2002)	Data Sources
		Min	Median	Max		
Pyrene	ng/L	N.D.	6.80	209	N/A	Muller, Berg et al. (2008), Ou, Liu et al. (2009), He, Hu et al. (2011), Zhang, Dong et al. (2012), Shi, Hu et al. (2013)
ΣPAHs	ng/L	20.0	1094	6306	N/A	Ou, Liu et al. (2009), He, Hu et al. (2011), Zhang, Dong et al. (2012), Shi, Hu et al. (2013)
ΣPCBs	ng/L	0.29	3.45	83.9	20	Han, Chen et al. (2009), Ou, Liu et al. (2009), Shi, Wang et al. (2011), Zhang, Shi et al. (2011)
Climbazole	ng/L	0.39	0.84	1.99	N/A	Liu, Zhao et al. (2015)
Clotrimazole	ng/L	N.D.	0.12	3.38	N/A	Liu, Zhao et al. (2015)
Miconazole	ng/L	0.18	0.28	4.62	N/A	Liu, Zhao et al. (2015)
DEET	ng/L	1.56	11.5	20.9	N/A	Liu, Zhao et al. (2015)
Sulfamethazine	ng/L	11.2	13.1	14.9	N/A	Wu, Huang et al. (2014)
Sulfamethoxazole	ng/L	8.3	225	701	N/A	Yang, Fu et al. (2011), Wu, Huang et al. (2014)
Triclocarban	ng/L	N.D.	5.73	54.3	N/A	Wu, Huang et al. (2014), Liu, Zhao et al. (2015)
Triclosan	ng/L	N.D.	2.04	23.1	N/A	Wu, Huang et al. (2014), Liu, Zhao et al. (2015)

Muller, Berg et al. (2008) in their study raised the question "how polluted is the Yangtze River?" Despite observations of ecosystem degradation, significant discharges of wastewater and agricultural activities including widespread use of fertilisers, pesticides and herbicides, the results of their extended sampling campaign in the lower Yangtze River indicated that concentrations of compounds originating from anthropogenic sources were comparable to other major rivers as a result of the diluting effect of the Yangtze's massive streamflow (Muller, Berg et al. 2008, Floehr, Xiao et al. 2013).

The results summarised in **Table 3-1** support this observation, with the majority of constituents conforming to the requirements of Chinese raw water class III (where applicable). However, there is some evidence that short term pollution at the estuary may be occurring; maximum concentrations of COD and BOD_5 exceed the class III thresholds and minimum dissolved oxygen levels are also below the specified threshold indicating elevated concentrations of oxidisable matter that could be associated with a pollution source such as wastewater discharge. Maximum chloride and sodium concentrations also exceed class III thresholds and are likely the result of saline intrusion in the estuary. The only constituents with median concentrations exceeding the class III thresholds are Total Nitrogen and Total Phosphorous. Nutrient enrichment is problematic to water supply as it can lead to the proliferation of algae that has implications for downstream treatment operations. Concentrations of all trace metals are low, with maximum concentrations below Class III levels. Most trace organic compounds are at low concentrations with the minimum values for many compounds below the limit of detection. The only trace organic compounds with maximum values exceeding Class III requirements are diethylhexyl phthalate (DEHP), Benzo(a)pyrene and combined polychlorinated biphenyls (ΣPCBs).

Caution should be applied in assuming that there is no risk to water quality in the Yangtze River resulting from trace metals or trace organic compounds for three key reasons:

1. The available data is from a limited number of samples which are probably insufficient to fully characterise the complexity of the system. As discussed in **Section 2.2**, the Yangtze River is an enormous system, with highly seasonal streamflow, and is subject to significant anthropogenic influence in the form of dams, diversions, urbanisation, agriculture and more. The Yangtze Estuary is over 100 km long, with multiple inflows including rivers, canals, and wastewater discharge locations, and is subject to tidal and saline influences. Water is extracted from at least 3 locations, Chenhang, Qingcaosha and Dongfengxisha, all of which are influenced by different hydraulic, hydrological and water quality factors. The potential characteristics and variations of water quality parameters are not sufficiently reflected through a single average value per month or per year to represent the whole estuary.
2. Although many of these constituents have no guideline set in the Environmental Quality Standards for Surface Water, this does not necessarily mean that they pose no risk to human

or environmental health; and

3. Presence in the water column is not necessarily the only pathway for these constituents to end up in the municipal supply. For example, decreases in measured trace metal loads in the Yangtze River are mainly caused by the retention of suspended particles in the many reservoirs and not by a decrease in emission of these contaminants to the river. Locations where these loads are being detained may become hot spots for contamination (Müller, Berg et al. 2012).

Muller, Berg et al. (2008) estimated that there could be as much as 500 to 3500 kg of industrial organic chemicals being discharged from the Yangtze per day and noted that when compared with previous monitoring data, the amounts of almost all observed parameters has increased (Muller, Berg et al. 2008). A detailed review of available studies was conducted by Floehr, Xiao et al. (2013) to further understand pollution in the Yangtze River; the conclusions of this study concur with the observations from Muller, Berg et al. (2008) that the immense amounts of water reduce the risk from pollution along the river but do not entirely eliminate it. Both studies highlighted the risks of both these pollutant loads being able to accumulate in the ecosystem, that continued increases in discharged pollutants could have disastrous effects for the Yangtze River and Estuary and that further monitoring of water quality in the river was required.

In this study, the following constituents are considered to be of concern:

- Salinity – because it affects the operation of coastal reservoirs and determines when water can be withdrawn from the estuary;
- Key nutrients nitrogen and phosphorous – because they have median concentrations that exceed Class III thresholds and can lead to algal blooming in coastal reservoirs; and
- Total suspended solids – because they are affected by coastal reservoir operation (pre-sedimentation) and can be a pathway for adsorbed contaminants.

Salinity is examined in further detail in **Section 3.2** and nutrients and suspended sediments in **Section 3.3**. Trace metals and trace organics are not considered further in this study as there is insufficient evidence to suggest that they are constituents of concern for municipal supply. In this thesis local sources of pollution have been largely ignored because collected water quality data indicates that at present, the diluting capacity of the Yangtze River's streamflow is sufficient to make average concentrations problematic pollutants low enough that they are not an issue for water supply. For short periods where extremely high concentrations of problematic constituents occur (e.g. chemical spills), it is assumed that the operating rules of the coastal reservoirs are sufficient to prevent issues with the water supply.

It is recommended, especially in consideration of the pace and scale of development in Shanghai Municipality and the Yangtze Estuary, that further studies including intensive

sampling in and around Shanghai's coastal reservoirs to ascertain that trace metals and trace organics, especially emerging contaminants, do not pose a risk to Shanghai's water supply and that the water quality impacts of local development and pollution sources should be considered in more detail in future research on water supply in from the Yangtze Estuary

3.2 Saline Intrusion

Salinity and its extent in the Yangtze estuary is of serious concern as it can have a significant effect on the intake of freshwater from the estuary for water supply in Shanghai; this could have a severe impact on water security (Qiu and Zhu 2013). Salinity is a measure of total dissolved solids (TDS), which usually comprises calcium, magnesium, sodium and potassium cations, as well as carbonate, bicarbonate, chloride, sulphate and nitrate anions (World Health Organization 2003). The quality of a water source with respect to salinity can generally be characterised by its palatability as there is no reliable data available on the health effects of TDS in drinking water (World Health Organization 2003):

- Excellent: TDS < 300 mg/L
- Good: TDS = 300 – 600 mg/L
- Fair: TDS = 600 – 900 mg/L
- Poor: TDS = 900 – 1200 mg/L
- Unacceptable: TDS > 1200 mg/L

Another consideration for water with TDS concentrations higher than 500 mg/L is that certain constituents such as chlorides, sulphates, calcium and carbonates can cause corrosion or scaling in water distribution systems and water heating devices (World Health Organization 2003). China's Environmental Quality Standards for Surface Water (SEPA 2002) requires that Chloride concentrations be restricted to 250 mg/L. The ratio of Chloride to total ions in seawater is approximately 19.2 g/kg to 34.7 g/kg (55.3%) (Byrne, Mackenzie et al. 2020). Therefore, a maximum TDS concentration of approximately 450 mg/L (250 mg/L multiplied by 34.7/19.2) would be required in order to meet the required raw water standard unless desalination technologies were applied during the water treatment process.

Multiple numerical modelling studies have been done to investigate hydrodynamic conditions in the estuary and the factors that influence the pattern and intensity of saline intrusion events. These numerical studies indicate that saline intrusion into the estuary is primarily controlled by the hydrodynamic behaviour in the estuary, which is mainly influenced by freshwater discharge from the Yangtze River and tidal effects at the estuary mouth, but is also affected by wind speed and direction (Zhang and Chen 2003, Dai, Chu et al. 2011, Cai, Savenije et al. 2015, Li, Chen et al. 2015). Another significant factor affecting the hydrodynamic behaviour of the estuary is the bathymetry of the estuary which has undergone significant changes as a result of both natural processes such as tide and wave action and changes in river streamflow, and the influence of the many engineering projects carried out not only in the nearshore zone (refer **Section 2.2.2**) but also damming and other activities in the Yangtze Basin which alter the supply of sediment to the estuary (Mei, Dai et al. 2018). Modelling conducted by Wan, Gu et al. (2014) to investigate the effect of bathymetric changes in the estuary on hydrodynamic behaviour found that the peak water level in the main channel of the Yangtze Estuary increased between 1998-2009 by 0.2-0.5 m as a

result of the changing bathymetry. While the effects of these bathymetric changes are remarkable, the changes could not be attributed to any one local project and is a result of a combination of factors including natural processes, extreme meteorological effects and engineered interventions (Wan, Gu et al. 2014). It is unclear what the future impacts of the hydrodynamic evolution of the estuary and its influence on conditions in the estuary will be (Wan, Gu et al. 2014).

The discharge of freshwater from the Yangtze River is a key factor controlling salinity levels in the estuary region where Shanghai sources drinking water. The difference between the flood and dry seasons on salinity is significant. In the flood season, salinity in the south branch is restricted by the significant freshwater flow, and salinity in the upper half of the north branch can be controlled by freshwater flow. As a result, intrusion into the south branch (Refer **Figure 3-2**) generally weakens around Changxing Island (80-100 km from Xulijing). During the dry season however, when the river discharge is low and the tide is high, salinity exceeding acceptable limits for water supply can occur near the Chenhang Reservoir intake or spill into the South Branch via the North Branch prevents extraction for drinking water can be as far up the estuary as Xuliujing where the river and estuary meet (Dai, Chu et al. 2011, Li, Chen et al. 2015). Due to the configuration of the Yangtze Estuary, the north branch receives less than 1% of the freshwater inflow from the Yangtze River and as a result water entering through the north branch can reach TDS concentrations as high as 25,000 mg/L (virtually 100% seawater) (Zhang, Savenije et al. 2011, Qiu and Zhu 2013, Li, Chen et al. 2015).

Figure 3-2: The Yangtze Estuary and Distances from Xuliujing where the river and estuary meet. Key locations are marked in red and salinity measurement stations in yellow. Aerial photo: NASA Earth Observatory (2017)

The highest contributions from the north branch occur during the low flow December to March period, during spring tides, especially when accompanied by strong south-easterly winds (Webber, Li et al. 2015). In 1978-1979, during one of the driest years on record, the mouth of the Huangpu River (70 km from Xuliujing) had a salinity that exceeded the drinkable limits (TDS > 0.45 mg/L) for 102 consecutive days (Yang and Kelly 2015). Serious saline intrusions also occurred reaching the Chenhang Reservoir (45 km from Xuliujing) during 1978-1979, 2001-2002 and 2006-2007 (Webber, Li et al. 2015). During the drought year 2006, saline intrusion occurred during 285 days in the estuary; 75 of these days recorded chloride concentrations over 250 mg/L (the drinking water limit, TDS 450 mg/L) and 60% of these events occurred in October and December. In the same year, there were 48 occurrences of chloride concentrations over 400 mg/L (the limit for industry and agriculture, TDS 620 mg/L), of which 40% occurred in October (Dai, Chu et al. 2011).

As discharge measured at Datong falls below critical levels, high salinity conditions at the Yangtze Estuary are increasingly likely. The intensity and duration of elevated salinity levels is generally controlled by how low the flow rate falls below this threshold and how long it holds at low rates. (Li, Chen et al. 2015). Li, Chen et al. (2015) compared salinity levels at three locations in the estuary with streamflow in the Yangtze River at Datong accounting for the travel time between Datong and the estuary (7 days). The three locations considered were Gaoqiao near the mouth of the Huangpu River, Chenhang near the Chenhang reservoir and Chongtou where the north and south branch of the estuary (refer **Figure 3-2**). The relationship between lagged flow at Datong and TDS is presented in **Figure 3-3**. It is estimated water will be unsuitable for water supply with regards to TDS concentration will occur when flow at Datong falls below approximately 11,000 m^3/s, 12,500 m^3/s, and 14,800 m^3/s at Gaoqiao, Chenhang and Chongtou respectively. Based on these thresholds, periods of raw water unsuitability can be expected to mainly occur in January, February and December, and could also be an issue in March and November in particularly dry years (refer **Figure 2-9** for monthly streamflow at Datong). It should be noted that there is a high degree of variability in these estimates which could be caused by multiple factors including natural effects (wind, waves, tides, streamflow variation) and the effects of engineering projects and changing bathymetry in the estuary. Also, the effect of saline intrusion via the north branch of the estuary is evident with the mean TDS at Chongtou and Chenhang exceeding the critical threshold at higher streamflows than Gaoqiao.

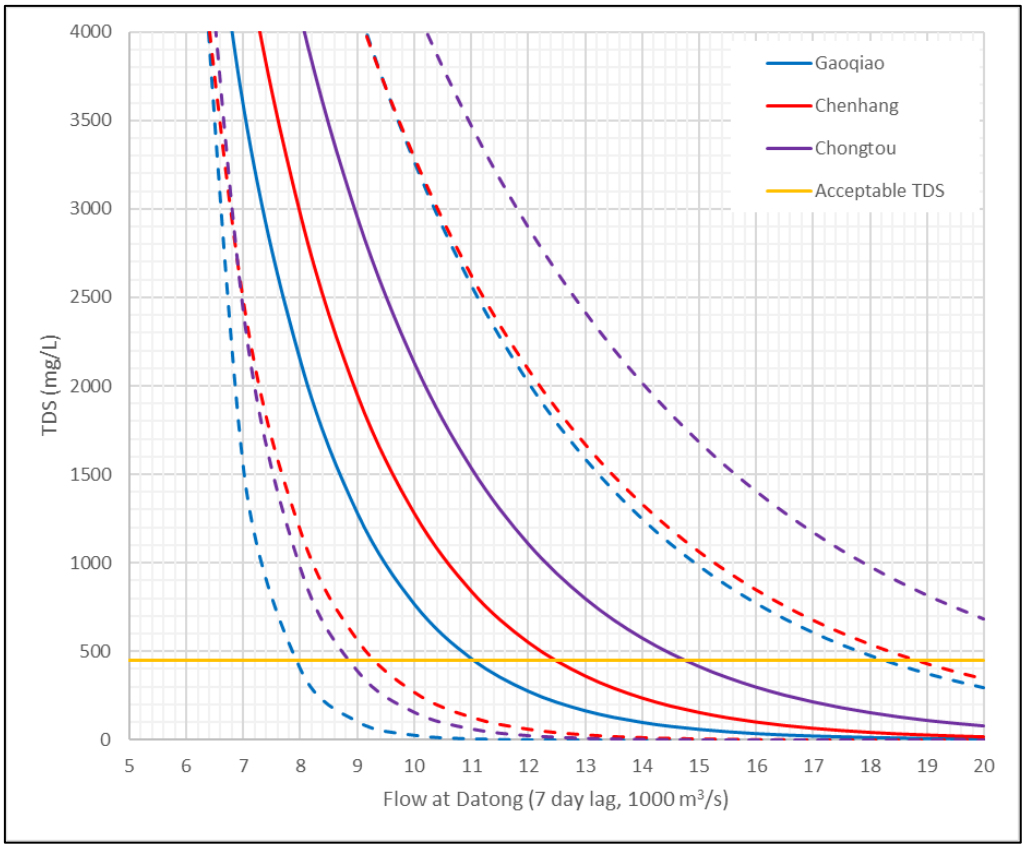

Figure 3-3: Comparison between flow at Datong with 7-day lag and TDS at the estuary. Adapted from Li, Chen et al. (2015). Note that conversion has been made from practical salinity to TDS for convenience assuming S = 1 is equivalent to TDS 1000 mg/L. Dashed lines represent estimates of maxima and minima.

There are additional factors that could affect the risk of saline intrusion into the estuary including engineering projects such as dams and water diversions which alter the seasonality and/or quantity of freshwater arriving at the estuary as well as factors such as sea level rise. As discussed in **Section 2.2.2**, while the operation of dams in the Yangtze River appears to have had no effect on the overall volume of water discharged from the river, the operation of the Three Gorges Dam has had a redistributive effect on flows in the river. 3D hydrodynamic modelling conducted by (Qiu and Zhu 2013) suggests that the runoff regulation by the Three Gorges Dam has a significant effect on the behaviour of saline intrusion in the estuary. The occurrence of saline intrusion in the estuary occurs earlier during the autumn season with slightly increased intensity, however significantly reduced the intensity and duration of saline intrusion around the locations where Shanghai withdraws its drinking water (Qingcaosha, Chenhang and Dongfengxisha). It was estimated that the duration of water with salinity too high for use as drinking water (TDS > 450 mg/L) at these locations was reduced by 48%, 73% and 16% respectively as a result of the dam's operation. The Three Gorges Dam therefore can be considered to have a mitigating effect on the risk of saline intrusion at the estuary.

Unlike the effect of dams, the effect of water diversions, especially those in the Lower Yangtze River downstream of Datong, have the potential to significantly reduce flow at critical times and

increase the risk of saline intrusion (Chen, Webber et al. 2013). As discussed in **Section 2.2.2**, the capacity for withdrawal from the Lower Yangtze River between Datong and Xuliujing is 5,600 m^3/s during the dry season alone. Full capacity extraction during the dry season in this reach of the river would exacerbate the risk of salinity preventing water diversion for water supply from the estuary. The significant abstraction capacity downstream of Datong is also a limitation of using streamflow measurements at Datong as the basis for determining critical levels of flow in the estuary; these abstractions for the use in surrounding cities have the potential to significantly vary flow relative to values observed at Datong (Chen, Webber et al. 2013).

The effect of sea level rise has the potential to push saline water further upstream in estuaries, which in the Yangtze Estuary could have similar implications for the magnitude and duration of high salinity in areas relevant to Shanghai's water supply as periods of low streamflow from the Yangtze River (Chen, Chen et al. 2016)(Zhang and Chen 2003, Dai, Chu et al. 2011, Li, Chen et al. 2015). The first projections of local sea level rise along Shanghai's coastline were made in 1996 and indicated rises of 10-25 cm by 2010, 20-40 cm by 2030 and 50-70 cm by 2050 relative to a 1991 benchmark (Cheng, Chen et al. 2018). There are several factors that contribute to change in relative sea level in Shanghai's coastal area and the Yangtze Estuary which are summarised as follows:

- Eustatic sea level rise caused by climate change;
- Changes in geodetic height of Shanghai Municipality resulting from tectonic subsidence and local subsidence; and
- Changes in local sea level due to geomorphic changes in the estuary.

Eustatic sea level rise has accelerated as a result of climate change with climate research suggesting that human activities will lead to a long term future sea level rise of up to 1.9m higher by 2100 (Cheng, Chen et al. 2018). The loss of geodetic height in Shanghai was noticed and monitored from as early as 1932. The majority of loss in height was the result of excessive groundwater withdrawals in Shanghai which up until the 1960's the average subsidence rate of 40 mm/a (Webber, Barnet et al. 2015, Cheng, Chen et al. 2018). Due to strict legislation controlling the extraction of groundwater and artificial recharge of groundwater, the average subsidence rate is less than 5 mm/a (Cheng, Chen et al. 2018). The contribution of tectonic subsidence to overall loss of geodetic height is approximately 1 mm/a (Cheng, Chen et al. 2018). Local factors causing local sea level rise include land reclamation projects in the estuary (the North Branch Reclamation Project, the Hengsha Reclamation Project, The Pudong International Airport and Nanhui Siltation Reclamation Project) and the Deepwater Navigation Channel Project (Cheng, Chen et al. 2018). Some local sea level fall is predicted due to erosion associated with a decrease in sediment supply to the estuary (Cheng, Chen et al. 2018).

Analysis by Cheng, Chen et al. (2018) suggests that local sea level rise in the Yangtze Estuary is lower than the 1996 estimates with only a 5.2 cm increase in measured sea level rise having

occurred by 2010. Based on a tectonic subsidence rate of 1 mm/a, an urban subsidence rate of 3-5 mm/a, a eustatic sea level rise of 2 mm/a (total of 4 cm between 2011 and 2030), a local sea level rise of 8-10 cm due to local engineering projects and a local sea level fall of 2-10 cm due to erosion in the estuary, a total local sea level rise of 10-16 cm is predicted by 2030 (relative to 2010 levels) (Cheng, Chen et al. 2018). This prediction of local sea level rise in Shanghai is equal to 15.2-21.2 cm between 1991 and 2030, which is lower than the initial 1996 estimate of 20-40 cm.

The rise in eustatic sea level could pose a particular issue in the years to 2100 considering that there a significant difference between the estimated 4 cm increase predicted by Cheng, Chen et al. (2018) and the potential 1.9m rise that may arise from human induced climate change. Chen, Chen et al. (2016) investigated the effects of eustatic sea level rise on the availability of fresh water (i.e. TDS < 250 mg/L) at Shanghai's coastal reservoirs under a 0.5 m, 1 m, and 2 m sea level rise scenarios using a 3D hydrodynamic model. Results of this investigation indicate that:

- Under a 0.5 m sea level rise scenario, the increase in total number of days in an average month during the dry season that salinity exceeds TDS 450 mg/L relative to current conditions is 0.6 days at Qingcaosha, is 4.9 days at Chenhang and is 4 days Dongfengxisha;
- Under a 1 m sea level rise scenario, the increase in total number of days in an average month during the dry season that salinity exceeds TDS 450 mg/L relative to current conditions is 18.3 days at Qingcaosha, is 26 days at Chenhang and is 27.6 days Dongfengxisha;
- Under a 2 m sea level rise scenario, the increase in total number of days in an average month during the dry season that salinity exceeds TDS 450 mg/L relative to current conditions is 18.3 days at Qingcaosha, is 28.4 days at Chenhang and is 31 days Dongfengxisha;
- A sea level rise of 1 m or greater would result in the Qingcaosha Reservoir and Dongfengxisha Reservoir having virtually no access to freshwater during the dry season (approximately 30 days per month); and
- At Chenhang reservoir, under 1 m sea level rise, the longest period of successive salinity exceeding drinking water standards is estimated to be 11.7 days, while under the 2 m sea level rise scenario, the reservoir would have no access to freshwater during the dry season (approximately 30 days per month).

The effects of sea level rise and water abstraction from the Lower Yangtze River pose a significant risk to ensuring fresh water supply from the estuary, especially during the dry season. To secure water supplies from the estuary it will be necessary to increase both the volume of water that Shanghai can store in the estuary and the length of time it can be stored for to meet these challenges.

3.3 Nutrients and Sediment Concentrations at the Yangtze Estuary

3.3.1 Characterisation of Nutrient and Sediment Concentrations

The key nutrients Nitrogen and Phosphorous, and Total Suspended Solids were identified in **Section 3.1** as constituents of concern. Data was collected from published literature for both Datong Station and the Estuary between Xuliujing and the estuary mouth from the time period 1990-2015. In addition to concentration data for Total Nitrogen and Total Phosphorous, data for dissolved inorganic fractions were also collected. Data on organic fractions is not readily available and has been excluded from this analysis; total suspended solids concentrations give some insight into the likely trends of organic nitrogen and organic phosphorous which are typically bound up in these suspended solids. Data reduction techniques were applied to produce an annual series and a monthly series with one concentration estimate per time step. Data sources are summarised in **Appendix 2**.

The annual series of concentrations of Total Nitrogen and Phosphorous and their inorganic fractions have been plotted in **Figure 3-4** and **Figure 3-5**. The relative lack of data points for TN and TP at Datong makes it difficult to compare results with those observed at the Estuary. Comparison of the annual series for Nitrate and Ammonium concentration between Datong and the Estuary shows that average concentrations at the two stations are comparable, however do not directly correspond. This is to be expected as not only do methods, timescales, and sampling times vary between studies, but there is also over 500 km (7 days travel time) between the two locations which is heavily developed. Similar observations can be made for DIP and TSS, both stations are within the same order of magnitude, but otherwise do not correspond. In general, similarity between the two stations indicates that data captured at Datong actually provides reasonable insight into the average concentrations for dissolved inorganic nitrogen (DIN) and DIP at the estuary.

General increases in concentration over time for both Nitrate and Ammonium concentration can be observed, however no clear increase over time for TN is observable due to lack of data. There is an inter-annual variability in the Nitrate and Ammonium annual series that is larger than the overall long-term increase in mean concentration. This variability indicates that either monthly variability or local factors like local pollution sources, mixing, tides have a significant effect on the reported concentrations. Concentrations for TP and DIP concentrations also appear to be increasing over time. As there are lower amounts of intra-annual data available for these parameters, it is difficult to observe the significance of variability compared with the overall average. The few years that do have a range of data appear to show that the intra-annual generally larger than the inter-annual variability.

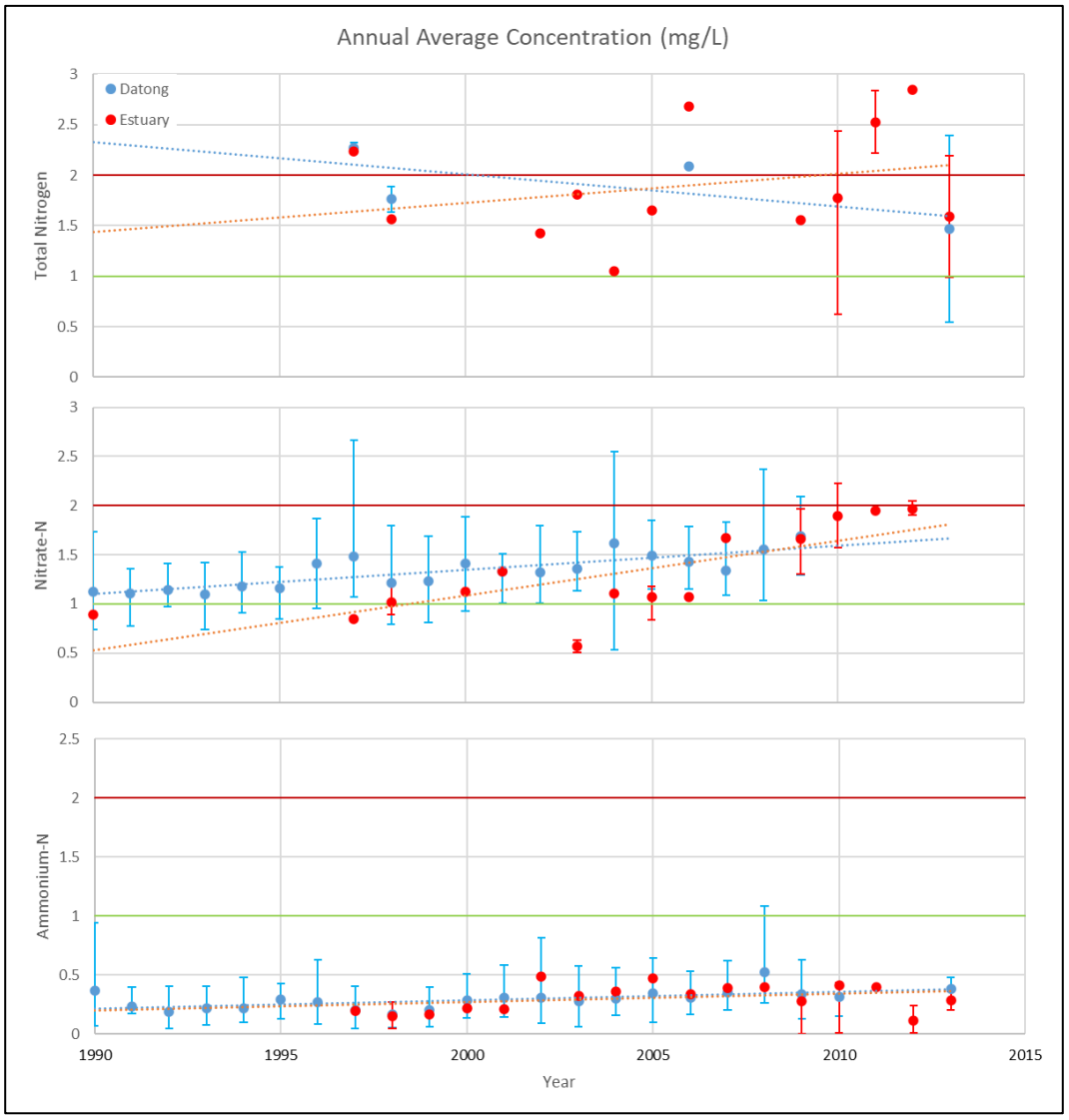

*Figure 3-4: Annual Average Concentration (1990-2013) of Total Nitrogen, Nitrate and Ammonium at Datong and the Estuary. Refer to **Appendix 1** for data source tables. Error bars represent range. Dotted lines are lines of best fit. Green lines represent Chinese water quality class III threshold for TN and Ammonium and maroon line represents class V threshold for TN and Ammonium. Nitrate is compared with the TN thresholds*

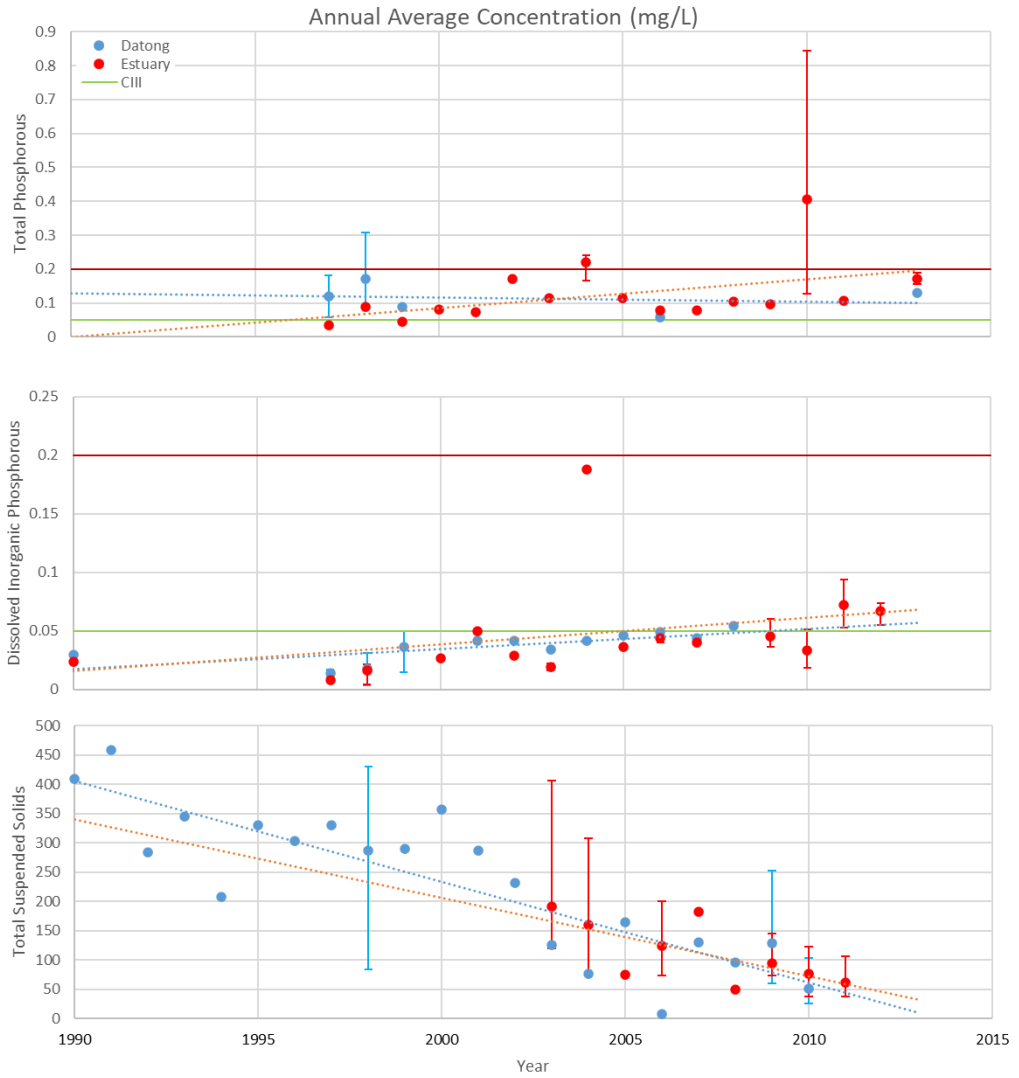

Figure 3-5: Annual Average Concentration (1990-2013) of Total Phosphorous, Dissolved Inorganic Phosphorous and Total Suspended Solids at Datong and the Estuary. Refer to ***Appendix 1*** *for data source tables for TP and DIP. TSS data at Datong is from Dai, Du et al. (2011). Refer* ***Table 3-1*** *for the source of TSS data at the estuary. Error bars represent range. Dotted lines are lines of best fit. Green lines represent Chinese water quality class III threshold for TP for lakes and reservoirs and maroon line represents class V threshold for TP for lakes and reservoirs. The lakes and reservoirs threshold has been selected as this water will be diverted to coastal reservoirs for use. DIP is compared with the TP thresholds. No quality restrictions are available for TSS.*

To assess the likelihood of a trend being present in the data, a Mann-Kendall analysis was conducted. Mann-Kendall analysis is a simple method for detecting a monotonic trend in time series data that compares each value in the series against all previous values to determine if the overall direction of the data is increasing, decreasing or no change is evident (Meals, Spooner et al. 2011, Helsel, Hirsch et al. 2020). The Mann-Kendall test is a method for trend testing recommended by the US Geological Survey for water resources that can be applied to data sets that do not conform to any particular distribution and contain missing data (Meals, Spooner et al. 2011, Helsel, Hirsch et al. 2020). The seasonal version of the Mann-Kendall test has been previously applied to detect trends in nutrient concentrations at Xuliujing (Gao, Li et al. 2012).

A null hypothesis that no trend in the data is present was adopted, and the significance testing with a confidence level (α) of 0.05 was conducted. The results of the Mann-Kendall test are summarised in **Table 3-2**. The results indicate that increasing trends are present in the Nitrate and DIP concentration at both the Estuary and Datong which may be caused by increased fertiliser application in the basin. Increasing trends in Nitrate and Phosphate (DIP) at Xuliujing were also detected by Gao, Li et al. (2012) using the seasonal Mann-Kendall test. Increasing trends in Ammonium concentration at Datong were detected which may indicate the presence of fresh pollution, and that a decreasing trend is present in TSS at Datong which is likely the result of upstream dam construction. Factors affecting nutrient and sediment concentrations arriving from the Yangtze River are examined further in **Section 3.3.2**. For TN and TP as well as Ammonium and TSS at the estuary, there is insufficient evidence to support rejecting the null hypothesis. It is possible that the small sample sizes make it hard to detect the presence of a trend. To determine the magnitude of the trends predicted in the Mann Kendall analysis, Sen's Slope can be used (Meals, Spooner et al. 2011, Helsel, Hirsch et al. 2020). Sen's Slope was calculated for each series and linear trends estimating the average concentration of each series using Sen's Slope with upper and lower 95% confidence intervals have been plotted in **Figure 3-6** to **Figure 3-11**.

Chinese raw water quality standards (refer **Section 2.3.1**) require that class III (drinking) water requires TN of less than 1 mg/L and TP of 0.2 mg/L for rivers or 0.05 mg/L for reservoirs. All observed mean concentrations of TN (**Figure 3-4**) at both stations exceeded Class III thresholds. In fact, class V thresholds (the worst class) were exceeded in 1997, 2006, 2011 and 2012. With the exception of 2012, all of these years were drier than average (Refer **Figure 2-8** in **Section 2.3.1**) and elevated concentrations may have been caused by the lower streamflow having a lower capacity to dilute TN concentrations. All observed mean concentrations of TP after the year 2000 (**Figure 3-5**) also exceeded Class III thresholds for reservoirs, which is probably the more relevant target considering Shanghai's use of coastal reservoirs. Class V thresholds (0.2 mg/L for reservoirs) were also exceeded by TP concentrations in 2004 and 2010.

Concentrations of Nitrate, Ammonium and DIP appear to be forming and increasingly large portion of TN and TP concentrations. All concentrations of Nitrate at Datong and most

concentrations at the Estuary (except 1990, 1997 and 2003) greater than 1 mg/L, meaning that the class III threshold for TN is exceeded by nitrate concentration is exceeded by the Nitrate fraction alone. The trend of annual average nitrate concentration presented in **Figure 3-7** indicates that Nitrate concentrations at Datong could exceed the TN Class V threshold alone by 2027, while **Figure 3-6** indicates that this may have already happened at the estuary. For DIP, the estimated trends indicate that DIP concentrations exceeded the Class III threshold for TP in 2007 (**Figure 3-9**) at the estuary and 2008 at Datong (**Figure 3-10**). While it appears unlikely that DIP could exceed the Class V TP threshold (0.2 mg/L) alone, after 2005 DIP appears to account for as much as 50% of TP present at the Estuary (**Figure 3-5**).

Table 3-2: Mann-Kendall Test Summary for Nutrient Data in the Yangtze Estuary

	TN		NO_3-N		NH_4-N		TP		DIP		TSS	
	Estuary	**Datong**	**Estuary**	**Datong**	**Estuary**	**Datong**	**Estuary**	**Datong**	**Estuary**	**Datong**	**Estuary**	**Datong**
Number of samples, n	12	4	13	20	17	22	16	5	15	12	9	19
Mann Kendall Statistic	14	-4	54	125	37	114	33	-2	63	38	-18	-105
Standard Error	14.58	2.94	16.39	30.82	24.28	35.41	21.81	4.08	20.07	14.25	9.59	28.58
z-statistic	0.89	-1.02	3.23	4.02	1.48	3.19	1.47	-0.24	3.09	2.60	-1.77	-3.64
p-value (assuming twin tailed distribution)	0.37	0.31	0.001	0.0001	0.14	0.001	0.14	0.81	0.002	0.009	0.076	0.0003
Trend Detected?	No	No	Yes Increasing	Yes Increasing	No	Yes Increasing	No	No	Yes Increasing	Yes Increasing	No	Yes Decreasing

Note: for details of Mann-Kendall method and terminology refer to Helsel, Hirsch et al. (2020)

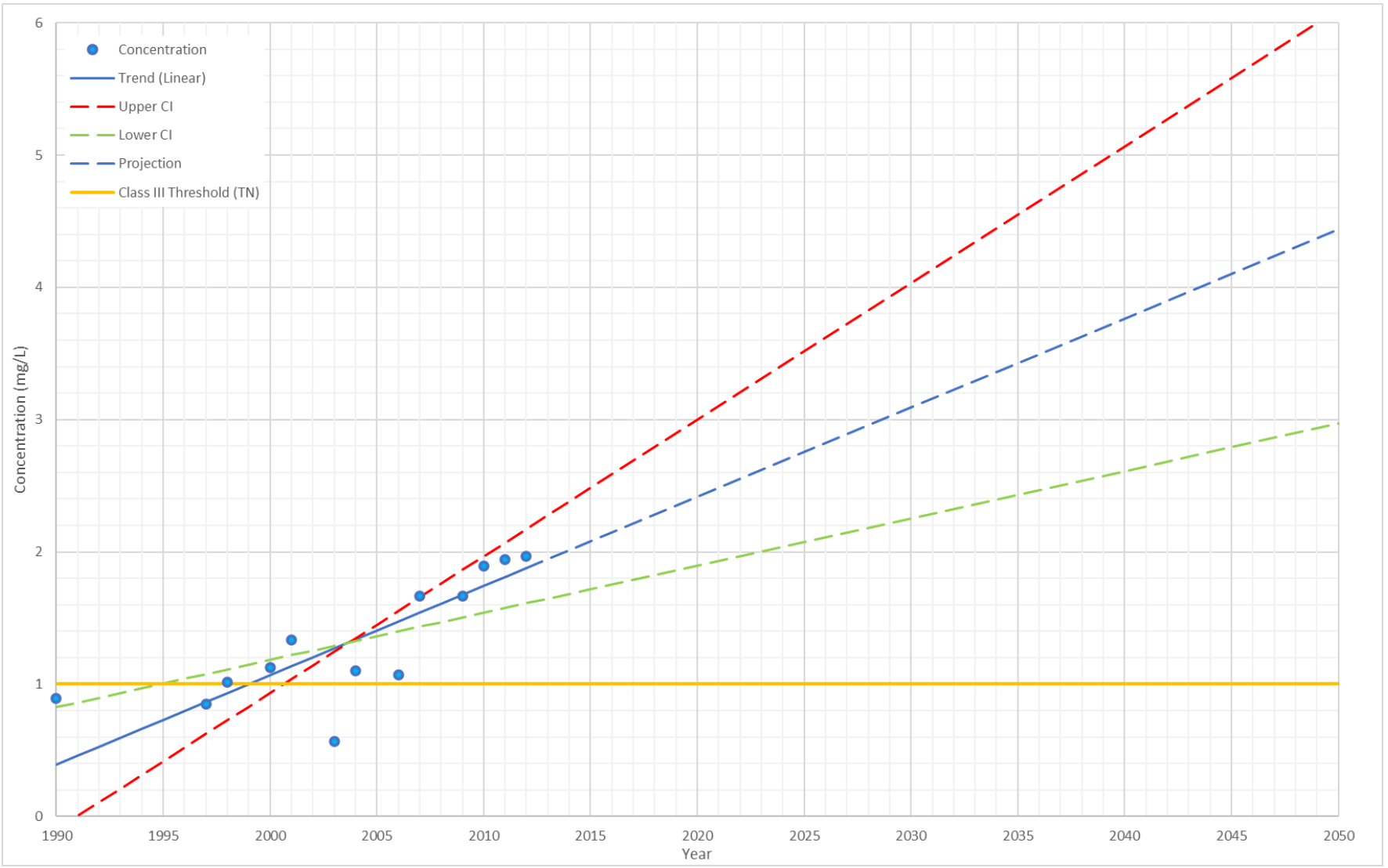

*Figure 3-6: Nitrate-N concentration at the Yangtze Estuary with linear trend calculated using Sen's slope. Refer to **Appendix 1** for data source tables.*

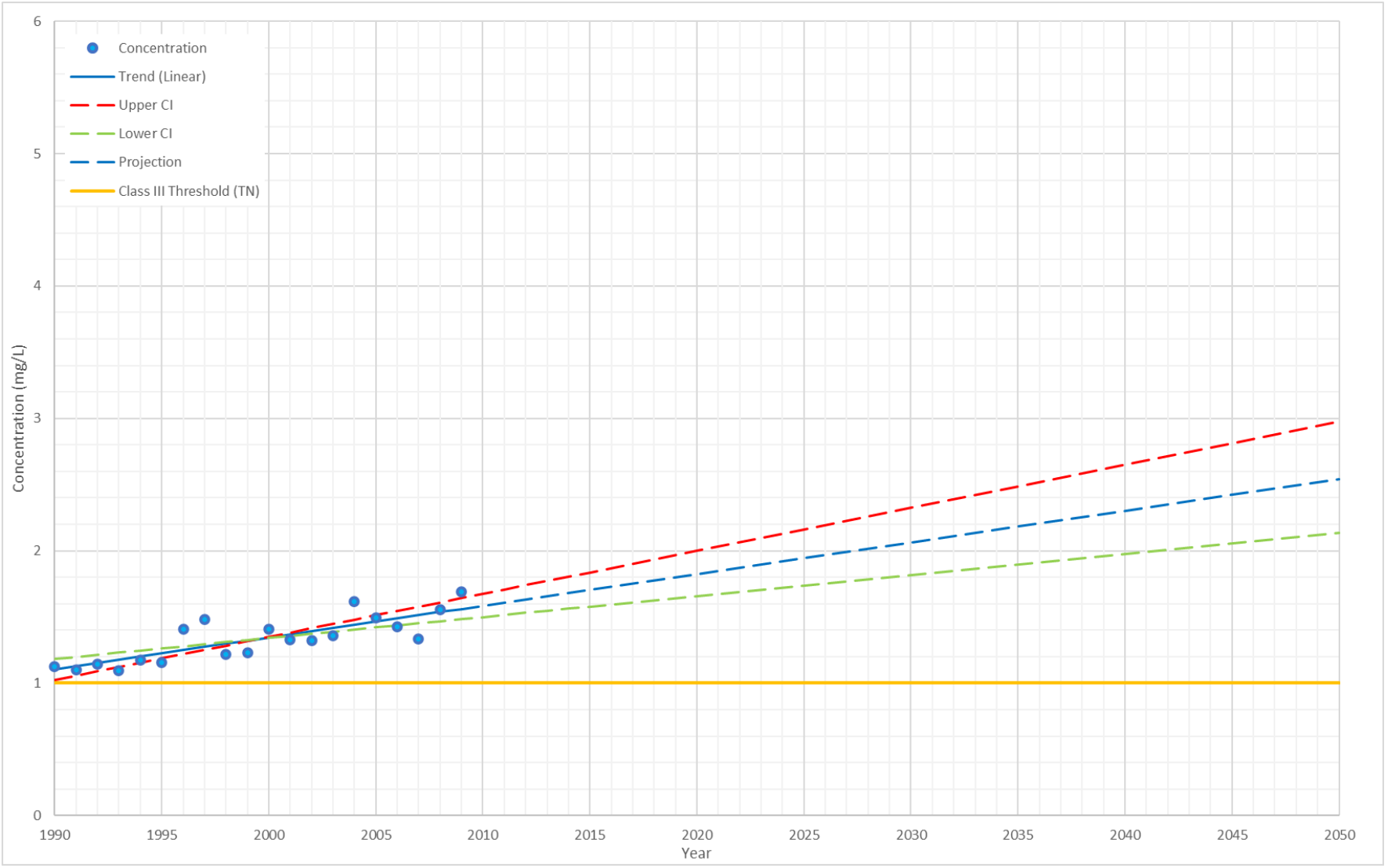

Figure 3-7: Nitrate-N concentration at the *Datong* with linear trend calculated using Sen's slope. Refer to Appendix 1 for data source tables.

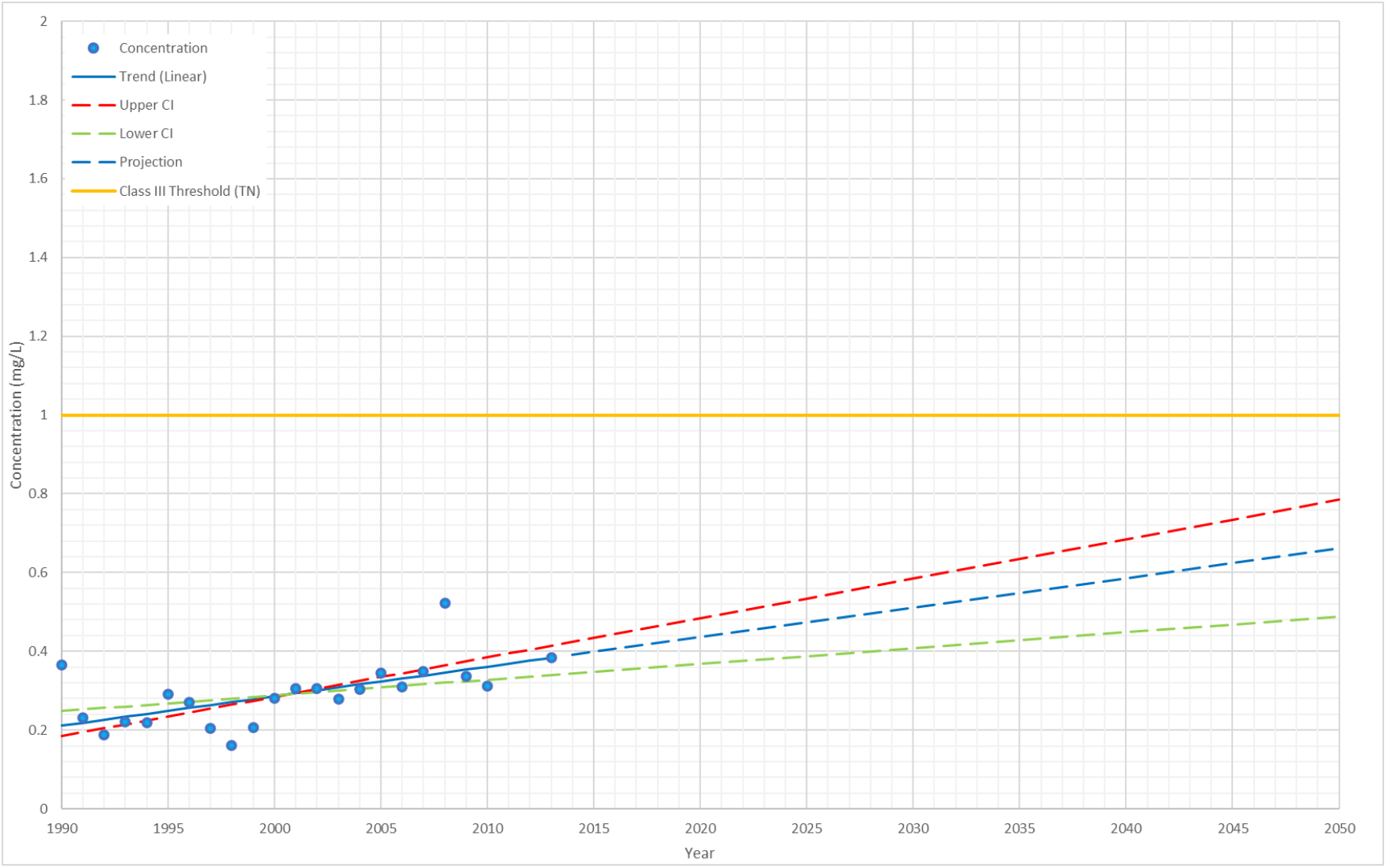

*Figure 3-8: Ammonium-N concentration at the Datong with linear trend calculated using Sen's slope. Refer to **Appendix 1** for data source tables.*

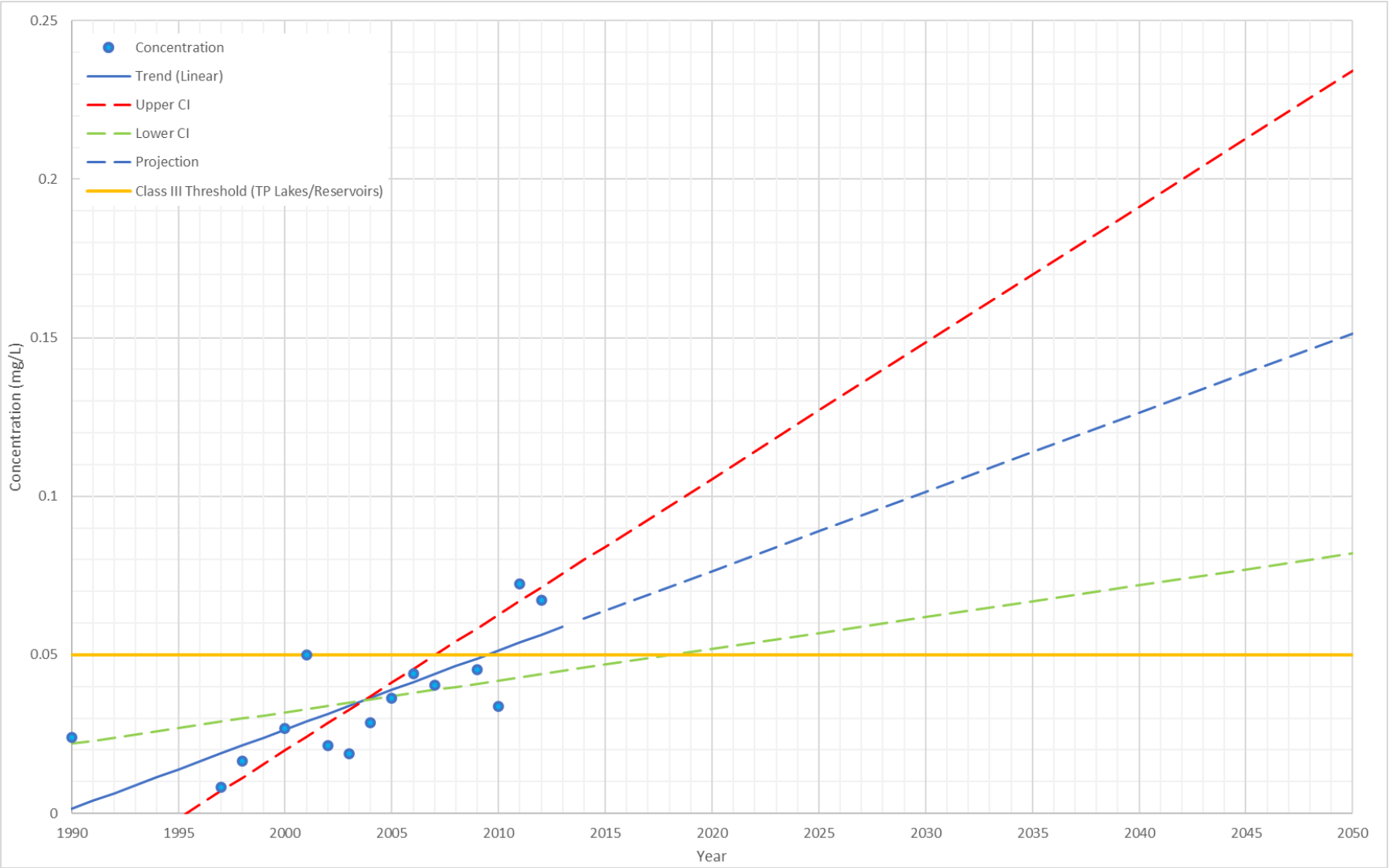

*Figure 3-9: DIP Concentration at the Estuary with linear trend calculated using Sen's slope. Refer to **Appendix 1** for data source tables.*

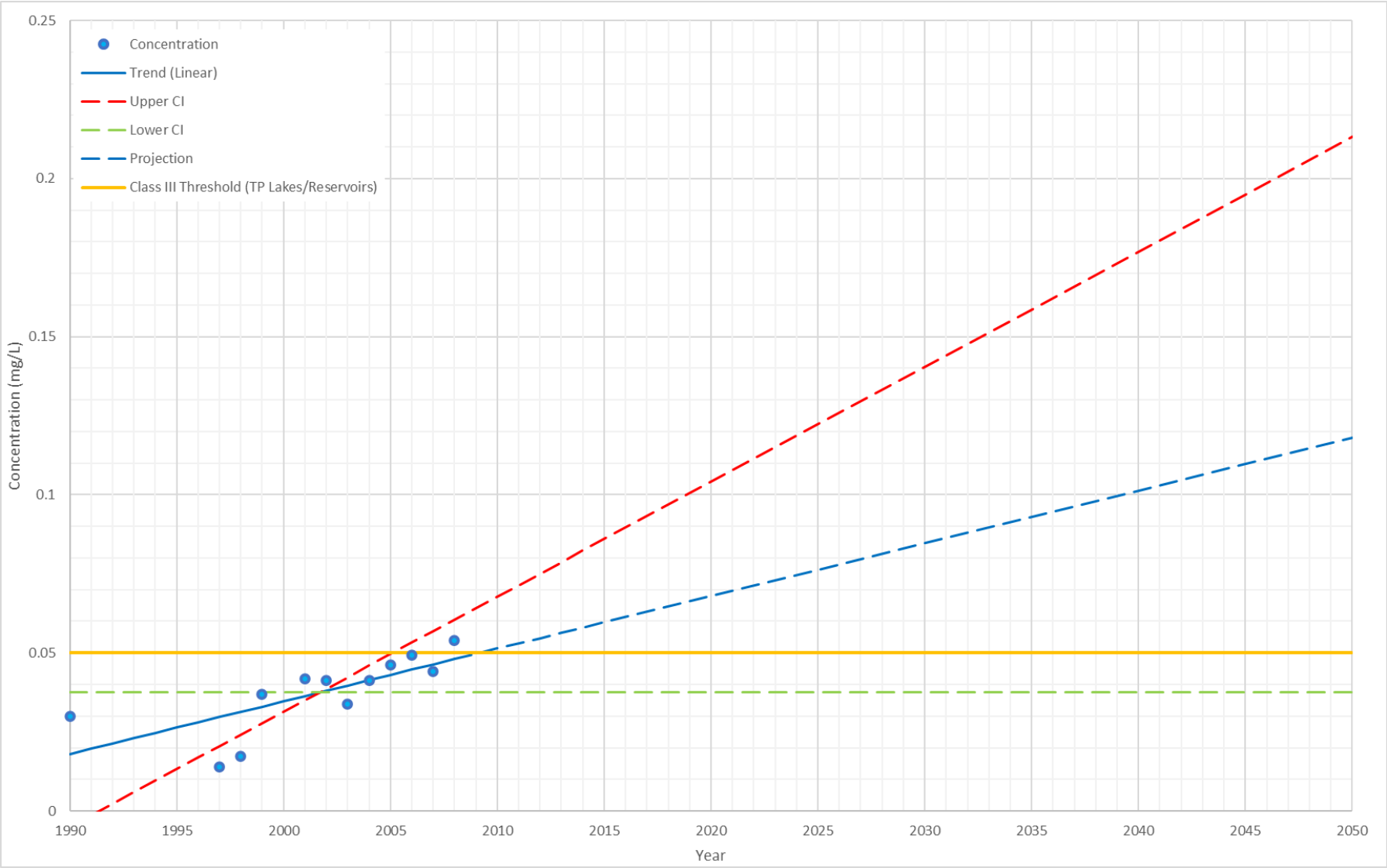

*Figure 3-10: DIP Concentration at Datong with linear trend calculated using Sen's slope. Refer to **Appendix 1** for data source tables*

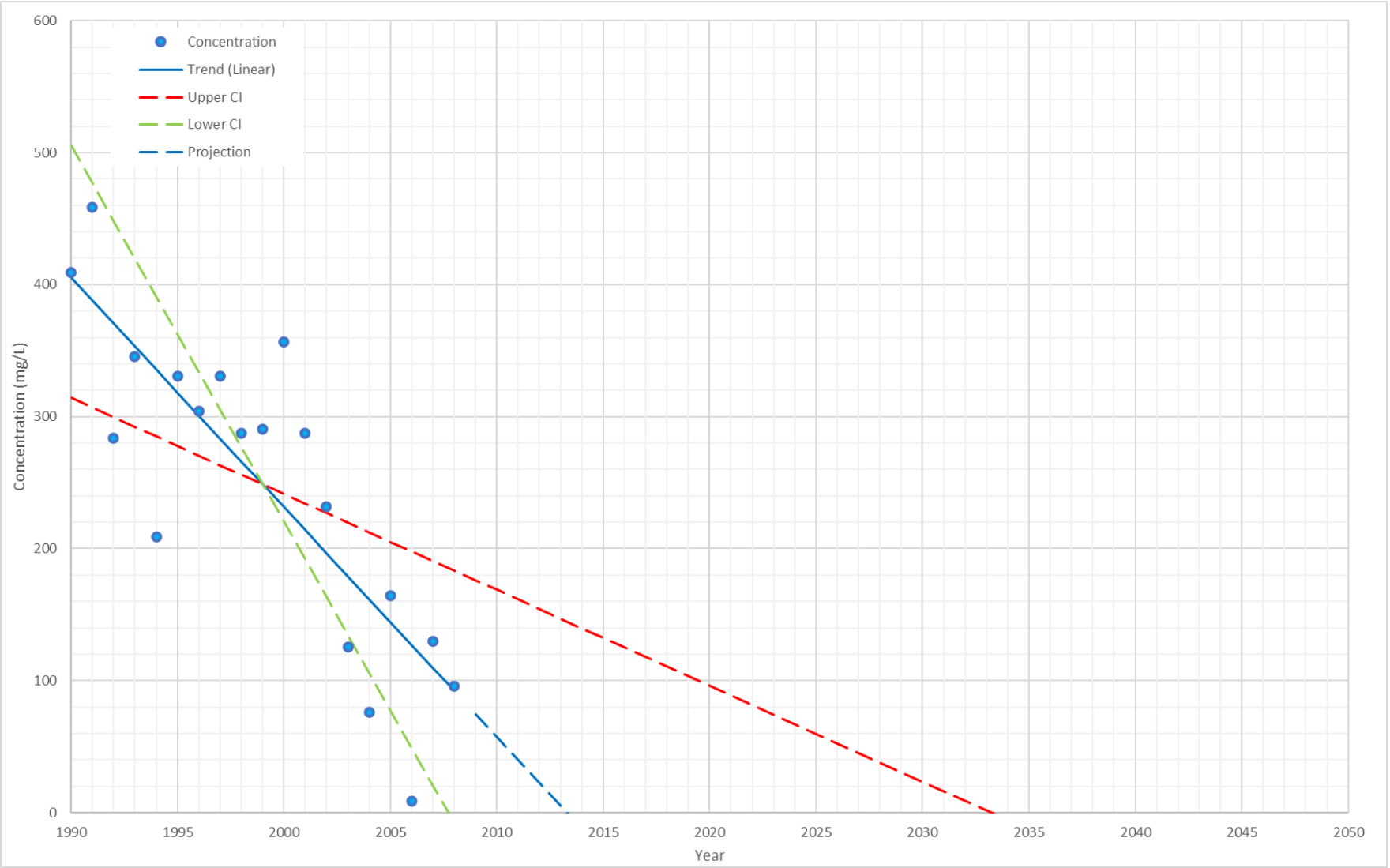

Figure 3-11: TSS Concentration at Datong with linear trend calculated using Sen's slope. Data from Dai, Du et al. (2011).

Several studies have also observed significant increases in concentrations of nutrients in historical data, in particular inorganic nitrogen. Yan, Zhang et al. (2003) examined nitrogen (as Nitrate) concentrations in the Yangtze River from 1968-1997 at Datong and found that concentrations had increased tenfold over this period. It was observed that Nitrogen fertiliser application and population density were good predictors of nitrate concentration and flux in the Yangtze River. Sun, Shen et al. (2013) conducted further analysis into dissolved inorganic nitrogen from 1990-2009 and found concentrations at Datong continued to increase over the period of record. Analysis by Gao, Li et al. (2012) found that the concentrations of both Nitrate and Phosphate were increasing over time at the estuary as well. The projected trends estimated using Sen's slope in this thesis indicate that unless the conditions in the Yangtze River basin do not change, significant increases in inorganic nutrient concentrations are likely to continue.

The long-term trend for TSS concentration is decreasing (**Figure 3-11**), which has been attributed to the effect of large-scale damming the in the catchment. Up to the closure of the Three Gorges Dam in 2003, the effects of dams on reducing sediment loads in the Yangtze River was mostly offset by enhanced soil erosion in the basin cause by changes in land use (Dai, Fagherazzi et al. 2016). After 2003, a significant decrease in sediment load at the river downstream of the Three Gorges Dam is observed. This decrease is mainly attributed to the construction of the Three Gorges Dam, however water and soil conservation strategies implemented in the upper basin also contribute to this decrease (Dai, Fagherazzi et al. 2016). It should be noted that the predicted trend in **Figure 3-11** is unrealistic outside of the available data as it is unlikely that TSS concentrations will be reduced to zero; erosion and resuspension are expected to compensate to some extent the reduction in TSS originating from the upper catchment.

Based on average streamflow measurements at Datong and TSS concentrations at the estuary, TSS load is estimated to have reduced from 376 million t/a in 1990 to 78 million t/a, which is approximately a 79% decrease in load (**Table 3-3**). Decreases in TSS loads are expected to have an effect on TN and TP concentrations by reducing the particulate fractions of these nutrients; the average nutrient concentrations in sediment for the Yangtze River is estimated to be 0.98 g/kg and 0.75 g/kg of nitrogen and phosphorous respectively (Yang, Gao et al. 2017). The estimated reduction in sediment bound nitrogen supply to the estuary is estimated to have reduced from 0.368 million t/a to 0.077 million t/a between 1990 and 2008, and sediment bound phosphorous reduced from 0.282 million t/a to 0.059 million t/a. This is a significant reduction in overall nutrient supply to the estuary. Based on these numbers, the estimated Particulate Nitrogen concentration be approximately 0.4 mg/L in 1990 down to 0.09 mg/L in 2008 and the estimated Particulate Phosphorous concentration would be approximately 0.3 mg/L in 1990 down to approximately 0.07 mg/L in 2008.

Table 3-3: Estimated Annual Loads of TSS, PN and PP from the Yangtze Estuary.

Year	Average Streamflow m3/s *	Average TSS Concentration mg/L **	Average TSS Load million t/a	Average PN Concentration mg/L	Average PN Load million t/a	Average PP Concentration mg/L	Average PP Load million t/a
1990	29200	408	376	0.400	0.368	0.306	0.282
2008	26200	95	78	0.093	0.077	0.071	0.059

*Refer **Figure 2-8**; ** Refer **Figure 3-11**

An additional effect of the construction of dams has been to significantly decrease the median particle size of the sediment load carried by the Yangtze River downstream (Luo, Yang et al. 2012). Particle size is significant as it can affect the settleability of suspended sediment loads which has implications for water treatment. Particle size distribution at Datong and Jiangyin (Refer **Figure 2-3**) is presented in **Figure 3-12**. Jiangyin is taken to be representative of the estuary. Particle size distributions for bed material at both locations and suspended sediment at Datong indicate that the majority of particles are fine than medium sand (< 0.2mm, ISO 14688-1:2002); Suspended matter at Jiangyin is mostly finer than coarse silt (<0.02mm). For both bed material and suspended sediment, particle sizes are finer at Jiangyin than Datong, probably due to a reduction in channel slope (resulting in lower velocity) between Datong and the Estuary relative to upstream areas (Gao 2014).

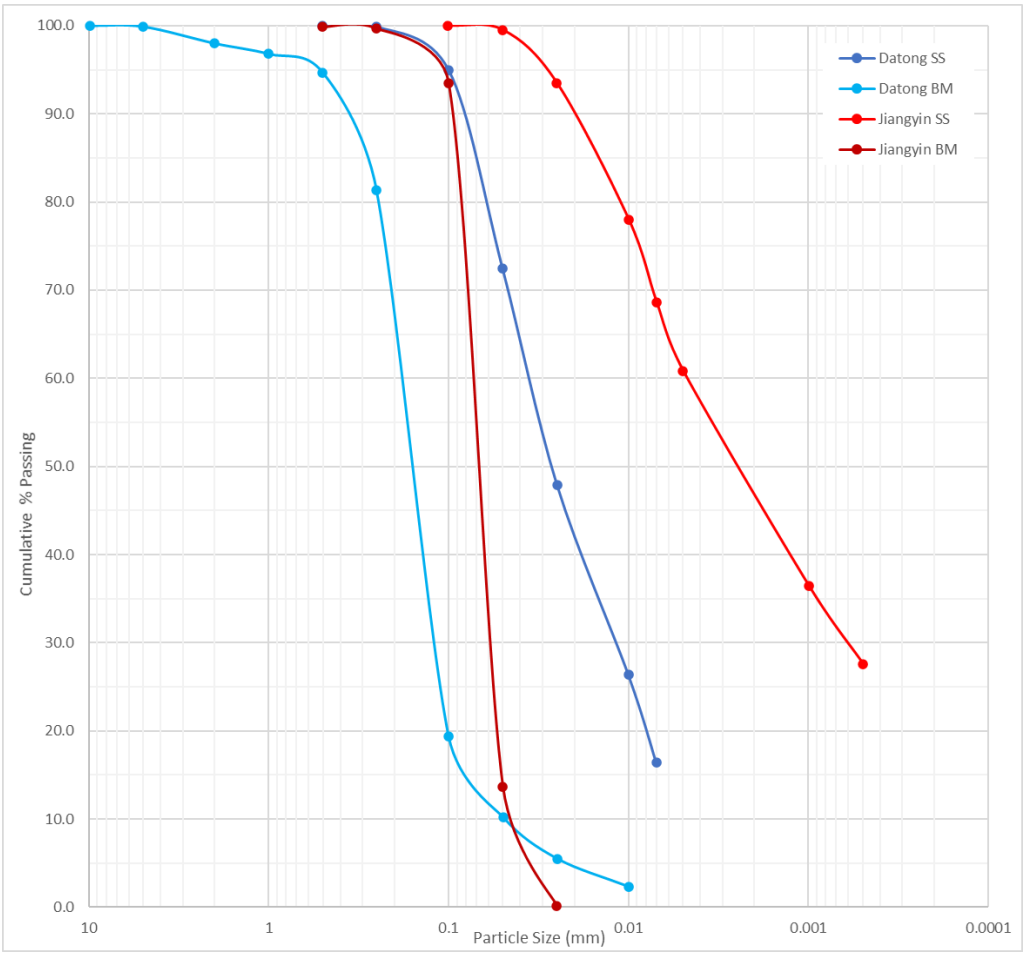

*Figure 3-12: Particle size distribution of Suspended Sediment (SS) and Bed Material (BM) at Jiangyin and Datong (Refer **Figure 2-3** for locations). Adapted from Gao (2014).*

Monthly series for all parameters between 1990 and 2013 have been plotted in **Figure 3-13** and **Figure 3-14**. Poor data quality is also apparent in the monthly plot for TN concentrations (**Figure 3-13**). At Datong Station, no data is available for January to April as well as September and at the Estuary, both February and March have missing values. This makes it difficult to determine any clear patterns in behaviour and the single values presented in some months may not give true representations of the actual concentration especially given the variability observable in Nitrate and Ammonium measurements. For Nitrate there are also no clear seasonal patterns in concentration and while the monthly means for Datong and the Estuary are within the same order of magnitude however there appears to be no clear relationship. Nitrate concentrations are consistently between 1 and 2 mg/L all year around. One possibility is that increased streamflow from the wet season and increased agricultural runoff resulting in higher loads of nitrate in the river occur at the same time resulting dilution of the increased nitrate load and subsequently a fairly consistent concentration to downstream areas occurs.

For Ammonium concentrations, Summer months generally appear to have lower mean concentrations when compared with Winter months for both Datong and the Estuary. Gao, Li et al. (2012) suggested that this may be due to increased biological activity and oxidation of Ammonium to Nitrate during warmer months. Ammonium concentrations at the estuary appear to all be consistently lower that at Datong in all months. Ammonium is generally associated with fresh pollution, so this is strange considering that Datong station is fairly far away from locations that are sources of fresh pollution (another reason it is typically used to assess likely concentrations in the Yangtze) while the estuary has many potential locations of fresh pollution. This observation supports the idea that the Yangtze River oxidises significant amounts of Ammonium to Nitrate as it travels downstream. On this basis it is probably not appropriate to rely on measurements of Ammonium at Datong for insight into concentrations and behaviour at the estuary.

There appears to be no strong seasonal patterns in observed TP or DIP concentrations at Datong or the Estuary (**Figure 3-14**). When comparing the two stations TP and DIP concentrations appear to be consistently higher on a monthly basis at the estuary than Datong. The monthly data represented at Datong were mostly sampled around 1997-1999 while the monthly data from the estuary was captured much later at around 2009-2013. Considering the observed increasing annual trend, these two series are not comparable. On the other hand, TSS concentrations are higher during the flood season that the dry season at both Datong and the Estuary. TSS at Datong appears to peak in August while at the Estuary it peaks in September. TSS concentrations at the estuary are likely affected by the tidal dynamics of the estuary and resuspension mechanisms.

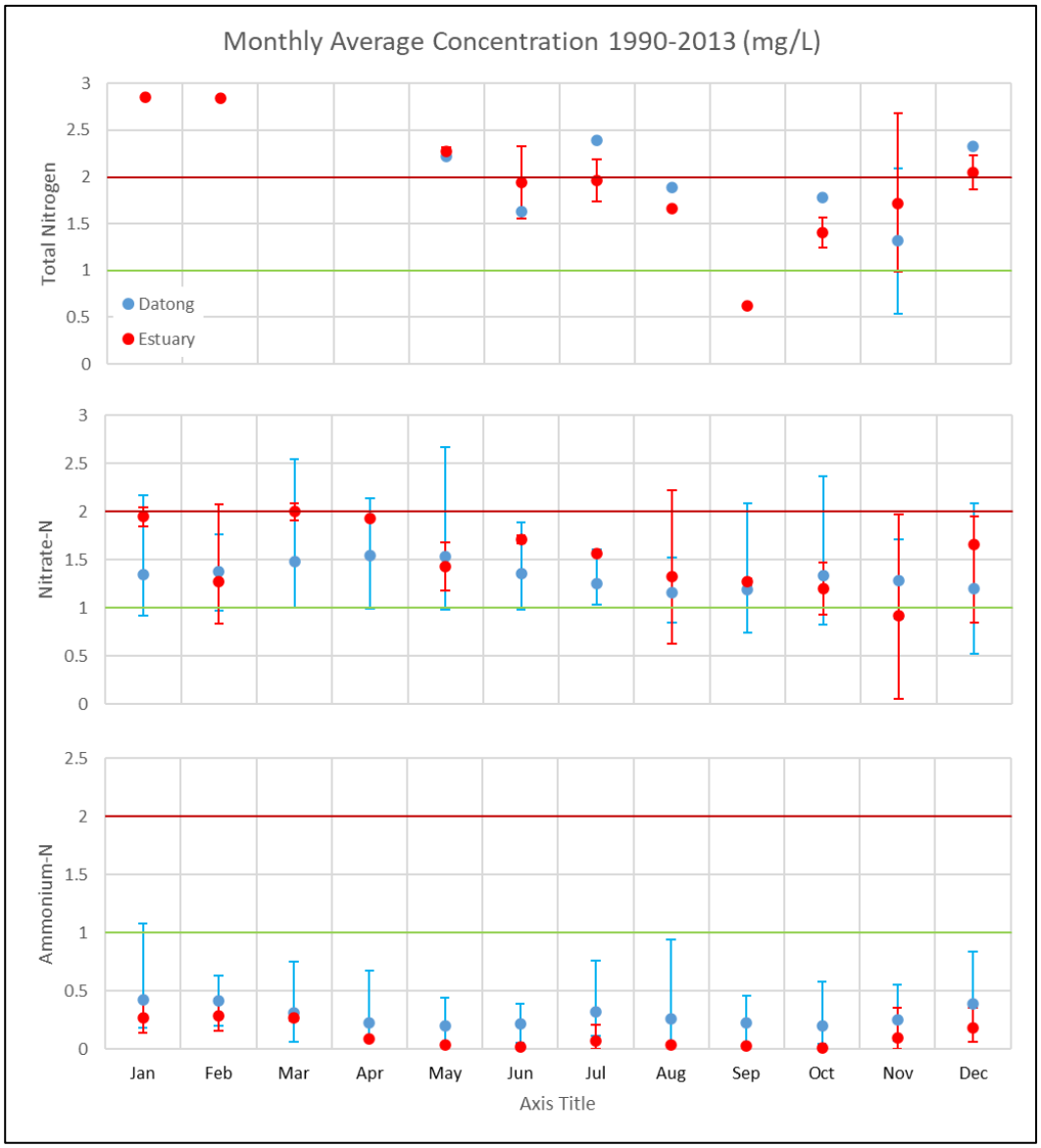

*Figure 3-13: Monthly Average Concentration (1990-2013) of Total Nitrogen, Nitrate and Ammonium at Datong and the Estuary. Refer to **Appendix 1** for data source tables. Error bars represent range. Green lines represent Chinese water quality class III threshold for TN and Ammonium and maroon line represents class V threshold for TN and Ammonium. Nitrate is compared with the TN thresholds*

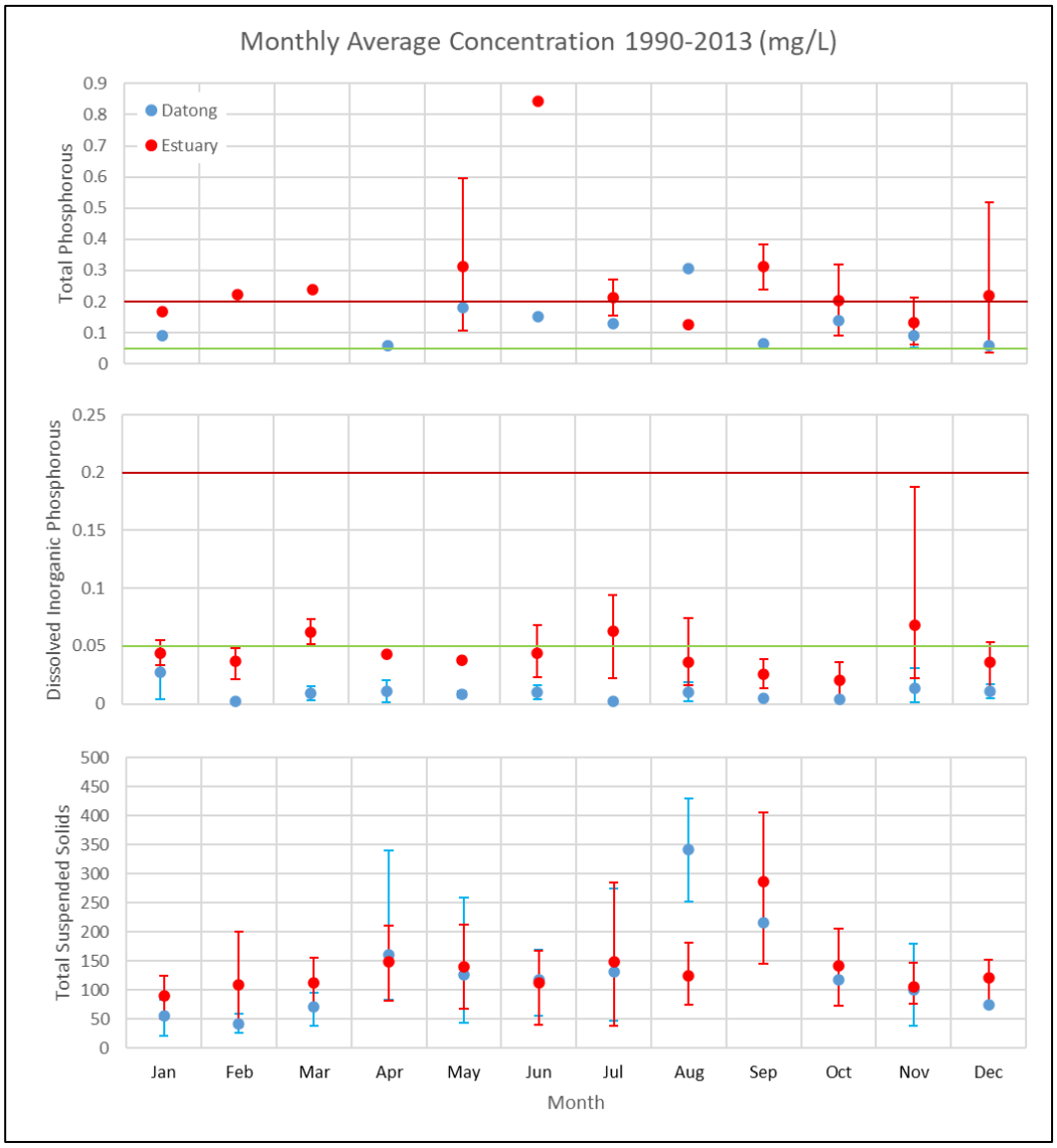

Figure 3-14: Monthly Average Concentration (1990-2013) of Total Phosphorous, Dissolved Inorganic Phosphorous and Total Suspended Solids at Datong and the Estuary. Refer to ***Appendix 1*** *for data source tables for TP and DIP. TSS data at Datong is from Dai, Du et al. (2011). Refer* ***Table 3-1*** *for the source of TSS data at the estuary. Error bars represent range. Green lines represent Chinese water quality class III threshold for TP for lakes and reservoirs and maroon line represents class V threshold for TP for lakes and reservoirs. The lakes and reservoirs threshold has been selected as this water will be diverted to coastal reservoirs for use. DIP is compared with the TP thresholds. No quality restrictions are available for TSS.*

Table 3-4 presents a comparison of some key nutrient fractions to other rivers and estuaries in China and around the world. Additionally, comparison has been made to Meybeck's 1982 estimation of average nutrient concentrations that would be expected in a typical unpolluted river. Mean nutrient concentrations in the Yangtze are significantly above the levels Meybeck estimated for an unpolluted river, being some 14 times higher for nitrate, 20 times higher for ammonium and 3 times higher for DIP which indicates that the water in the Yangtze is nutrient enriched by anthropogenic activities. Nitrate levels in the Yangtze are similar to that of the Huang He (Yellow River), lower than the Yalu Jiang and higher than other rivers in China. Ammonium levels in the Yangtze are higher than other rivers in China with the exception of the Huang He and DIP levels higher than all except the Daliao He. Compared with World Rivers, the Yangtze's nutrient pollution is lower relative to most of the rivers of Europe as well as the Mississippi River, but more polluted than the Amazon and the Zaire.

Table 3-4: Mean Concentration of Nutrients in Rivers and Estuaries (mg/L); Mean concentrations for the Yangtze estimated from data collected from this dataset in the years 1990-2015. Other rivers adapted from Shen and Liu (2009), Liu, Zhang et al. (2003) and Chai, Yu et al. (2009), estimate for unpolluted river from Meybeck (1982)

Rivers	**DIN**	**NO_3-N**	**NH_4-N**	**TP**	**DIP**
Yangtze (at Datong)	-	1.419	0.301	0.121	0.033
Unpolluted River*	0.116	0.100	0.015		0.010
Huang He (China)	2.101	1.420	0.644	-	0.012
Zhu Jiang (China)	0.684	0.658	0.168	0.068	0.004
Luan He (China)	-	1.044	-	-	0.016
Daliao He (China)	0.280	0.105	0.175	-	0.053
Yalu Jiang (China)	1.820	1.806	0.020	-	0.005
Rhine (Germany/Netherlands)	2.016	1.484	0.531	-	0.210
Seine (France)	-	6.006	-	-	1.000
Loire (France)	2.618	2.576	0.053	-	0.079
Rhone (France)	1.554	-	-	-	0.004
Po (Italy)	2.436	2.100	0.336	-	0.142
Zaire (Congo)	0.099	0.091	0.006	-	0.025
Estuaries					
Yangtze	-	1.522	0.484	0.798	0.039
Huang He (China)	0.574	-	-	-	0.022
Zhu Jiang (China)	1.610	-	-	-	0.031
Amazon (Brazil)	0.234	0.224	0.006	-	0.025
Orinoco (Venezuela)	-	0.112	-	-	6.194
Mississippi (U.S.)	-	2.38	0.070	-	0.108
Chesapeake (U.S.)	1.890	-	-	-	0.028
Seine (France)	-	4.298	0.994	-	0.025
Rhone (France)	-	1.148	0.010	-	0.040
Thames (England)	0.490	-	-	-	0.108
Danube (Ukraine/Romania)	3.500	-	-	-	0.146

3.3.2 Factors Affecting Nutrients and Sediments in the Yangtze Estuary

Historically, the increase in nutrients in the Yangtze River resulted from reduced streamflow, hence reducing dilution (e.g. drought), or serious erosion which promotes the leaching of nutrients from the soil (Liu, Zhang et al. 2003). However, studies have found that alongside increasing trends of nitrogen and phosphorous, meta-silicate (SiO_3) concentrations associated with natural rock weathering were found to be evenly distributed along the river, indicating that the excess nitrogen and phosphorous originated from anthropogenic activities (Wu 2005, Gao and Wang 2008, Shen and Liu 2009). Excess nutrients now come from a variety of additional sources including increased application of fertiliser, livestock waste, aquaculture, and industrial and domestic wastewater discharge (Varis and Vakkilainen 2001, Anderson, Glibert et al. 2002, Wu 2005, Gao and Wang 2008, Jiang 2009, Li, Mander et al. 2009, Hogan 2012).

With a growing population, China has increased its demand for food while simultaneously decreasing available space for agricultural development. Arable land in China is decreasing with an expected 10% decline between 2000 and 2030, with most of this loss being the result of land reallocation for industrial and residential use and some loss to desertification, (Varis and Vakkilainen 2001, Liu, Zhang et al. 2003). These dual requirements have led to the ability of China to feed its population mainly coming from intensifying farming practices, which involves increasing irrigation and use of fertilisers (Varis and Vakkilainen 2001, Liu, Zhang et al. 2003, Wang, Wang et al. 2007). China's agricultural industry is now considered to be a major polluter, releasing over 13 million t of effluent into waterways annually (Aregay and Minjuan 2012). This increase in fertiliser application and irrigation practices has been supported by the Chinese Government, which has made considerable effort to enhance productivity, and as a result, China is now the largest global consumer of fertiliser and has the largest irrigated area. (Varis and Vakkilainen 2001, Aregay and Zhao 2012)

Chinese farmers are over applying fertiliser. This has two main negative impacts; not only does over application increase the potential for excess nutrients to enter waterways, but also can negatively affect crop response to chemical fertiliser, meaning that applying fertiliser is becoming less effective for boosting production (Aregay and Minjuan 2012). Nitrogen use efficiency for fertiliser was around 30-35% in the 1990s which dropped to 26-28% in the early 2000s, while for phosphorous, fertiliser use efficiency was 59% in 1980, dropping to 36% by 2005 (Ma, Zhang et al. 2013, Yan, Ti et al. 2014). Animal production in China has also intensified in as animal protein plays an increasing role in the Chinese diet. There are indications that animal production could be responsible for as much as 20% of nitrogen and 40% of phosphorous pollution in aquatic systems in China (Jiang, Yu et al. 2012). Before the agricultural revolution in 1978, Chinese agriculture was dominated by combined crop and animal production. There was little use for synthetic fertilisers as animal manure was recycled for application to crops. With the sharp growth in the use of synthetic fertilisers, animal waste was increasingly discharged into river systems around China; in the 1970s, less than 5% of animal manure was discharged directly to river systems,

however, by the year 2000, this had increased to somewhere between 30-70% (Chen, Chen et al. 2008, Jiang, Yu et al. 2012, Ma, Zhang et al. 2013).

Also, to help improve food security, aquaculture in China has intensified in China, with the Yangtze River contributing a sizable proportion of national production. China accounted for approximately 60% of world aquaculture production since the 1990s and aquaculture accounts for 76% of China's total fisheries production. Aquaculture in the middle and lower reaches of the Yangtze River is thought to contribute between 9-54% of TN and 13-33% of TP non-point source pollution (Zhang, Bleeker et al. 2015).

In addition to food production activities, urbanisation, sewage discharge and damming also have an effect on the nutrient loads entering the Yangtze River. With the rapid increase of population in the Yangtze River Basin, increasing amounts of wastewater is discharged to the river. It is estimated that in 2014 the average de facto re-use rate of the Yangtze River at Shanghai is 2.5% and can reach as high as 14% during low flow periods (Wang, Shao et al. 2017). Nutrients are difficult to remove from wastewater with conventional treatment systems and this is expected to affect concentrations of nutrients arriving at the estuary.

The impact of damming in the Yangtze Basin has resulted in a massive decrease in sediment concentration in the downstream portion of the river. A decline in sediment loads can be expected to have some effect on nutrient delivery to the lower reaches of the Yangtze River; as noted previously, average nutrient concentrations in sediment for the Yangtze River is around 0.98 g/kg and 0.75 g/kg for nitrogen and phosphorous respectively (Yang, Gao et al. 2017). Damming is particularly thought to have had an effect on particulate phosphorous loads in the Yangtze River. Soil losses, particularly from the upper basin, were thought to account for a large proportion of total particulate phosphorous concentrations; the upper basin was estimated contributing around 60% of the catchment total (Duan, Liang et al. 2008, Shen and Liu 2009). Particulate phosphorous at the Yangtze Estuary has declined by 86% since the closure of the TGD (Meng, Yu et al. 2015). Additional dams of comparable size to the Three Gorges Dam are proposed in the upper reaches of the Yangtze River along the Jinsha River and Jialing River (Dai and Lu 2014, Dai, Fagherazzi et al. 2016). These two tributaries of the Yangtze River are estimated to provide 51% and 23% of the total sediment load measured at Yichang station on the mainstem of the Yangtze River. It is estimated that when the four proposed cascaded dams on the Jinsha River (Wodongbe, Baihetan, Xiloudu and Xingjiaba Dams), up to 95% of the sediment from the Jinsha River could be trapped (Dai and Lu 2014). These additional dams could have a significant effect on the flow and sediment regimes in the Yangtze Estuary. It is not clear as to the exact effect these dams would have and they should be considered in any further research into water quality in the Yangtze Estuary.

Data on key factors that are considered to have an effect on nutrient concentrations have been collected from the Chinese National Bureau of Statistics for provinces and municipalities in the

Yangzte Basin (National Bureau of Statistics of China 2017). These factors are specifically population, total number on livestock, area irrigated, application of nitrogenous fertiliser and phosphate fertiliser and the amount of area used for freshwater aquaculture. Based on this data, estimates were made for these factors within the Yangtze River Basin for each year. A Mann-Kendall assessment was run on each of these series to determine if a trend was present in the data (confidence level $\alpha = 0.05$) and Sen's Slope calculated to determine the magnitude of any observed trends. Results of the Mann-Kendall assessment is summarised in **Table 3-5**. The data series are plotted in **Figure 3-15** to **Figure 3-21**. Results of the Mann-Kendall assessment indicate the presence of increasing trends in all the examined parameters.

Population in the Yangtze River basin (**Figure 3-15)** was around 200 million people in 1962, which has more than doubled to over 440 million people by 2014. The population growth rate after 2000 appears to be increasing at a slower rate than earlier years, and it appears that the predicted trend using Sen's slope overestimates the likely future growth. In 1978, the total applied fertiliser was approximately 2 million t (effective component) climbing to around 17 million t in 2014. The increase in total fertiliser application in the basin (**Figure 3-16)** has been relatively steady. Growth in applied fertiliser rates appears to have slowed in 2011-14. This has occurred previously in 1995-2000 before accelerating again, and as such slowing application rates in 2011-2014 does not necessarily indicate applications rates will remain at 17 million t/a in the long term. Nitrogenous fertiliser application (**Figure 3-17)** rates have increased from approximately 0.4 million t in 1965 to 6.8 million t in 2015. Rapid growth in nitrogenous fertiliser application can be observed from the start of the agricultural revolution in 1978 up until 1998. After 1998, growth in the application rate of nitrogenous fertiliser has slowed and after 2012 begun decreasing. A similar pattern can be observed in application rates for phosphorous fertiliser application (**Figure 3-18)** which has increased from 0.2 million t in 1966 to 2.8 million t in 2015. This indicates that Chinese farmers may be changing their habits with regards to fertiliser application, changing the quantity and/or type of fertiliser they are applying, and that the predicted trends using Sen's slope may be overestimating future fertiliser usage. It is possible however that like total fertiliser application after 2000, application rates may increase again in the future.

While the change in the amount of irrigated farmland in the Yangtze Basin (**Figure 3-19)** has fluctuated, it has generally trended upwards, increased from 14.2 million ha in 1978 to nearly 18 million ha in 2014. The amount of irrigated farmland in the basin has increased exponentially after 2006, perhaps reflecting intensifying agricultural practices. Total livestock in the basin (**Figure 3-20)** has increased from around 180 million livestock in 1978 to approximately 280 million in 2015. Two shifts in the livestock data can be observed after 1995 and 2005 that could be the result of significant events in the basin such as extreme drought or a change in the way that the number of livestock is counted or reported. After 2009, the growth rate in the number of livestock has slowed. The area used for aquaculture in the basin (**Figure 3-21)** has steadily increased from 1.1 million ha in 1978 to 2.6 million ha in 2015. Similar to number of livestock, a shift in the data can

be observed in 2005 that might be the result of a change in measurement or recording practices.

Despite some of the rates of change showing signs of slowing or even decreasing rather than increasing in recent years, on the whole, all of the factors associated with increasing nutrients in the Yangtze River have increased significantly over the period observed. If conditions in the basin continue to follow the long-term trends, nutrient concentrations in the Yangtze River will continue to increase.

Table 3-5: Mann-Kendall Summary for Land Uses in the Yangtze Basin

	Population	Total Fertiliser Application	Nitrogenous Fertiliser Application	Phosphorous Fertiliser Application	Irrigated Area	Livestock	Aquaculture Area
Number of Samples, n	39	37	53	53	37	38	38
Mann Kendall Statistic	731	658	1230	1271	554	517	613
Standard Error	82.67	76.46	130.37	130.37	76.46	79.54	79.54
z-statistic	8.831	8.593	9.427	9.742	7.233	6.487	7.694
p-value (assuming twin tailed distribution)	1.0×10^{-18}	8.5×10^{-18}	4.2×10^{-21}	2.0×10^{-22}	4.7×10^{-13}	8.8×10^{-11}	1.4×10^{-14}
Trend Detected?	Yes Increasing	Yes Increasing	Yes Increasing	Yes Increasing	Yes Increasing	Yes increasing	Yes Increasing

Note: for details of Mann-Kendall method and terminology refer to Helsel, Hirsch et al. (2020)

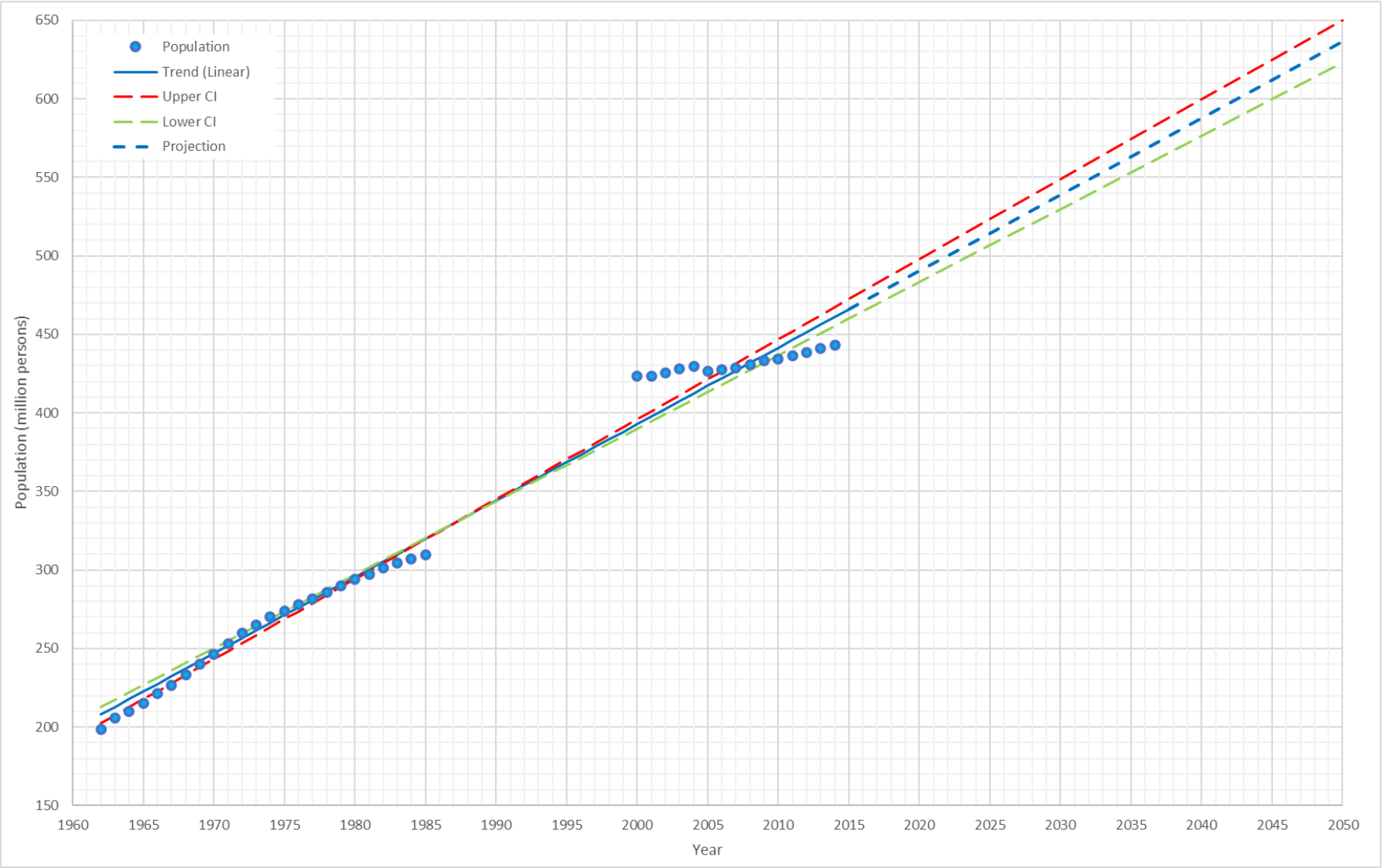

Figure 3-15: Population in the Yangtze Basin with linear trend calculated using Sen's slope. Data from National Bureau of Statistics of China (2017) and Duan, Xu et al. (2007)

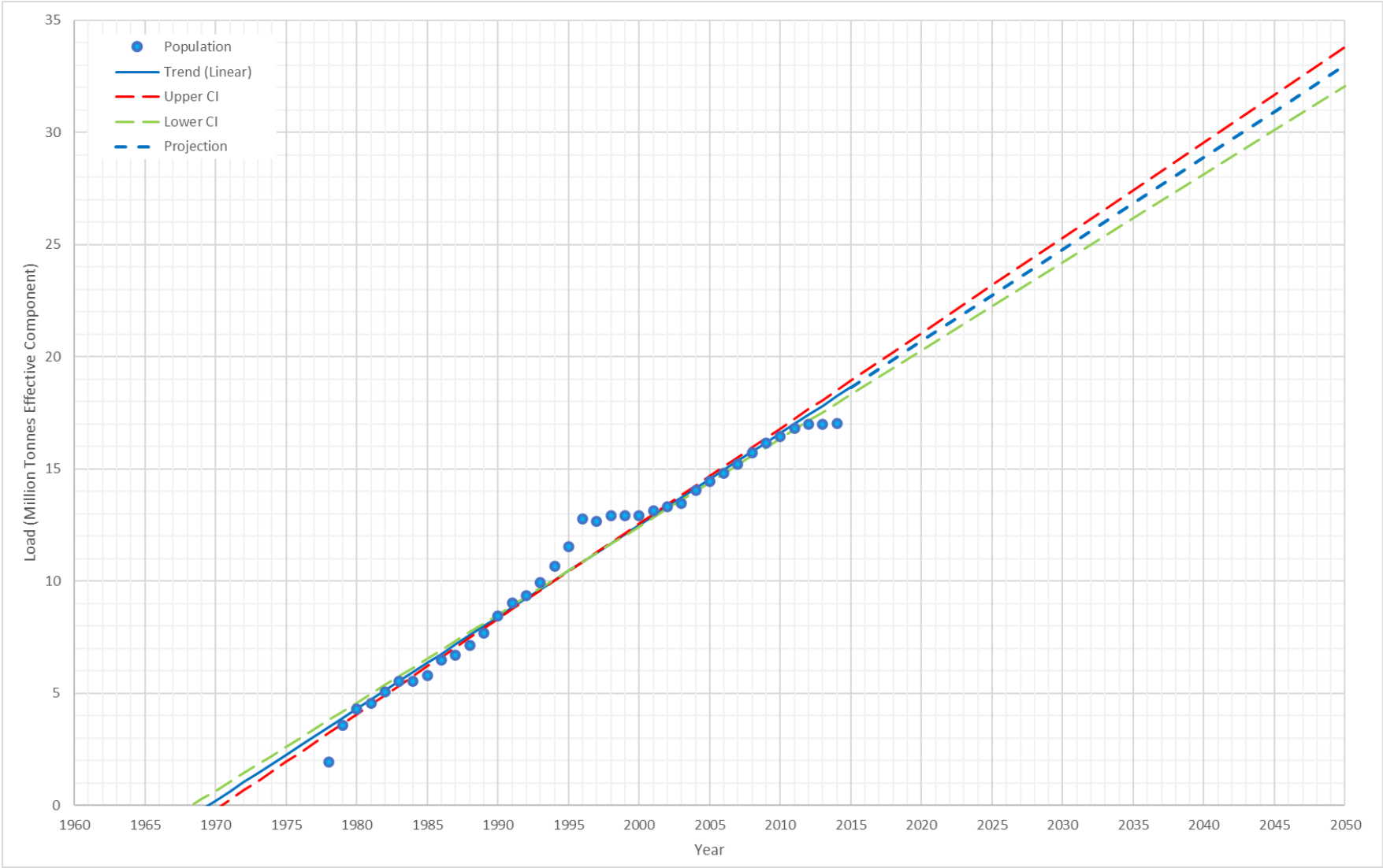

Figure 3-16: Total Fertiliser Application in the Yangtze Basin with linear trend calculated using Sen's slope. Data from National Bureau of Statistics of China (2017)

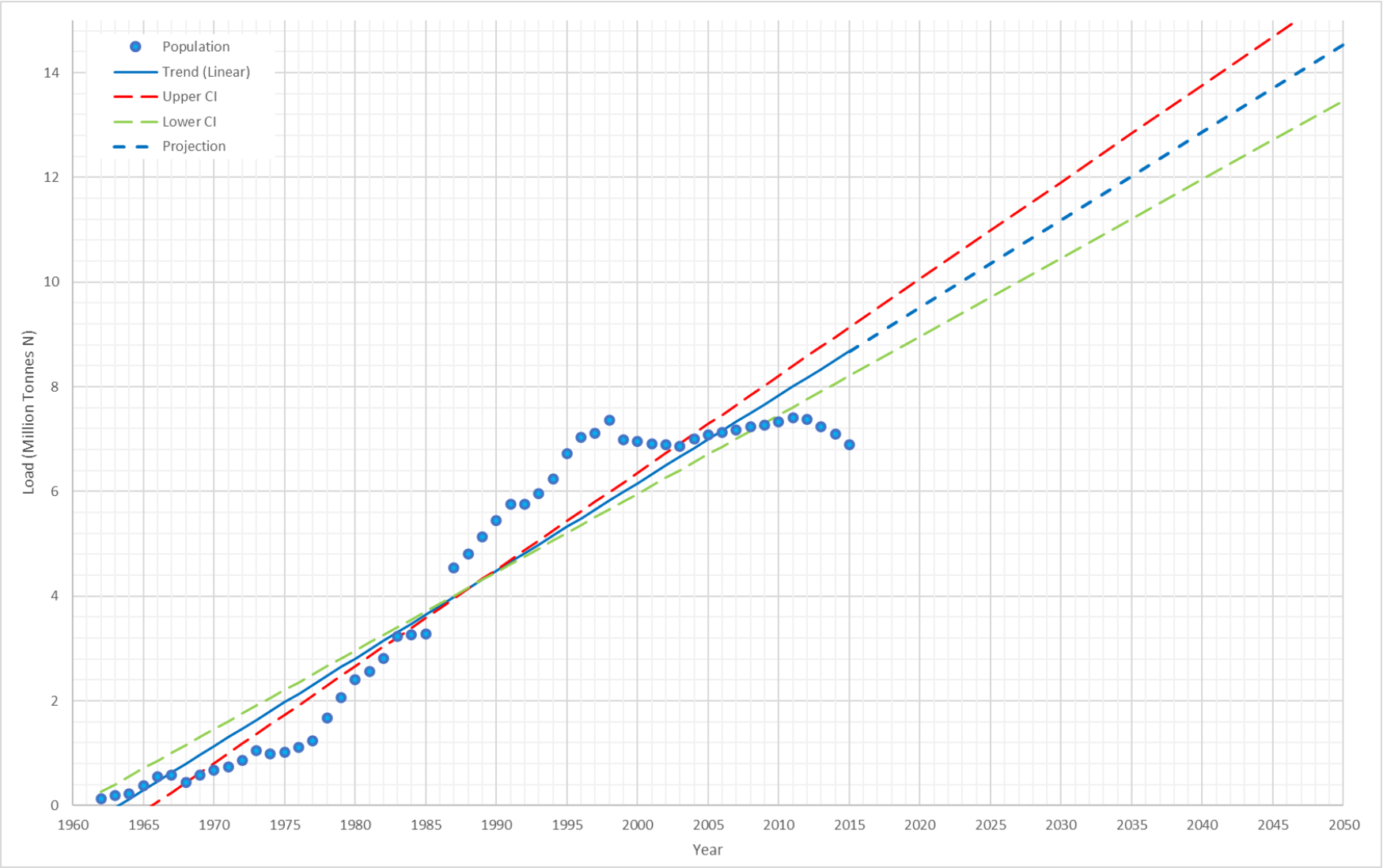

Figure 3-17: Nitrogenous Fertiliser Application in the Yangtze Basin with linear trend calculated using Sen's slope. Data from National Bureau of Statistics of China (2017)

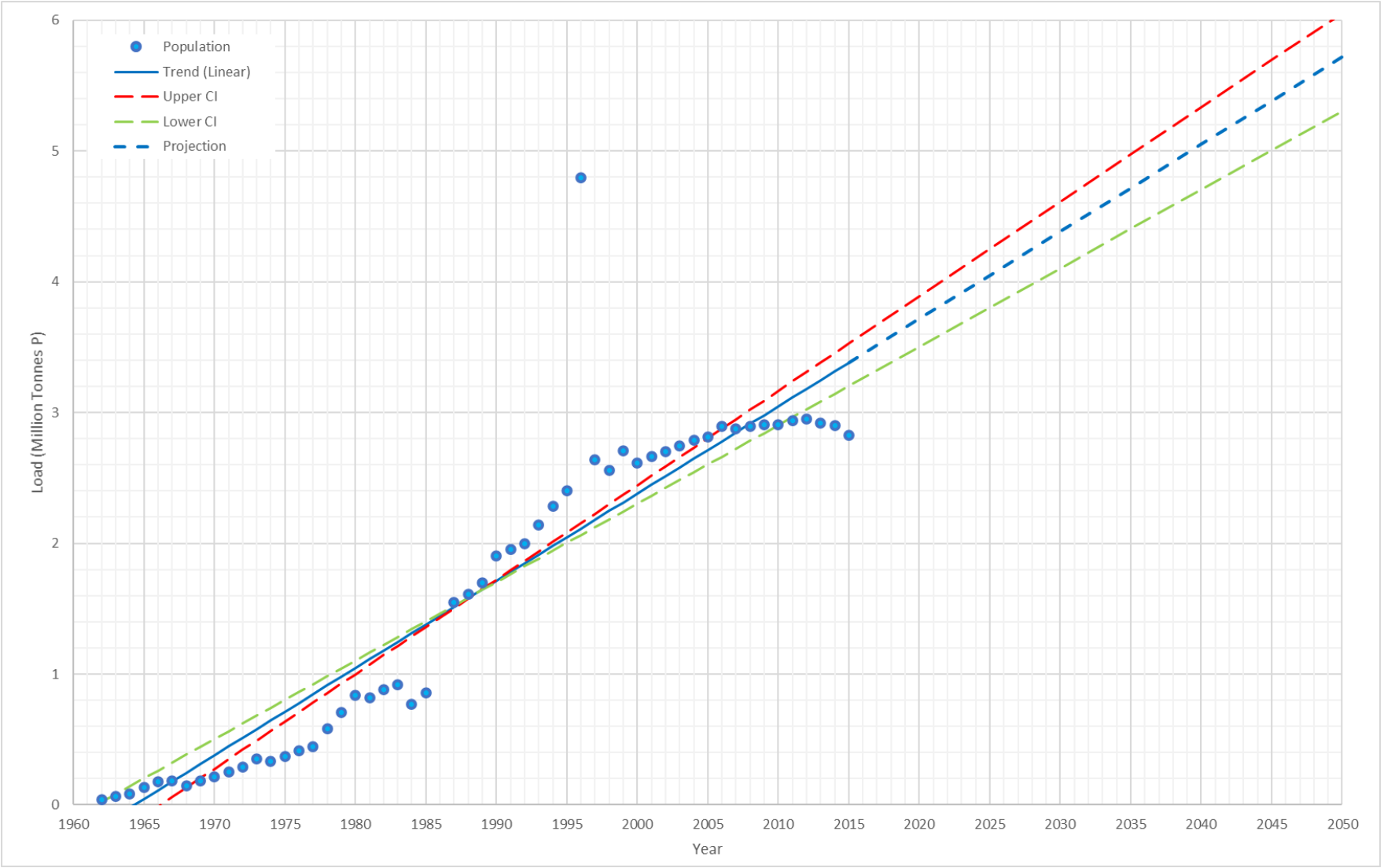

Figure 3-18: Phosphorous Fertiliser Application in the Yangtze Basin with linear trend calculated using Sen's slope. Data from National Bureau of Statistics of China (2017)

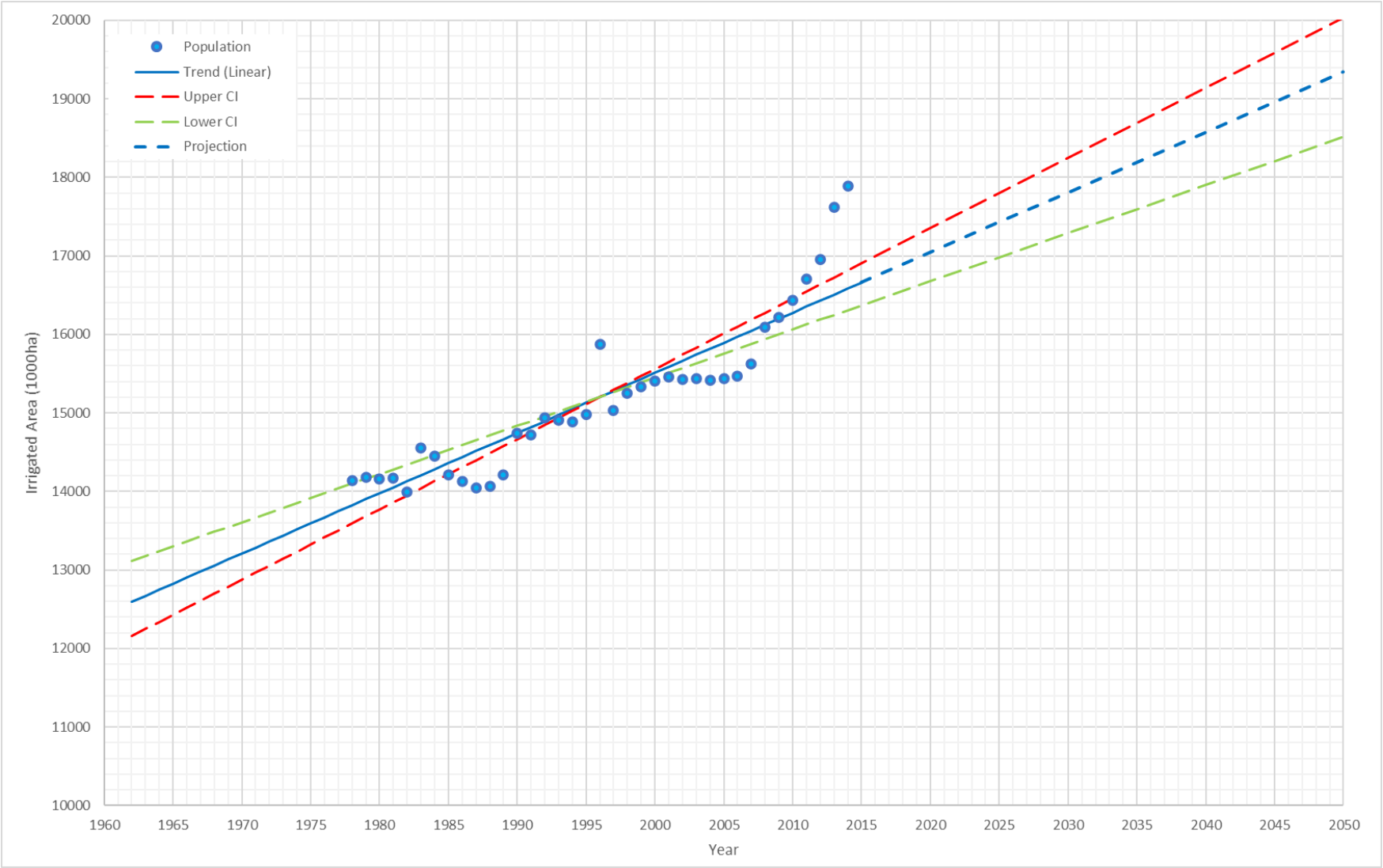

Figure 3-19: Irrigated Area in the Yangtze Basin with linear trend calculated using Sen's slope. Data from National Bureau of Statistics of China (2017)

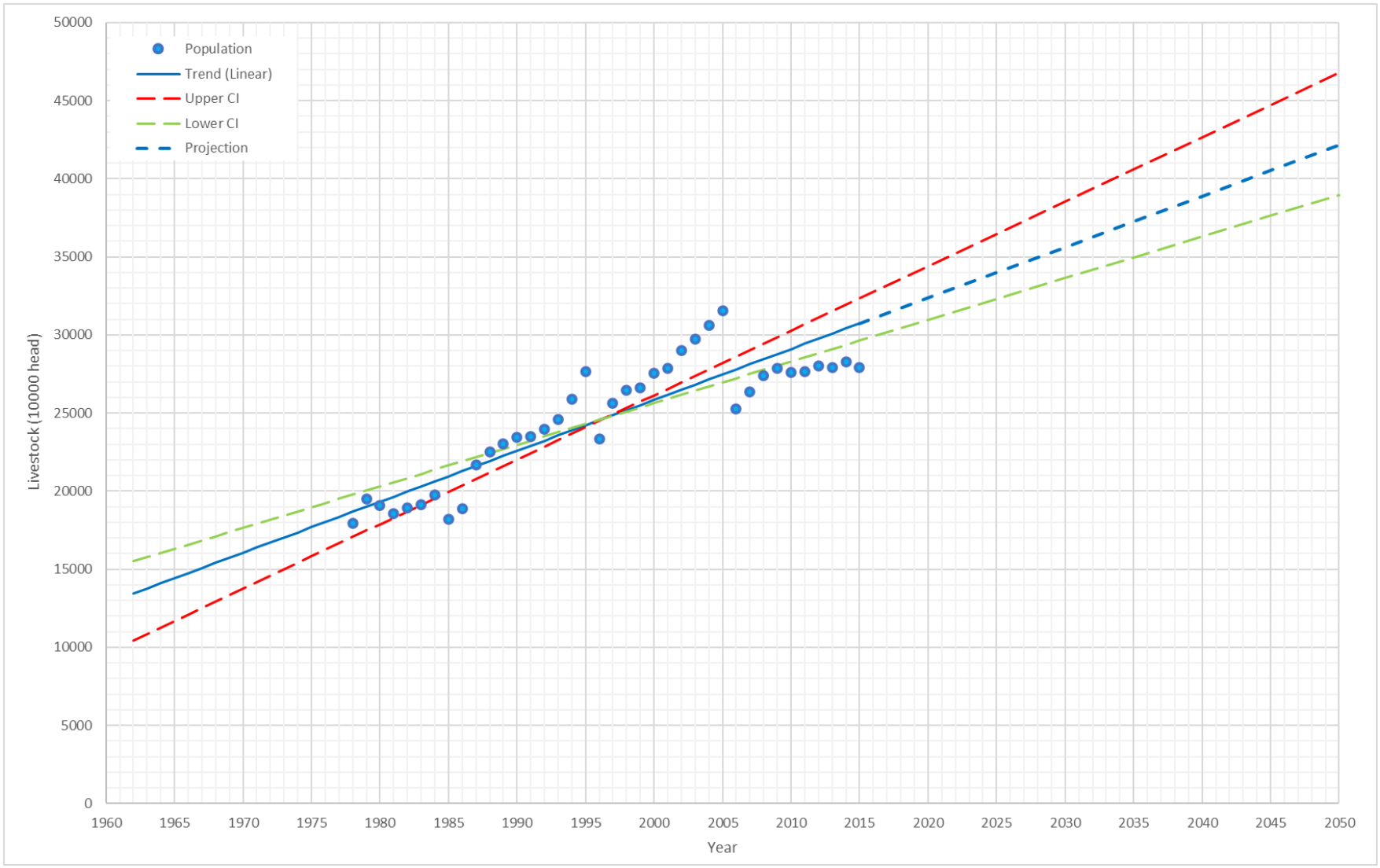

Figure 3-20: Livestock in the Yangtze River Basin with linear trend calculated using Sen's slope. Data from National Bureau of Statistics of China (2017)

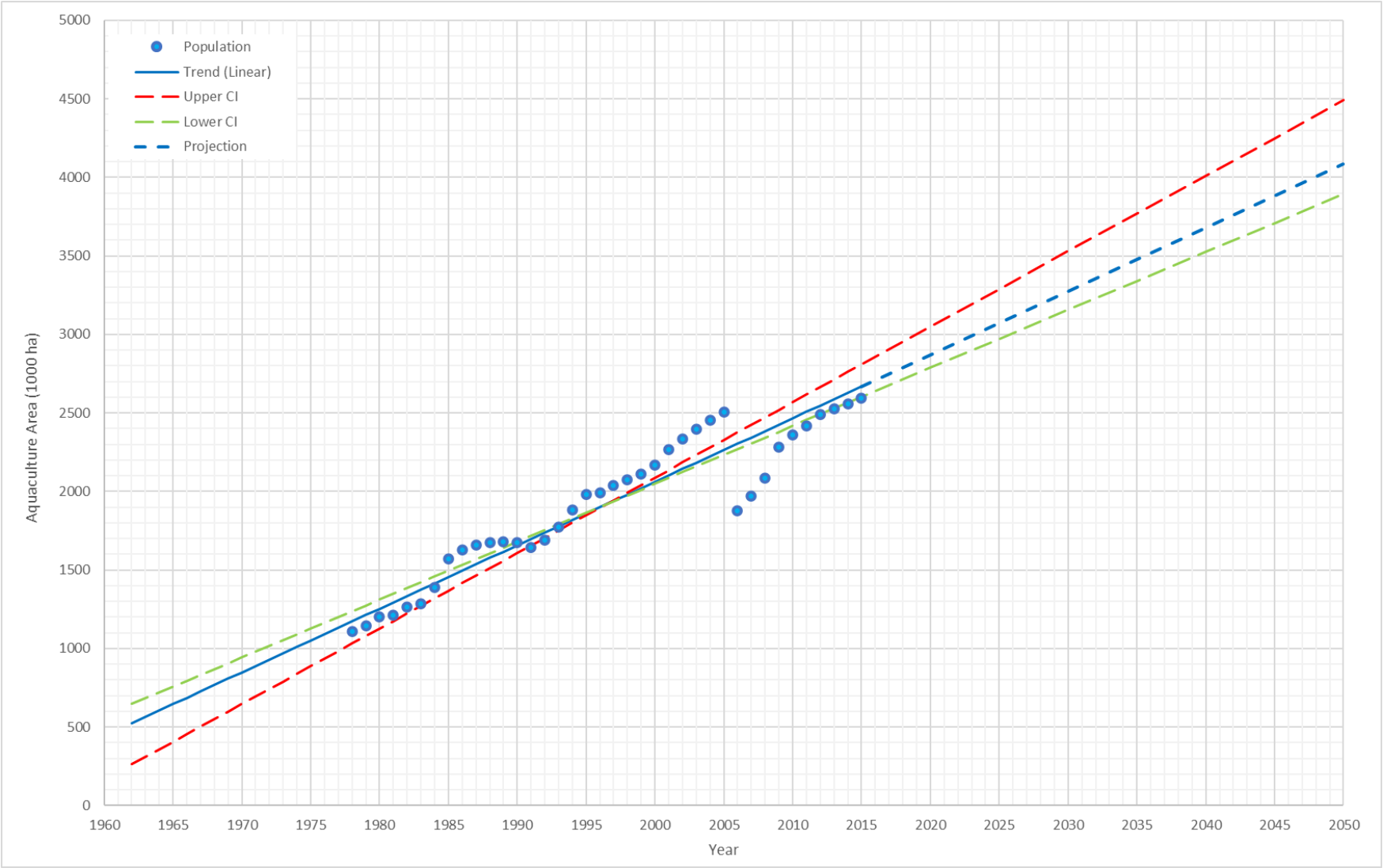

Figure 3-21: Aquaculture area in the Yangtze Basin with linear trend calculated using Sen's slope. Data from National Bureau of Statistics of China (2017)

3.3.3 Eutrophication and Algal Blooms

Eutrophication is defined as the process whereby an aquatic environment acquires a higher amount of nutrients often promoting the excessive growth of algae (Naeem, Idrees et al. 2013). The most significant contribution to this process is additions to nutrient levels originating from mineral nutrients that are used as fertiliser in agricultural practice. Surface runoff, sewage effluent, animal excreta and organic debris are also some important contributors of nutrients. Aquatic ecosystems can be classified by their trophic state into three general types (Naeem, Idrees et al. 2013):

- Oligotrophic: a system with poor productivity and low nutrient concentrations
- Mesotrophic: a system with moderate productivity and nutrient concentrations
- Eutrophic: a system with high productivity and concentrations of nutrients

There are two main nutrients that are associated with eutrophication due to their relative importance in macro and microphyte biology; nitrogen and phosphorous. While there are 19 essential elements for the growth of plants, nitrogen and phosphorous are the most covered in literature. Nitrogen and phosphorous are the usual limiting nutrients for plant growth, hence their widespread application as chemical fertilisers (Naeem, Idrees et al. 2013).

Nitrogen is critical to plant growth because of its key role in the formation of amino acids and Chlorophyll, and hence is a key component of all plant development and the photosynthesis process. Nitrogen is available to plants in its mineral forms; the ions nitrate and ammonium. Nitrate is the dominant form of inorganic nitrogen, is a macro-nutrient for plants and is a common component in chemical fertilisers. It can also occur in natural cycling of nitrogen species, usually during the decomposition/oxidation of ammonia and ammonium through the process of nitrification. Nitrite is a highly reactive form of inorganic nitrogen that often originates as an intermediate product during the nitrification process. In natural systems, its concentration should be very low. Ammonium is the first of the inorganic nitrogens created during the mineralisation of organic matter. Organic sources of nitrogen, including amino acids, proteins and urea, amongst others convert to ammonium through a process called ammonification or deamination. Ammonium is found in wastewater and fertiliser runoff and because of its instability, is a good indicator of fresh pollution.

Phosphorous is a major component in DNA and RNA structures, plays a critical role in energy storage and transfer and is critical in the young cells of a plant and hence is used in root development, flower growth and seed and fruit development. DIP (also referred to as phosphate, orthophosphate or SRP) is the fraction of phosphorous that is taken up by plants as nutrient (Naeem, Idrees et al. 2013). It has a variety of sources including chemical fertilisers, from the breakdown of polyphosphates originating in household products and from the mineralisation of organic matter. Typically, the majority of phosphorous in aquatic systems is bound to particulate matter with orthophosphate fractions being adsorbed and desorbed from these particles.

Phosphorous is often the limiting nutrient in freshwater systems and high phosphorous loading can encourage the proliferation of cyanobacteria.

As key components of plant nutrition, the supply rate of nitrogen and phosphorous strongly influence the growth of algae and vascular plants in aquatic ecosystems. In addition to Nitrogen and Phosphorous, Silicon in the form of reactive silica is also important for the growth of the diatom group of algae (Naeem, Idrees et al. 2013) As a result of high nutrient supply rates, eutrophication can cause imbalance in the trophic structure of aquatic systems as the excess nutrients stimulate the primary production of macro and microphytes (Zhang, Liu et al. 2007, Naeem, Idrees et al. 2013). In particular, eutrophication can lead to the occurrence of harmful algal blooms (often abbreviated as HABs), which have the potential to cause the build-up of toxic substances in the water and food web, the death of marine animals and birds, reduced biodiversity in aquatic systems, the alteration of aquatic habitats and complications during water treatment operations (Anderson, Glibert et al. 2002, Kennish 2002, Heisler, Glibert et al. 2008, Zhou, Shen et al. 2008, Pawelczyk 2012). Waters that are affected by algal blooms can be considered useless for human use because they are very difficult and expensive to remove (Naeem, Idrees et al. 2013). The supply of Nitrogen and Phosphorous strongly influences the growth of algae in freshwater and marine ecosystems; there is correlation between increased nutrient influx and more frequent occurrence of algal blooms (Kennish 2002, Wu 2005, Heisler, Glibert et al. 2008). High nutrient concentrations are often recorded prior to the formation of algal bloom; these concentrations, especially nitrate and phosphate, are low after the occurrence of a bloom as they are absorbed and retained by the algal cells (Naeem, Idrees et al. 2013).

The concept of nutrient limitation implies that one key nutrient should be the limiting factor for plant growth in an ecosystem, the rate of growth of plants is proportional to rate of supply of this key nutrient and that the control of eutrophication can be achieved by the controlling the supply of this key nutrient (Naeem, Idrees et al. 2013). In freshwater systems, phosphorous is the primary nutrient that is least available and is therefore often the limiting nutrient on the growth of photosynthetic organisms, however in the marine environment nitrogen is usually more important. In lower estuaries, both nitrogen and phosphorous can be the limiting nutrient (Anderson, Glibert et al. 2002, Heisler, Glibert et al. 2008). The Nitrogen to Phosphorous ratio, called the Redfield Ratio, is an important indicator that helps identify the limiting nutrient for algal growth. If the Redfield Ratio exceeds 16:1, then Phosphorous is most likely the limiting factor for algal growth, while lower ratios indicate that nitrogen is of more importance. The composition of nutrient inputs to an aquatic environment can impact the type of organism that flourishes, for example, the high phosphorous loadings encourage the growth of the toxic cyanobacteria blooms in freshwater environments (Anderson, Glibert et al. 2002, Heisler, Glibert et al. 2008). In 1997, the N:P ratio was around 142.1 at the estuary during the dry season and during the wet season 38.4; during this time DIN:DIP ratio was 309.6 in the dry season and 310 in the wet season at the estuary (Shen and Liu 2009). By 2010, the N:P ratio in the freshwater section of the estuary was about 75 (Li,

Wang et al. 2016). These ratios would indicate that the estuary was Phosphorous limited.

Excessive phosphorous loading can be a prerequisite for cyanobacterial harmful algal blooms. Phosphate is the primary form of phosphorous used during algal blooming. Dissolved organic phosphorous can also be used, though not as readily as phosphate. Particulate phosphorous can also serve as a source of dissolved inorganic phosphorous, especially during hypoxic and anoxic periods (Paerl 2008). Organic nitrogen and ammonium rich conditions can favour cyanobacteria over other types of algae and increase the toxicity of the bloom genera (Paerl 2008). When the dissolved silicon to nitrate nitrogen ratio is 1:1, aquatic food webs which are associated with diatoms may thrive resulting in the occurrence of harmful algal blooms (Naeem, Idrees et al. 2013).

In certain environments, algae have the capacity to store large quantities of nitrogen and phosphorous in their cells in order to support multiplication for future cell generations. This allows algae to potentially avoid the effects of nutrient limitation during future growth periods (Naeem, Idrees et al. 2013). Algal blooms in lake or reservoir environments can also acquire a semi-permanent nature when their lifecycle begins to control the cycling of nutrients; surface algae can limit light penetration into the water, causing the lower layers to cool resulting in stratification. Reduced oxygen supply causes the lower layers to become oxygen deficient, promoting the activities of anaerobic organisms which produce a number of organic substances that are intermediate metabolites of algae metabolism. At night when the surface layer cools, mixing can be induced, supplying oxygen and leading to the mineralisation of these partial metabolites. Therefore nutrients for algal growth can also be derived from the lower layer of the water body, from decaying organic matter and mineral sediments (Naeem, Idrees et al. 2013).

In systems where Nitrogen and Phosphorous are being supplied at close to non-limiting rates, other factors may be controlling algal growth (Paerl 2008). In reservoirs and rivers, light is commonly the limiting resource, often controlled by abiotic turbidity, sediment loading and mixing (Anderson, Glibert et al. 2002). When nutrient rich water is detained in a slow-moving water body, the settling of suspended matter increases the light penetration resulting in algal growth. This algal growth is further exacerbated by long retention times and low flushing rates, elevated temperatures and vertical stratification (Paerl 2008, Naeem, Idrees et al. 2013). For freshwater species of algae, salinity can also be a limiting factor.

Algal blooms have severe impacts on fish, seabirds and marine mammals, as well as marine fishery, aquiculture and public health (Anderson, Glibert et al. 2002, Kennish 2002, Zhou, Shen et al. 2008, Wang and Wu 2009). Algae may die suddenly, resulting in masses of dead and degrading organic matter. Subsequently, a huge amount of organic matter decomposes depleting water of oxygen leading to the death of other aquatic fauna and flora. This can cause widespread destruction of valuable resources such as lobster, crabs and flat fish (Naeem, Idrees et al. 2013).

Of particular concern are cyanobacterial blooms, which are often unsightly and strong odoured, and have the capacity to cause harm to both ecosystems and public health. They are potentially inedible and toxic to consumer species causing food web alterations, detrimental to nutrient cycling, as described above, and can cause scums and mats that lead to hypoxia when decomposing that has negative impacts on other aquatic life (Paerl 2008). Algal blooms produce a variety of odour and taste compounds like geosmins (earth smell) and DMIB (dimethyl isoborneol) potentially rendering affected waters unsuitable for drinking (Paerl 2008). Numerous cyanobacterial blooms also produce alkaloid, peptide and other compounds which are toxic upon contact or ingestion (Paerl 2008).

Near the Yangtze Estuary, harmful algal blooms were rarely reported before the 1960s, but are increasing in frequency and tend to be present at the nutrient front where the river meets the sea where the high TN loading and sufficient light are present to promote algal growth (Gao and Wang 2008, Wang and Wu 2009). Total zooplankton biomass in the Yangtze Estuary and nearby waters of the East China Sea has more than doubled between 1959 and 1999 (Gao and Wang 2008). Blooms off the coast of China have increased in scale (km^2 to tens of km^2) and duration (days to months) (Heisler, Glibert et al. 2008). Between 1952 and 2002, at least 512 occurrences of HABs were documented, and between 2001 and 2006, 67 HAB events involved the production of toxic algal species, the principle species being Gymnodinium mikimotoi and K. mikimotoi (Wang and Wu 2009). As additional evidence of these excess nutrients in the Yangtze River, eutrophication in lakes and reservoirs linked to the river, as well as in the Yangtze Estuary are becoming increasingly apparent (Kennish 2002, Shen and Liu 2009, Wang 2013).

3.4 Summary

- Water quality data for the Yangtze Estuary was collected from literature and constituents of concern for municipal supply using coastal reservoirs were identified using the following considerations:
    - Comparison with Chinese raw water quality standard class III (drinking water);
    - Would have an implication for municipal treatment or would be affected by the operation of the coastal reservoirs;
    - Median concentrations were consistently at high levels;
    - Posed a risk to public health.
- Examination of available water quality data at the Yangtze Estuary indicates that generally very few parameters exceeded the required thresholds for drinking water use. Based on the available data, the diluting power of the Yangtze River appears sufficient to maintain the concentrations of most constituents despite contributions of upstream and local human activities, municipal, agricultural and industrial, at levels where they do not preclude municipal water supply
- Caution, however, should be applied in assuming that there is no risk to water quality in the Yangtze River resulting from trace metals or trace organic compounds for three key reasons:
    - The available data is from a limited number of samples which are probably insufficient to fully characterise the complexity of the system;
    - Although many of these constituents have no guideline set in the Environmental Quality Standards for Surface Water, this does not necessarily mean that they pose no risk to human or environmental health; and
    - Presence in the water column is not necessarily the only pathway for these constituents to end up in the municipal supply.
- The following constituents are considered to be of concern:
    - Salinity – because it affects the operation of coastal reservoirs and determines when water can be withdrawn from the estuary;
    - Key nutrients nitrogen and phosphorous – because they have median concentrations that exceed Class III thresholds and can lead to algal blooming in coastal reservoirs; and
    - Total suspended solids – because they are affected by coastal reservoir operation (pre-sedimentation) and can be a pathway for adsorbed contaminants.
- The Yangtze estuary is subject to regular occurrences of high salinity associated with seawater penetration into the estuary. Salinity becomes a problem for water supply operations when TDS concentrations exceed 450 mg/L.
- Concentrations exceeding this threshold are expected to occur at Gaoqiao, Chenhang and Chongtou when Yangtze River streamflow drops below 11,000 m3/s, 12,500 m3/s and 14,800 m3/s respectively.

- Streamflow is expected to drop below these thresholds during January, February, and December. During particularly dry years, issues could occur in March or November as well. Large scale water diversion in the Lower Yangtze River and sea level rise both have the potential to exacerbate this issue, increasing the risk that high salinity will occur and the duration of high salinity events.
- Increasing frequency and severity of high salinity events in the estuary could restrict Shanghai's ability to source freshwater. It will be necessary to construct additional reservoirs and enhance their ability to store water for longer periods to protect against this risk.
- Nutrient enrichment has occurred in the Yangtze River as a result of anthropogenic activities in the basin especially food production and municipal wastewater discharge.
- Total Nitrogen and Total Phosphorous concentrations at the estuary have consistently exceeded Chinese raw water quality standards Class III (drinking water source) since 1990.
- Inorganic fractions of Nitrogen and Phosphorous make up an increasing portion of Total Nitrogen and Total Phosphorous at the estuary. Nitrate and Dissolved Inorganic Phosphorous concentrations now exceed Class III requirements for Total Nitrogen and Total Phosphorous alone.
- Trajectories in the change of these inorganic nutrient concentrations and the land uses driving them appear to be increasing, and without significant changes in the rate of population growth or improvements in food production that minimise nutrient discharge to the river, these will continue to grow.
- High nutrient concentrations and the subsequent risk of algal blooming could complicate Shanghai's municipal water treatment process and lead to significant cost increases for water treatment.
- The behaviour of suspended sediments and their settleability in coastal reservoirs could have implications for Shanghai's water treatment operations. Suspended sediments in the Yangtze Estuary are fine grained, with almost all particles being classified as silt or finer. Small particles like silts and clays can be difficult to remove without techniques like coagulation and flocculation.
- Although suspended sediment concentrations have been decreasing in the Yangtze River, concentrations are still quite high and need to be removed prior to end use. Coastal reservoirs serve as pre-sedimentation storage that contributes to the overall treatment.

Chapter 4

4. Water Quality Shanghai's Qingcaosha Reservoir

Shanghai's coastal reservoirs form a crucial component of Shanghai's municipal water supply and are used for the capture and storage of water from the estuary. This chapter aims to explore the role of coastal reservoirs in Shanghai's water supply in more detail in an attempt to investigate their effect on downstream treatment processes.

Significant withdrawals for municipal water supply from the Yangtze Estuary began as early as 1996 with the construction of a pumping station and reservoir at Chenhang (Refer **Figure 4-1**) on the southern bank of the estuary (Li, Chen et al. 2015, Webber, Barnet et al. 2015). The next reservoir, the Qingcaosha Reservoir, was constructed to increase the supply of from the Yangtze Estuary and when it commenced operation in 2011, the Yangtze estuary became the primary source of water for Shanghai's municipal water supply (Finlayson, Barnett et al. 2012, Liu, Pan et al. 2016). At full operation, Qingcaosha was designed to provide 7.19 million m^3 of drinking water. Another smaller reservoir, Donfengxisha Reservoir, has also been constructed to capture water in the estuary, and together with Qingcaosha and Chenhang can supply 70% of Shanghai's water (based on 2012 demand) (Huang, Xie et al. 2014, Li, Chen et al. 2015, Liu, Pan et al. 2015). Key data on Shanghai's coastal reservoirs is summarised in **Table 4-1**.

Figure 4-1: Locations of Shanghai's coastal reservoirs. Aerial photo from NASA Earth Observatory (2017)

Table 4-1: Shanghai's Coastal Reservoirs Key Data Summary, Adapted from Yuan and Wu (2018)

Reservoir	**Chenhang**	**Qingcaosha**	**Dongfengxisha**
Year Construction Commenced	1990	2007	2011
Year Operation Commenced	1992	2011	2014
Size (km^2)	1.336	66.15	3.74
Effective Storage Capacity (million m^3)	9.5	438	8.9
Max Transfer Rate (million m^3/d)	1.3	7.19	0.215
Annual Supply Capacity (million m^3)	475	2624	78
Continuous Days' Supply Without Refill	7	68	41

Data has been collected from published articles and summarised in **Section 4.1** to characterise conditions and water quality in the Qingcaosha Reservoir. Due to the relative availability of data when compared with the other reservoirs, the Qingcaosha Reservoir will be focused on here. Locations of samples collected in the Qingcaosha reservoir are presented in **Figure 4-2**. Analysis of water quality processes occurring in the reservoir is presented in **Section 4.2** and discussion on water quality in the Qingcaosha reservoir, its effect on downstream treatment operations and potential management strategies are discussed in **Section 4.3**.

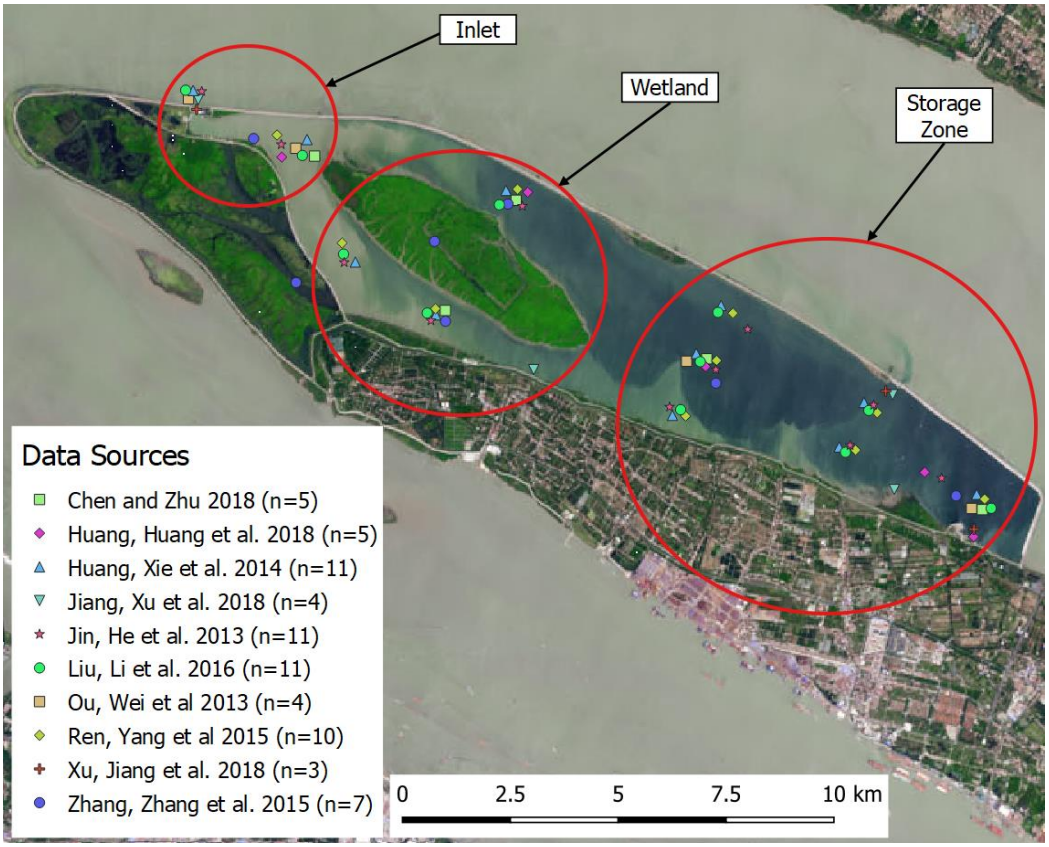

Figure 4-2: Data sources and sample locations in the Qingcaosha Reservoir. Aerial photo from NASA Earth Observatory (2017)

4.1 Qingcaosha Reservoir and its Water Quality

4.1.1 Physical Characteristics

The Qingcaosha Reservoir was constructed adjacent to Changxing Island and incorporates the two existing estuarine wetlands, the Qingcaosha Wetland and Zhongyangsha Wetland. Key components and locations in and around the Qingcaosha Reservoir are presented in **Figure 4-3**. The reservoir embankment comprises two dikes, the old dyke which was originally a component of Changxing Island's seawall and the new dyke which forms the outer border of the reservoir. The combined length of the dike is 48.4 km, and the total area of the reservoir is 66.15 km^2 (Yuan and Wu 2018). The construction of the Qingcaosha Reservoir began on the 5th of June 2007 and operation of the reservoir commenced on the 8th of June 2011 (Yuan and Wu 2018).

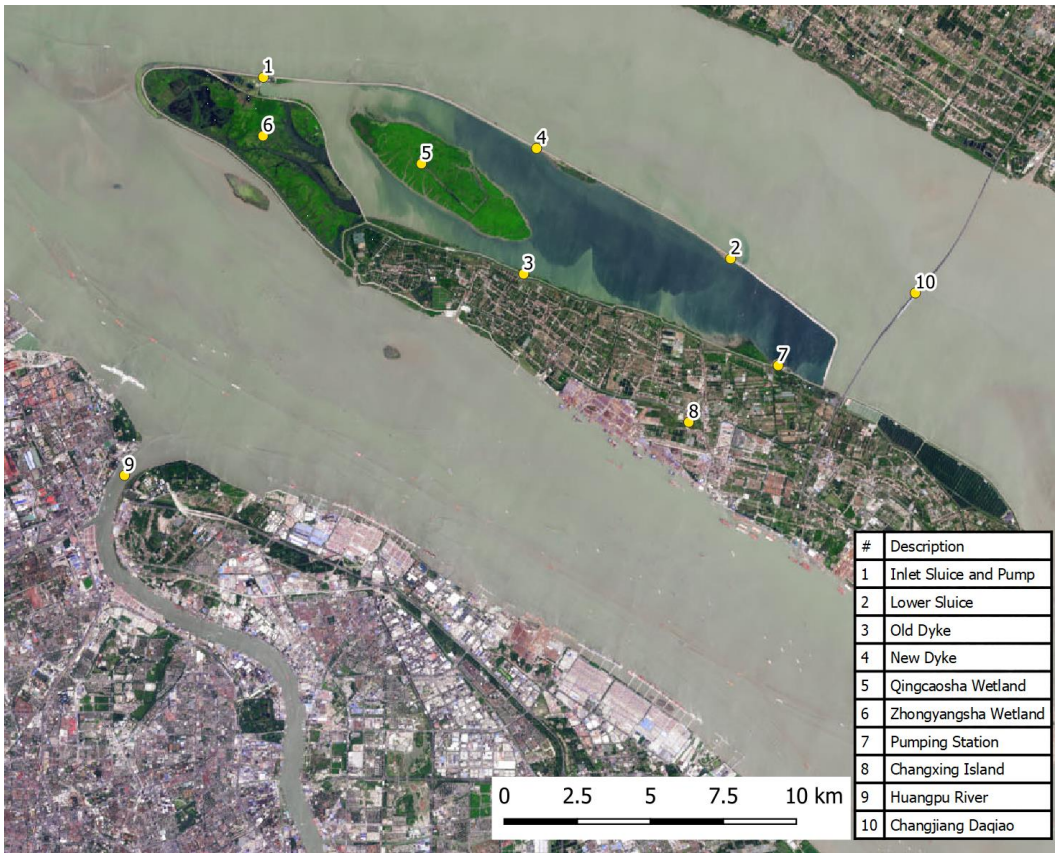

Figure 4-3: The Qingcaosha Reservoir. Aerial photo from NASA Earth Observatory (2017). Key locations from Sogreah Consultants (2008)

The reservoir bathymetry (**Figure 4-4**) ranges from relatively shallow on the western end of the reservoir at around 0m elevation (Wusong Datum) to getting progressively deeper towards the eastern end. Two channels exist on either side of Qingcaosha Wetland connecting the inlet zone to the reservoir storage area. The lowest bed level in the reservoir is below -10m elevation near the outlet and pumping station. The reservoir depth varies depending on the operating condition of the reservoir. The reservoir was designed to operate under two conditions in the estuary, in the dry season when saline intrusion is occurring and in the flood season when saline intrusion is not occurring. For this reason, the intake to the Qingcaosha reservoir consists of both a sluice and a pump system. During the flood season, inflow to the reservoir is controlled using the sluices, allowing for the tides and gravity to fill the reservoir (Sogreah Consultants 2008). The upper inlet sluice gate's net width is 70m and its lowest elevation -1.5 m. A outlet sluice gate at the eastern end of the reservoir has been included to allow for discharge of excess water and to control the reservoir's hydraulic retention time (HRT). This gate has a width of 20m and a lowest elevation of -1.5 m when fully open (Sogreah Consultants 2008, Yuan and Wu 2018). The maximum operation water level during the flood season is 4 m and the average operation water level 2.7 m. During the dry season, pumps at the inlet location are used to fill the reservoir to its maximum storage level of 7 m (Yuan and Wu 2018). These pumps can operate at a maximum capacity of 200 m^3/s (Sogreah Consultants 2008).

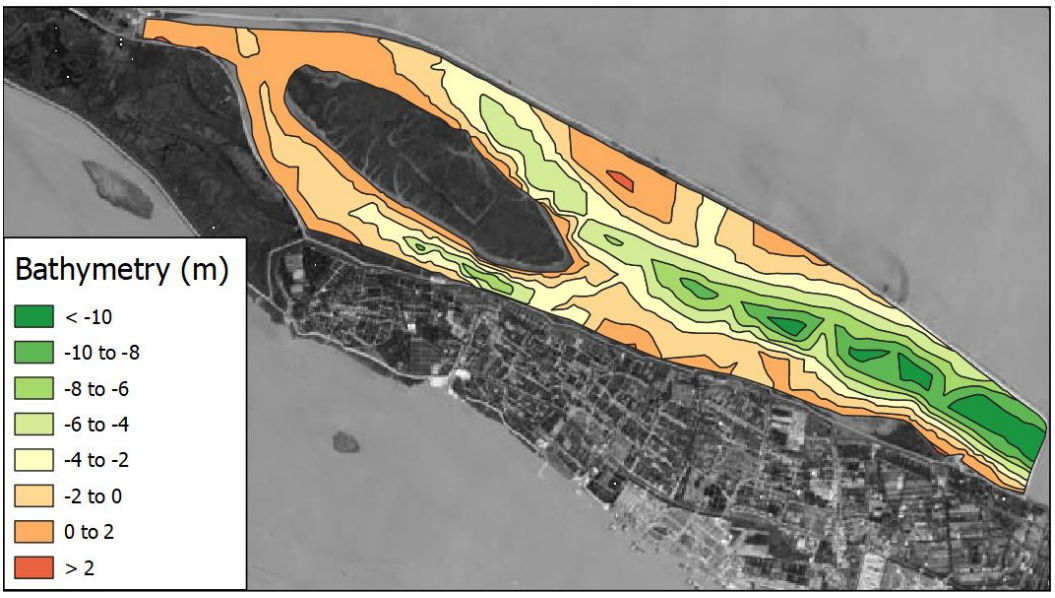

Figure 4-4: Bathymetry in the Qingcaosha Reservoir. Aerial photo from NASA Earth Observatory (2017). Bathymetry data digitised from Liu, Pan et al. (2016).

The Qingcaosha Reservoir has a dead storage level of -1.5m, a (total) maximum storage capacity of 527 million m^3 and an effective storage capacity of 438 million m^3 (Yuan and Wu 2018). The reservoir has a design daily water supply of 7.19 million m^3 from the outlet pumping station located at the south-western end of the reservoir. The reservoir is large enough to supply 68 days' supply without interruption when at full storage and was designed to operate with a typical HRT of 15-20 days and a maximum HRT of 30 days under standard (i.e. no saline intrusion) operating conditions (Sogreah Consultants 2008, Yuan and Wu 2018). A shorter HRT of 7-10 days is being considered to "flush" the reservoir as a potential water quality management strategy (Yuan and Wu 2018). Estimated average depths and storage volumes under different operating conditions are presented in **Table 4-2**.

Table 4-2: Estimated Average Depth and Storage under various operating water levels.

Operating Water Level	Water Level (m)	Estimated Average Depth (m)	Estimated Storage Volume (million m^3)
Minimum	-1.5	3.9*	89
Flood Season Typical	2.7	5.4*	281*
Flood Season Maximum	4.0	6.7*	349*
Dry Season Maximum	7.0	8.0*	527

Note: *Estimated depths and volumes calculated using water levels in Sogreah Consultants (2008) and Yuan and Wu (2018), and bathymetry from Liu, Pan et al. (2016). The level of the Qingcaosha wetland was estimated by setting the volume at 7 m water level elevation to 527 million m^3 as reported in Yuan and Wu (2018). Minimum volume has been calculated as total storage minus effective storage.

Wind conditions at the Qingcaosha reservoir have been summarised in **Table 4-3** and **Table 4-4**. During spring and summer, the dominant wind directions are from the East, South and Southeast. During autumn the dominant wind direction is from the East, followed by Southeast and Northwest. During winter, the dominant wind direction is from the Northwest, followed by the East. The estimated average wind speed is around 2.91 m/s.

Table 4-3: Typical Wind Direction (%) at the Qingcaosha Reservoir. Adapted from Liu, Pan et al. (2016)

	N	NE	E	SE	S	SW	W	NW	Calm
Spring	5.20	3.12	29.10	26.50	17.67	3.12	0.00	9.87	5.43
Summer	1.20	3.01	15.06	30.72	19.88	4.22	7.23	13.25	5.43
Autumn	4.6	5.26	37.49	13.81	6.58	0.66	2.63	15.78	13.19
Winter	3.36	3.36	23.49	12.58	7.55	0.84	0.84	33.55	14.44
Average	**3.59**	**3.69**	**26.29**	**20.90**	**12.92**	**2.21**	**2.68**	**18.11**	**9.62**

Table 4-4: Estimated Average Wind Speed (m/s) at the Qingcaosha Reservoir. Adapted from Liu, Pan et al. (2016)

	N	NE	E	SE	S	SW	W	NW	Calm	Seasonal
Spring	2.6	2.7	3.0	3.4	4.0	2.7	0.0	3.4	0.85	**3.2**
Summer	2.3	2.3	3.5	3.2	3.6	2.9	2.5	2.8	0.85	**3.0**
Autumn	3.7	2.3	2.9	2.8	3.0	3.5	2.3	3.3	0.85	**2.7**
Winter	2.6	2.3	2.9	2.7	3.2	2.3	2.3	3.5	0.85	**2.8**
Average	**2.80**	**2.40**	**3.08**	**3.03**	**3.45**	**2.85**	**1.78**	**3.25**	**0.85**	**2.91**

An estimate of reservoir fetch (**Table 4-5**) was calculated by taking the average length of open water in each wind direction weighted by typical wind directions presented in **Table 4-3**. Fetch is an indicator of the likelihood that wind will induce wave action or mixing in a large water body. The estimated fetch of the Qingcaosha reservoir was found to be approximately 8050 m.

Table 4-5: Estimated Reservoir Fetch.

Wind Direction	Fetch (m)
N	4450
NE	3800
E	7650
SE	12500
S	4450
SW	3800
W	7650
NW	12500
Calm	0
Weighted Average	**8051**

Average monthly temperature in the Qingcaosha Reservoir is presented in **Figure 4-5.** Strong seasonality is evident with temperatures peaking around 30°C in late summer and reaching around 7°C in January. Chen and Zhu (2018) reported that during their period of observation temperatures reached as low as 2.5°C in winter and as high as 32.5°C in summer. During this period, they reported that there was also very little spatial change in temperature within the reservoir and no evidence of a thermocline observed (Chen and Zhu 2018). In the deeper areas of the reservoir, depths can reach up to 14 m in normal operation and 17 m when filled to the maximum level. At depths in this range stratification is likely, and it is unusual that none was observed.

Average monthly dissolved oxygen (DO) is presented in **Figure 4-6**. Seasonality is also apparent with higher DO concentrations observed in winter than in summer, which is to be expected considering that the capacity for water to hold oxygen in dissolved form is inversely proportional to its temperature. **Figure 4-6** indicates that the maximum DO concentration is around 12 mg/L while the minimum is around 7.5 mg/L. During their period of observation, Chen and Zhu (2018) reported a range of DO concentration between 6mg/L and 14mg/L, and that there were significant variations in DO concentration observed between the surface water and deeper water. This difference reached up to 6 mg/L difference and was ascribed to both phytoplankton growth and poor water exchange in the reservoir (Chen and Zhu 2018). DO concentrations of 12 mg/L-14 mg/L are near saturation levels (depending on temperature) and are mostly associated with algae rather than reaeration induced by flow, wind or rain. Average monthly pH is presented in **Figure 4-7** and shows a pH range from approximately 7.8 to 8.6 which means that the water is neutral to slightly alkaline. pH appears generally higher in the warmer months than the colder months.

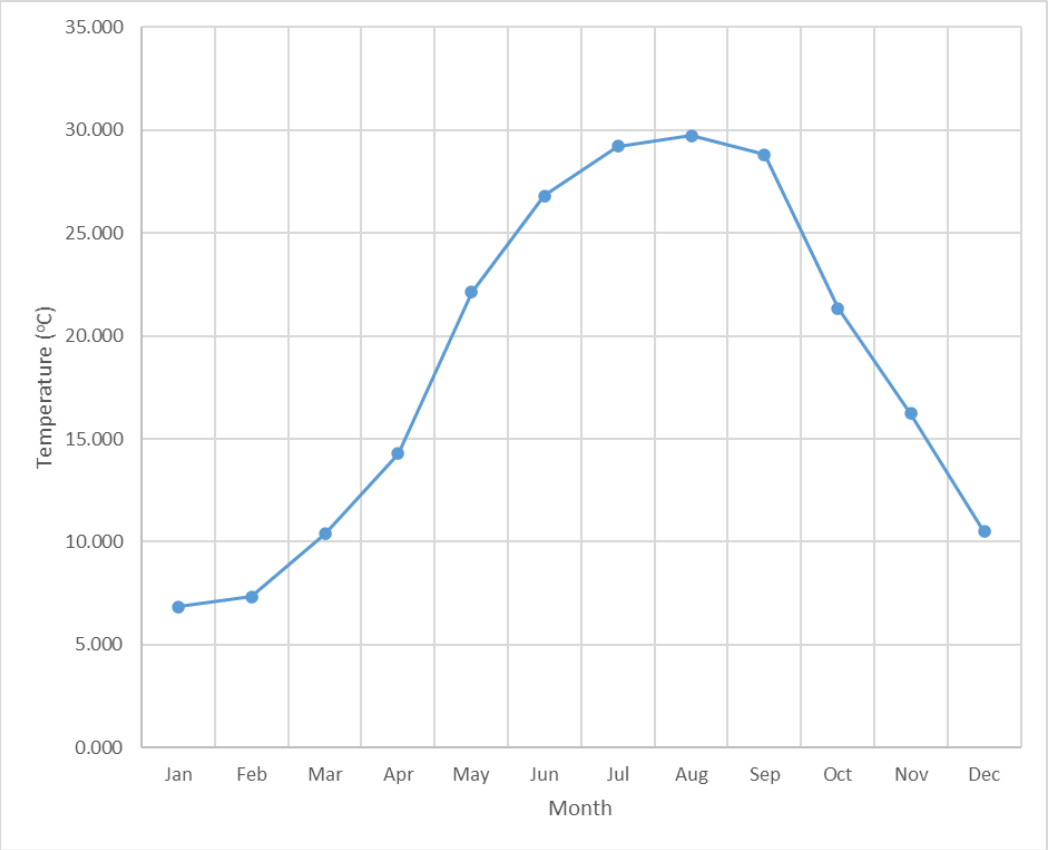

Figure 4-5: Average Monthly Water Temperature in the Qingcaosha Reservoir; Data sources: Liu, Li et al. (2016) and Jiang, Xu et al. (2018)

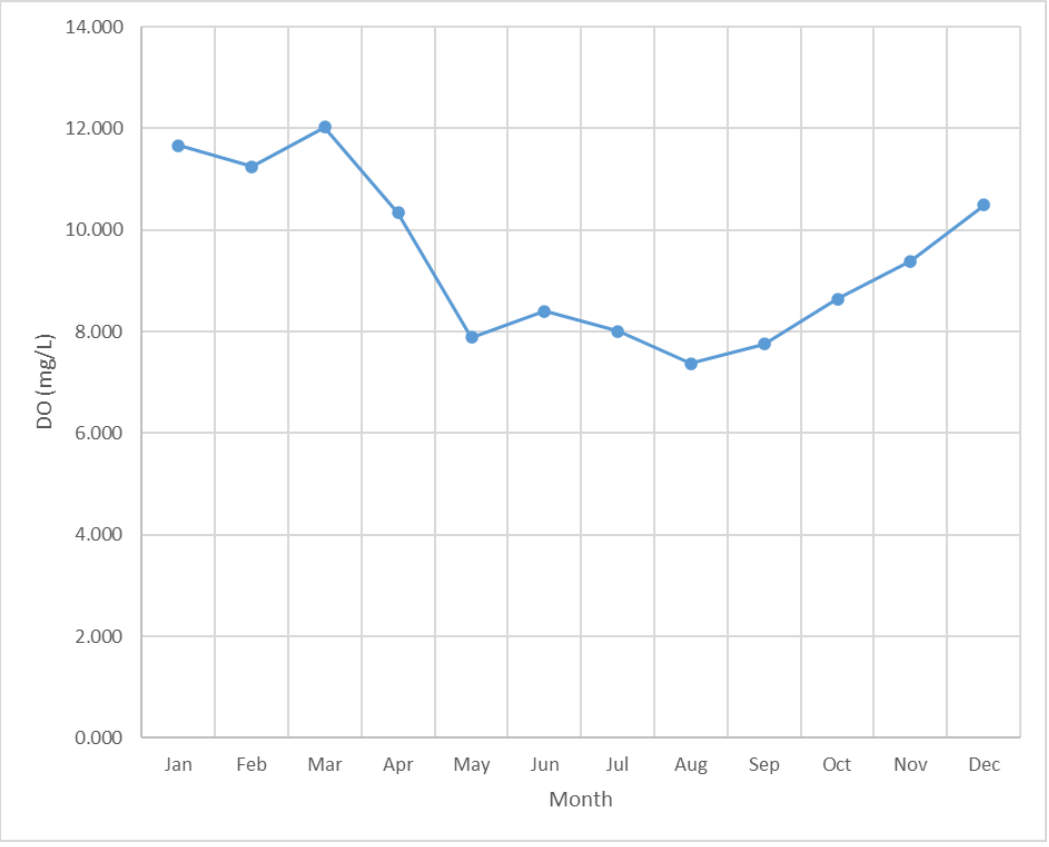

Figure 4-6: Average monthly DO concentration in the Qingcaosha Reservoir; Data sources: Liu, Li et al. (2016), Jin, He et al. (2013) and Jiang, Xu et al. (2018)

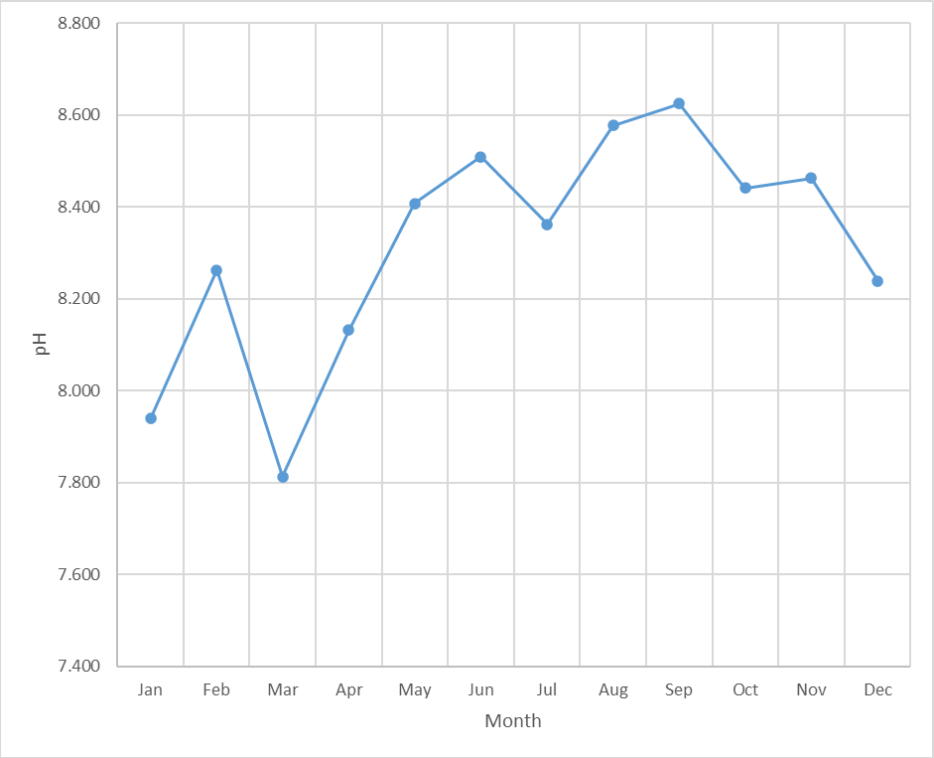

Figure 4-7: Average monthly pH in the Qingcaosha Reservoir; Data sources: Liu, Li et al. (2016), Huang, Huang et al. (2018) and Jiang, Xu et al. (2018)

Due to an absence of available data on total suspended solids in the reservoir, average transparency measured with a secchi disk (i.e. secchi depth) and turbidity have been considered here instead. While these measurements are not exact substitutes for TSS (Turbidity measures the reflectance of light in water rather that mass of non-filterable particles), at high turbidities, TSS is often the major contributing component. Average transparency (or Secchi Depth) from June 2009 to October 2013 is plotted in **Figure 4-8** and ranges from approximately 1.7 m to 0.4 m. Generally, the water clarity was higher before the reservoir commenced operation in 2010, except for the period in late 2009 when significant algal growth occurred. Conditions in the reservoir are characterised by slow moving water, reported as 0.02-0.04 m/s by Liu, Pan et al. (2015) and 0.05 m/s by Huang, Huang et al. (2018). These conditions promote the settling of particulates and transparency increases as result as water progresses down the reservoir (Liu, Li et al. 2016, Chen and Zhu 2018). Average monthly transparency is presented in **Figure 4-9** with results showing that transparency is at its highest in winter and lowest in summer, potentially showing the effect of summer algal growth in the reservoir on water clarity. Longitudinal changes in transparency and turbidity have been plotted in **Figure 4-10** and **Figure 4-11**. Results indicate that as water progresses through the reservoir, average transparency increases, and turbidity decreases. This is indicative of sedimentation of particles occurring in the reservoir. It should be noted that clarity in the reservoir is extremely variable and the data in **Figure 4-10** indicates that the clarity in the storage zone of the reservoir can be as low as the inlet.

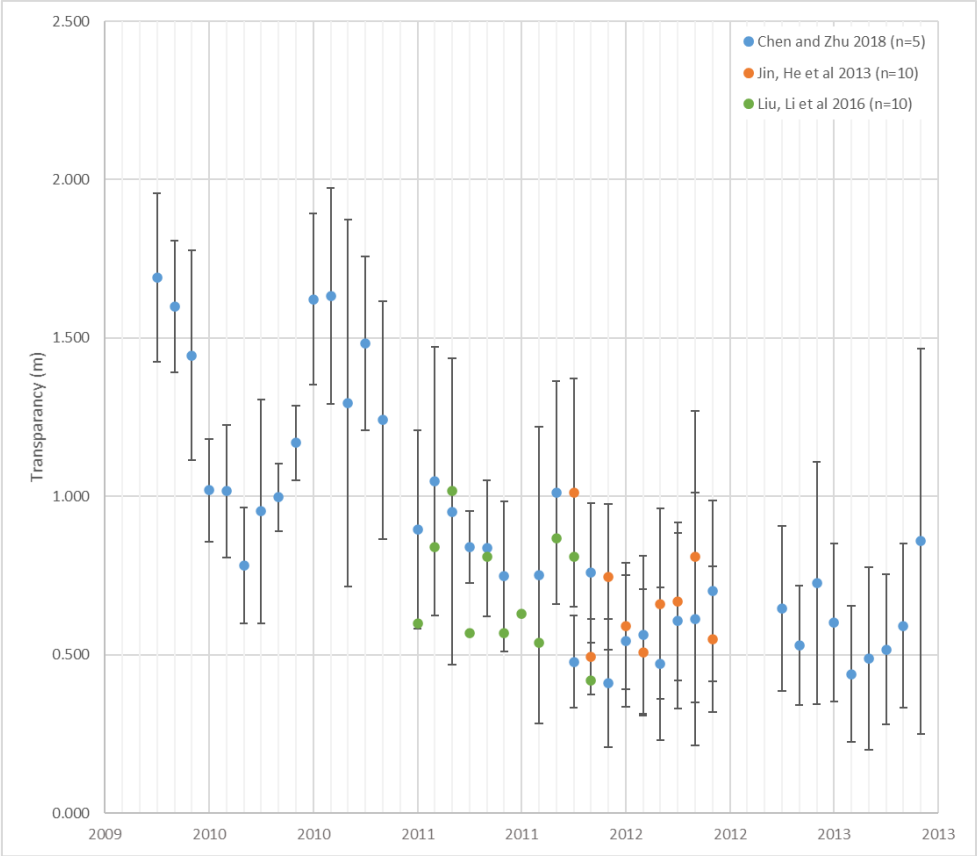

Figure 4-8: Average Transparency in the Qingcaosha Reservoir Jun 2009 to Oct 2013. Error bars refer to standard deviation. Data Sources: Chen and Zhu (2018), Jin, He et al. (2013), and Liu, Li et al. (2016)

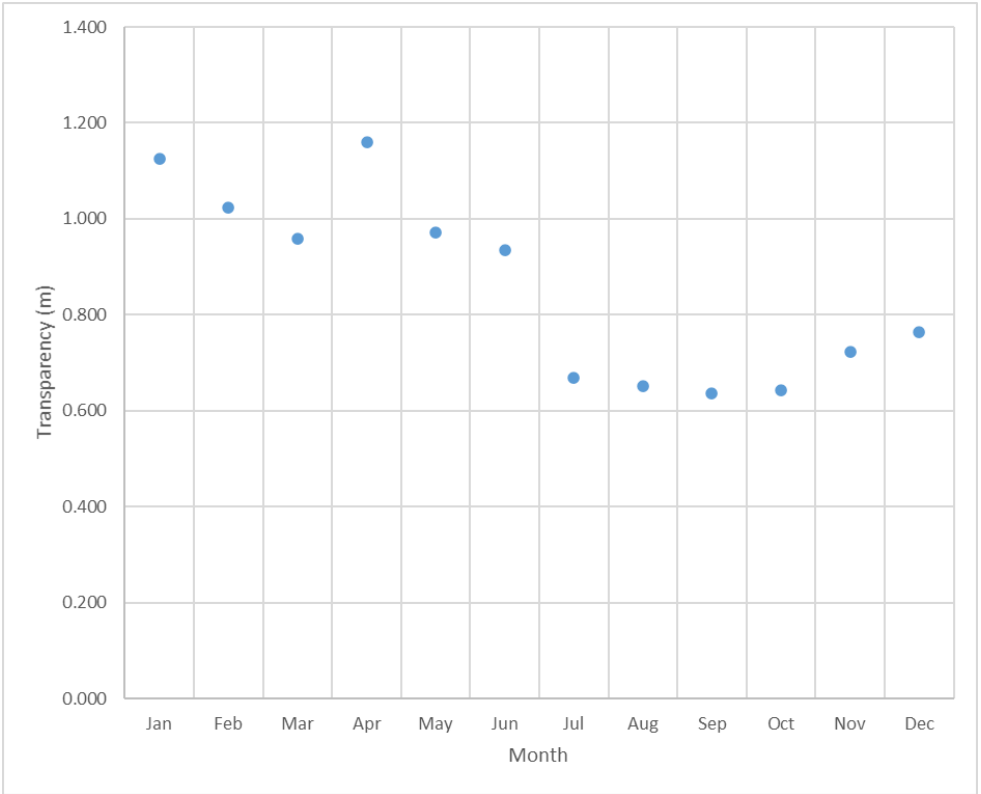

Figure 4-9: Average Monthly Transparency in the Qingcaosha Reservoir. Data source: Chen and Zhu (2018)

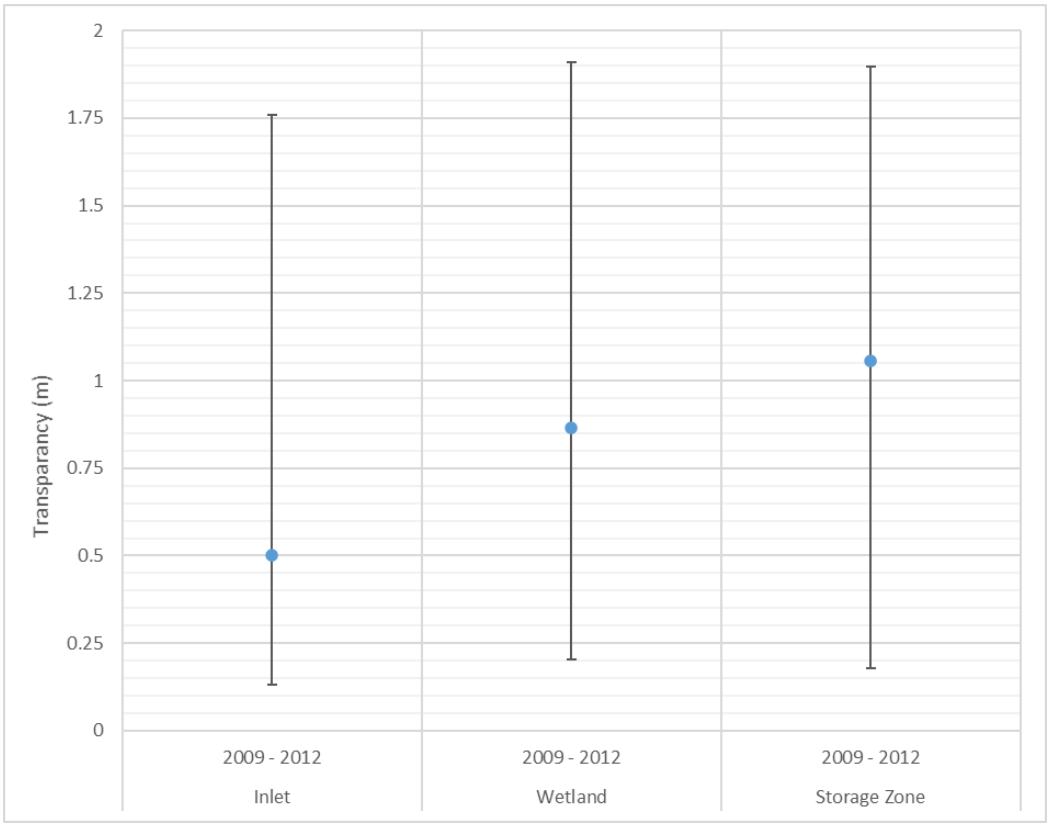

*Figure 4-10: Longitudinal Change in Transparency in the Qingcaosha Reservoir. Data source from Chen and Zhu (2018). Refer to **Figure 4-2** for locations. Error bars refer to standard deviation.*

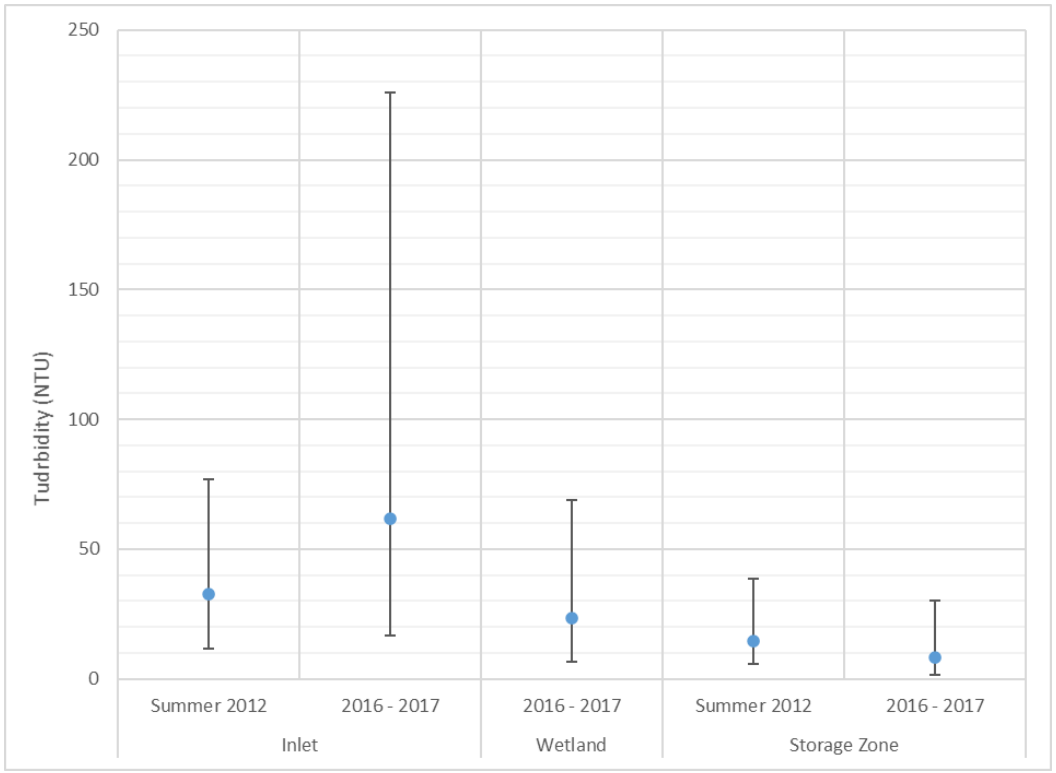

*Figure 4-11: Longitudinal Change in Turbidity in the Qingcaosha Reservoir. Data sourced from Ou, Wei et al. (2013) and Jiang, Xu et al. (2018). Refer to **Figure 4-2** for locations. Error bars refer to range in summer 2012 and standard deviation in other years.*

4.1.2 Nutrients

Average measurements of Total Nitrogen (TN) are presented in **Figure 4-12**. TN concentrations are generally comparable with the concentrations presented in **Section 3.3**, falling between 1-2 mg/L which is above the upper threshold for Class III water (1 mg/L). An exception to this is a significant decrease in concentration during 2009 and consistently low concentrations during 2010 while the reservoir was closed; during this period there were no inflows from the river to replenish TN in the reservoir. For the time period after 2009 and 2010 when the reservoir was open there is no clear long-term pattern to TN concentrations.

Monthly concentrations of TN are plotted in **Figure 4-13**. The value for January is based off a single estimate at the beginning of 2011 and may not give the best representation of what TN concentration is likely to be. Otherwise, the lowest TN concentrations appear to occur in February and late summer to early autumn. The drop in concentration appears to occur in 2011, 2012, 2014 and 2016 (**Figure 4-12**) and may indicate uptake of nitrogen during algal growth in late summer early autumn. Longitudinal concentrations for TN are plotted in **Figure 4-14**. No clear longitudinal behaviour can be observed, the 2009-2012 data and summer 2014 data indicate a decrease in average concentration at the storage area relative to the inlet where the summer 2012 data indicates an increase in TN concentration. The data from summer 2012 indicates a much higher variability in TN concentration than all other estimates in this study reaching as high as 7.6 mg/L. This suggests that the current data available may not be adequate enough to accurately characterise nutrient concentrations in the Qingcaosha reservoir.

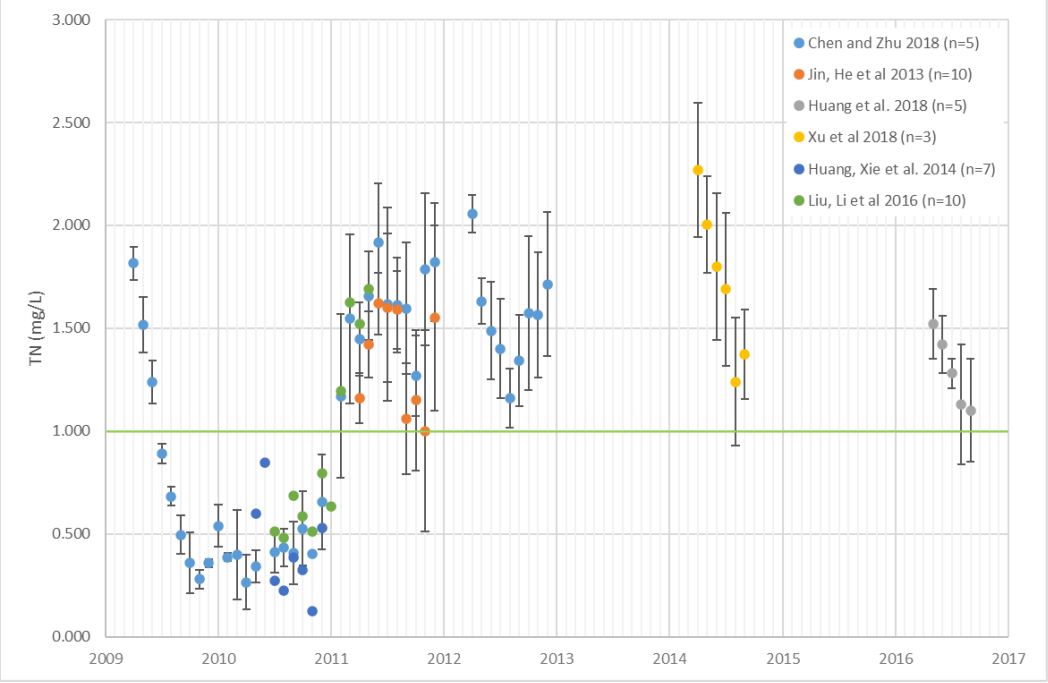

Figure 4-12: Average TN the Qingcaosha Reservoir 2009-2017. Error bars refer to standard deviation. Data source: Chen and Zhu (2018), Jin, He et al. (2013), Huang, Huang et al. (2018), Xu, Jiang et al. (2018), Huang, Xie et al. (2014), and Liu, Li et al. (2016). Green line represents Class III threshold for TN.

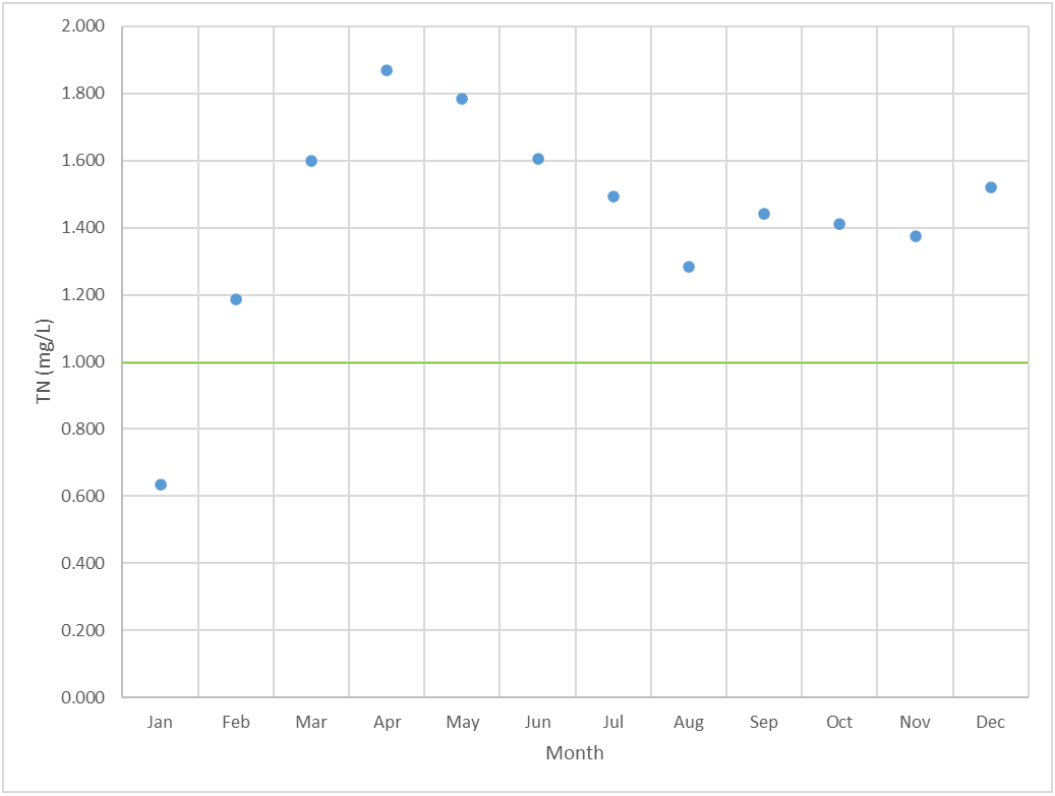

Figure 4-13: Average Monthly TN the Qingcaosha Reservoir 2011-2017. Data source: Chen and Zhu (2018), Jin, He et al. (2013), Huang, Huang et al. (2018), Xu, Jiang et al. (2018), Huang, Xie et al. (2014), and Liu, Li et al. (2016) Green line represents Class III threshold for TN.

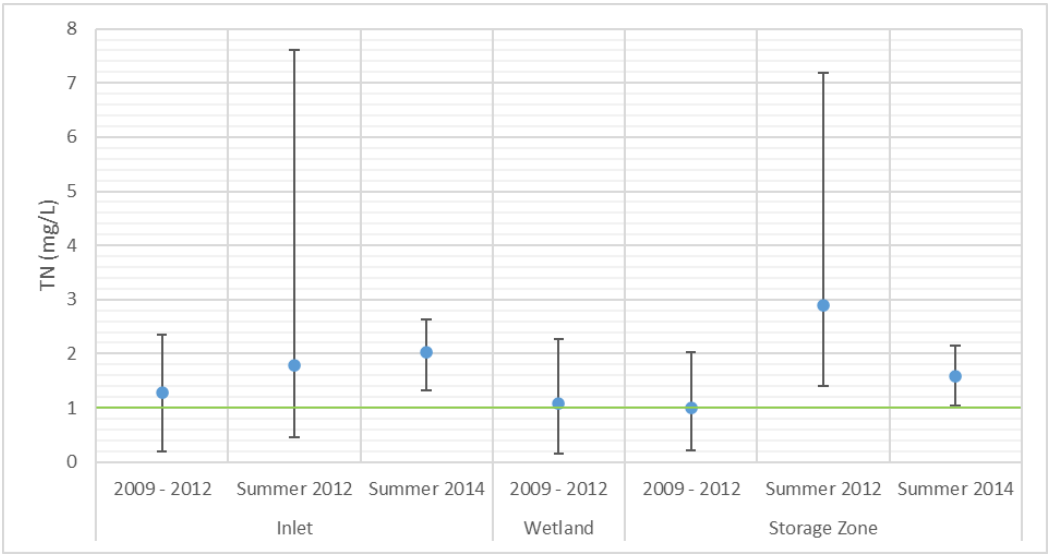

*Figure 4-14: Longitudinal Change in TN in the Qingcaosha Reservoir. Data source: Chen and Zhu (2018), Ou, Wei et al. (2013), and Xu, Jiang et al. (2018). Refer to **Figure 4-2** for locations. Error bars refer to range in summer 2012 and standard deviation in other years. Green line represents Class III threshold for TN.*

Average TP concentrations presented in **Figure 4-15** before 2011 are generally lower than the concentrations presented in **Section 3.3**¸while after the start of 2011 when the reservoir entered full operation, the estimates are more comparable. Many of the TP measurements also exceed the Class III threshold for lakes and reservoirs (0.05 mg/L) especially after 2011. The difference between these two time periods may be the result of additional particle settling during the long closure period in 2009 and 2010. Monthly average TP concentration estimates are presented in **Figure 4-15** and it appears that the lowest concentrations of TP occur during the winter months. This estimate is based on a limited dataset and it might not truly reflect the behaviour of TP on a monthly basis. Longitudinal concentration estimates for TP are plotted in **Figure 4-16**. Similar to TN, no clear pattern is observable here; the 2009-2012 data and summer 2014 data indicate a decrease in average concentration at the storage area relative to the inlet where the summer 2012 data indicates an increase in concentration. The variability of the estimate from summer 2012 is much larger than the other estimates, with maximum concentrations even exceeding Class V thresholds (0.2 mg/L for lakes and reservoirs).

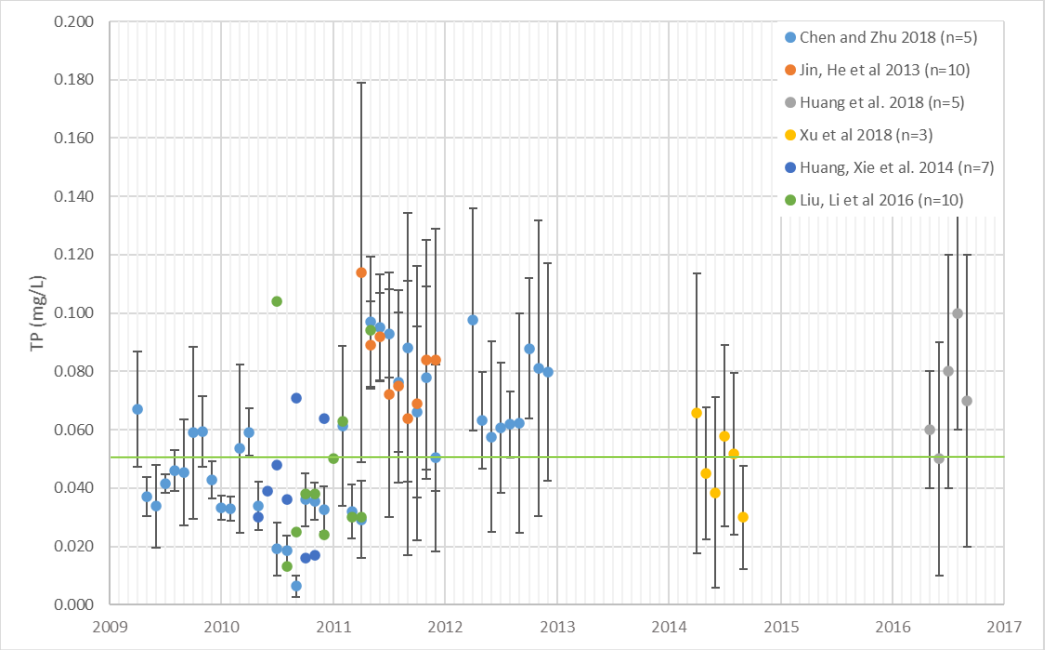

Figure 4-15: Average TP the Qingcaosha Reservoir 2009-2017. Data source: Chen and Zhu (2018), Jin, He et al. (2013), Huang, Huang et al. (2018), Xu, Jiang et al. (2018), Huang, Xie et al. (2014), and Liu, Li et al. (2016). Error bars refer to standard deviation. Green line represents Class III threshold for TP in lakes and reservoirs.

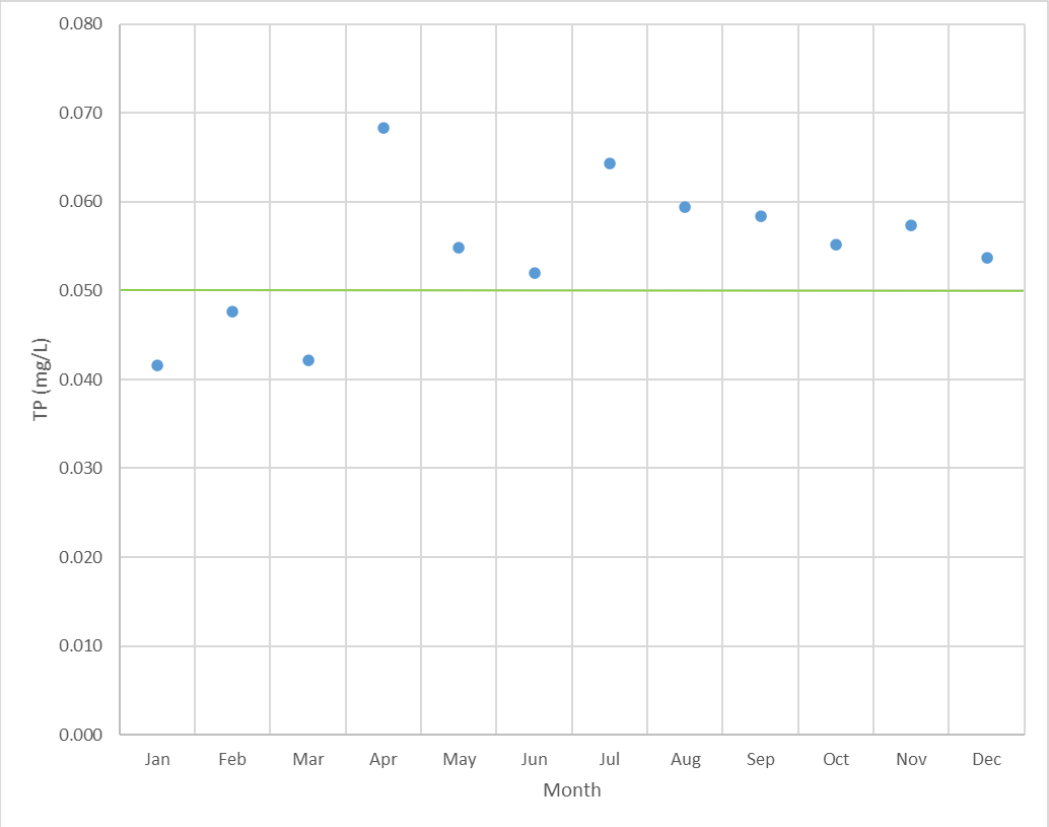

Figure 4-16: Average Monthly TP the Qingcaosha Reservoir 2009-2017. Data source: Chen and Zhu (2018), Jin, He et al. (2013), Huang, Huang et al. (2018), Xu, Jiang et al. (2018), Huang, Xie et al. (2014), and Liu, Li et al. (2016). Green line represents Class III threshold for TP in lakes and reservoirs.

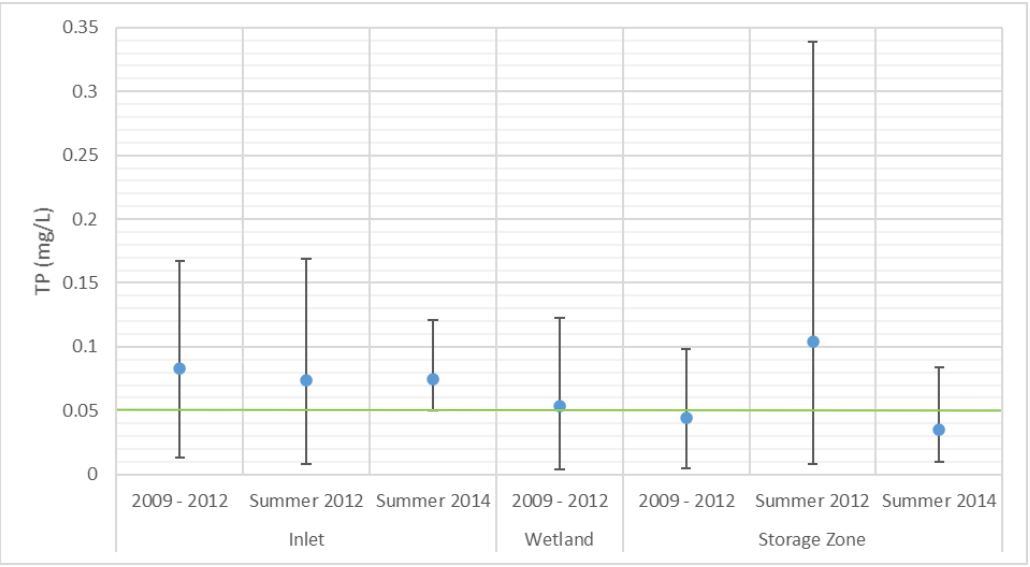

*Figure 4-17: Longitudinal Change in TP in the Qingcaosha Reservoir. Data source: Chen and Zhu (2018), Ou, Wei et al. (2013), and Xu, Jiang et al. (2018). Refer to **Figure 4-2** for locations. Error bars refer to range in summer 2012 and standard deviation in other years. Green line represents Class III threshold for TP in lakes and reservoirs.*

The TN to TP ratio has been plotted along with average TN and TP concentrations in **Figure 4-7.** TN to TP ratio ranges between around 10 to 115 and has mostly been above Redfield ratio (N:P molar ratio = 16) in periods where the reservoir was open; in these periods the river can replenish TN in the reservoir and the system is likely Phosphorous limited if only nutrients are considered as limiting factors. During the closure period, the TN to TP ratio dropped below the Redfield ratio several times, which indicates Nitrogen limitation and that nitrogen fixing algae (i.e. cyanobacteria) would have an advantage. However Liu, Pan et al. (2015) noted during their observation period (2010-2012) that the reservoir was at a nutrient abundant state and changes in TN or TP concentrations appeared to have no significant effect on algal growth in the reservoir.

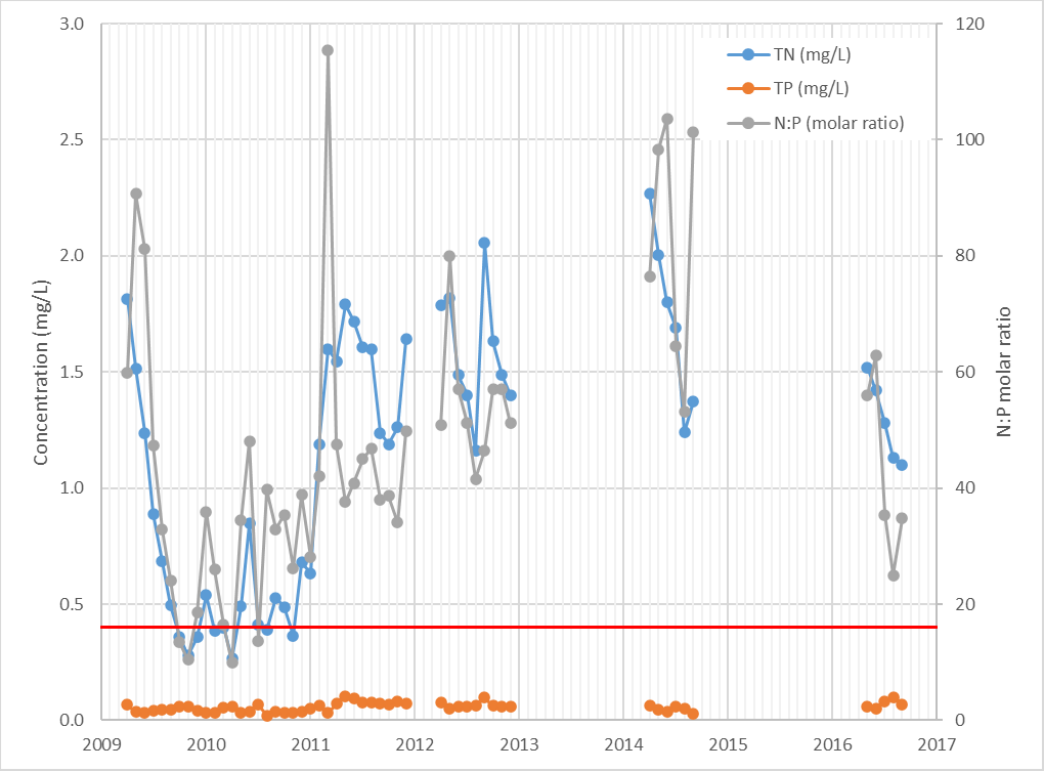

Figure 4-18: TN, TP, and estimated TN:TP molar ratio. Data sourced from Chen and Zhu (2018), Jin, He et al. (2013), Huang, Huang et al. (2018), Xu, Jiang et al. (2018), Huang, Xie et al. (2014), and Liu, Li et al. (2016). The red line represents the Redfield ratio (N:P molar ratio = 16)

4.1.3 Algae

Concentrations of Chlorophyll a, Cyanobacteria and Chlorophyta in the reservoir have been plotted in **Figure 4-19**. Elevated concentrations of Chlorophyll a during Summer in 2009, 2011 and 2016 can be observed. An algal bloom occurred in Summer 2009 that included elevated concentrations of Cyanobacteria and Chlorophyta; during this peak Cyanobacteria accounted for as much as 32-53% total algae (Zhang, Zhang et al. 2015). The following summer, nutrient levels the reservoir dropped while the reservoir was closed because there was no additional nutrient input from the river; the resulting nutrient levels were insufficient to support significant phytoplankton growth (Chen and Zhu 2018). After the reservoir entered full operation, the algal biomass increased sharply, and the dominant species became monopolistic. The cyanobacteria bloom in Summer 2011 only consisted of 4 species, the most dominant of which were Microcystis Incerta and Microcystis Aeruginosa (Ren, Yang et al. 2015, Liu, Li et al. 2016).

Seasonal average Chlorophyll a concentrations have been plotted in **Figure 4-20**. The highest concentrations occur during early autumn indicating that biological growth is at its highest during this time. The lowest concentrations occur during winter. Longitudinal Chlorophyll a concentrations have been plotted in **Figure 4-21**. While the highest maximum concentration and largest variability in concentration occur in the inlet zone, the average concentration of Chlorophyll a is highest in the wetland zone followed by the storage zone.

A few studies have attempted determine the predominant species comprising of the total algal biomass occurring in the reservoir and in which months they are predominant. During the 2010-2011 period, 282 species of phytoplankton were detected in the reservoir and two key temporal periods in algal behaviour were observed (Ren, Yang et al. 2015, Liu, Li et al. 2016):

- Late summer to autumn: where Cyanobacteria dominates; and
- Winer to early spring; where nearly no Cyanobacteria occur, and the community is made up of mostly Chlorophytes, Diatoms and Cryptophytes.

Between May 2015 and September 2016 63 taxa of algae were detected, including 6 species of Cyanobacteria which were dominant during Summer and Autumn, 21 species of Bacillariaphyceae (Diatoms) which were dominant during Winter, 27 species of Chlorophyta which occurred all year round, but peaked in Winter and 3 species of Chrysophyta which were prevalent in spring (Huang, Huang et al. 2018).

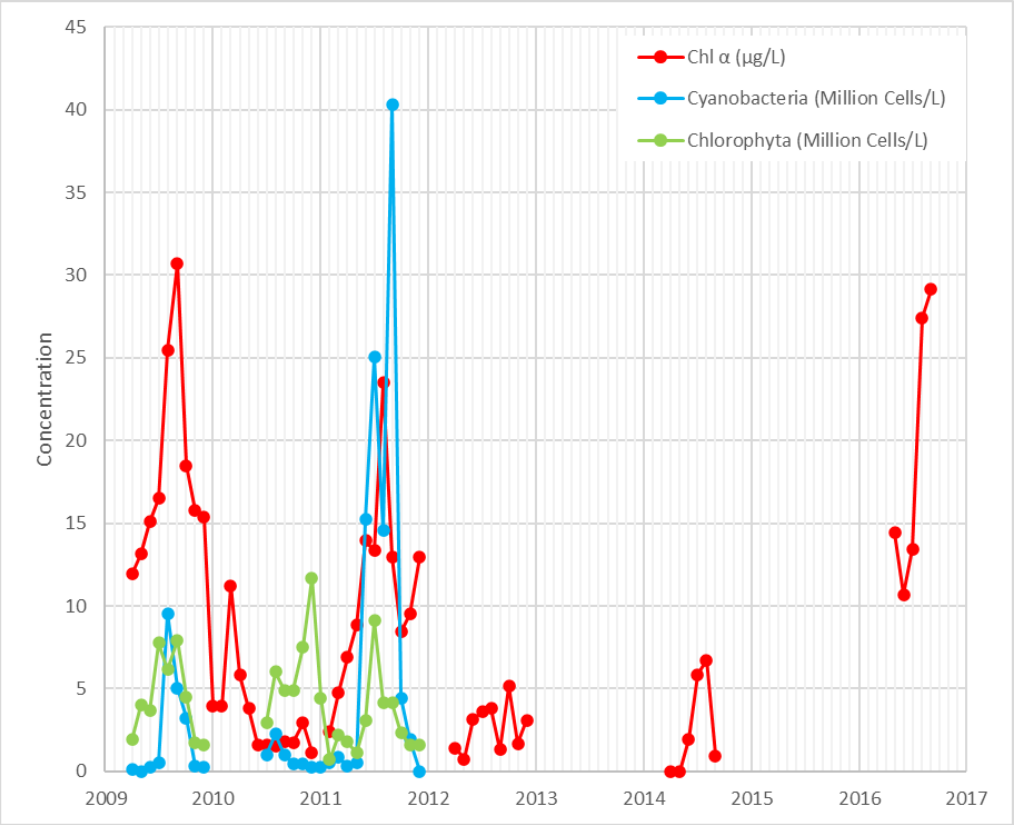

Figure 4-19: Chlorophyll a, Cyanobacteria and Chlorophyta in the Qingcaosha Reservoir. Data source: Chen and Zhu (2018), Jin, He et al. (2013), Huang, Huang et al. (2018), Xu, Jiang et al. (2018), Huang, Xie et al. (2014), Ren, Yang et al. (2015) and Zhang, Zhang et al. (2015).

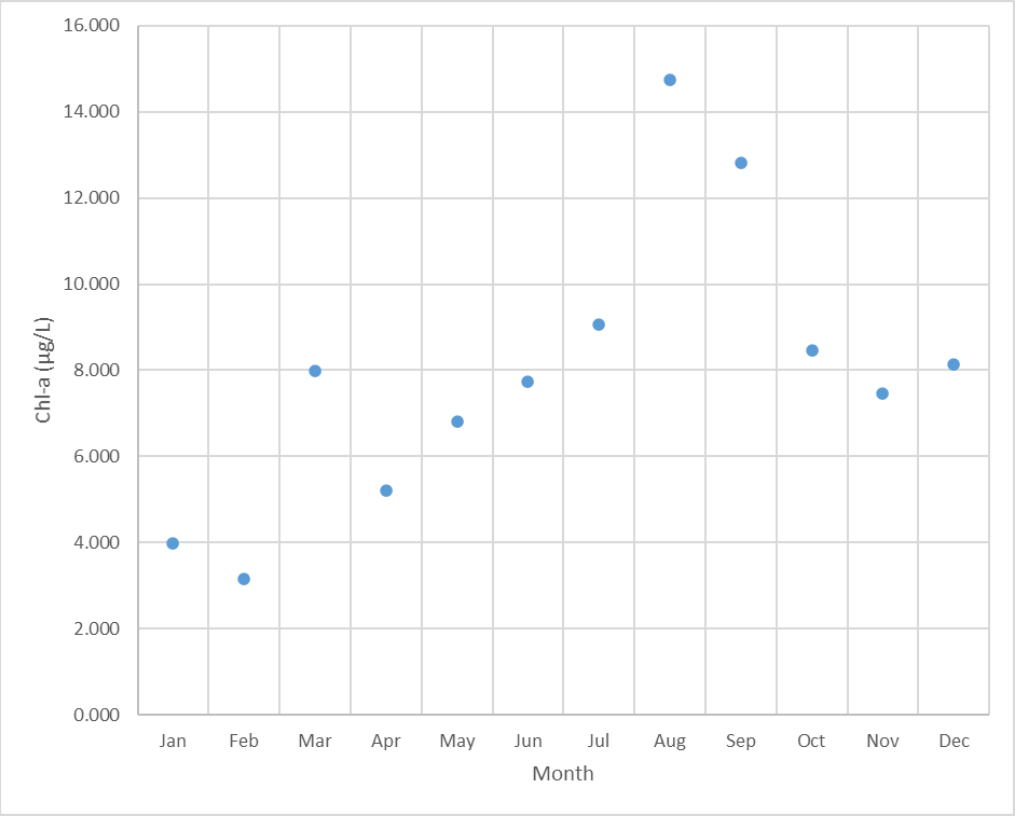

Figure 4-20: Monthly Average Chlorophyll-a concentration in the Qingcaosha Reservoir. Data source: Chen and Zhu (2018), Jin, He et al. (2013), Huang, Huang et al. (2018), and Xu, Jiang et al. (2018)

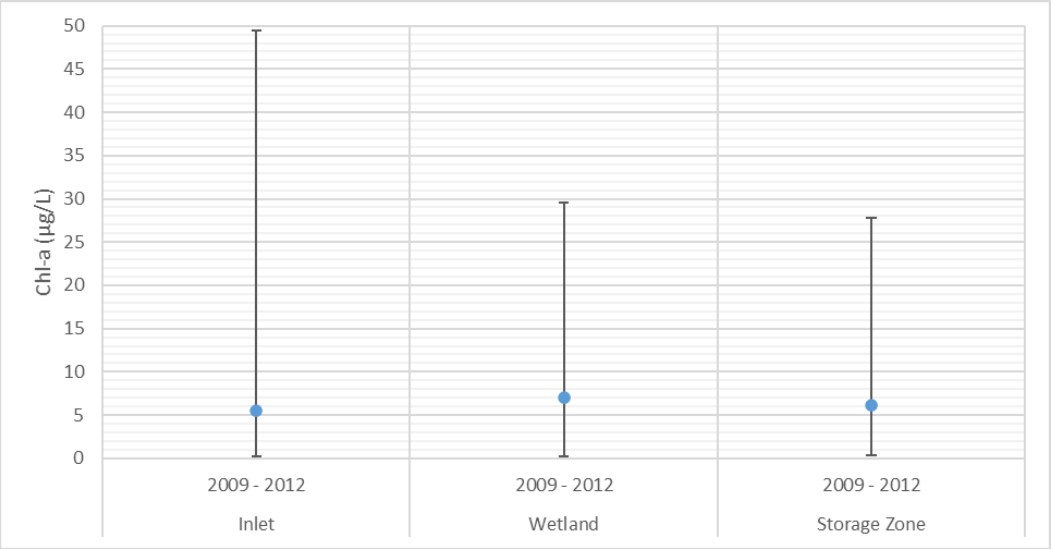

Figure 4-21: Longitudinal Change in TP in the Qingcaosha Reservoir. Chen and Zhu (2018). Refer to ***Figure 4-2*** *for locations. Error bars refer to standard deviation*

Water temperature and light are considered significant factors contributing to the growth and speciation of algae. In July and August 2011, the temperature ranged between 25 to 30ºC and light intensity near the surface ranged between 11,900-171,410 Lux (Ren, Yang et al. 2015). This high temperature contributed to a near maximum growth rate of Cyanobacteria and while light intensity that is too high can be lethal to some Cyanobacteria, the local climate has many rain events during summer and autumn. These events provided intermittent periods of low light intensity in between high intensity exposures which also may have contributed to high growth rates of Cyanobacteria (Ren, Yang et al. 2015). In winter 2009, while temperatures were low, Diatoms accounted for 53-62% of total algal cells (Zhang, Zhang et al. 2015). Dominance of Diatoms and Chlorophyta during winter was also observed in winter in 2011 and 2016, likely because Diatoms and Chlorophyta have growth rates of two to four times higher than Cyanobacteria at 20 degrees Celsius (Ren, Yang et al. 2015).

4.2 Water Quality Processes Occurring in the Qingcaosha Reservoir

As discussed in **Chapter 3**, both suspended sediments and high nutrient concentrations are expected to have implications to the operation of coastal reservoirs and municipal water treatment operations that warrant further investigation. This section applies analytical techniques with the data available to gain insight on mechanisms in the Qingcaosha reservoir relevant to sedimentation and biological growth.

4.2.1 Sedimentation

A common engineering technique for understanding the settleability of suspended sediment loads in a basin or reservoir is using the concept of an ideal settling basin. The terminal settling velocity of a discrete, non-flocculent particle that does not undergo a change in size, shape or specific gravity can be estimated by applying Stokes Law (Mines 2014) (**Equation 4-1**).

$$V_S = \frac{g(\rho_p - \rho_w)d^2}{18\mu} \qquad \textit{Equation 4-1}$$

Where: V_S = Terminal Settling Velocity (m/s)
g = Acceleration Due to Gravity (m/s^2)
ρ_p = Density of Particle (kg/ m^3)
ρ_w = Density of Water (kg/ m^3)
μ = Dynamic Viscosity of Water (Pa.s)

The ability of an ideal settling basin to capture particles is determined by its overflow rate (Mines 2014) (**Equation 4-2**)

$$V_o = \frac{Q}{A_S} \qquad \textit{Equation 4-2}$$

Where: V_s = Overflow rate (m^3/d/sq.m)
Q = Flow rate (m^3/d)
A_S = Surface Area (sq.m)

By comparing the overflow rate and particle settling velocity, the ability of an ideal basin to settle particles can be determined. Theoretically, all particles with a settling velocity greater than or equal to the overflow rate will be removed by the basin (Mines 2014).

Settling velocities were calculated for various particle sizes (**Table 4-6**). Particle size classifications were based on those specified in ISO 14688-1:2017 and a particle density of 2650 kg/ m^3, which is typical for weathered minerals like suspended clays, was adopted. Fraction of each particle size classification by weight was calculated and is presented in **Table 4-6** (based on **Figure 3-12)**. Particle grading at Jiangyin is taken to be representative to the suspended sediment load in freshwater arriving at the estuary. 47% of sediment (by weight) arriving at the estuary is expected to be clay fraction, 22% fine silt, 21% medium silt and the remaining 10% coarse silt. Silt particles have extremely slow settling times estimated to be between approximately 0.3 m/d (4 x 10^{-6} m/s) and 300 m/d (3.6 x 10^{-3} m/s). Clay settles extremely slowly and is can also exhibit colloidal properties which can prevent it from fully settling under gravity (Mines 2014).

Overflow rates were estimated for the various operating hydraulic conditions of the Qingcaosha reservoir,

- HRT = 8.5 days, volume = 281 million m^3 and water level = 2.7m – representing condition of the reservoir when flushing operations are occurring;
- HRT = 17.5 days, volume = 281 million m^3 and water level = 2.7m – representing the condition of the reservoir during typical (no saline intrusion) operation with a typical HRT of 15-20 days;
- HRT = 30 days, volume = 281 million m^3 and water level = 2.7m – representing the condition of the reservoir when at maximum HRT during typical operation; and
- HRT = 68 days, volume 527 million m^3 and water level = 7.0m – representing the condition of the reservoir during the dry season when saline intrusion is occurring.

Estimated flow rates, horizontal velocities and overflow rates are presented in **Table 4-7**. The estimated overflow rates are low enough that during typical operation, it is expected that most particles or equal weight or heavier than fine silt could be removed from the reservoir. The minimum particle size estimated to be settleable for each HRT are compared with sediment particle size distribution at Jiangyin in **Figure 4-22**. Estimated sediment removal fractions are 48%, 52%, 57% and 59% for 8.5 days, 17.5 days, 30 days, and 68 days respectively. The majority of remaining particles are predominantly clays which may require coagulation and flocculation to be applied in order to be removed.

Table 4-6: Estimated Settling Velocities based on Particle Grading Classification (ISO 14688-1:2017) and Classification of Suspended Solids and Bed Material at Jiangyin and Datong. Sediment data from Gao (2014)

Category	Name	Size (mm, > than)	Settling Velocity (mm/s)	Settling Velocity (m/d)	Fraction Suspended Solids (%)		Fraction Bed Material (%)	
					Jiangyin	Datong	Jiangyin	Datong
Very Coarse Soil	Large Boulder	630	Really Fast	Really Fast	0	0	0	0
	Boulder	200			0	0	0	0
	Cobble	63			0	0	0	0
Coarse Soil	Coarse Gravel	20			0	0	0	0
	Medium Gravel	6.3			0	0	0	0
	Fine Gravel	2			0	0	0	2
	Coarse Sand	0.63	357	30821	0	0	0	2
	Medium Sand	0.2	36.0	3106	0	2	2	36
	Fine Sand	0.063	3.57	308.2	0	16	48	48
Fine Soil	Coarse Silt	0.02	0.360	31.1	10	39	50	9.7
	Medium Silt	0.0063	0.0357	3.1	21	26	0	2.3
	Fine Silt	0.002	0.00357	0.3	22	17	0	0
	Clay	$\leqslant$ 0.002	$\leqslant$ 0.00357	$\leqslant$ 0.3	47	0	0	0

Table 4-7: Estimated Horizontal Velocity and Overflow Rate at various Hydraulic Retention Times

HRT (days)	Flow to Shanghai (million m^3/d)	Sluice Outflow Rate (million m^3/d)	Average Horizontal Velocity (m/s)*	Overflow Rate ($m^3/(d.m^2)$)**
8.5 – Flushing	7.19	25.87	0.020	0.636
17.5 – Typical Operation	7.19	8.87	0.010	0.309
30 – Typical Operation; Max HRT	7.19	2.18	0.006	0.180
68 – Dry season; Max HRT	7.19	0.00	0.004	0.116

* calculated at an average section assuming a reservoir width of 3.5km and depth of 5.4m
**calculated using reservoir water surface area of 51.95 km^2 for flushing and typical operations when the water level is at 2.7 m and using an area of 66.15 km^2 for the dry season max HRT when the water level is at 7 m and the reservoir is full.

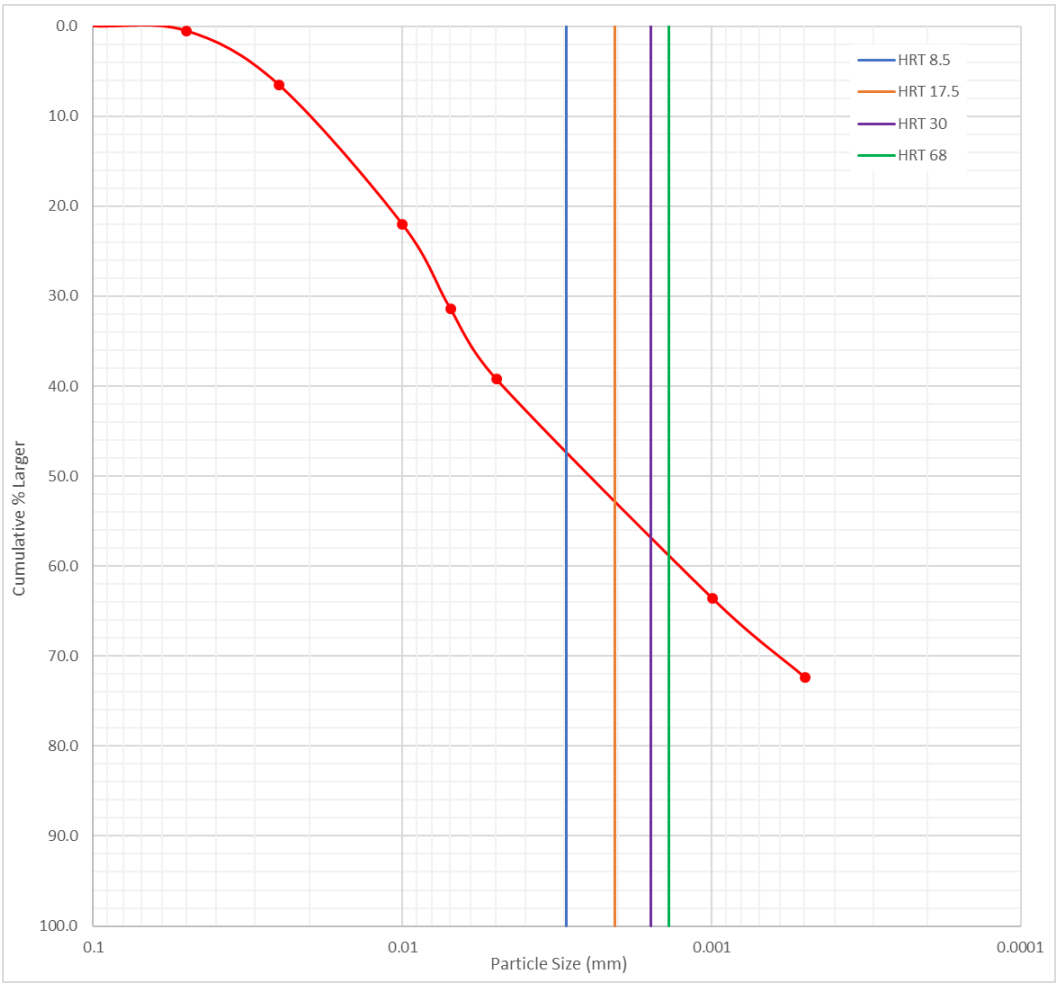

*Figure 4-22: Sediment particle distribution at Jiangyin and estimated minimum settleable particle size at the overflow rates calculated in **Table 4-7**. Particle size distribution: Gao (2014) suspended sediment at Jiangyin*

The results of this calculation are generally consistent with the longitudinal behaviour observed in **Figure 4-10** and **Figure 4-11**, where particles settle out and water transparency improves as water passes through the reservoir. The predicted behaviour is also visible in aerial imagery of the reservoir as displayed in **Figure 4-23**. Despite this, there are limitations to treating the reservoir as an ideal settling basin for the purposes of estimating sediment removal:

- Firstly, this technique does not consider resuspension mechanisms such as wind action, hydraulic turbulence and animal induced resuspension;
- Secondly, the reservoir demonstrates clear spatial variability in suspended sediment (**Figure 4-23**) which is not reflected in this method; and
- Finally, this method assumes spherical particles and that free settling is occurring, which may not be the case for fine particles such as silts and clays.

Real settling velocities in the in the Qingcaosha reservoirs will depend on the variable depths and cross sections in the reservoir and their influence on flow velocities in the reservoir. In shallower sections, the flow velocity is increased, hindering settling, while settling is

enhanced in deeper sections of the reservoir which have reduces flow velocities. This can be observed by comparing the observed settling of particles in **Figure 4-23** with the bathymetry presented in **Figure 4-4** where the suspended particles can be observed in the shallow sections of the reservoir, especially to the south of the Qingcaosha wetland, while improved clarity can be observed in the deeper portion of the reservoir. To further understand the sediment transport dynamics in the reservoir, using a hydrodynamic model with coupled sediment transport modules would be more appropriate as it would allow for detailed estimation of velocities and sediment movement to be calculated. However, additional data collection at key locations in the reservoir would be required to employ this technique.

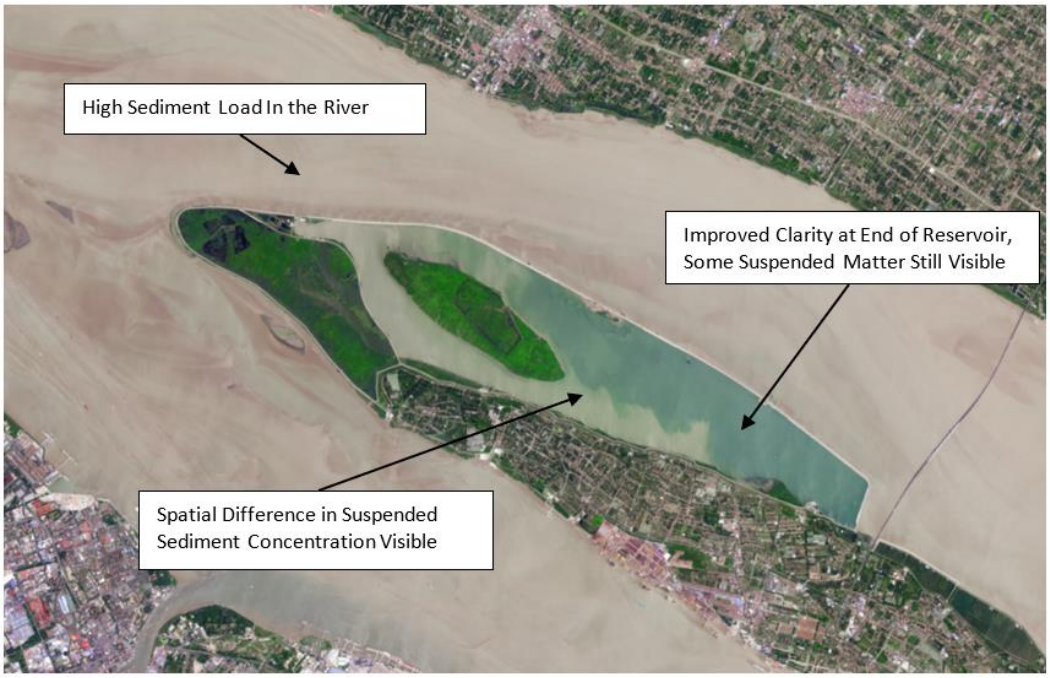

Figure 4-23: Aerial Photo captured in 2016 where Suspended Sediment the Qingcaosha Reservoir can be observed (NASA Earth Observatory 2017)

4.2.2 Biological Processes

A model-based approach was used to investigate the effects on nutrient levels in the Yangtze Estuary source water (eutrophication) on algal production. Load-response curves for a hypothetical system approximating the Qingcaosha Reservoir were derived for multiple operating conditions. The model PCLake+ (version 6.13.16) was selected for this task. The full PCLake+ model including supporting documentation can be accessed at https://github.com/pcmodel.

PCLake is a one-dimensional lake ecosystem model of intermediate complexity that combines a short run-time and limited data requirement (typical to a simple model) with a level of complexity suitable to answer lake water quality related questions (Janssen, Teurlincx et al. 2019). Based on the low flow velocities expected in the Qingcaosha Reservoir, an assumption was made that ecological behaviour in the reservoir is sufficiently analogous to that of a lake.

The PCLake model was designed to simulate the main nutrient and food web dynamics of a non-stratifying lake in response to eutrophication and related restoration measures. It was calibrated against nutrient, transparency, Chlorophyll a and vegetation data of > 40 lakes and a systematic sensitivity and uncertainty analysis was performed (Janse, De Senerpont Domis et al. 2008). PCLake dynamically models closed nutrient cycles allowing for quantified analysis of primary production of macrophytes and phytoplankton and then calculates the water quality parameters Chlorophyll a, transparency phytoplankton types and the density of submerged macrophytes. It also calculates the distribution and fluxes nitrogen and phosphorous (Janse 1997).

Input into the model are lake/reservoir hydrology, nutrient loading, dimension and sediment characteristics. The model then describes the water column and upper sediment layer (default 0.1m) and an optional wetland zone with helophytes (Janse 1997, Janse, De Senerpont Domis et al. 2008). The base of the model are water and nutrient budgets (in- and outflow). A physico-chemical model describes the exchange of detritus, inorganic matter and nutrients between the sediment and water (and wetland zone if included) and two modules, a phytoplankton and a macrophyte module, describe the primary production of the system (Janse 1997). A simple food web module consisting of zooplankton, macro-zoobenthos, planktivorous and predatory fish has been used and all biota are modelled on the basis of functional groups. This allows for the effects of the food web structure on nutrient cycles in the lake to be accounted for (Janse 1997, Janse, De Senerpont Domis et al. 2008).

PCLake is well suited to studying the impacts of eutrophication and oligotrophication processes of lake ecology and water quality and has been applied in many specific cases to assess critical nutrient loading in specific lakes (Janssen, Teurlincx et al. 2019). PCLake can be used for transient and bifurcation analysis:

- Transient analysis is used to study temporal dynamics and impacts of the system's history as captured by the initial conditions. For a transient analysis, the user needs to carefully consider all initial state variables by using field data or estimates at time zero. A major challenge in transient analysis is that these conditions are often partly unknown.
- Bifurcation analysis is used to study the equilibrium of the model in response to changing parameters. This technique is particularly suited to creating a load response curve for critical nutrient loads, and for examining the presence of hysteresis between alternative stable states; in this case a clear state representing a macrophyte dominated ecological system and turbid state representing an algae dominated system (Janssen, Teurlincx et al. 2019).

PCLake was upgraded to PCLake+ in 2019 to extend its application domain to cover a wide range of freshwater lakes that differ in thermal stratification modes and climate-related process, while remaining as close as possible to the original model formulations and scientific niche. Additional input parameter verification for deeper lakes was undertaken to supplement previous input verification (Janssen, Teurlincx et al. 2019). Further modification to PCLake+ to incorporate buoyancy regulation and nitrogen fixation of Cyanobacterial species was also undertaken in 2020 (Chang, Teurlincx et al. 2020).

In this study, bifurcation analysis is used to observe the Chlorophyll a response to Total Nitrogen and Phosphorous loading under different operation conditions:

- HRT = 8.5 days, volume = 281 million m^3 and water level = 2.7m – representing condition of the reservoir when flushing operations are occurring;
- HRT = 17.5 days, volume = 281 million m^3 and water level = 2.7m – representing the condition of the reservoir during typical (no saline intrusion) operation with a typical HRT of 15-20 days;
- HRT = 30 days, volume = 281 million m^3 and water level = 2.7m – representing the condition of the reservoir when at maximum HRT during typical operation; and

Dry season operation (HRT 68 days) was not considered in this assessment because there is no regularity to conditions that cause the reservoir to close for long periods of time (i.e. saline intrusions and pollution events). Bifurcation analysis involves running the model to equilibrium over a period of at least 20 years and the effects of these closures would not be observed in the results. Temporal analysis is more appropriate to assess the effects of dry season closures, however at this stage these is inadequate data to calibrate and run a temporal analysis.

The procedure followed to undertake this analysis is as follows:

1. Collect and collate data for input factors of the Qingcaosha Reservoir and input into the model;
2. Select initial values for turbid and clear states for bifurcation analysis;
3. Run initial conditions to equilibrium to initialise the model, once for the turbid State (Run 0) and once for the clear State (Run 1);
4. Adopt the values determined at the end of the first year of the initialisation run as initial values for the bifurcation analysis (replacing the previous assumptions);
5. Identify a range of input nutrient loadings to assessed with the bifurcation analysis;
6. For each nutrient loading value, the model needs to run twice to equilibrium, once for clear conditions and once for turbid conditions;
7. The output variable, in this case Chlorophyll a, is then averaged over the year or target season; and
8. The output variables of all input nutrient loading values can then be plotted to produce a load response curve. Input loads were converted to concentrations to conveniently compare with concentrations in the Yangtze Estuary.

The input data and settings for the model are described in **Appendix 3**. Bifurcation analysis was run on TP loading range of 0 to 0.1 gP/sq.m/d in 21 increments, which was determined sufficient to cover a range of concentrations from the estuary (including estuary average, Class III threshold and Class V threshold) at difference hydraulic loading rates. TN loading was coupled to TP loading at a ratio of 19.4, which was estimated to be the average ratio between these two parameters at the estuary. For this study, Run ID 0 was used to calculate response curves starting from clear conditions and progressing towards turbid conditions (eutrophication) and run ID 1 was used to calculate the response curve starting from turbid conditions and progressing towards clear conditions (oligotrophication).

Chlorophyll a response to nutrient concentrations under typical operating conditions (HRT 17.5 days) is presented in **Figure 4-24**. Responses for both the annual average and summer only have been plotted. The estimated Chlorophyll a concentration response to a TP concentration matching the estuary average is approximately 4 µg/L over the whole year and 7.5 µg/L. Increasing TP concentration results in expected increases in Chlorophyll a concentration. Compared with annual average conditions, Chlorophyll a concentrations are expected to be higher during summer which is expected due to increased light and higher temperatures. The gradient of the summer response curve is steeper, indicating that algal growth in the reservoir is more sensitive to high phosphorous concentrations during summer. At TP concentrations equivalent to the class III thresholds, there is approximately 2 µg/L difference between summer and annual average Chlorophyll a concentrations. At TP concentrations equivalent to class V thresholds, this difference is 6 µg/L. Increasing TP loads appear to increase the risk of algal growth particularly during the summer.

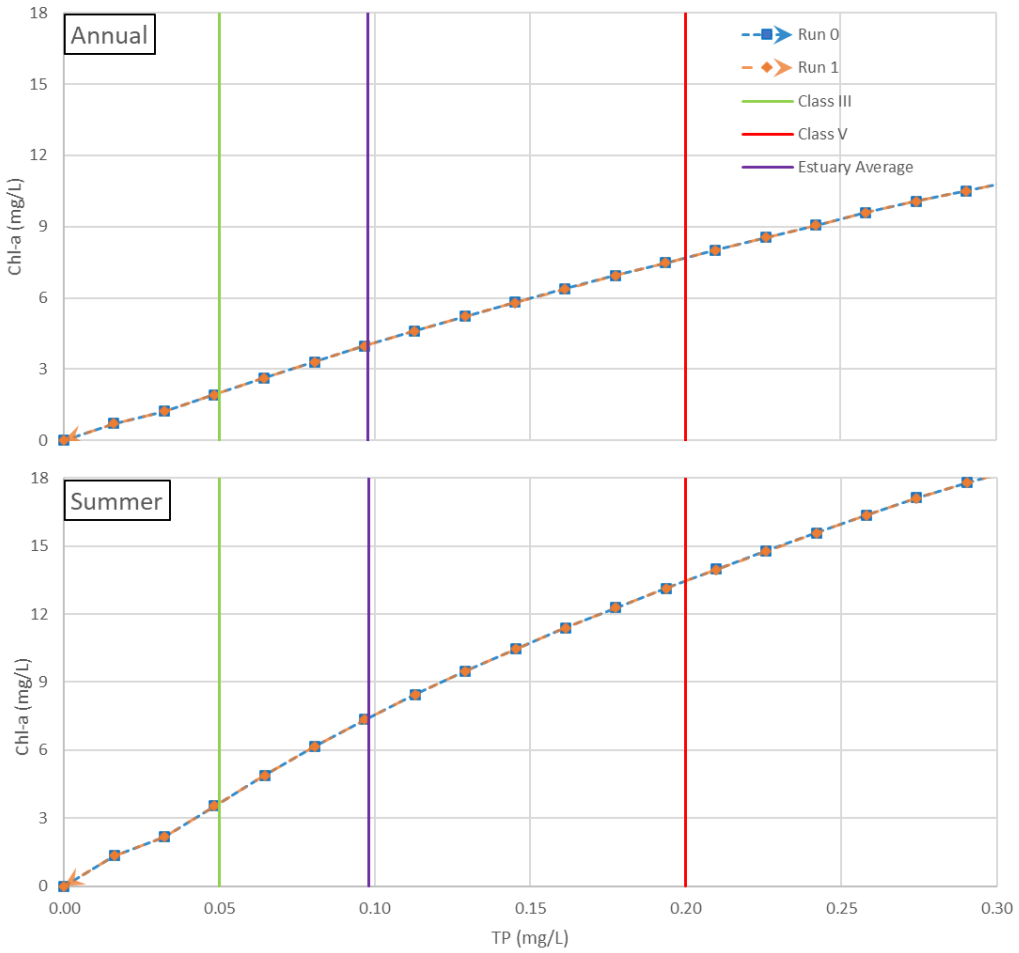

Figure 4-24: Comparison of estimated annual and summer Chlorophyll-a concentrations at varying phosphorous concentrations under typical operating conditions. Run ID 0 was used to calculate response curves starting from clear conditions and progressing towards turbid conditions (eutrophication) and run ID 1 was used to calculate the response curve starting from turbid conditions and progressing towards clear conditions (oligotrophication). The green line represents the Chinese water class III threshold for TP (lakes and reservoirs) and the red line represents class V. The purple line represents average TP concentration at the estuary 1990-2015 based on the data collected in Chapter 3.

Phosphorous concentration Chlorophyll a response curves under the three operating conditions have been plotted in **Figure 4-25** (Annual average) and **Figure 4-26** (Summer average). In general, reductions in HRT appear to reduce the Chlorophyll a response to phosphorous concentration. For the annual average, there is little difference between the response curves for typical operation HRT (17.5 days) and flushing HRT (8.5), but at maximum flood season operation HRT (30 days) there is a difference of 1.5 µg/L or more at TP concentrations between class III and class V thresholds. In summer, the difference between typical operation HRT and flushing HRT is small at TP concentrations lower than the class III threshold, but there is a difference of 1.5 µg/L when TP concentrations are at the estuary average. The maximum flood season operation HRT during summer results in much high Chlorophyll a responses than the other tested conditions. It is likely that the cause of the difference between these curves is the effect that lower HRTs have on particle settling time. As shown in **Section 4.2.1** longer retention times increase particle settling in the reservoir. This causes increased light penetration, particularly in summer, resulting in increased

biological growth. As such, manipulation of HRT may provide some assistance in managing algal blooms particularly during summer.

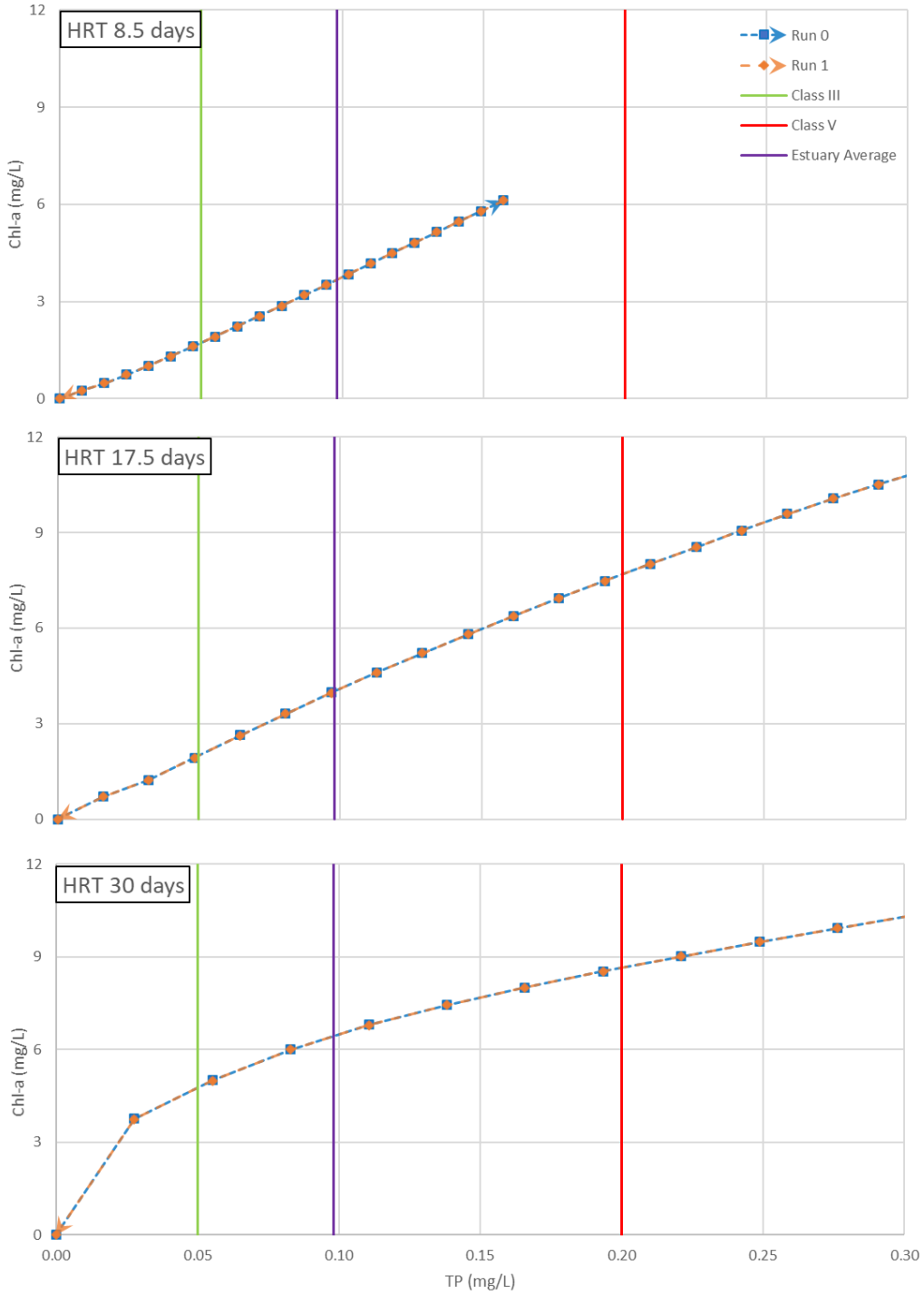

Figure 4-25: Comparison of estimated annual Chlorophyll-a concentrations at varying phosphorous concentrations under different hydraulic loading. Run ID 0 was used to calculate response curves starting from clear conditions and progressing towards turbid conditions (eutrophication) and run ID 1 was used to calculate the response curve starting from turbid conditions and progressing towards clear conditions (oligotrophication). The green line represents the Chinese water class III threshold for TP (lakes and reservoirs) and the red line represents class V. The purple line represents average TP concentration at the estuary 1990-2015 based on the data collected in Chapter 3.

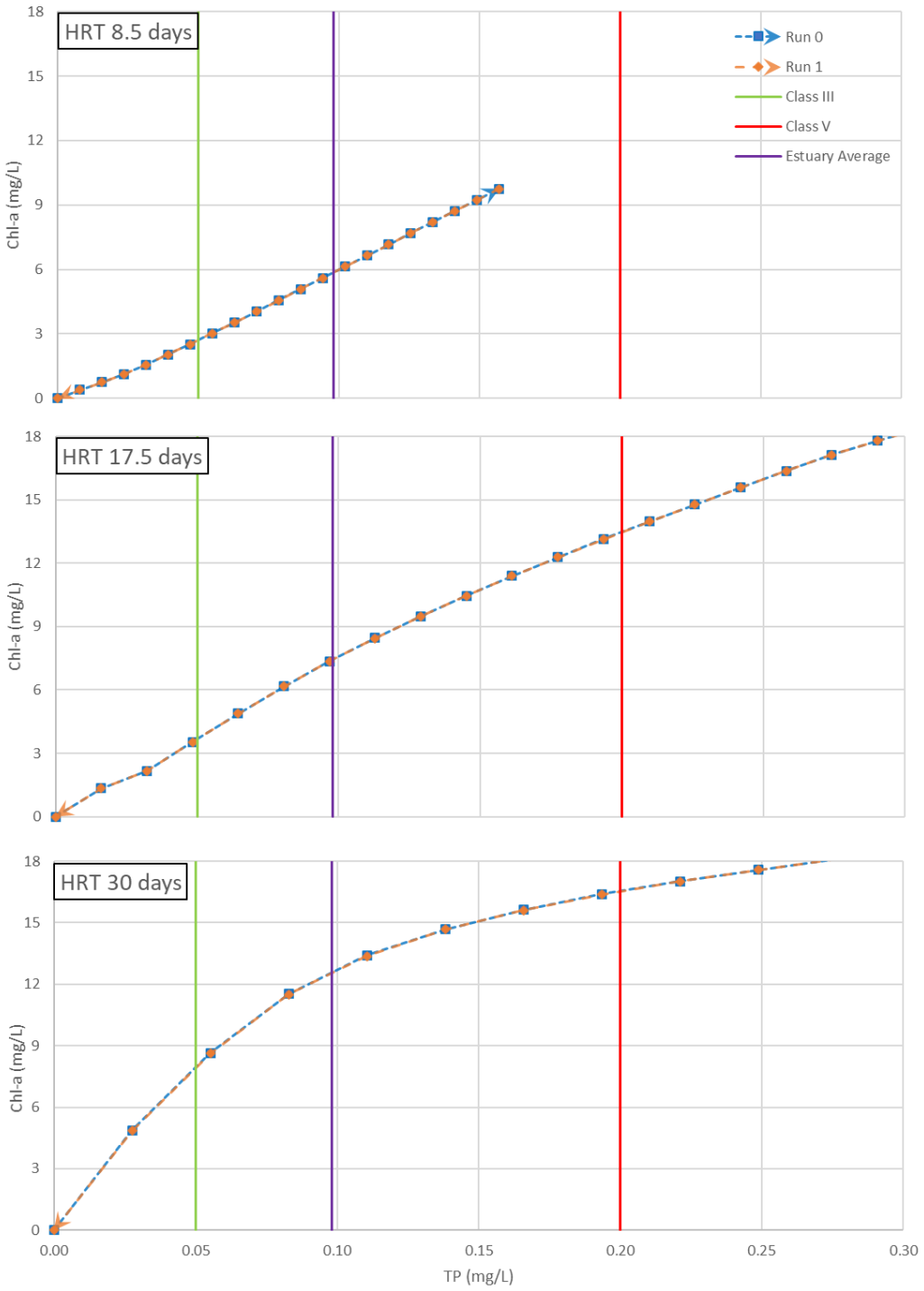

Figure 4-26: Comparison of estimated summer Chlorophyll-a concentrations at varying phosphorous concentrations under different hydraulic loading. Run ID 0 was used to calculate response curves starting from clear conditions and progressing towards turbid conditions (eutrophication) and run ID 1 was used to calculate the response curve starting from turbid conditions and progressing towards clear conditions (oligotrophication). The green line represents the Chinese water class III threshold for TP (lakes and reservoirs) and the red line represents class V. The purple line represents average TP concentration at the estuary 1990-2015 based on the data collected in Chapter 3.

The total amount of vegetation in the reservoir was considered to see if it would have an effect on nutrient uptake and thereby effect algal growth. Phosphorous concentration Chlorophyll a response curves under the three different marsh coverage rates (0.3 – existing, 0.4 and 0.5 representing increased marsh coverage) have been plotted in **Figure 4-27** (Annual average) and **Figure 4-28** (Summer average). Overall, the Chlorophyll a response to TP loading with different marsh coverage is subtle both on average and in summer with increasing marsh coverage slightly decreasing Chlorophyll a response at equivalent TP load. In all bifurcation runs, hysteresis was not observed. Hysteresis is a characteristic where a stable ecological state will resist change to another state. In the context of a lake environment two typical regimes occur, a clear macrophyte dominated system and a turbid, algae dominated system. The resistance of these states to change under different nutrient loadings is often observable in bifurcation analysis with two separate load response curves forming (Janse, De Senerpont Domis et al. 2008). The absence of hysteresis from the Qingcaosha reservoir results could indicate that only one regime in the reservoir is possible in the current conditions. High suspended sediment loads minimising light penetration into the water column could be preventing a stable colony of underwater macrophytes from establishing.

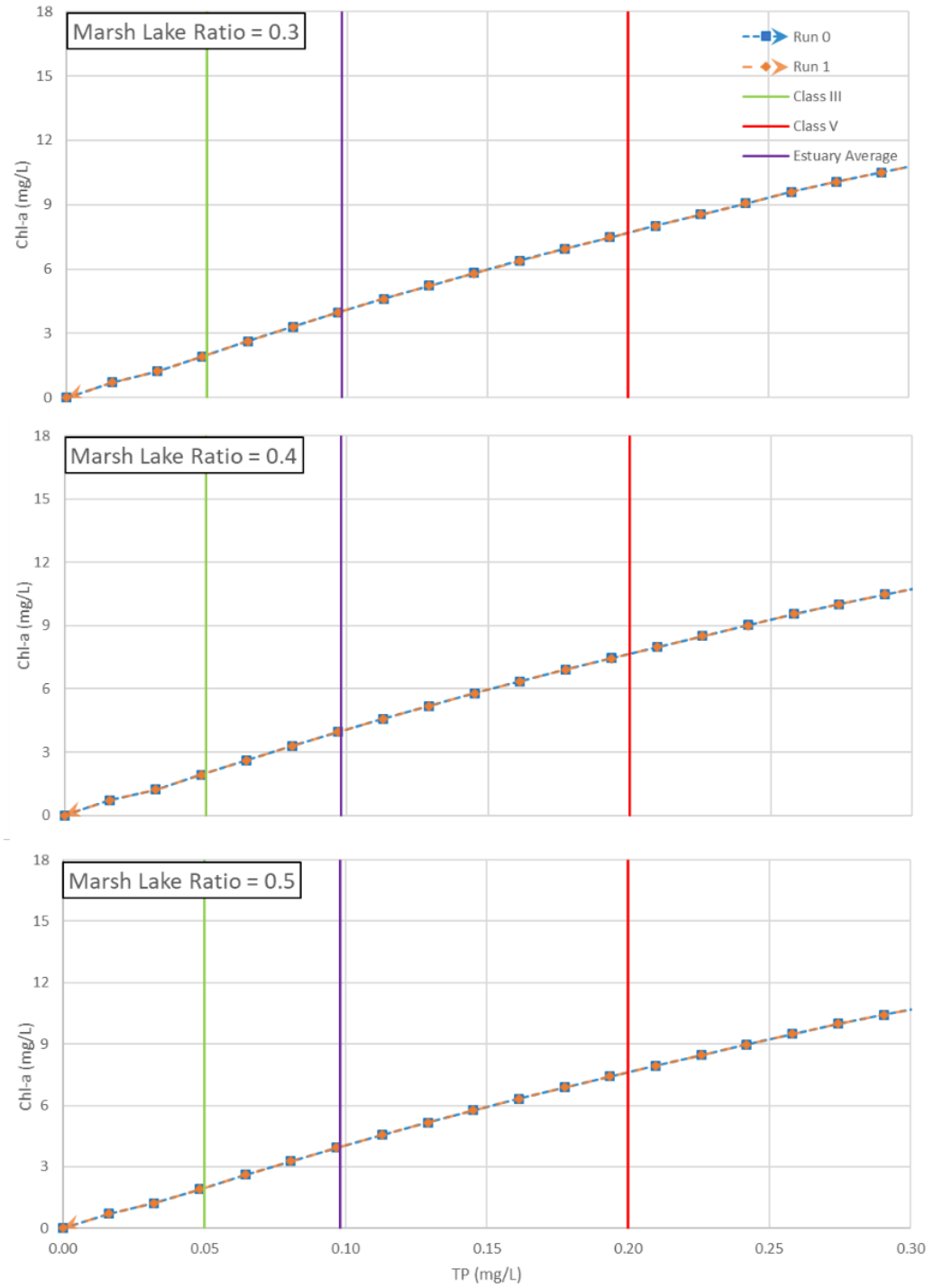

Figure 4-27: Comparison of estimated annual Chlorophyll-a concentrations at varying phosphorous concentrations with different marsh coverage fractions. Run ID 0 was used to calculate response curves starting from clear conditions and progressing towards turbid conditions (eutrophication) and run ID 1 was used to calculate the response curve starting from turbid conditions and progressing towards clear conditions (oligotrophication). The green line represents the Chinese water class III threshold for TP (lakes and reservoirs) and the red line represents class V. The purple line represents average TP concentration at the estuary 1990-2015 based on the data collected in Chapter 3.

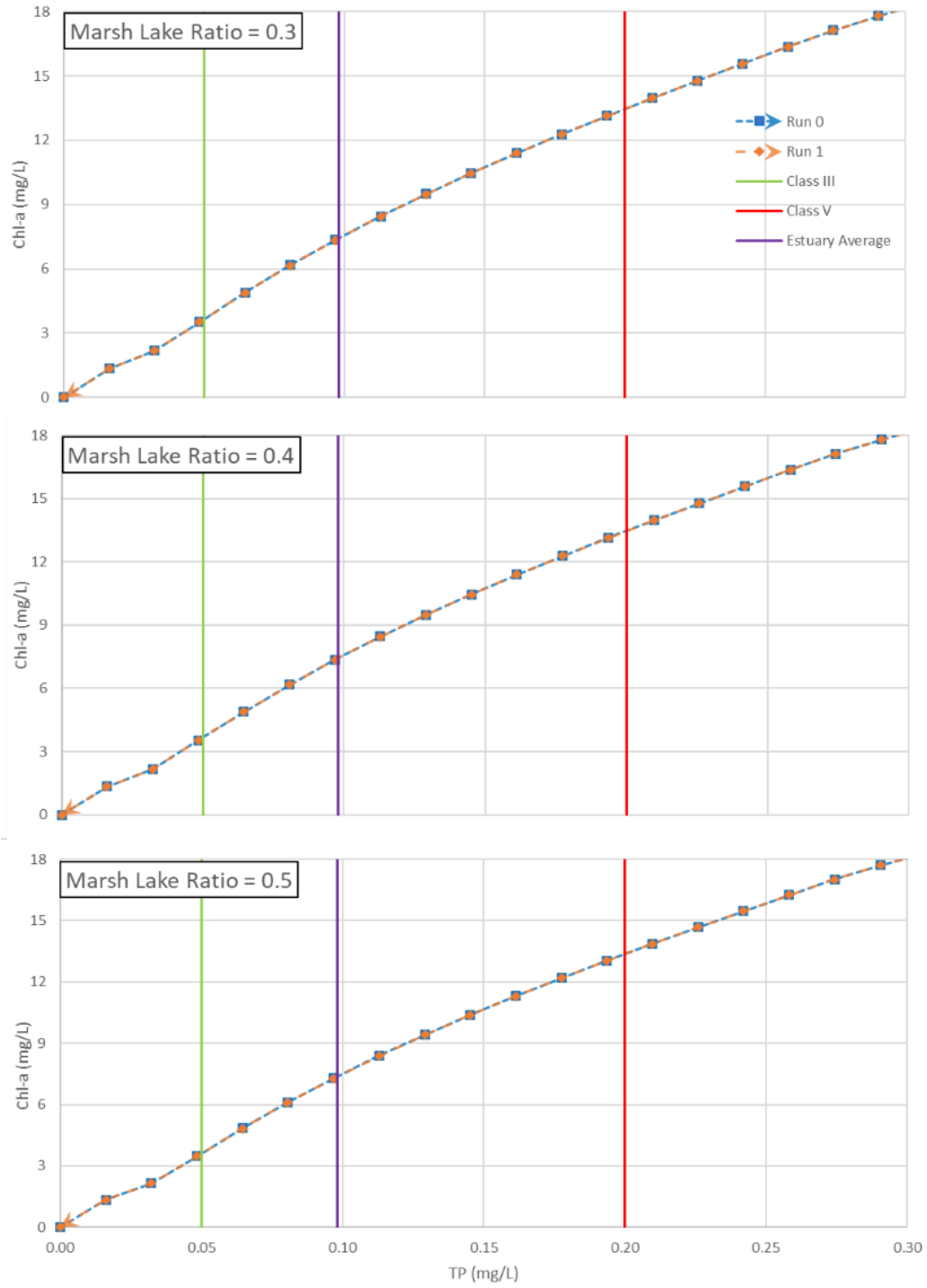

Figure 4-28: Comparison of estimated summer Chlorophyll-a concentrations at varying phosphorous concentrations with different marsh coverage fractions. Run ID 0 was used to calculate response curves starting from clear conditions and progressing towards turbid conditions (eutrophication) and run ID 1 was used to calculate the response curve starting from turbid conditions and progressing towards clear conditions (oligotrophication). The green line represents the Chinese water class III threshold for TP (lakes and reservoirs) and the red line represents class V. The purple line represents average TP concentration at the estuary 1990-2015 based on the data collected in Chapter 3.

To explore the effect of suspended sediment on Chlorophyll a response, further bifurcation analyses were run varying the clay (lutum) fraction of sediments and total suspended solids loading. Results of these analyses are presented in **Figure 4-29** and **Figure 4-30**. Reduction in either the amount of suspended sediment that is clay, which is difficult to settle, or in the total concentration of suspended solids leads to an increase in Chlorophyll a concentration. The effects of reduction in suspended solids are more pronounced in summer relative to the annual average. In these results, again no evidence of hysteresis is present. In these tests, TP concentrations were set at the estuary average concentration which may be too high for a stable macrophyte dominated system to occur.

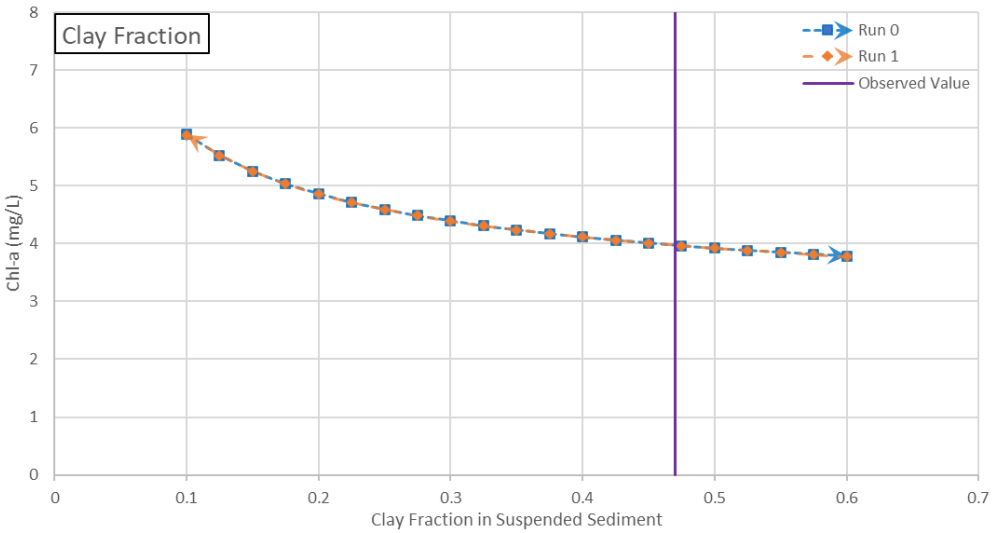

Figure 4-29: Chlorophyll a response to clay fraction of suspended sediment. Run ID 0 was used to calculate response curves starting from clear conditions and progressing towards turbid conditions (eutrophication) and run ID 1 was used to calculate the response curve starting from turbid conditions and progressing towards clear conditions (oligotrophication).

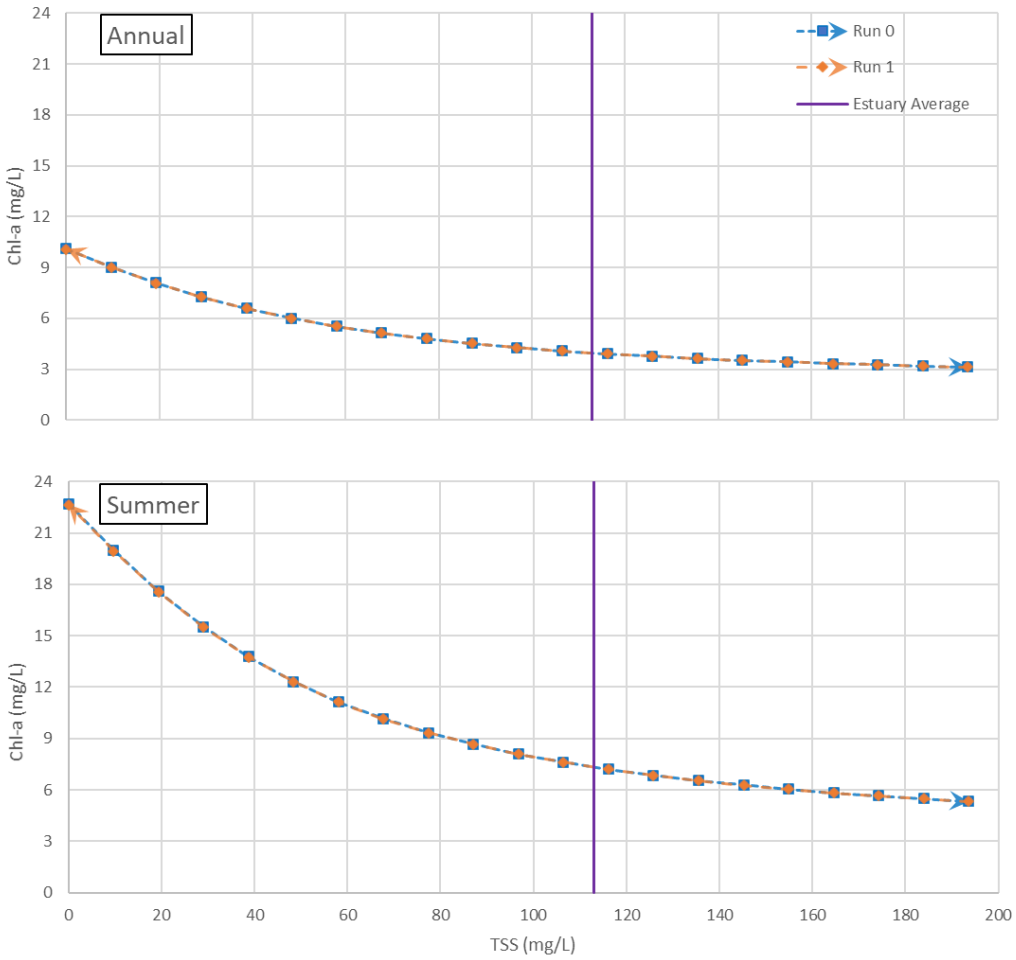

Figure 4-30: Annual average and summer average Chlorophyll a response to suspended sediment concentration. Run ID 0 was used to calculate response curves starting from clear conditions and progressing towards turbid conditions (eutrophication) and run ID 1 was used to calculate the response curve starting from turbid conditions and progressing towards clear conditions (oligotrophication).

There are several limitations that should be considered when interpreting the results of this study:

- Data limitation is an issue. The model is sensitive to parameters such as sediment load and therefore it is important to have an accurate characterisation of the likely conditions. In addition, with the limited data available, performing an output calibration is not possible and the model must rely on calibration of the input data;
- The model is 1D and does not account for the spatial variability in the system. As shown in previous sections, spatial variability in the reservoir does occur and should be accounted for in future studies;
- The application of this model relies on the assumption that the ecological systems in the reservoir in analogous to a lake. The Qingcaosha Reservoir is a relatively new system, and the existing ecosystem would have had to adapt from an estuarine environment to a mainly freshwater environment. Despite slow moving water (especially relative to the adjacent river), it may be the case that the ecological systems have not yet adapted to match those occurring in a lake; and

- The model applied a deterministic approach to algal growth which is actually a stochastic process.

Despite these limitations, the model takes a mass balance approach and probably points in the correct direction with regards to estimating the capability for the system to produce algal blooms and does offer some insight into the expected behaviour of the system. Based on the results of the modelling undertaken, the following conclusions can be drawn:

- The most significant factors that affect Chlorophyll response are sediment concentration and higher temperatures and light during summer. Probably the most effective management strategies would involve some kind of method to limit and water temperature especially in summer;
- Reductions in reservoir HRT do appear to have a beneficial effect on Chlorophyll a response. As such, flushing using the tides and operation of the reservoirs sluice gates could be a useful management technique especially in summer;
- High HRTs increase the risk that algae will form. This could be a significant risk during long closure periods; and
- High sediment loads may prevent a macrophyte based regime from occurring in the reservoir due to light limitation. As such, natural techniques for water quality management like wetlands may not be effective unless management techniques for sediment control are also employed. Floating wetland may be a viable alternative that would avoid the effects of sediment induced light limitation.

4.3 The Effect of Coastal Reservoir and Potential Management Strategies

Shanghai's coastal reservoirs, Qingcaosha, Chenhang and Dongfengxisha, have a combined effective storage capacity of 456.7 million m^3 (refer **Table 4-1**). This supply is critical to Shanghai's water security and can meet Shanghai's current water supply consumption of approximately 8.5 million m^3/d for 53 days consecutively (assuming sufficient pumping capacity) without water intake or being supplemented by water sourced from the Huangpu or Taipu Rivers (based on current water supply demand of approximately 3.1 billion m^3/a). A reduction in the length of time that Shanghai can store water would increase the risk of running out of water during an intense saline intrusion event similar to the events that occurred in 1978-1979, 2001-2002 or 2006-2007 (Refer **Section 3.2**).

By 2050, water supply consumption in Shanghai could reach between 11.8 million m^3/d to 15.6 million m^3/d (based on the low and high growth scenario estimates of 4.3 billion m^3/a and 5.7 billion m^3/a; refer **Figure 2-17**). Under these demands, combined reservoir storage would only last approximately 30-39 days. To achieve an equivalent 53 days of consecutive supply from the Yangtze Estuary alone, combined reservoir effective capacity would need to be increased to between 625.4 million m^3 and 826.8 million m^3; a 36.9% to 81.0% increase. To meet this increase, another reservoir providing between 168.7 million m^3 and 370.1 million m^3 effective storage would be required. There is a risk that increasing water transfers from the Yangtze River and sea level rise could further increase the duration and intensity of saline intrusion at the estuary. To meet these risks, longer storage capabilities might be required beyond the estimates provided above, otherwise desalination technologies may need to be implemented in Shanghai's water treatment process as an emergency measure.

In addition to securing fresh water supply, another useful function provided by coastal reservoirs is as a pre-sedimentation system, reducing the suspended sediment load that will need to be removed at the water treatment facility. It is estimated that the Qingcaosha reservoir, for example, is capable of removing up to 52% of suspended sediments during typical operations (HRT = 17.5 days, refer **Figure 4-22**). Assuming a median total suspended sediment concentration of 122.9 mg/L (**Table 3-1**), during typical operations the reservoir will remove approximately 1026 of the total 1974 t of suspended sediment passing through the reservoir on a typical day. In the 7.19 million m^3/d flow that could be piped to Shanghai for municipal supply from the Qingcaosha Reservoir, the sediment load arriving at water treatment plants is estimated to be reduced from 884 t/d to 424 t/d. This accumulated sediment would need to be dredged from the reservoir regularly to maintain its storage capacity.

The amount of sediment expected to be removed is controlled by the hydraulic retention time of the reservoir. For the Qingcaosha reservoir, in addition to its typical operating hydraulic

retention time of 15-20 days, longer durations are expected when the reservoir must close due to inadequate water quality in the estuary and a shorter duration of between 7-10 days for "flushing" the reservoir is also being considered. During the flushing operation, estimated sediment removal is estimated to drop to 48% while during the longest closure duration of 68 days, removal is estimated to reach up to 59%. It should be noted that while the fraction of sediments settled reduces as HRT decreases, the shorter retention time is driven by passing a larger volume of water through the reservoir in an equivalent period of time. As such, both the loading of water and sediment is increased; for a HRT of 8.5 days and the median concentration of total suspended sediment of 122.9 mg/L, the an estimated 1950 of 4063 t/d will accumulate in the reservoir. This nearly doubles the amount of sediment required to be dredged from the reservoir. During a closure period however, beyond the initial intake of water, additional loading of water and sediment is zero.

The majority of suspended particles arriving at the estuary are predominantly in the clay and silt grain size categories. The majority of the particles estimated to be removed through pre-sedimentation are from the silt category or larger. Very fine particles like clay, are often kept afloat by hydraulic turbulence or by electrostatic repulsion and will not be settle under gravity alone (Ongley 1996, Mines 2014). An estimated 47% of particles arriving at the estuary are clay, and these particles will likely need the application of coagulation, flocculation and filtration processes during water treatment to be fully removed (Mines 2014).

At present, a significant risk to water quality operations in the reservoir is from algal blooms, which can cause undesirable byproducts and complicate the water treatment process (refer **Section 3.3.3**). Based on the available data, elevated Chlorophyll a concentrations indicating algal blooms have been observed in the reservoir in 2009, 2011 and 2016 (**Figure 4-19**). The consequences of algal blooms include byproducts such as taste and odour compounds 2-Methylisoborneol (2MIB) and Geosmin which have odour thresholds of 5-10 ng/L (Liu, Pan et al. 2016, Huang, Huang et al. 2018). Even small concentrations of these compounds make water quality unpalatable for drinking use. The effective and economic removal of taste and odour compounds is challenging and usually advanced technologies such as ozonation, permanganate oxidation and adsorption by activated carbon are required (Liu, Pan et al. 2016). These compounds including 2MIB and Geosmin were detected in the Qingcaosha Reservoir several times with peak Geosmin reaching around 25 ng/L in late 2010 and peak 2MIB reaching over 300 ng/L in summer 2012 (Liu, Pan et al. 2016). 2MIB concentrations were found to be higher during the warm seasons and correlate strongly with the growth of Cyanobacteria (Zhang, Zhang et al. 2015, Liu, Pan et al. 2016). During the period of their study, Liu, Pan et al. (2016) observed that complaints about taste and odour compounds occurred between 1-4 times per year. A more important consequence of algal blooming would be the growth of toxin-producing species that would require additional treatment technologies to remove like activated carbon.

There are many potential options for managing algal blooms and their byproducts in drinking water reservoir. These options can be categorised as follows:

- **Prevention** – options that manipulate conditions in the reservoir so that algal blooms do not form;
- **Control -** options that remove or remediate algal blooms in the reservoir once they have occurred; and
- **Treatment –** options that remove the algae or byproducts during the water treatment phase prior to drinking.

A summary of potential management options that could be applied to manage algal blooming in Shanghai's coastal reservoirs is provided in **Table 4-8**. The most effective and cost-effective method for controlling algal blooms is phosphorous limitation. Phosphorous reductions can be highly effective even without corresponding nitrogen limitations because they may reduce they have the capability to firstly reduce essential nutrient supply to all algal taxa, but also have the ability to give the less problematic eukaryotic algae an advantage (Paerl 2008). The reduction of nitrogen without a proportional reduction in phosphorous can also lead to a low Redfield Ratio, which merely can promote the growth of diazotropic (nitrogen gas fixing) nuisance algae like cyanobacteria without reducing the total algal biomass (Naeem, Idrees et al. 2013).

Table 4-8: Potential Management Measures for Algal Blooms in Drinking Water Reservoirs. Adapted from Stroom and Kardinaal (2016), Paerl (2008), Tang, Wu et al. (2011), and Zeng, He et al. (2017).

Prevention	**Control**	**Treatment**
Watershed Protection	Flushing	Inlet Screening
Nutrient Reduction Using Macrophytes and Wetlands • Constructed Wetlands • Floating Wetlands • Submerged Macrophytes	Biomass Removal • Algaecide (copper sulphate, hydrogen peroxide) • Flocculation • Scum harvesting	Pre-oxidation • Chlorine • Ozone • Potassium Permanganate
Compartmentalisation and Fetch Reduction	Mixing • Vertical (disrupting stratification) • Horizontal (preventing stagnation)	Advanced treatments • Activated Carbon • Membranes
Food web manipulation • Fish management • Dreissenid mussels	Monitoring and Warning Systems	
Substrate management • Capping • Dredging • Iron enhancement		
Light management • Flocculation • Water level drawdown or Shoaling		

Watershed protection, essentially by capturing pollution close to the source or preventing it from occurring to begin with, is an effective way of reducing nutrient concentrations arriving at the reservoir, thereby reducing the risk of algal blooms from occuring. For example, reductions in wastewater and agricultural phosphorous inputs have been shown to lead to decreased cyanobacterial blooms in large European and Asian lakes (Paerl 2008). In the context of Shanghai's coastal reservoirs, while watershed management could provide reductions in nutrients to the reservoirs, almost the entire catchment is out of the control of the Shanghai Municipal Government and as such, this should not form the basis of water quality management in the reservoirs.

Methods for nutrient reduction that can be applied within or immediately upstream of the reservoir are the provision of constructed wetlands, floating wetlands, or establishment of submerged macrophytes (hydrophytes). Constructed wetlands are engineered systems that utilise natural processes that occur resulting from interactions between constituents in the water column and the wetland macrophytes, substrate and microbial communities which can be an effective method to reduce nitrogen and phosphorous loading in a water body (Tang, Wu et al. 2011, Naeem, Idrees et al. 2013). High nutrient removal in wetland can be achieved if sufficient oxygenation of the wetland is achieved. This can be done using fluctuations in wetland water level or through mechanical means such as injection of compressed air into the root zone (Tang, Wu et al. 2011). In locations where the water column is too deep for typical constructed wetlands to be established, floating wetlands could be applied. Floating wetland can be an effective tool in improving water quality in reservoirs. The plant roots grow through the floating substrate and are in direct contact with the water column, which allows the floating wetlands to function as water filters zone (Tang, Wu et al. 2011). In addition to providing many of the functions of typical constructed wetlands, floating wetlands also provide shade to the water column. Submerged macrophytes have been successful for ecological restoration and water quality enhancement. These plants are in direct contact with the water column and compete with algae for light and nutrients. Some hydrophytes can also release chemicals that inhibit the growth of algae or enhance particle settling, and also can improve the oxygen availability in the water column zone (Tang, Wu et al. 2011). The restoration of submerged macrophytes absorbs nutrients in the water column, stabilises sediments minimising the release of additional nutrients, and provides shelter for zooplankton and planktivorous fish (Zeng, He et al. 2017). A study conducted in Wuguitan Lake (a sub-lake of Hangzhou's West Lake) showed that submerged macrophyte restoration techniques significantly improved macrophyte coverage and biomass in the lake while significantly decreasing nutrient loading and phytoplankton biomass (Zeng, He et al. 2017). The success of submerged macrophytes in the reservoir relies on sufficient light reaching the plants through the water column. Some techniques for light managements are water level drawdown or shoaling, where the aim is to increase light penetration to the bed of the lake or reservoir by keeping the water column shallow in order to improve water clarity and macrophyte coverage (Stroom and Kardinaal 2016).

Compartmentalisation of the reservoir increases the acceptable nutrient loading threshold with small shallow lakes being more resilient to high nutrient loading than large deep lakes. Compartmentalisation also reduces wind fetch, which subsequently reduces resuspension of sediments in the reservoir. This helps to reduce nutrient loads in the reservoir and improves light conditions, favouring the growth of submerged macrophytes. Compartmentalisation can also influence the success of other applied measures because small water bodies are easier to manage (Stroom and Kardinaal 2016). Compartmentalisation and fetch reduction can be achieved through constructing dams or islands and for fetch reduction alone (without compartmentalisation) rows of poles to disrupt the waves can be used (Stroom and Kardinaal 2016).

Two techniques for food web manipulation could also be applied to help control algae growth; fish management and the introduction of dreissenid mussels. The introduction of Dreissenid mussels to filter water in the reservoir and remove phytoplankton in particular has shown promise in lakes where it has been applied. Surveys assessing the impact of dreissenid mussels in lakes found that turbidity could be reduced by 41%, Chlorophyll-a by 47%, phytoplankton by 58% and zooplankton by 51%, while the amounts of littoral periphyton increased by 171%, macrophytes by 182% and zoobenthos (excluding dreissenids) by 212%(Stroom and Kardinaal 2016). Dreissenids were found to be most successful when established at depths shallower than 8m where a suitable substrate like sand, rock, clay, wood, macrophytes and other bivalve shells, are provided (Stroom and Kardinaal 2016). A key risk in applying food web manipulation techniques for algae control is that they will lead to the dominance of toxic or inedible species of algae (Paerl 2008).

Capping the base of a reservoir with sand may help to reduce the amount of nutrients, especially phosphorous, released from the sediment at the base of the reservoir. This approach can be done by adding a layer of sand, gravel or clay above the enriched material or by chemical fixation of phosphates. Capping is only likely to be effective in the case that incoming nutrient loading is low (Stroom and Kardinaal 2016). In small or moderated sized shallow lakes, dredging of enriched sediments is a feasible, but costly option. Dredging will also potentially damage macrophytes and other biota on the invert of the reservoir and can cause changes to the ecosystem, sometimes beneficial and other times detrimental (Stroom and Kardinaal 2016). Enhancement of the substrate through dredging or capping of soft sediments can also improve conditions for submerged macrophyte growth by providing a better surface to anchor to and resist dislodgement by drag forces caused by currents and waves (Stroom and Kardinaal 2016).

Potential control methods that could be applied for algal blooms include flushing both vertical and horizontal mixing, and the application of algaecide. Flushing is a technique that is currently

applied in the Qingcaosha reservoir in an attempt to manage blooms occurring. Flushing of a reservoir works by reducing the retention time of stored water relative to the growth rate of algal cells so that algal cells are flushed from the reservoir before a bloom can occur. Ideally, residence times should be reduced to a few days or weeks to be effective (Stroom and Kardinaal 2016). The application of physical mixing can be effective for managing algal blooms; however the construction, maintenance and operation costs of mixing systems are high (Stroom and Kardinaal 2016).

Algaecide can be used to kill off algal cells preventing the formation of blooms. Algaecides like Chlorine, Ozone and Potassium Permanganate are not suitable for use in a lake or reservoir due to their adverse effects on other aquatic organisms. Copper sulphate is commonly used to control cyanobacterial blooms and is relatively effective and easy to apply. However, it is not ideal due to its toxicity to other organisms and can accumulate in sediments. Hydrogen peroxide is another algaecide and is particularly selective for cyanobacteria. As a control measure, its main advantage is that it leaves no harmful remnants in the environment (Stroom and Kardinaal 2016). Algaecide should not be used in drinking water reservoirs and is often uneconomical for application in larger bodies of water (Paerl 2008).

The use of monitoring and warning systems are useful for identifying when other control and treatment measures should be activated. A warning system and advanced treatment measure was proposed by Liu, Pan et al. (2016) who estimated that action was required when the following triggers occurred in the Qingcaosha Reservoir:

- TOCC reached 100 ng/L;
- A single algal bloom reached 2 km^2 surface area; or
- The cumulative surface area of algal bloom reached 10 km^2.

In addition, they recommended that emergency measures (including the application of advanced treatment technologies are applied when the reservoir water temperature exceeds 25 Celsius which is when algal blooms are more likely to occur (Liu, Pan et al. 2016).

The most effective combination of management options that could be applied in Shanghai's coastal reservoirs would meet the following goals:

- Maintain effective sedimentation under all operation conditions and preferably capture it in a location where it could be easily dredged and removed;
- Either reduce nutrient concentrations or improve the systems resilience to nutrient loading;
- Be effective even when water is required to be stored for long periods of time;
- Be entirely within the control of the Shanghai municipal government.

While the current flushing technique applied to Qingcaosha could assist with the management of algal blooms, it does so at the cost of increased sediment deposition in the reservoir and also cannot be used in situations where water quality in the estuary is unsuitable for diversion into the water supply. Additionally, while emergency warning systems are essential for safe operation of a water supply system, relying on this and additional treatment measures ignores the opportunity for potentially cheaper options applied within the reservoir itself.

Instead of the current strategies applied, a potential solution would be to compartmentalise the reservoir into multiple zones and consider each zone as a part of a treatment process. An example of how this could be applied is presented in **Figure 4-31**. Such a configuration would allow for efficient sediment removal and dredging at the beginning of the process, minimising the disruption to downstream components. Finer particles that are not removed effectively by sedimentation could be removed in a shallow wetland or submerged macrophytes zone, which would also help with nutrient removal by uptake and sequestration of sediments. A transition zone with floating wetlands would further assist with fine sediment and nutrient removal and has the added advantage of providing some shade and temperature control to the water column which would help minimise algal growth in summer. Finally, a deep zone for long term storage of high clarity and low nutrient raw water would complete the process. In this zone, monitoring of water quality could be conducted and other emergency control techniques such as flocculation or mechanical mixing could be used in the event that an algal bloom did occur. A system of this could still be effective during periods where long hydraulic retention time is required. This is but one potential example that could be applied that has been based on high level principles. Alternative options could be explored and further sampling, modelling and calculation could be undertaken to find the most effective and efficient solution to manage the Qingcaosha Reservoir.

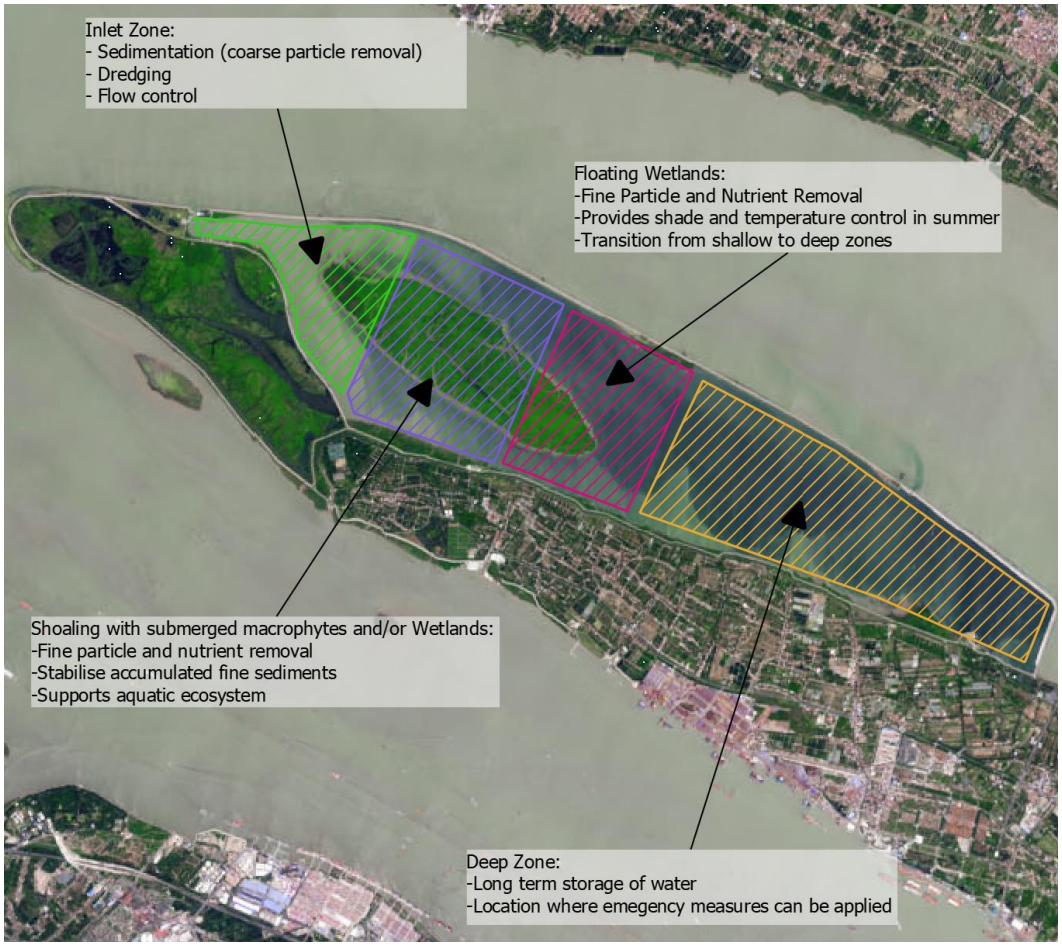

Figure 4-31: Example of Implementation of Reservoir Management Measures in Qingcaosha Reservoir. Aerial photo from NASA Earth Observatory (2017)

4.4 Summary

- Shanghai's coastal reservoirs form a crucial component of Shanghai's municipal water supply and are used for the capture and storage of water from the estuary.
- The Qinghcaosha, Chenhang and Donfengxisha reservoirs provide a cumulative storage of 456.7 million m^3 of water and supply approximately 70% of Shanghai's municipal water supply. This combined volume can supply Shanghai for 53 consecutive days without water intake or being supplemented by water sourced from the Huangpu or Taipu Rivers.
- By 2050, water supply consumption in Shanghai could reach between 11.8 million m^3/d to 15.6 million m^3/d. To maintain 53 days storage capacity under these scenarios, combined reservoir effective capacity would need to be increased to between 625.4 million m^3 and 826.8 million m^3. To meet this increase, another reservoir providing between 168.7 million m^3 and 370.1 million m^3 effective storage would be required.
- There is a risk that increasing water transfers from the Yangtze River and sea level rise could further increase the duration and intensity of saline intrusion at the estuary which may require even more storage being required to secure the future water supply.
- The Qingcaosha reservoir provides pre-sedimentation for Shanghai's municipal water supply. Average water transparency increases and turbidity decreases as water progresses down the reservoir.
- Sedimentation was analysed in the reservoir by treating the reservoir as an ideal settling basin. It is estimated that the reservoir could settle between 48% and 59% of incoming sediment depending on which HRT the reservoir is operating. Sedimentation efficiency will increase with higher HRT.
- Real settling velocities in the in the Qingcaosha reservoirs will depend on the variable depths and cross sections in the reservoir and their influence on flow velocities in the reservoir. In shallower sections, the flow velocity is increased, hindering settling, while settling is enhanced in deeper sections of the reservoir which have reduces flow velocities.
- Observed average TN and TP concentrations in the Qingcaosha reservoir are frequently above the Chinese water quality Class III threshold while the reservoir has been in operation.
- N:P ratio in the reservoir is mostly above the Redfield ratio indicating that the reservoir is generally phosphorous limited. However it has been observed that levels of nutrients are abundant and appear to have no significant effect on algal growth in the reservoir.
- Algal blooming has been observed in the reservoir. During late summer and autumn, the predominant algal species in the reservoir are types of Cyanobacteria while

during winter to early spring, no cyanobacteria occur, and the algal community is mostly made up of Chlorophytes, Diatoms and Cryptophytes. The significant factors controlling the type of algae dominant in the reservoir are water temperature and light.

- Bifurcation analysis was undertaken using the lake ecology model PCLake+ to determine the nutrient load Chlorophyll a response for the reservoir under various scenarios. Results of the modelling indicate that:
    - The most significant factors that affect Chlorophyll a response are sediment concentration and higher temperatures and light during summer. Probably the most effective management strategies would involve some kind of method to limit and water temperature especially in summer;
    - Reductions in reservoir HRT do appear to have a beneficial effect on Chlorophyll a response. As such, flushing using the tides and operation of the reservoirs sluice gates could be a useful management technique especially in summer;
    - High HRTs increase the risk that algae will form. This could be a significant risk during long closure periods; and
    - High sediment loads may prevent a macrophyte based regime from occurring in the reservoir due to light limitation. As such, natural techniques for water quality management like wetlands may not be effective unless management techniques for sediment control are also employed. Floating wetland may be a viable alternative that would avoid the effects of sediment induced light limitation.
- A range of management strategies could be applied to manage the risk of algal blooms in the Qingcaosha reservoir. The most effective combination of management options would meet the following goals:
    - Maintain effective sedimentation under all operation conditions and preferably capture it in a location where it could be easily dredged and removed;
    - Either reduce nutrient concentrations or improve the systems resilience to nutrient loading;
    - Be effective even when water is required to be stored for long periods of time;
    - Be entirely within the control of the Shanghai municipal government.
- A potential solution would be to compartmentalise the reservoir into multiple zones and consider each zone as a part of a treatment process. This is an opportunity to explore management options that could be cheaper that flushing the reservoir or relying on advanced treatment processes in Shanghai’s water treatment plants.

Chapter 5

5. Conclusions and Recommendations

5.1 Conclusions from this Study

Shanghai's coastal reservoirs, in their current context in Shanghai's water supply, perform several useful functions, the most important of which is to secure Shanghai's water supply from the Yangtze Estuary. The coastal reservoirs allow for selective intake and long term storage of freshwater while avoiding the periods of high salinity that regularly occur in the estuary. Salinity avoidance is significant for Shanghai's water supply as it removes the need to implement expensive and energy intensive desalination treatment technologies in Shanghai's water treatment plants. Some other useful functions performed by Shanghai's coastal reservoirs are to protect against acute occurrences of poor water quality, such as accidental spills and discharges of pollution, and also provides a pre-sedimentation function before water is diverted from the reservoir to water treatment plants.

To meet its future needs, Shanghai will need to increase its reliance on the Yangtze River estuary because other local water resources are inadequate from both quantity and quality perspectives. By 2050, Shanghai could require between 4.2 and 5.7 billion m^3 of raw water for municipal supply per year, which represents a 35% to 83% increase in consumption (relative to 2013 levels). At present, Shanghai's municipal supply has a raw water pumping capacity of 5.8 billion m^3/a (with most spare capacity associated with pumps in the Huangpu River), a treatment capacity of 4.2 billion m^3 and a combined reservoir storage capacity in the estuary of 456.7 million m^3 (Qingcaosha, Chenhang and Dongfengxisha) which can last up to 53 days without additional inflows and without supplement from the Huangpu or Taipu Rivers. By 2050, additional pumping capacity, up to five new 1.5 million m^3/d water treatment plants and 370.1 million m^3 additional storage in coastal reservoirs could be required under the highest growth projection. This would allow Shanghai to maintain the current level of service up to 2050.

Examination of available water quality data at the Yangtze Estuary indicates that very few parameters exceeded the required thresholds for drinking water use. Based on the available data, the diluting power of the Yangtze River appears sufficient to maintain the concentrations of most constituents despite contributions of upstream human activities, municipal, agricultural and industrial, at levels where they do not preclude municipal water supply. Despite this, caution should be applied in assuming that there is no risk to water quality in the Yangtze River resulting from trace metals or trace organic compounds. The available data is drawn from a limited number of samples which are probably insufficient to characterise the extent and complexity of the Yangtze River and its Estuary and many emerging pollutants have not been considered in this study. Additionally, despite the significant dilution effect of the Yangtze River streamflow, there is still the potential for

extremely high discharge of trace organic compounds and heavy metals. Presence in the water column is not the only way for these constituents to end up in drinking water supplies. Suspended particles are another potential pathway for the transport and accumulation of sediments in coastal reservoirs that could be a significant risk to Shanghai's water supply in the future.

Three key constituents of concern that affect or are affected by Shanghai's coastal reservoir and downstream water treatment operations can be identified. Firstly, the Yangtze estuary is subject to regular occurrences of high salinity associated with seawater penetration into the estuary. Salinity becomes a problem for water supply operations when TDS concentrations associated with seawater exceed 450 mg/L as corresponding Chloride concentrations are expected to exceed the 250 mg/L threshold stipulated in Chinese raw water quality guidelines. Concentrations exceeding this threshold are expected to occur at Gaoqiao, Chenhang and Chongtou when Yangtze River streamflow drops below 11,000 m^3/s, 12,500 m^3/s and 14,800 m^3/s respectively. These locations are near to the points where water is diverted into Shanghai's Qingcaosha, Chenhang and Dongfengxisha Reservoirs respectively, and high salinity preventing water diversion for municipal supply is expected mainly during January, February, and December. During particularly dry years, problems could occur in March or November as well. Historically, intense saline intrusions that would have prevented the coastal reservoirs from operating for long periods of time occurred 1987-1989, 2001-2002 and 2006-2008. As factors such as diversions in the Lower Yangtze River and sea level rise increase in the near future, the risk of a long duration saline intrusion that prevents water diversion to the coastal reservoir also increases.

Secondly, nutrient enrichment has occurred in the Yangtze River as a result of anthropogenic activities in the basin especially food production and municipal wastewater discharge. Total Nitrogen and Total Phosphorous concentrations at the estuary have consistently exceeded Chinese raw water quality standards Class III (drinking water source) since 1990. Inorganic fractions of Nitrogen and Phosphorous make up an increasing portion of Total Nitrogen and Total Phosphorous at the estuary. Nitrate and Dissolved Inorganic Phosphorous concentrations now exceed Class III requirements for Total Nitrogen and Total Phosphorous alone. Increases in these inorganic fractions appear to be sufficient to compensate for a loss of particulate nitrogen and phosphorous associated with the decline of suspended sediment concentrations in the river. Trajectories in the change of these inorganic nutrient concentrations and the land uses driving them appear to be increasing, and without significant changes in the rate of population growth or improvements in food production that minimise nutrient discharge to the river, these will continue to grow. Even if these sorts of changes were to occur to factors controlling nutrient discharge, the issue of nutrient concentrations at the estuary would not necessarily be resolved. Currently, nutrient concentrations are probably already past levels where they limit biological growth and as a result, algal blooms are now a regular occurrence offshore. Eutrophic conditions can be an issue

for water supply with reservoirs often providing ideal conditions for algal growth. Removing algae and its byproducts, which are sometimes toxic, can be difficult and expensive.

Algal blooming has been observed in the Qingcaosha Reservoir. During late summer and autumn, the predominant algal species in the reservoir are types of Cyanobacteria while during winter to early spring, no cyanobacteria occur, and the algal community is mostly made up of Chlorophytes, Diatoms and Cryptophytes. The significant factors controlling the type of algae dominant in the reservoir are water temperature and light. To assess the factors controlling algal growth in the reservoir, bifurcation analysis was undertaken using the lake ecology model PCLake+ to determine the nutrient load - Chlorophyll a response for the reservoir under various scenarios. Results of the modelling indicate that:

- The most significant factors that affect Chlorophyll a response are sediment concentration and higher temperatures and light during summer. Probably the most effective management strategies would involve some kind of method to limit light and water temperature especially in summer;
- Reductions in reservoir HRT do appear to have a beneficial effect on Chlorophyll a response. As such, flushing using the tides and operation of the reservoirs sluice gates could be a useful management technique especially in summer;
- High HRTs increase the risk that algae will form. This could be a significant risk during long closure periods; and
- High sediment loads may prevent a macrophyte based regime from occurring in the reservoir due to light limitation. As such, natural techniques for water quality management like wetlands may not be effective unless management techniques for sediment control are also employed. Floating wetland may be a viable alternative that would avoid the effects of sediment induced light limitation.

Finally, although suspended sediment concentrations have been decreasing in the Yangtze River, concentrations are still quite high and need to be removed prior to end use. Coastal reservoirs serve as pre-sedimentation storage that contributes to the overall treatment. Suspended sediments in the Yangtze Estuary are fine grained, with almost all particles being classified as silt or finer. Small particles like silts and clays can be difficult to remove without techniques like coagulation and flocculation. Sedimentation was analysed in the reservoir by treating the reservoir as an ideal settling basin. It is estimated that the reservoir could settle between 48% and 59% of incoming sediment depending on which HRT the reservoir is operating. Sedimentation efficiency will increase with higher HRT. Real settling velocities in the in the Qingcaosha reservoirs will depend on the variable depths and cross sections in the reservoir and their influence on flow velocities in the reservoir. In shallower sections, the flow velocity is increased, hindering settling, while settling is enhanced in deeper sections of the reservoir which have reduces flow velocities.

A range of management strategies could be applied to manage the risk of algal blooms in the Qingcaosha reservoir. The most effective combination of management options would meet the following goals:

- Maintain effective sedimentation under all operation conditions and preferably capture it in a location where it could be easily dredged and removed;
- Either reduce nutrient concentrations or improve the systems resilience to nutrient loading;
- Be effective even when water is required to be stored for long periods of time;
- Be entirely within the control of the Shanghai municipal government.

A potential solution would be to compartmentalise the reservoir into multiple zones and consider each zone as a part of a treatment process. This is an opportunity to explore management options that could be cheaper that flushing the reservoir or relying on advanced treatment processes in Shanghai's water treatment plants

5.2 Recommendations for Further Research

The following recommendations for further research are made:

- More extensive and intensive sampling should be undertaken in the Yangtze Estuary and Shanghai's Coastal Reservoirs to fully understand the probable conditions that could affect Shanghai's water supply. Additional sampling should aim to directly monitor suspended sediment concentration and adsorbed compounds, saline intrusion and dissolved concentrations of trace metals and trace organics to fill in the knowledge gap regarding these parameters. Consideration should also be given to undertaking continuous monitoring of some indicator analytes which can assist in tracking where water that arrives at the reservoir has originated from (e.g. identifying the differences in characteristics of water originating from the Yangtze River versus water that is discharged locally from Shanghai). These kinds of data would allow more detailed modelling (both numerical and statistical) to be undertaken and could also form the basis of an effective decision support tool for the operation of the reservoirs;
- A more detailed review of existing modelling studies, including hydraulic and transport modelling, should be undertaken, and potentially additional modelling carried out to better characterise the conditions in the estuary, as well as the internal behaviour of flows and water quality processes within the reservoirs. Clearer understanding of these behaviours would allow more effective decisions regarding the management of these reservoirs such as when to intake water or how effective different management strategies will be, and also allow for better quantification of the risks to water supply from the Yangtze Estuary identified in this thesis (especially saline intrusion and algal blooming,

but also the effects of changing conditions in the estuary and impacts of dams and diversions in the Yangtze Basin). Further modelling would also be foundational to selecting suitable locations for additional reservoir space in the estuary;

- More detailed assessment on the risk of saline intrusion into the estuary is required. It is clear that increasing risk arising from saline intrusion will be exacerbated by diversion structures in the Lower Yangtze River and sea level rise. The potential future saline intrusion behaviour needs to be assessed in detail to support strategic planning of future reservoirs in the estuary, as it affects the number of days that water supplies need to be stored and ultimately the additional storage volume required in the estuary.
- Alternative management strategies should be explored for Shanghai's coastal reservoirs. An ideal solution would achieve maintain effective sedimentation under all operation conditions and preferably capture it in a location where it could be easily dredged and removed, reduce nutrient concentrations or improve the systems resilience to nutrient loading, be effective even when water is required to be stored for long periods of time and be entirely within the control of the Shanghai municipal government. There is the opportunity to reconfigure the coastal reservoirs to operate as a treatment train of compartmentalised zones, with each performing separate functions. Learning how to manage water quality cheaply and effectively in coastal reservoirs is critical to the long term water security of Shanghai and other coastal cities planning to use this technology to secure their water supply.
- It is recommended that authorities and universities in Shanghai be contacted for any further research on this topic to explore potential collaboration and gain access to more extensive datasets.

By undertaking these research activities, the risk to long term water supply from the estuary and the overall cost of municipal water supply operations could be reduced.

6. Bibliography

Anderson, D. M., P. M. Glibert and J. M. Burkholder (2002). "Harmful algal blooms and eutrophication: Nutrient sources, composition, and consequences." Estuaries **25**(4B): 704-726.

Aregay, F. A. and Z. Minjuan (2012). "Impact of Irrigation on Fertilizer Use Decision of Farmers in China: A Case Study in Weihe River Basin." Journal of Sustainable Development **5**(4).

Aregay, F. A. and M. J. Zhao (2012). "Impact of Irrigation on Fertilizer Use Decision of Farmers in China: A." Journal of Sustainable Development **5**(4): 74-82.

Bai, X., X. Zhang, Q. Sun, X. Wang and B. Zhu (2006). "Effect of water source pollution on the water quality of Shanghai water supply system." J Environ Sci Health A Tox Hazard Subst Environ Eng **41**(7): 1271-1280.

Byrne, R. H., F. t. Mackenzie and A. C. Duxbury (2020). Seawater. Encyclopedia Britannica.

Cai, H., H. H. G. Savenije, S. Zuo, C. Jiang and V. P. Chua (2015). "A predictive model for salt intrusion in estuaries applied to the Yangtze estuary." Journal of Hydrology **529**: 1336-1349.

Chai, C., Z. Yu, Z. Shen, X. Song, X. Cao and Y. Yao (2009). "Nutrient characteristics in the Yangtze River Estuary and the adjacent East China Sea before and after impoundment of the Three Gorges Dam." Sci Total Environ **407**(16): 4687-4695.

Chang, M., S. Teurlincx, J. Janse, H. Paerl, W. Mooij and A. Janssen (2020). "Exploring How Cyanobacterial Traits Affect Nutrient Loading Thresholds in Shallow Lakes: A Modelling Approach." Water **12**(9).

Chen, D., M. Webber, B. Finlayson, J. Barnett, Z. Chen and M. Wang (2013). "The impact of water transfers from the lower Yangtze River on water security in Shanghai." Applied Geography **45**: 303-310.

Chen, J., X. Gao, D. He and X. Xia (2000). "Nitrogen Contamination in the Yangtze River System, China." Journal of Hazardous Materials **A73**: 107-113.

Chen, M., J. Chen and F. Sun (2008). "Agricultural phosphorus flow and its environmental impacts in China." Sci Total Environ **405**(1-3): 140-152.

Chen, W., K. Chen, C. Kuang, D. Z. Zhu, L. He, X. Mao, H. Liang and H. Song (2016). "Influence of sea level rise on saline water intrusion in the Yangtze River Estuary, China." Applied Ocean Research **54**: 12-25.

Chen, X., Y. Zong, E. Zhang, J. Xu and S. Li (2001). "Human impacts on the Changjiang (Yangtze) River basin, China, with special reference to the impacts on the dry season water discharges into the sea." Geomorphology **41**(2): 111-123.

Chen, Y., R. Liu, C. Sun, P. Zhang, C. Feng and Z. Shen (2012). "Spatial and temporal variations in nitrogen and phosphorous nutrients in the Yangtze River Estuary." Mar Pollut Bull **64**(10): 2083-2089.

Chen, Y. and J. Zhu (2018). "Reducing eutrophication risk of a reservoir by water replacement: a case study of the Qingcaosha reservoir in the Changjiang Estuary." Acta Oceanologica Sinica **37**(6): 23-29.

Cheng, H. and Y. Hu (2011). "Improving China's water resources management for better adaptation to climate change." Climatic Change **112**(2): 253-282.

Cheng, H. Q., J. Y. Chen, Z. J. Chen, R. L. Ruan, G. Q. Xu, G. Zeng, J. R. Zhu, Z. J. Dai, X. Y. Chen, S. H. Gu, X. L. Zhang and H. M. Wang (2018). "Mapping Sea Level Rise Behavior in an Estuarine Delta System: A Case Study along the Shanghai Coast." Engineering **4**(1): 156-163.

Chetelat, B., C. Q. Liu, Z. Q. Zhao, Q. L. Wang, S. L. Li, J. Li and B. L. Wang (2008). "Geochemistry of

the dissolved load of the Changjiang Basin rivers: Anthropogenic impacts and chemical weathering." Geochimica et Cosmochimica Acta **72**(17): 4254-4277.

Crissman, L. and L. Berman (2012). ChinaHydro Basins. G. W. S. A. C. f. G. Analysis, Harvard Dataverse.

Dai, S. B. and X. X. Lu (2014). "Sediment load change in the Yangtze River (Changjiang): A review." Geomorphology **215**: 60-73.

Dai, Z., A. Chu, M. Stive, X. Zhang and H. Yan (2011). "Unusual Salinity Conditions in the Yangtze Estuary in 2006: Impacts of an Extreme Drought or of the Three Gorges Dam?" Ambio **40**(5): 496-505.

Dai, Z., J. Du, X. Zhang, N. Su and J. Li (2011). "Variation of riverine material loads and environmental consequences on the Changjiang (Yangtze) Estuary in recent decades (1955-2008)." Environmental Science and Technology **45**(1): 223-227.

Dai, Z., S. Fagherazzi, X. Mei and J. Gao (2016). "Decline in suspended sediment concentration delivered by the Changjiang (Yangtze) River into the East China Sea between 1956 and 2013." Geomorphology **268**: 123-132.

Ding, T., J. Gao, S. Tian, G. Shi, F. Chen, C. Wang, X. Luo and D. Han (2014). "Chemical and isotopic characteristics of the water and suspended particulate materials in the Yangtze river and their geological and environmental implications." Acta Geologica Sinica **88**(1): 276-360.

Duan, S., T. Liang, S. Zhang, L. Wang, X. Zhang and X. Chen (2008). "Seasonal changes in nitrogen and phosphorus transport in the lower Changjiang River before the construction of the Three Gorges Dam." Estuarine, Coastal and Shelf Science **79**(2): 239-250.

Duan, S., Z. Shen and H. Huang (2000). "Transport of dissolved inorganic nitogen from the major rivers to estuaries in China." Nutrient Cycling in Agroecosystems **57**: 13-22.

Duan, S., F. Xu and L.-J. Wang (2007). "Long-term changes in nutrient concentrations of the Changjiang River and principal tributaries." Biogeochemistry **85**(2): 215-234.

Duan, S. 段., S. 章. Zhang, X. 陈. Chen, X. 张. Zhang, L. 王. Wang and W. 晏. Yan (2000). "Concentrations of nitrogen and phosphorus and nutrient transport to estuary of the Yangtze River 长江下游氮_磷含量变化及其输送量的估计_段水旺." Environmental Science 环境科学 **21**: 53-56.

Edmond, J. M., A. Spivack, B. C. Grant, M. Hu, Z. Chen, S. Chen and X. Zeng (1985). "Chemical Dynamics of the Changjiang Estuary." Continental Shelf Research **4**(1/2): 17-36.

Fick, S. E. and R. J. Hijmans (2017). "WorldClim 2: new 1-km spatial resolution climate surfaces for global land areas." International Journal of Climatology **37**(12): 4302-4315.

Finlayson, B. L., J. Barnett, T. Wei, M. Webber, M. Li, M. Y. Wang, J. Chen, H. Xu and Z. Chen (2012). "The drivers of risk to water security in Shanghai." Regional Environmental Change **13**(2): 329-340.

Floehr, T., H. Xiao, B. Scholz-Starke, L. Wu, J. Hou, D. Yin, X. Zhang, R. Ji, X. Yuan, R. Ottermanns, M. Ross-Nickoll, A. Schaffer and H. Hollert (2013). "Solution by dilution?--A review on the pollution status of the Yangtze River." Environ Sci Pollut Res Int **20**(10): 6934-6971.

Fu, R. and H. Shen (2002). "The fluxes of the dissolved inorganic nitrogen and phosphorus at freshwater end-member in the Changiiang Estuary." Acta Oceanologica Sinica **24**(4): 34-43.

Gao, K. C. (2014). "Analysis of the Characteristics of Discharged Sediment in Yangtze River Estuary." Applied Mechanics and Materials **501-504**: 2049-2055.

Gao, L., D. Li, J. Ishizaka, Y. Zhang, H. Zong and L. Guo (2015). "Nutrient dynamics across the river-sea interface in the Changjiang (Yangtze River) estuary-East China Sea region." Limnology and

Oceanography **60**(6): 2207-2221.

Gao, L., D. Li and Y. Zhang (2012). "Nutrients and particulate organic matter discharged by the Changjiang (Yangtze River): Seasonal variations and temporal trends." Journal of Geophysical Research **117**(G4).

Gao, S. and Y. P. Wang (2008). "Changes in material fluxes from the Changjiang River and their implications on the adjoining continental shelf ecosystem." Continental Shelf Research **28**(12): 1490-1500.

Guo, L. and Q. He (2011). "Freshwater flocculation of suspended sediments in the Yangtze River, China." Ocean Dynamics **61**(2-3): 371-386.

Han, F., J. Chen, Z. Jiang, L. Chen and W. Ji (2013). "Volatile and Semi-volatile Organic Compounds in the Lower Yangtze River and Surface Waters of Three Chinese Provinces." Pol. J. Environ. Stud. **22**(3): 683-690.

Han, F. a. 韩., L. 陈. Chen, W. 吉. Ji, X. 李. Li, C. 周. Zhou, Y. 胡. Hu, R. 陆. Lu, Z. 将. Jiang and S. 杨. Yang (2009). "A comparison of VOCs, SVOCs contents of Yangtze River water and main surface water in Jiangsu, Zhejiang and Shandong 江苏长江水与苏鲁浙主要地表水 VOCs_SVOCs 检测." Journal of Preventative Medicine Information 预防医学情报杂志 **25**(3): 161-167.

He, H., G. J. Hu, C. Sun, S. L. Chen, M. N. Yang, J. Li, Y. Zhao and H. Wang (2011). "Trace analysis of persistent toxic substances in the main stream of Jiangsu section of the Yangtze River, China." Environ Sci Pollut Res Int **18**(4): 638-648.

Heisler, J., P. M. Glibert, J. M. Burkholder, D. M. Anderson, W. Cochlan, W. C. Dennison, Q. Dortch, C. J. Gobler, C. A. Heil, E. Humphries, A. Lewitus, R. Magnien, H. G. Marshall, K. Sellner, D. A. Stockwell, D. K. Stoecker and M. Suddleson (2008). "Eutrophication and harmful algal blooms: A scientific consensus." Harmful Algae **8**(1): 3-13.

Helsel, D. R., R. M. Hirsch, K. R. Ryberg, S. A. Archfield and E. J. Gilroy (2020). Statistical methods in water resources: U.S. Geological Survey Techniques and Methods, book 4, chapter A3, USGS.

Hogan, C. M. (2012). Yangtze River, The Encyclopedia of Earth.

Hu, G., C. Sun, J. Li, Y. Zhao, H. Wang and Y. Li (2009). "POPs accumulated in fish and benthos bodies taken from Yangtze River in Jiangsu area." Ecotoxicology **18**(6): 647-651.

Huang, X., Z. Huang, X. P. Chen, D. Zhang, J. Zhou, X. Wang and N. Gao (2018). "The predominant phytoplankton of Pseudoanabaena holding specific biosynthesis gene-derived occurrence of 2-MIB in a drinking water reservoir." Environ Sci Pollut Res Int **25**(19): 19134-19142.

Huang, Z., B. Xie, Q. Yuan, W. Xu and J. Lu (2014). "Microbial community study in newly established Qingcaosha Reservoir of Shanghai, China." Appl Microbiol Biotechnol **98**(23): 9849-9858.

Janse, J. H. (1997). "A model of nutrient dynamics in shallow lakes in relation to multiple stable states." Hydrobiologia **342/343**.

Janse, J. H., L. N. De Senerpont Domis, M. Scheffer, L. Lijklema, L. Van Liere, M. Klinge and W. M. Mooij (2008). "Critical phosphorus loading of different types of shallow lakes and the consequences for management estimated with the ecosystem model PCLake." Limnologica **38**(3-4): 203-219.

Janssen, A. B. G., S. Teurlincx, A. H. W. Beusen, M. A. J. Huijbregts, J. Rost, A. M. Schipper, L. M. S. Seelen, W. M. Mooij and J. H. Janse (2019). "PCLake+: A process-based ecological model to assess the trophic state of stratified and non-stratified freshwater lakes worldwide." Ecological Modelling **396**: 23-32.

Jiang, T., Z. Yu, X. Song and X. Cao (2012). "Nitrogen budget in the Changjiang River drainage area."

Chinese Journal of Oceanology and Limnology **30**(4): 654-667.

Jiang, Y. (2009). "China's water scarcity." J Environ Manage **90**(11): 3185-3196.

Jiang, Y., C. Xu, X. Wu, Y. Chen, W. Han, K. Gin, Yew-Hoong and Y. He (2018). "Occurrence, Seasonal Variation and Risk Assessment of Antibiotics in Qingcaosha Reservoir." Water **10**(115).

Jiang, Z., J. Liu, J. Chen, Q. Chen, X. Yan, J. Xuan and J. Zeng (2014). "Responses of summer phytoplankton community to drastic environmental changes in the Changjiang (Yangtze River) estuary during the past 50 years." Water Res **54**: 1-11.

Jin, X., Y. He, G. Kirumba, Y. Hassan and J. Li (2013). "Phosphorus fractions and phosphate sorption-release characteristics of the sediment in the Yangtze River estuary reservoir." Ecological Engineering **55**: 62-66.

Jin, X., Y. He, B. Zhang, Y. Hassan and K. George (2013). "Impact of sulfate and chloride on sediment phosphorus release in the Yangtze Estuary Reservoir, China." Water Sci Technol **67**(8): 1748-1756.

Jing, X., S. Zhang, J. Zhang, Y. Wang and Y. Wang (2017). "Assessing efficiency and economic viability of rainwater harvesting systems for meeting non-potable water demands in four climatic zones of China." Resources, Conservation and Recycling **126**: 74-85.

Kennish, M. J. (2002). "Environmental threats and environmental future of estuaries." Environmental Conservation **29**(1): 78-107.

Lehner, B., C. Reidy Liermann, C. Revenga, C. Vorosmarty, B. Fekete, P. Crouzet, P. Doll, M. Endejan, K. Frenken, J. Magome, C. Nilsson, J. C. Robertson, R. Rodel, N. Sindorf and D. Wisser (2011). Global Reservoir and Dam Database, Version 1 (GRanDv1): Dams, Revision 01. Palisades, NY, NASA Socioeconomic Data and Applications Center (SEDAC).

Li, M., J. Chen, B. Finlayson, Z. Chen, M. Webber, J. Barnett and M. Wang (2019). "Freshwater Supply to Metropolitan Shanghai: Issues of Quality from Source to Consumers." Water **11**(10).

Li, M., Z. Chen, B. Finlayson, T. Wei, J. Chen, X. Wu, H. Xu, M. Webber, J. Barnett and M. Wang (2015). "Water diversion and sea-level rise: Potential threats to freshwater supplies in the Changjiang River estuary." Estuarine, Coastal and Shelf Science **156**: 52-60.

Li, M., B. Finlayson, M. Webber, J. Barnett, S. Webber, S. Rogers, Z. Chen, T. Wei, J. Chen, X. Wu and M. Wang (2017). "Estimating urban water demand under conditions of rapid growth: the case of Shanghai." Regional Environmental Change **17**(4): 1153-1161.

Li, M., H. Wang, Y. Li, W. Ai, L. Hou and Z. Chen (2016). "Sedimentary BSi and TOC quantifies the degradation of the Changjiang Estuary, China, from river basin alteration and warming SST." Estuarine, Coastal and Shelf Science **183**: 392-401.

Li, X. Z., Ü. Mander, Z. G. Ma and Y. Jia (2009). "Water quality problems and the potential for wetlands as treatment systems in the Yangtze River Delta, China." Wetlands **25**(4): 1125-1132.

Li, Y., C. Tang, C. Wang, D. O. Anim, Z. Yu and K. Acharya (2013). "Improved Yangtze River Diversions: Are they helping to solve algal bloom problems in Lake Taihu, China?" Ecological Engineering **51**: 104-116.

Liu, C., G.-L. Yuan, Z.-F. Yang, T. Yu, X.-Q. Xia, Q.-Y. Hou and L. Chen (2010). "Levels of organochlorine pesticides in natural water along the Yangtze River, from headstream to estuary, and factors determining these levels." Environmental Earth Sciences **62**(5): 953-960.

Liu, H., Y. Li, F. Leng and W. Schmidt (2016). "Stage Variation of Phytoplankton and Environmental Factors in a Large Drinking Water Reservoir: from Construction to Full Operation." Water, Air, & Soil Pollution **227**(9).

Liu, H., D. Pan and P. Chen (2015). "A two-year field study and evaluation of water quality and trophic state of a large shallow drinking water reservoir in Shanghai, China." Desalination and Water Treatment: 1-10.

Liu, H., D. Pan, M. Zhu and D. Zhang (2016). "Occurrence and Emergency Response of 2-Methylisoborneol and Geosmin in a Large Shallow Drinking Water Reservoir." CLEAN - Soil, Air, Water **44**(1): 63-71.

Liu, S.-m., J. Zhang, H. T. Chen, Y. Wu, H. Xiong and Z. F. Zhang (2003). "Nutrients in the changjiang and its tributaries." Biogeochemistry **62**: 1-18.

Liu, S. M., J. Zhang, H. T. Chen, Y. Wu, H. Xiong and Z. F. Zhang (2003). "Nutrients in the Changjiang and its tributaries." Biogeochemistry **62**(1): 1-18.

Liu, S. Q. (2007). "Urban water supply management in Shanghai." Water Supply **7**(2): 41-47.

Liu, W. R., J. L. Zhao, Y. S. Liu, Z. F. Chen, Y. Y. Yang, Q. Q. Zhang and G. G. Ying (2015). "Biocides in the Yangtze River of China: spatiotemporal distribution, mass load and risk assessment." Environ Pollut **200**: 53-63.

Liu, X., Z. Yu, X. Song and X. Cao (2009). "The nitrogen isotopic composition of dissolved nitrate in the Yangtze River (Changjiang) estuary, China." Estuarine, Coastal and Shelf Science **85**(4): 641-650.

Lu, G.-H., Y.-L. Yang, S. Taniyasu, L. W. Y. Yeung, J. Pan, B. Zhou, P. K. S. Lam and N. Yamashita (2013). "Potential exposure of perfluorinated compounds to Chinese in Shenyang and Yangtze River Delta areas." Environmental Chemistry **8**(4): 407.

Lu, Z., L. Zhang, J. Yang, S. Zhang and L. Lin (2010). Picoplankton distribution as sensitive indicators of eutrophication in typical freshwater bodies around Shanghai. AIP Conference Proceedings.

Lu, Z., L. Zhang, J. Yang, S. Zhang and L. Lin (2010). Picoplankton Distribution as Sensitive Indicators of Eutrophication in Typical
Freshwater Bodies around Shanghai. Second International Symposium on Aqua Science, Water Resource, and Low Carbon Energy, AIP Conference Proceedings.

Luo, X. X., S. L. Yang and J. Zhang (2012). "The impact of the Three Gorges Dam on the downstream distribution and texture of sediments along the middle and lower Yangtze River (Changjiang) and its estuary, and subsequent sediment dispersal in the East China Sea." Geomorphology **179**: 126-140.

Ma, L., W. F. Zhang, W. Q. Ma, G. L. Velthof, O. Oenema and F. S. Zhang (2013). "An analysis of developments and challenges in nutrient management in china." J Environ Qual **42**(4): 951-961.

McDonald, R. I., K. F. Weber, J. Padowski, T. Boucher and D. Shemie (2016). "Estimating watershed degradation over the last century and its impact on water-treatment costs for the world's large cities." Proc Natl Acad Sci U S A **113**(32): 9117-9122.

Meals, D. W., J. Spooner, S. A. Dressing and J. B. Harcum (2011). Technotes 6: Statistical Analysis for Monotonic Trends. U. S. E. P. Agency. Fairfax, Tetra Tech.

Mei, X., Z. Dai, W. Wei, W. Li, J. Wang and H. Sheng (2018). "Secular bathymetric variations of the North Channel in the Changjiang (Yangtze) Estuary, China, 1880–2013: Causes and effects." Geomorphology **303**: 30-40.

Meng, J., Z. Yu, Q. Yao, T. S. Bianchi, A. Paytan, B. Zhao, H. Pan and P. Yao (2015). "Distribution, mixing behavior, and transformation of dissolved inorganic phosphorus and suspended particulate phosphorus along a salinity gradient in the Changjiang Estuary." Marine Chemistry **168**: 124-134.

Meng, W. 孟., Y. 秦. Qin, B. 郑. Zheng, G. 富. Fu, Z. 李. Li, K. 雷. Lei and L. 张. Zhang (2004). "Analysis of nitrogen, phosphorus nutrients and cod in waters of Yangtze River Estuary 长江口水体中氮

、磷含量及其化学耗氧量的分析." Environmental Science 环境科学 **25**(6): 65-68.

Meybeck, M. (1982). "Carbon, Nitrogen and Phosphorous Transport by World Rivers." Americal Journal of Science **282**: 401-450.

Mines, R. O. J. (2014). Design of Water Treatment Systems. Environmental Engineering: Principles and Practice, John Wiley & Sons.

Müller, B., M. Berg, B. Pernet-Coudrier, W. Qi and H. Liu (2012). "The geochemistry of the Yangtze River: Seasonality of concentrations and temporal trends of chemical loads." Global Biogeochemical Cycles **26**(2): n/a-n/a.

Muller, B., M. Berg, Z. P. Yao, X. F. Zhang, D. Wang and A. Pfluger (2008). "How polluted is the Yangtze river? Water quality downstream from the Three Gorges Dam." Sci Total Environ **402**(2-3): 232-247.

Naeem, N., M. Idrees, M. Masroor, A. Khan, M. A. Moinuddin and A. A. Ansari (2013). Task of Mineral Nutrients in Eutrophication. Eutrophication: Causes, Consequences and Control. A. A. Ansari. Dordrecht, Springer**:** 224-234.

NASA Earth Observatory (2017). World of Change: Sprawling Shanghai.

NASA LP DAAC (2015). ASTER Level 1 Precision Terrain Corrected Registered At-Sensor Radiance V003 [Data set]. N. E. L. P. DAAC.

National Bureau of Statistics of China (2017). http://data.stats.gov.cn/english/easyquery.htm.

Nie, M., C. Yan, W. Dong, M. Liu, J. Zhou and Y. Yang (2015). "Occurrence, distribution and risk assessment of estrogens in surface water, suspended particulate matter, and sediments of the Yangtze Estuary." Chemosphere **127**: 109-116.

Ongley, E. (1996). Chapter 13 - Sediment Measurements. Water Quality Monitoring - A Practical Guide to the Design and Implementation of Freshwater Quality Studies and Monitoring Programs. J. Batram and R. Ballence, United Nations Environment Programme and the World Health Organization.

Ou, D. 欧., M. 刘. Liu, S. 许. Xu, S. 程. Cheng, L. 侯. Hou and L. 王. Wang (2009). "Distribution and ecological risk assessment of polycyclic aromatic hydrocarbons in overlying waters and surface sediments from the Yangtze estuarine and coastal 长江口滨岸水和沉积物中多环芳烃分布特征与生态风险评价." Environmental Science 环境科学 **30**(10): 3043-3049.

Ou, H. S., C. H. Wei, Y. Deng and N. Y. Gao (2013). "Principal component analysis to assess the composition and fate of impurities in a large river-embedded reservoir: Qingcaosha Reservoir." Environ Sci Process Impacts **15**(8): 1613-1621.

Paerl, H. W. (2008). Chapter 10: Nutrient and other environmental controls of harmful cyanobacterial blooms along the freshwater-marine continuum. Cyanobacterial Harmful Algal Blooms ; State of the Science and Research Needs. N. Beck, A. Lajtha and R. Paoletti, Springer.

Pan, C. G., G. G. Ying, J. L. Zhao, Y. S. Liu, Y. X. Jiang and Q. Q. Zhang (2014). "Spatiotemporal distribution and mass loadings of perfluoroalkyl substances in the Yangtze River of China." Sci Total Environ **493**: 580-587.

Pan, G. and C. You (2010). "Sediment-water distribution of perfluorooctane sulfonate (PFOS) in Yangtze River Estuary." Environ Pollut **158**(5): 1363-1367.

Pawelczyk, A. (2012). "Assessment of health hazard associated with nitrogen compounds in water." Water Sci Technol **66**(3): 666-672.

Qiu, C. and J.-R. Zhu (2013). "Influence of seasonal runoff regulation by the Three Gorges Reservoir on

saltwater intrusion in the Changjiang River Estuary." Continental Shelf Research **71**: 16-26.

Ren, X., K. Yang, Y. Che, M. Wang, L. Zhou and L. Chen (2015). "Spatial and temporal assessment of the initial pattern of phytoplankton population in a newly built coastal reservoir." Frontiers of Earth Science.

Robinson, N., J. Regetz and R. P. Guralnick (2014). "EarthEnv-DEM90: A nearly-global, void-free, multi-scale smoothed, 90m digital elevation model from fused ASTER and SRTM data." ISPRS Journal of Photogrammetry and Remote Sensing **87**: 57-67.

SEPA (2002). GB 3838 - 2002: Environmental quality standards for surface water 地表水环境质量表示. S. E. P. A. PRC and 国家环境保护总局.

Shanghai Municipal Government. (2009). "Geographic Location and Natural Condition." Retrieved 4th October, 2018, from http://www.shanghai.gov.cn/shanghai/node23919/node24059/node24061/userobject22ai36485.html.

Shanghai Municipal People's Government (2010). The Encyclopedia of Shanghai. The Encyclopedia of Shanghai Editorial Comittee. Shanghai, Shanghai Scientific and Technical Publishers,.

Shen, Z. L. and Q. Liu (2009). "Nutrients in the Changjiang River." Environ Monit Assess **153**(1-4): 27-44.

Shi, J., X. Liu, Q. Chen and H. Zhang (2014). "Spatial and seasonal distributions of estrogens and bisphenol A in the Yangtze River Estuary and the adjacent East China Sea." Chemosphere **111**: 336-343.

Shi, W., G. Hu, S. Chen, S. Wei, X. Cai, B. Chen, J. Feng, X. Hu, X. Wang and H. Yu (2013). "Occurrence of estrogenic activities in second-grade surface water and ground water in the Yangtze River Delta, China." Environ Pollut **181**: 31-37.

Shi, W., X. Wang, G. Hu, Y. Hao, X. Zhang, H. Liu, S. Wei, X. Wang and H. Yu (2011). "Bioanalytical and instrumental analysis of thyroid hormone disrupting compounds in water sources along the Yangtze River." Environ Pollut **159**(2): 441-448.

Shi, W., S. Wei, X. X. Hu, G. J. Hu, C. L. Chen, X. R. Wang, J. P. Giesy and H. X. Yu (2013). "Identification of thyroid receptor ant/agonists in water sources using mass balance analysis and monte carlo simulation." PLoS One **8**(10): e73883.

Shi, X., S. Jiang, H. Xu, F. Jiang, Z. He and J. Wu (2016). "The effects of artificial recharge of groundwater on controlling land subsidence and its influence on groundwater quality and aquifer energy storage in Shanghai, China." Environmental Earth Sciences **75**(3).

Sogreah Consultants (2008). R3 - Summary of QingCaoSha Reservoir Environmental Assessment.

Song, J. X., D. An and B. Anderson (2010). "A Survey of Current Drinking Water Supply for Shanghai." Advanced Materials Research **113-116**: 68-70.

Song, Y., J. Ji, C. Mao, Z. Yang, X. Yuan, G. A. Ayoko and R. L. Frost (2010). "Heavy metal contamination in suspended solids of Changjiang River — environmental implications." Geoderma **159**(3-4): 286-295.

Stroom, J. M. and W. E. A. Kardinaal (2016). "How to combat cyanobacterial blooms: strategy toward preventive lake restoration and reactive control measures." Aquatic Ecology **50**(3): 541-576.

Sun, C. C., Z. Y. Shen, M. Xiong, F. B. Ma, Y. Y. Li, L. Chen and R. M. Liu (2013). "Trend of dissolved inorganic nitrogen at stations downstream from the Three-Gorges Dam of Yangtze River." Environ Pollut **180**: 13-18.

Sun, G., A. M. Michelsen, Z. Sheng, A. F. Fang, Y. Shang and H. Zhang (2015). "Featured collection

introduction: Water for megacities - challenges and solutions." Journal of the American Water Resources Association **51(3)**: 585-588.

Tang, X., M. Wu, W. Yang, W. Yin, F. Jin, M. Ye, N. Currie and M. Scholz (2011). "Ecological Strategy for Eutrophication Control." Water, Air, & Soil Pollution **223**(2): 723-737.

Tang, Z., Q. Huang, Y. Yang, X. Zhu and H. Fu (2013). "Organochlorine pesticides in the lower reaches of Yangtze River: occurrence, ecological risk and temporal trends." Ecotoxicol Environ Saf **87**: 89-97.

UN DESA. (2018). "World Urbanisation Prospects 2018 -Worlds Largest Cities." World Urbanisation Prospects Retrieved 4th October, 2018, from https://www.un.org/development/desa/publications/graphic/world-urbanization-prospects-2018-worlds-largest-cities.

Varis, O. and P. Vakkilainen (2001). "China's 8 challenges to water resources management in the first quarter of the 21st century." Geomorphology **41**(2): 93-104.

Wan, Y., F. Gu, H. Wu and D. Roelvink (2014). "Hydrodynamic evolutions at the Yangtze Estuary from 1998 to 2009." Applied Ocean Research **47**: 291-302.

Wang, F., Y. Wang and J. Zhang (2007). "A decade of variation of COD in the Changjiang River (Yangtze River) and its variation trend analysis." Chinese Journal of Geochemistry **26**(4): 366-373.

Wang, J. and J. Wu (2009). "Occurrence and potential risks of harmful algal blooms in the East China Sea." Sci Total Environ **407**(13): 4012-4021.

Wang, J., Q. Yuan and B. Xie (2014). "Temporal dynamics of cyanobacterial community structure in Dianshan Lake of Shanghai, China." Annals of Microbiology **65**(1): 105-113.

Wang, L., Y. Wang, W. Zhang, C. Xu and Z. An (2013). "Multivariate statistical techniques for evaluating and identifying the environmental significance of heavy metal contamination in sediments of the Yangtze River, China." Environmental Earth Sciences **71**(3): 1183-1193.

Wang, L. Z., L. J. Chen and Y. Q. Zhu (2015). Competitive spatiotemporal dataset on population distribution and its natural-social-economic driving factors from 1949 to 2013. C. a. A. R. S. D. C. a. Lanzhou.

Wang, M., M. Webber, B. Finlayson and J. Barnett (2008). "Rural industries and water pollution in China." J Environ Manage **86**(4): 648-659.

Wang, W., W. Xing, T. Yang, Q. Shao, S. Peng, Z. Yu and B. Yong (2013). "Characterizing the changing behaviours of precipitation concentration in the Yangtze River Basin, China." Hydrological Processes **27**(24): 3375-3393.

Wang, Z., D. Shao and P. Westerhoff (2017). "Wastewater discharge impact on drinking water sources along the Yangtze River (China)." Sci Total Environ **599-600**: 1399-1407.

Wang, Z. H. (2013). Police protect essential drinking water supply. Aberdeen, China Daily.

Ward, R. M. and W. Liang (1995). "Shanghai Water Supply and Wastewater Disposal." Americal Geographical Society **85**(2): 141-156.

Webber, M., J. O. N. Barnet, Z. Chen, B. Finlayson, M. Wang, D. A. N. Chen, J. Chen, M. Li, T. Wei, S. Wu and H. A. O. Xu (2015). "Constructing Water Shortages on a Huge River: The Case of Shanghai." Geographical Research **53**(4): 406-418.

Webber, M., J. Barnett, B. Finlayson and M. Wang (2018). Water Supply in a Mega-city: A Political Ecology Analysis of Shanghai. Cheltenham, UK, Edward Elgar Publishing.

Webber, M., M. T. Li, J. Chen, B. Finlayson, D. Chen, Z. Y. Chen, M. Wang and J. Barnett (2015).

"Impact of the Three Gorges Dam, the South–North Water Transfer Project and water abstractions on the duration and intensity of salt intrusions in the Yangtze River estuary." Hydrology and Earth System Sciences **19**(11): 4411-4425.

Wong, C. M., C. E. Williams, J. Pittock, U. Collier and P. Schelle (2007). World's top 10 rivers at risk. Switzerland, World Wildlife Fund.

World Health Organization (2003). Total dissolved solids in drinking-water. Background document for preparation of WHO Guidelines for drinking-water quality. W. H. Organization. Geneva.

World Health Organization (2017). Guidelines for Drinking-water Quality: Fourth Edition Incorporating the First Amendment. Geneva.

Wu, C., X. Huang, J. D. Witter, A. L. Spongberg, K. Wang, D. Wang and J. Liu (2014). "Occurrence of pharmaceuticals and personal care products and associated environmental risks in the central and lower Yangtze river, China." Ecotoxicol Environ Saf **106**: 19-26.

Wu, J. Y. (2005). "Assessing surface water quality of the Yangtze Estuary with genotoxicity data." Mar Pollut Bull **50**(12): 1661-1667.

Xinhua News Agency (2006). Economic growth saps water resources from Yangtze River Delta. Xinhua News Agency - CIES,.

Xu, Z., Y. Jiang, S. Te, Y. He and K. Gin (2018). "The Effects of Antibiotics on Microbial Community Composition in an Estuary Reservoir during Spring and Summer Seasons." Water **10**(2): 154.

Yan, Q., L.-b. Chen, W. Guo and H.-t. Jiang (2013). "Variation of Flow Rate and Water Quality of Changjiang River at Xuliujing Section in 1997-2011." Journal of Ecology and Rural Environment **29**(5): 577-580.

Yan, W. and Z. Shen (2003). "The composition and bioavailability of phosphorous transport through the Changjiang (Yangtze) River during the 1998 flood." Biogeochemistry **65**: 179-194.

Yan, W., S. Zhang, P. Sun and S. P. Seitzinger (2003). "How do nitrogen inputs to the Changjiang basin impact the Changjiang River nitrate: A temporal analysis for 1968-1997." Global Biogeochemical Cycles **17**(4): n/a-n/a.

Yan, X., C. Ti, P. Vitousek, D. Chen, A. Leip, Z. Cai and Z. Zhu (2014). "Fertilizer nitrogen recovery efficiencies in crop production systems of China with and without consideration of the residual effect of nitrogen." Environmental Research Letters **9**(9): 095002.

Yang, H.-j., Z.-m. Shen, J.-p. Zhang and W.-h. Wang (2007). "Water quality characteristics along the course of the Huangpu River (China)." Journal of Environmental Sciences **19**(10): 1193-1198.

Yang, S.-Q. and S. Kelly (2015). "The Use of Coastal Reservoirs and SPP Strategy to Provide Sufficient High Quality Water to Coastal Communities." Journal of Geoscience and Environment Protection **03**(05): 80-92.

Yang, S. L., J. D. Milliman, P. Li and K. Xu (2011). "50,000 dams later: Erosion of the Yangtze River and its delta." Global and Planetary Change **75**(1-2): 14-20.

Yang, S. L., K. H. Xu, J. D. Milliman, H. F. Yang and C. S. Wu (2015). "Decline of Yangtze River water and sediment discharge: Impact from natural and anthropogenic changes." Sci Rep **5**: 12581.

Yang, Y., J. Deng, M. Zhang, Y. Li and W. Liu (2015). "The synchronicity and difference in the change of suspended sediment concentration in the Yangtze River Estuary." Journal of Geographical Sciences **25**(4): 399-416.

Yang, Y., J. Fu, H. Peng, L. Hou, M. Liu and J. L. Zhou (2011). "Occurrence and phase distribution of selected pharmaceuticals in the Yangtze Estuary and its coastal zone." J Hazard Mater **190**(1-3): 588-596.

Yang, Y., B. Gao, H. Hao, H. Zhou and J. Lu (2017). "Nitrogen and phosphorus in sediments in China: A national-scale assessment and review." Sci Total Environ **576**: 840-849.

Yao, Q.-Z., Z.-G. Yu, H.-T. Chen, P.-X. Liu and T.-Z. Mi (2009). "Phosphorus transport and speciation in the Changjiang (Yangtze River) system." Applied Geochemistry **24**(11): 2186-2194.

Yin, Z. Y., S. Walcott, B. Kaplan, J. Cao, W. Lin, M. Chen, D. Liu and Y. Ning (2005). "An analysis of the relationship between spatial patterns of water quality and urban development in Shanghai, China." Computers, Environment and Urban Systems **29**(2): 197-221.

Yuan, J. Z. and C. E. Wu (2018). "Shanghai Coastal Reservoirs: Their Development and Experience from their Design." Hydrolink **1**: 10-13.

Yuan, J. Z. and C. E. Wu (2018). Shanghai Coastal Reservoirs: Their Development and Experience From Their Design. Hydrolink.

Zeng, L., F. He, Z. Dai, D. Xu, B. Liu, Q. Zhou and Z. Wu (2017). "Effect of submerged macrophyte restoration on improving aquatic ecosystem in a subtropical, shallow lake." Ecological Engineering **106**: 578-587.

Zeng, X., Z. W. Kundzewicz, J. Zhou and B. Su (2012). "Discharge projection in the Yangtze River basin under different emission scenarios based on the artificial neural networks." Quaternary International **282**: 113-121.

Zhang, E. and X. Chen (2003). "Changes of water discharge between Datong and the Changjiang Estuary during the dry season." Acta Geographica Sinica **58**(2): 231-238.

Zhang, E., H. H. G. Savenije, S. Chen and J. Chen (2012). "Water abstraction along the lower Yangtze River, China, and its impact on water discharge into the estuary." Physics and Chemistry of the Earth, Parts A/B/C **47-48**: 76-85.

Zhang, E., H. H. G. Savenije, H. Wu, Y. Kong and J. Zhu (2011). "Analytical solution for salt intrusion in the Yangtze Estuary, China." Estuarine, Coastal and Shelf Science **91**(4): 492-501.

Zhang, J., S. M. Liu, J. L. Ren, Y. Wu and G. L. Zhang (2007). "Nutrient gradients from the eutrophic Changjiang (Yangtze River) Estuary to the oligotrophic Kuroshio waters and re-evaluation of budgets for the East China Sea Shelf." Progress in Oceanography **74**(4): 449-478.

Zhang, K., T. Zhang, Y. Deng, N. Gao and Y. Yang (2015). "Occurrence of algae and algae-related taste and odour (T&O) compounds in the Qingcaosha Reservoir, China." Journal of Water Supply: Research and Technology - Aqua **64**(7): 824-831.

Zhang, L., L. Dong, L. Ren, S. Shi, L. Zhou, T. Zhang and Y. Huang (2012). "Concentration and source identification of polycyclic aromatic hydrocarbons and phthalic acid esters in the surface water of the Yangtze River Delta, China." Journal of Environmental Sciences **24**(2): 335-342.

Zhang, L., S. Shi, L. Dong, T. Zhang, L. Zhou and Y. Huang (2011). "Concentrations and possible sources of polychlorinated biphenyls in the surface water of the Yangtze River Delta, China." Chemosphere **85**(3): 399-405.

Zhang, Q., M. Gemmer and J. Chen (2008). "Climate changes and flood/drought risk in the Yangtze Delta, China, during the past millennium." Quaternary International **176-177**: 62-69.

Zhang, Q., C. Y. Xu, V. P. Singh and T. Yang (2009). "Multiscale variability of sediment load and streamflow of the lower Yangtze River basin: Possible causes and implications." Journal of Hydrology **368**(1-4): 96-104.

Zhang, Y., A. Bleeker and J. Liu (2015). "Nutrient discharge from China's aquaculture industry and associated environmental impacts." Environmental Research Letters **10**(4): 045002.

Zhou, J., Z. Liu, W. Meng, Z. Li and J. Z. Li (2006). "The Characteristics Of Nutrients Distribution in the Yangtze River Estuary." Research of Environmental Sciences **19**(6): 139-144.

Zhou, M. J., Z. L. Shen and R. C. Yu (2008). "Responses of a coastal phytoplankton community to increased nutrient input from the Changjiang (Yangtze) River." Continental Shelf Research **28**(12): 1483-1489.

7. Appendices

A1 - Supplementary Data Tables

Table A1-1: Total Nitrogen (TN) Data Source Table

Estuary-Monthly		**Datong-Monthly**	
1997/12	(Shen and Liu 2009)	1962-1985	Ministry of Water Conservancy (reported in Chen, Gao et al. (2000))
1998/10	(Shen and Liu 2009)	1997/5	(Duan, Shen et al. 2000)
2002/11	(Chai, Yu et al. 2009)	1997/12	(Shen and Liu 2009)
2003/11	(Chai, Yu et al. 2009)	1998/6	(Duan, Shen et al. 2000)
2004/11	(Meng, Qin et al. 2004, Yang, Shen et al. 2007, Chai, Yu et al. 2009)	1998/8	(Duan, Shen et al. 2000)
2005/11	(Chai, Yu et al. 2009)	1998/10	(Shen and Liu 2009)
2006/11	(Muller, Berg et al. 2008, Chai, Yu et al. 2009)	2006/11	(Muller, Berg et al. 2008)
2009/6	(Lu, Zhang et al. 2010)	2013/7	(Liu, Zhao et al. 2015) (supp. data)
2010/5	(Huang, Xie et al. 2014)	2013/11	(Liu, Zhao et al. 2015) (supp. data)
2010/6	(Huang, Xie et al. 2014)		
2010/7	(Huang, Xie et al. 2014)		
2010/8	(Chen, Liu et al. 2012, Huang, Xie et al. 2014)		
2010/9	(Huang, Xie et al. 2014)		
2010/10	(Huang, Xie et al. 2014)		
2010/11	(Chen, Liu et al. 2012, Huang, Xie et al. 2014)		
2010/12	(Huang, Xie et al. 2014)		
2011/2	(Chen, Liu et al. 2012)		
2011/5	(Chen, Liu et al. 2012)		
2012/1	(Wu, Huang et al. 2014) (supp. data)		
(Liu, Zhao et al. 2015) (supp. Data)	(Liu, Zhao et al. 2015) (supp. data)		
(Liu, Zhao et al. 2015) (supp. Data)	(Liu, Zhao et al. 2015) (supp. data)		

Table A1-2: Nitrate-Nitrogen (NO_3-N) Data Source Table

Estuary		**Datong**	
1980/6	(Edmond, Spivack et al. 1985)	1962-1990	(Duan, Shen et al. 2000)
1981/11	(Edmond, Spivack et al. 1985)	1991-2009	Chang Jiang Water Resources Commission (CJWRC) reported in (Sun, Shen et al. 2013)
1997/12	(Shen and Liu 2009)		
1998/2	(Fu and Shen 2002)		
1998/9	(Fu and Shen 2002)		
1998/10	(Shen and Liu 2009)		
2003/8	(Zhou, Liu et al. 2006)		
2003/11	(Zhou, Liu et al. 2006)		
2004/11	(Meng, Qin et al. 2004, Yang, Shen et al. 2007)		
2006/2	(Liu, Yu et al. 2009)		
2006/5	(Liu, Yu et al. 2009)		
2006/8	(Chetelat, Liu et al. 2008, Liu, Yu et al. 2009)		
2006/11	(Muller, Berg et al. 2008, Liu, Yu et al. 2009)		
2007/6	(Gao, Li et al. 2012)		
2009-2010	(Gao, Li et al. 2012)		
2011/12	(Gao, Li et al. 2015)		
2012/1	(Gao, Li et al. 2015)		
2012/3	(Gao, Li et al. 2015)		
2012/12	(Wu, Huang et al. 2014)		

Annual Data series for nitrate at the estuary was supplemented with data from Jiang, Liu et al. (2014).

Table A1-3: Ammonium-Nitrogen (NH_4-N) Data Source Table

Estuary - Monthly		**Datong Monthly**	
1998/2	(Fu and Shen 2002)	1966-1985	Ministry of water as reported in (Duan, Xu et al. 2007)
1998/9	(Fu and Shen 2002)	1990-2009	Chang Jiang Water Resources Commission (CJWRC) reported in (Sun, Shen et al. 2013)
2003/8	(Zhou, Liu et al. 2006)	2009-2010	(Müller, Berg et al. 2012)
2003/11	(Zhou, Liu et al. 2006)	2013/7	(Liu, Zhao et al. 2015) (supp. Data)
2004/11	(Meng, Qin et al. 2004, Yang, Shen et al. 2007)	2013/11	(Liu, Zhao et al. 2015) (supp. Data)
2006/2	(Liu, Yu et al. 2009)		
2006/5	(Liu, Yu et al. 2009)		
2006/8	(Liu, Yu et al. 2009)		
2006/11	(Muller, Berg et al. 2008, Liu, Yu et al. 2009)		
2007/6	(Gao, Li et al. 2012)		
2009-2010	(Gao, Li et al. 2012)		
2011/12	(Gao, Li et al. 2015)		
2012/1	(Gao, Li et al. 2015)		
2012/3	(Gao, Li et al. 2015)		
2012/7	(Gao, Li et al. 2015)		
2012/12	(Wu, Huang et al. 2014)		
(Liu, Zhao et al. 2015) (supp. Data)	(Liu, Zhao et al. 2015) (supp. data)		
(Liu, Zhao et al. 2015) (supp. Data)	(Liu, Zhao et al. 2015) (supp. data)		

Annual Data series for Ammonium at the estuary was supplemented with data from (Yan, Chen et al. 2013).

Table A1-4: Total Phosphorous (TP) Data Source Table

Estuary - Monthly		**Datong Monthly**	
1997/5	(Duan, Zhang et al. 2000, Yan and Shen 2003)	1997/5	(Duan, Zhang et al. 2000),(Yan and Shen 2003)
1997/12	(Shen and Liu 2009)	1997/12	(Shen and Liu 2009)
1998/6	(Duan, Zhang et al. 2000, Yan and Shen 2003)	1998/6	(Duan, Zhang et al. 2000),(Yan and Shen 2003)
1998/8	(Duan, Zhang et al. 2000, Yan and Shen 2003)	1998/8	(Duan, Zhang et al. 2000),(Yan and Shen 2003)
1998/10	(Shen and Liu 2009)	1998/10	(Shen and Liu 2009)
1998/11	(Yan and Shen 2003)	1998/11	(Yan and Shen 2003)
1999/1	(Yan and Shen 2003)	1999/1	(Yan and Shen 2003)
2006/4	(Yao, Yu et al. 2009)	2006/4	(Yao, Yu et al. 2009)
2006/9	(Yao, Yu et al. 2009)	2006/9	(Yao, Yu et al. 2009)
2006/11	(Muller, Berg et al. 2008)	2006/11	(Muller, Berg et al. 2008)
2013/7	(Liu, Zhao et al. 2015) (supp. Data)	2013/7	(Liu, Zhao et al. 2015) (supp. Data)
2013/11	(Liu, Zhao et al. 2015) (supp. Data)	2013/11	(Liu, Zhao et al. 2015) (supp. Data)

Annual Data series for TP at the estuary was supplemented with data from (Yan, Chen et al. 2013).

Table A1-5: Dissolved Inorganic Phosphorous (DIP) Data Source Table

Estuary - Monthly		**Datong Monthly**	
1980/6	(Edmond, Spivack et al. 1985)	1997/5	(Yan and Shen 2003)
1981/11	(Edmond, Spivack et al. 1985)	1997/12	(Shen and Liu 2009)
1997/12	(Shen and Liu 2009)	1998/6	(Duan, Zhang et al. 2000),(Yan and Shen 2003)
1998/2	(Fu and Shen 2002)	1998/8	(Duan, Zhang et al. 2000),(Yan and Shen 2003)
1998/9	(Fu and Shen 2002)	1998/10	(Shen and Liu 2009)
1998/10	(Shen and Liu 2009)	1998/11	(Yan and Shen 2003) (Duan, Liang et al. 2008)
2002/11	(Duan, Shen et al. 2000)	1999/1	(Yan and Shen 2003) (Duan, Liang et al. 2008)
2002/11	(Chai, Yu et al. 2009)	1999/3	(Duan, Liang et al. 2008)
2003/8	(Zhou, Liu et al. 2006)	2006/4	(Yao, Yu et al. 2009)
2003/11	(Chai, Yu et al. 2009)	2006/11	(Muller, Berg et al. 2008)
2004/11	(Meng, Qin et al. 2004, Chai, Yu et al. 2009)		
2005/11	(Chai, Yu et al. 2009)		
2006/11	(Muller, Berg et al. 2008, Chai, Yu et al. 2009)		
2007/6	(Gao, Li et al. 2012)		
2009-2010	(Gao, Li et al. 2012)		
2011/6	(Meng, Yu et al. 2015)		
2011/7	(Meng, Yu et al. 2015)		
2011/8	(Meng, Yu et al. 2015)		
2011/12	(Gao, Li et al. 2015)		
2012/1	(Gao, Li et al. 2015)		
2012/3	(Gao, Li et al. 2015)		
2012/7	(Gao, Li et al. 2015)		

Annual Data series for DIP at the estuary was supplemented with data from Jiang, Liu et al. (2014).

A2 - Chinese Water Quality Standards

Environmental Quality Standards for Surface Water <GB 3838 – 2002>

State Environmental Protection Agency

Table A2-1: Basic Water Quality Parameter Guidelines

Parameter	Unit	Class				
		1	2	3	4	5
Water temperature	(ºC)	The change in temperature in the man-made environment should be limited to: Rise in weekly average maximum temperature ≤ 1 Drop in weekly average maximum temperature ≤ 2				
pH	-	6 to 9				
Dissolved Oxygen	(mg/L)	90% saturation 90% (or 7.5)	6	5	3	2
Permanganate Index	(mg/L)	2	4	6	10	15
COD	(mg/L)	15	15	20	30	40
BOD_5	(mg/L)	3	3	4	6	10
NH_3-N	(mg/L)	0.15	0.5	1	1.5	2
TP (rivers)	(mg/L)	0.02	0.1	0.2	0.3	0.4
TP (lake/reservoir)	(mg/L)	0.01	0.025	0.05	0.1	0.2
TN	(mg/L)	0.2	0.5	1	1.5	2
Copper (Cu)	(mg/L)	0.01	1	1	1	1
Zinc (Zn)	(mg/L)	0.05	1	1	2	2
Fluoride (Fl^-)	(mg/L)	1	1	1	1.5	1.5
Selenium (Se)	(mg/L)	0.01	0.01	0.01	0.02	0.02
Arsenic (As)	(mg/L)	0.05	0.05	0.05	0.1	0.1
Mercury (Hg)	(mg/L)	0.00005	0.00005	0.0001	0.001	0.001
Cadmium (Cd)	(mg/L)	0.001	0.005	0.005	0.005	0.01
Hexavalent Chromium (Cr^{6+})	(mg/L)	0.01	0.05	0.05	0.05	0.1
Lead (Pb)	(mg/L)	0.01	0.01	0.05	0.05	0.1
Cyanide (CN^-)	(mg/L)	0.005	0.05	0.2	0.2	0.2
Volatile Phenol	(mg/L)	0.002	0.002	0.005	0.01	0.1
Oils	(mg/L)	0.05	0.05	0.05	0.5	1
Anionic Surfactants	(mg/L)	0.2	0.2	0.2	0.3	0.3
Sulphide (S^{2-})	(mg/L)	0.05	0.1	0.2	0.5	1
Total Coliforms	(count/L)	200	2000	10000	20000	40000

Table A2-2: Drinking Raw Water Supplementary Standards

Parameter	Unit	Guideline
Sulphate (SO42-)	(mg/L)	250
Chloride (Cl^-)	(mg/L)	250
Nitrate (NO_3--N)	(mg/L)	10
Iron (Fe)	(mg/L)	0.3
Manganese (Mn)	(mg/L)	0.1

Table A2-3: Drinking Raw Water Specific Guidelines

Parameter	**Unit**	**Guideline**
Antimony (Sb)	mg/L	0.005
Barium (Ba)	mg/L	0.7
Beryllium (Be)	mg/L	0.002
Boron (B)	mg/L	0.5
Molybdenum (Mo)	mg/L	0.07
Nickel (Ni)	mg/L	0.02
Thallium (Tl)	mg/L	0.0001
Cobalt (Co)	mg/L	1
Vanadium (V)	mg/L	0.05
Titanium (Ti)	mg/L	0.1
1,2 Dichloroacetic Acid	mg/L	0.03
Dichloromethane	mg/L	0.02
Chloral (Trichloroacetaldehyde)	mg/L	0.01
2,4,6, Trichlorophenol	mg/L	0.2
Tribromomethane	mg/L	0.1
Heptachlor	mg/L	-
Heptachlorepoxide	mg/L	0.0002
Maldison/Malathion	mg/L	0.05
Pentachlorophenol	mg/L	0.009
Hexachlorobenzene	mg/L	0.05
Dimethoate	mg/L	0.08
Parathion	mg/L	0.003
Methyl Parathion	mg/L	0.002
Chlorothalonil	mg/L	0.01
Lindane	mg/L	0.002
Dichlorvos	mg/L	0.05
Atrazine	mg/L	0.003
Deltamethrin	mg/L	0.02
DDT	mg/L	0.001
Ethylbenzene	mg/L	0.3
Xylene (total)	mg/L	0.5
1,1 - Dichloroethelene	mg/L	0.03
1,2 - Dichloroethylene	mg/L	0.05
1,2 - Dichlorobenzene	mg/L	1
1,4 - Dichlorobenzene	mg/L	0.3
Trichloroethylene	mg/L	0.07
Trichlorobenzenes (total)	mg/L	0.02
Chlorobutadine	mg/L	0.002

Hexachlorobutadiene	mg/L	0.0006
Acrylamide	mg/L	0.0005
Tetrachlorethylene	mg/L	0.04
Toluene	mg/L	0.7
Phthalate Ester (total)	mg/L	0.003
Phthalate Ester (2 - ethylhexyl)	mg/L	0.008
Epichlorohydrin	mg/L	0.02
Benzene	mg/L	0.01
Styrene	mg/L	0.9
Benzo (a) pyrene	mg/L	0.0000028
Vinyl chloride	mg/L	0.005
Chlorobenzene	mg/L	0.3
Microcystins-LR	mg/L	0.001
Acetaldehyde	mg/L	0.05
Acrolein	mg/L	0.1
Cumene	mg/L	0.25
Tetrachlorodibenzodioxin	mg/L	0.02
Nitrobenzene	mg/L	0.017
Dinitrobenzene	mg/L	0.5
2,4-Dinitrotoluene	mg/L	0.0003
2,4,6-Trinitrotoluene	mg/L	0.5
Dinitrochlorobenzene	mg/L	0.05
2,4-Dinitrochlorobenzene	mg/L	0.5
2,4- Dichlorophenol	mg/L	0.093
Aniline	mg/L	0.1
Benzidine	mg/L	0.0005
Acrylonitrile	mg/L	0.1
Hydrazine Hydrate	mg/L	0.01
Tetraethyl Lead	mg/L	0.0001
Pyridine	mg/L	0.2
Turpentine	mg/L	0.2
Picric Acid	mg/L	0.5
Butyl Xanthate	mg/L	0.005
Active Chlorine	mg/L	0.01
Trichlorphon	mg/L	0.05
Demeton	mg/L	0.03
Carbaryl	mg/L	0.05
Methyl Mercury	mg/L	0.000001
Polychlorinated Biphenyls	mg/L	0.00002

A3 – PCLake+ input data

Modules

The following modules were activated in the model environment:

- Transport module = ON
- Vegetation module = ON
- Burial Module = ON
- Food Web Module = ON
- Marsh zone module = ON
- Season module = ON
- Stratification = OFF; based on Fig 3 in Janssen et al (2019), mixing depth is a function of depth. Average fetch was estimated to be 8000m resulting in a mixing depth estimate of 11.4m. This mixing depth is close to the maximum depth of the reservoir and far below the average depth and therefore stratification was deactivated for this model.
- Latitude module = ON
- Surface Layer Module (Cyanobacteria Buoyancy) = ON
- Nitrogen fixation module = ON
- Calculate mixing depth module = ON
- Calculate Evaporation module = ON

Hydrological Input

Flow through the reservoir determined using the following equation:

$$Average\ Flow\ (Q) = \frac{Volume\ (V)}{Hydraulic\ Retention\ Time\ (t)} \qquad \textit{Equation A3-1}$$

HRT was adopted as described above. Volume adopted from Table 4-2 assuming an average operational water level of 2.7m elevation. Inflow was assumed to be equal to the total flow for each HRT. Outflow to Shanghai is assumed as 7.19 million m^3/d with the outflow sluice making up the difference to ensure continuity. Derived flow rates are presented in the table below. Daily flow in and out of the reservoir was converted to mm/d by dividing by surface area which is required for input into the model.

Table A3-1: PCLake+ Hydrological Input

HRT	Operation Water Level (m)	Volume (million m^3)	Average Flow Rate (Qin) (million m^3/d)	Qin (mm/d)	Flow to Shanghai (million m^3/d)	Outflow Rate (Qout) (million m^3/d)	Qout (mm/d)
8.5	2.7	281	33.1	636.3	7.19	25.9	636.3
17.5	2.7	281	16.1	309.1	7.19	8.9	309.1
30	2.7	281	9.4	180.3	7.19	2.2	180.3

Reservoir Properties and Local Conditions

Input calibration parameters specific to the Qingcaosha reservoir and local conditions are summarised in the table below.

Table A3-2 PCLake+ Reservoir Properties and Local Conditions

Parameter	Unit	Model Value	Comment
Water Depth (sDepthW)	m	5.4	Refer Section 4.1
Wind Fetch (cFetch)	m	8050	Ranges from 4450m to 12500m based on wind direction
Wind Speed (-)	m/s	2.9	Ranges from approximately 0.85 to 4 m/s
Lutum Content of Sediment (fLutum)	%	47	Same as Clay as defined under ISO14688-1:2002 (i.e., fraction of particles ≤ 0.002 mm diameter)
Iron Content Sediment (fFeDIM)	gFe/gDW	0.03	Adopted from Lake Tai Values from Janssen et al (2017) in the absence of specific data assuming similarities in sediment/geological composition with Yangtze Estuary
Aluminium Content Sediment (fAlDIM)	gAl/gDW	0.03	Adopted from Lake Tai Values from Janssen et al (2017) in the absence of specific data assuming similarities in sediment/geological composition with Yangtze Estuary
Organic Fraction Sediment (fDOrgSM0)	gDW/gsed	0.02	Adopted from Lake Tai Values from Janssen et al (2017) in the absence of specific data assuming similarities in sediment/geological composition with Yangtze Estuary
Relative Marsh to Lake Area (fMarsh)	sq.m marsh/ sq.m lake	0.3	Estimated from aerial photo. Estimate at normal water level (2.7m)
Annual Average Radiation (cLDayAve)	J.sq.m/d	13.1×10^6	Adopted from Lake Tai Values from Janssen et al (2017) in the absence of specific data same latitude and climate zone
Annual Variation in Radiation (cLDayVar)	J.sq.m/d	7.0×10^6	Adopted from Lake Tai Values from Janssen et al (2017) in the absence of specific data same latitude and climate zone
Annual variation in day length (cfDayVar)	hrs variation/d	0.1	Adopted from Lake Tai Values from Janssen et al (2017) in the absence of specific data same latitude and climate zone

Parameter	Unit	Model Value	Comment
Temperature of Water (mTemp)	^{o}C	Varies	Refer graph in Chapter 4
N-Load:P-Load (_cNPLoadMeas_)	Ratio	19.4	Calculated from estuary averages in Chapter 3
PO4:TP (_fPO4In_)	Ratio	0.37	Calculated from estuary averages in Chapter 3
NH4:DIN (_fNH4DissIn_)	Ratio	0.2	Calculated from estuary averages in Chapter 3

Initial States

Model default values were adopted for pre-warm up initial states. Initial states adopted after the warm-up step are summarised in the table below.

Table A3-3: PCLake+ Post-warm-up Initial States

Parameter	**Turbid**	**Clear**
RunId	**0**	**1**
oNH4WHyp	0.366024	0.366024
oNO3WHyp	4.10222	4.10222
oPO4WHyp	0.848485	0.848485
oPAIMWHyp	0.000690958	0.000690958
oSiO2WHyp	6.6665	6.6665
oO2WHyp	6.91704	6.91704
oDDetWHyp	6.16687	6.16687
oNDetWHyp	0.419992	0.419992
oPDetWHyp	0.0613011	0.0613011
oSiDetWHyp	0.336682	0.336682
oDIMWHyp	2.02593	2.02593
oDDiatWHyp	0.00618313	0.00618313
oNDiatWHyp	0.000308909	0.000308909
oPDiatWHyp	3.61E-05	3.61E-05
oDGrenWHyp	0.01658	0.01658
oNGrenWHyp	0.00164675	0.00164675
oPGrenWHyp	0.000246188	0.000246188
oDBlueWHyp	0.419656	0.419656
oNBlueWHyp	0.0622182	0.0622182
oPBlueWHyp	0.010485	0.010485
oDZooHyp	0.0438986	0.0438986
oNZooHyp	0.0030729	0.0030729
oPZooHyp	0.000438986	0.000438986
aDFiAd	2.7614	0.0018157
aDFiJv	1.17291	0.000881418
aNFiAd	0.27614	0.00018157
aNFiJv	0.117291	8.81E-05
aPFiAd	0.0607509	3.99E-05
aPFiJv	0.025804	1.94E-05
aDPisc	0.000191995	0.000189125
aNH4S	0.249022	0.00611741
aNO3S	0.0753162	0.0412588

aPO4S	0.058649	0.00338403
aPAIMS	10.1709	2.77646
aDDetS	393.279	21.165
aNDetS	25.6772	1.35829
aPDetS	3.65225	0.194105
aSiDetS	21.4294	1.23652
aDHumS	5932.14	4619.13
aNHumS	309.024	231.519
aPHumS	42.0414	31.2304
aDIMS	27900.7	30909.8
aDDiatS	0.0324268	0.00159704
aNDiatS	0.00175453	7.93E-05
aPDiatS	0.000225646	9.88E-06
aDGrenS	0.0208741	0.000875932
aNGrenS	0.00194136	7.78E-05
aPGrenS	0.000286134	1.08E-05
aDBlueS	0.00715081	0.000414635
aNBlueS	0.000939427	5.24E-05
aPBlueS	0.000169158	9.61E-06
aDVeg	0.0471605	0.0471919
aNVeg	0.00164625	0.00164733
aPVeg	0.000164591	0.000164696
aVegHeight	2	2
aDBent	1.88515	0.00564117
aNBent	0.131961	0.000394882
aPBent	0.0188515	5.64E-05
uDepthWM	0.5	0.5
oNH4WM	0.81938	0.0302203
oNO3WM	4.43658	0.229883
oPO4WM	0.173011	0.00864524
oPAIMWM	0.000687791	7.14E-05
oSiO2WM	3.38069	3.02021
_oO2WM_	9.47931	9.96458
oDDetWM	5.01588	0.241029
oNDetWM	0.345639	0.0160591
oPDetWM	0.0492779	0.0022968
oSiDetWM	0.253696	0.0127824
oDIMWM	3.30322	3.15929
oDDiatWM	0.0151334	0.000710697

oNDiatWM	0.000827563	3.52E-05
oPDiatWM	0.000110141	4.52E-06
oDGrenWM	0.0398421	0.00157586
oNGrenWM	0.00368182	0.000138509
oPGrenWM	0.000541833	1.92E-05
oDBlueWM	0.111795	0.00620118
oNBlueWM	0.0146593	0.00078207
oPBlueWM	0.00264262	0.000143489
oDZooM	0.136272	0.0616284
oNZooM	0.00953903	0.00431399
oPZooM	0.00136272	0.000616284
aNH4SM	0.492062	0.00093088
aNO3SM	0.0571199	0.000101865
aPO4SM	0.0814463	0.00122728
aPAIMSM	11.523	0.318314
aDDetSM	1376.03	818.431
aNDetSM	60.7083	14.6762
aPDetSM	7.78884	2.56449
aSiDetSM	24.7976	1.37736
aDHumSM	3696.6	3153.21
aNHumSM	169.964	113.941
aPHumSM	19.861	13.3719
aDIMSM	30137.6	32103.7
aDRootPhra	6143.57	5381.61
aDShootPhra	1405.07	1230.18
aNRootPhra	190.227	91.154
aNShootPhra	43.506	20.8369
aPRootPhra	21.0175	16.1423
aPShootPhra	4.80683	3.68997
oNH4WEpi	0.685809	0.0363011
oNO3WEpi	4.45795	0.233981
oPO4WEpi	0.144319	0.00832786
oPAIMWEpi	0.00541137	0.000578867
oSiO2WEpi	3.17845	3.00906
oO2WEpi	6.92911	8.45396
oDDetWEpi	14.1162	0.679013
oNDetWEpi	0.972979	0.0452691
oPDetWEpi	0.138725	0.00647423
oSiDetWEpi	0.713848	0.035954

oDIMWEpi	26.9355	25.7583
oDDiatWEpi	0.068601	0.00323083
oNDiatWEpi	0.00374977	0.000160066
oPDiatWEpi	0.00049907	2.05E-05
oDGrenWEpi	0.0954047	0.00378837
oNGrenWEpi	0.00881114	0.000332736
oPGrenWEpi	0.00129655	4.60E-05
oDBlueWEpi	0.153834	0.00846423
oNBlueWEpi	0.02011	0.00106408
oPBlueWEpi	0.00363068	0.000195483
oDZooEpi	0.137154	0.061761
oNZooEpi	0.00960076	0.00432327
oPZooEpi	0.00137154	0.00061761
aDExtTotT	47285.1	48500
aNExtTotT	509.147	306.888
aPExtTotT	77.1816	45.1207
aSiExtTotT	50.4931	18.5506
aO2ExtTotT	38.8391	47.146